453

BNL 50298
NCSAC - 38
EANDC(US)-156 "U"
INDC(USA)-30 "U"

Reports to . . .

THE AEC NUCLEAR CROSS SECTIONS ADVISORY COMMITTEE

Meeting at

DUKE UNIVERSITY
DURHAM, NORTH CAROLINA

May 4-5, 1971

Compiled by . . .

R.E. Chrien, Secretary, NCSAC

PREFACE

The reports in this document were submitted to the AEC Nuclear Cross Sections Advisory Committee (NCSAC) at the meeting at Duke University, Durham, North Carolina, on May 4-5, 1971. The reporting laboratories are those having a substantial effort in measuring neutron and nuclear cross sections of relevance to the U. S. applied nuclear energy program. The material contained in these reports is to be regarded as comprised of informal statements of recent developments and preliminary data. Appropriate subjects are listed as follows:

1. Microscopic neutron cross sections relevant to the nuclear energy program, including shielding. Inverse reactions where pertinent are included.

2. Charged particle cross sections, where they are relevant to 1) above, and where relevant to developing and testing nuclear models.

3. Gamma-ray production, radioactive decay, and theoretical developments in nuclear structure which are applicable to nuclear energy programs.

4. Proton and alpha-particle cross sections, at energies of up to 1 GeV, which are of interest to the space program.

These reports cannot be regarded as a complete summary of the nuclear research effort of the AEC. A number of laboratories, whose research is less programmatically oriented do not submit reports; neither do the submitted reports reflect all the work related to nuclear cross sections in progress at the submitting laboratory. Budgetary limitations have made it mandatory to follow more strictly the subject guidelines described above and therefore to restrict the size of this document.

Persons wishing to make use of these data should contact the individual experimenter for further details. The data which appear in this document should be quoted only by permission of the contributor and should be referenced as private communication, and not by this document number.

This compilation has been produced almost completely from master copies prepared by the individual contributors listed in the Table of Contents. It is a pleasure to acknowledge their help in the preparation of these reports.

R. E. Chrien
Secretary, NCSAC
Brookhaven National Laboratory
Upton, New York 11973

TABLE OF CONTENTS

Previously submitted Reports to the AEC Nuclear Cross Sections Advisory Committee include the following:

December 1970 Meeting at Lawrence Radiation Laboratory	NCSAC- 33 EANDC(US)-150U INDC(US)- 25U
May 1970 Meeting at Argonne National Laboratory	NCSAC- 31 EANDC(US)-143U INDC(US)- 22U
September 1969 Meeting at Rice University	WASH-1136 EANDC(US)-122U INDC(US)- 14U
April 1969 Meeting at Oak Ridge, Tennessee	WASH-1127 EANDC(US)-120U INDC(US)- 10U
October 1968 Meeting at Columbia University	WASH-1124 EANDC(US)-111U INDC(US)- 9U
April 1968 Meeting at Los Alamos, New Mexico	WASH-1093 EANDC(US)-105U INDC(US)- 2U
October 1967 Meeting at Idaho Falls, Idaho	WASH-1079 EANDC(US)-104U INDC(US)- 12U
April 1967 Meeting at Brookhaven, New York	WASH-1074 EANDC(US)- 99U INDC(US)- 9U
November 1966 Meeting at Argonne, Illinois	WASH-1071 EANDC(US)- 91U INDC(US)- 5U
March 1966 Meeting at Washington, D.C.	WASH-1068 EANDC(US)- 85U INDC(US)- 3U

The following is an index to measurements in NCSAC 38 pertinent to listed in NCSAC-35, "Compilation of Requests for Nuclear Cross Section Measurements", (March 1971). This latter document has superseded the previously-issued WASH 1144. A CINDA-type index, prepared by L. T. Whitehead, of the Division of Technical Information, follows on page vii .

NCSAC-35 REQUEST #	MATERIAL	X-SECTION	NCSAC-38 PAGE #
1	H	Total	173
7	He-3	Elastic	116
25	Be-9	(n, p) Del Neut	125
28	B-10	(n,α)	76
29	B-10	(n,α)	76
31 - 33	C-12	Elastic	143
32	C-12	Elastic	1
38 , 39	N-14	Elastic	143
42	N-14	Gamma Prod	148
43	O-16	Elastic	143
56	Na-23	Tot Inelastic	159
73	Ca	Gamma Prod	162
82	Ti-47	(n, p)	1
84	V	Elastic	1
85	V	Inelastic	1
87	V	(n,γ)	173
90,91,94	Cr	(n, γ)	173
97	Fe	Elastic	1,172
99	Fe	Inelastic	1,159
103,104,105	Fe	Gamma Prod	77
118	Ni	Elastic	1,172
119	Ni	Inelastic	1
124	Ni-58	(n, p)	1
222	Mo	(n,γ)	76
227	Rh^{-103}	(n,γ)	74,76
240	Nd-143	(n,γ)	132
241	Nd-145	(n,γ)	132
249	Sm-147	(n,γ)	172
250	Sm-150	(n,γ)	172
275	Gd	(n,γ)	76
321	Ta-181	(n,γ)	76
324	W	Tot γ Prod	86
336	Au	(n,γ)	76,112
343	Pb-208	(n,γ)	117

NCSAC-35 REQUEST #	MATERIAL	X-SECTION	NCSAC-38 PAGE #
347	Th	(n,γ)	57,112
358,359	U-233	(n,F)	61
361,362	U-233	Nubar	174
387	U-235	(n,F)	61
388,389,390	U-235	(n,F)	261,95,117,162
393	U-235	Alpha	162
395	U-235	Nubar	174
396	U-235	Fission Neut Yield	5
398	U-235	Capt Spectra	27, 59, 60,
399	U-235	Delayed gamma Yield	27,66,105
400	U-235	Res Parameters	27,30
412	U-238	Elastic	1
413	U-238	Inelastic	1
417	U-238	Fission Ratio	2,112,85
421,422	U-238	(n,γ)	76,85,162
423	U-238	Tot Gamma Prod	13,158
427	U-238	Res Par	47,112,158
446	Pu-239	Emission	5
450,451	Pu-239	(n,F)	4
455	Pu-239	Alpha	115,162
463	Pu-240	Inelastic	1
471	Pu 240	Res Parameters	170
505	Cm-243	Total	81
508	Cm-244	Total	81
514	Cm-245	Total	81
515	Cm-245	Fission	81
517	Cm-246	Total	81
528	Cf-249	Fission	112
533	Cf-252	Fission	112

ELEMENT S	A	QUANTITY	TYPE	ENERGY MIN	ENERGY MAX	DOCUMENTATION REF	VOL	PAGE	DATE	LAB	COMMENTS	SERIAL NO.
H	001	TOTAL XSECT	EXPT-PROG	1.0 6	2.0 7	BNL-50298	173		5/71	RPI	CLEMENT+.TOF. ABST ONLY,NO DATA GIVN	55656
H	001	POLARIZATION	EXPT-PROG	5.0 6	2.5 7	BNL-50298	199		5/71	YAL	FIRK+. NO DATA GIVEN	55601
D	002	TOTAL XSECT	EXPT-PROG	1.0 6	2.0 7	BNL-50298	173		5/71	RPI	CLEMENT+.TOF. ABST ONLY,NO DATA GIVN	55655
D	002	N2N REACTION	EXPT-PROG	NDG		BNL-50298	116		5/71	LAS	GRAVES+.SCINTILLATOR. NO DATA GIVEN	55513
D	002	GAMMA N	EXPT-PROG	5.0 6	3.5 7	BNL-50298	199		5/71	YAL	FIRK+. NEUT POL MEASD 45-90DEG,NDG	55600
HE	003	ELASTIC	EXPT-PROG	7.9 6	2.4 7	BNL-50298	116		5/71	LAS	DROSG+.NO DATA GIVEN	55511
HE	003	DIFF ELASTIC	EXPT-PROG	7.9 6	2.4 7	BNL-50298	116		5/71	LAS	DROSG+.ANG DIST 19.4-118.5DEG. NDG	55512
HE	004	DIFF ELASTIC	EXPT-PROG	NDG		BNL-50298	186		5/71	DKE	STAMMBACH+. R-MATRIX ANAL,NO DATA	55604
HE	004	DIFF ELASTIC	EXPT-PROG	NDG		BNL-50298	188		5/71	DKE	WALTER+.SEE PR C5 2034(1970),NO DATA	55602
HE	004	POLARIZATION	EXPT-PROG	NDG		BNL-50298	186		5/71	DKE	STAMMBACH+. R-MATRIX ANAL,NO DATA	55603
LI	007	TOT INELASTC	EXPT-PROG	5	6	BNL-50298	159		5/71	ORL	PEREY+. NO DATA GIVEN	55688
BE	009	TOTAL XSECT	EXPT-PROG	5.0 5	2.0 7	BNL-50298	128		5/71	NBS	SCHWARTZ+. LINAC+TOF. CURVE	55627
BE	009	N,PROTON	EXPT-PROG	1.5 7		BNL-50298	125		5/71	LAS	AUGUSTSON+.DELAYED NEUT SIG, TBC,NDG	55628
B	010	N,ALPHA	EXPT-PROG	1. 3	1. 6	BNL-50298	76		5/71	GA	FRIESENHAHN. 1-3PC ACCURACY. TBD	55490
C		DIFF ELASTIC	EXPT-PROG	1.8 6	3.0 6	BNL-50298	1		5/71	ANL	SMITH+.ANAL TO BE COMPLETED,NO DATA	55572
C		DIFF ELASTIC	EXPT-PROG	7.0 6	1.4 7	BNL-50298	143		5/71	NEL	BUCHER+.2.5-15DEG,TBC,NO DATA GIVEN	55616
C		TOT INELASTC	EXPT-PROG	5	6	BNL-50298	159		5/71	ORL	PEREY+. NO DATA GIVEN	55682
C		DIFF INELAST	EXPT-PROG	1.8 6	3.0 6	BNL-50298	1		5/71	ANL	SMITH+.ANAL TO BE COMPLETED,NO DATA	55567
N		DIFF ELASTIC	EXPT-PROG	7.0 6	1.4 7	BNL-50298	143		5/71	NEL	BUCHER+.2.5-15DEG,TBC,NO DATA GIVEN	55615
N		NONEL GAMMAS	EXPT-PROG	1.5 7		BNL-50298	148		5/71	NEL	CIALELLA. GE(LI),ANAL TBC,NO DATA	55612
O		TOTAL XSECT	EXPT-PROG	2.4 6		BNL-50298	57		5/71	COL	KALYNA+. VDG. VALUE GIVN. TBP	55527
O		TOTAL XSECT	EXPT-PROG	5.0 5	2.0 7	BNL-50298	128		5/71	NBS	SCHWARTZ+. TRANS.,TBC,NO DATA GIVEN	55625
O		DIFF ELASTIC	EXPT-PROG	7.0 6	1.4 7	BNL-50298	143		5/71	NEL	BUCHER+.2.5-15DEG,TBC,NO DATA GIVEN	55614
O	016	TOTAL XSECT	EXPT-PROG	6		BNL-50298	151		5/71	ORL	FOWLER+.LI7(P,N) SOURCE,NO DATA GIVN	55611
O	016	TOTAL XSECT	EXPT-PROG	1.7 6	4.3 6	BNL-50298	152		5/71	ORL	FOWLER+. T(P,N) SOURCE,30KEV RESOL	55610
O	016	TOTAL XSECT	EXPT-PROG	2.4 6		BNL-50298	57		5/71	COL	KALYNA+. VDG. VALUE GIVN. TBP	55528
F	019	RESON PARAMS	EXPT-PROG	2.7 4	9.7 4	BNL-50298	47		5/71	COL	SINGH+. L J PI WN WG FOR 3RESON GIVN	55536
F	019	STRNTH FNCTN	EXPT-PROG	3	5	BNL-50298	47		5/71	COL	SINGH+. S0 AND S1 DERIVED,NO DATA	55535
NA	023	TOT INELASTC	EXPT-PROG	5.0 5	2.2 6	BNL-50298	159		5/71	ORL	PEREY+. CURVE	55684
AL	027	RESON PARAMS	EXPT-PROG	5.9 3	2.1 5	BNL-50298	47		5/71	COL	SINGH+. L J PI WN WG FOR 8RESON GIVN	55537
AL	027	STRNTH FNCTN	EXPT-PROG	3	5	BNL-50298	47		5/71	COL	SINGH+. S0 AND S1 DERIVED,NO DATA	55534
AL	027	NONEL GAMMAS	EXPT-PROG	8.6 5	1.7 7	BNL-50298	77		5/71	GA	ORPHAN+.LINAC.GE(LI) DET.NO DATA GVN	55488
SI		TOTAL XSECT	EXPT-PROG	5.0 5	2.0 7	BNL-50298	128		5/71	NBS	SCHWARTZ+. LINAC+TOF. CURVE	55626
SI		NONEL GAMMAS	EXPT-PROG	7.5 6		BNL-50298	117		5/71	LAS	DRAKE+. GE(LI) DET. 1.78MEV GAM,NDG	55508
SI		TOT INELASTC	EXPT-PROG	8.0 5	2.1 6	BNL-50298	159		5/71	ORL	PEREY+. CURVE	55683
AR		TOTAL XSECT	EXPT-PROG	1.0 5	1.0 6	BNL-50298	35		5/71	COL	CAMARDA+. TRANS. CURVE	55582
CA		NONEL GAMMAS	EXPT-PROG	5.9 6		BNL-50298	162		5/71	ORL	DICKENS+. NO DATA GIVEN	55687
CA	040	TOTAL XSECT	EXPT-PROG	1.0 6	2.1 6	BNL-50298	152		5/71	ORL	FOWLER+.LI7(P,N) SOURCE.4KEV RESOL	55698
TI		DIFF ELASTIC	EXPT-PROG	1.8 6	3.0 6	BNL-50298	1		5/71	ANL	SMITH+.ANAL TO BE COMPLETED,NO DATA	55570
TI		DIFF INELAST	EXPT-PROG	1.8 6	3.0 6	BNL-50298	1		5/71	ANL	SMITH+.ANAL TO BE COMPLETED,NO DATA	55565
TI	047	N,PROTON	EXPT-PROG	TR	4.4 6	BNL-50298	1		5/71	ANL	MEADOWS.EXCITATION FNCT,ANAL TBC,NDG	55579
V		TOTAL XSECT	EXPT-PROG	3		BNL-50298	173		5/71	RPI	STIEGLITZ+. SEE NP A163 592(1971)	55649
V		RESON PARAMS	EXPT-PROG	3		BNL-50298	173		5/71	RPI	STIEGLITZ+. SEE NP A163 592(1971)	55643
V		STRNTH FNCTN	EXPT-PROG	3		BNL-50298	173		5/71	RPI	STIEGLITZ+. SEE NP A163 592(1971)	55637
V		DIFF ELASTIC	EXPT-PROG	1.8 6	3.0 6	BNL-50298	1		5/71	ANL	SMITH+.ANAL TO BE COMPLETED,NO DATA	55569
V		DIFF INELAST	EXPT-PROG	1.8 6	3.0 6	BNL-90298	1		5/71	ANL	SMITH+.ANAL TO BE COMPLETED,NO DATA	55564
V		N,GAMMA	EXPT-PROG	3		BNL-50298	173		5/71	RPI	STIEGLITZ+. SEE NP A163 592(1971)	55631
CR	050	TOTAL XSECT	EXPT-PROG	3		BNL-50298	173		5/71	RPI	STIEGLITZ+. SEE NP A163 592(1971)	55654

ELEMENT S	A	QUANTITY	TYPE	ENERGY MIN	ENERGY MAX	DOCUMENTATION REF	VOL	PAGE	DATE	LAB	COMMENTS	SERIAL NO.
CR	050	RESON PARAMS	EXPT-PROG	3		BNL-50298	173		5/71	RPI	STIEGLITZ+. SEE NP A163 592(1971)	55648
CR	050	STRNTH FNCTN	EXPT-PROG	3		BNL-50298	173		5/71	RPI	STIEGLITZ+. SEE NP A163 592(1971)	55642
CR	050	N,GAMMA	EXPT-PROG	3		BNL-50298	173		5/71	RPI	STIEGLITZ+. SEE NP A163 592(1971)	55636
CR	052	TOTAL XSECT	EXPT-PROG	3		BNL-50298	173		5/71	RPI	STIEGLITZ+. SEE NP A163 592(1971)	55653
CR	052	RESON PARAMS	EXPT-PROG	3		BNL-50298	173		5/71	RPI	STIEGLITZ+. SEE NP A163 592(1971)	55647
CR	052	STRNTH FNCTN	EXPT-PROG	3		BNL-50298	173		5/71	RPI	STIEGLITZ+. SEE NP A163 592(1971)	55641
CR	052	N,GAMMA	EXPT-PROG	3		BNL-50298	173		5/71	RPI	STIEGLITZ+. SEE NP A163 592(1971)	55635
CR	053	TOTAL XSECT	EXPT-PROG	3		BNL-50298	173		5/71	RPI	STIEGLITZ+. SEE NP A163 592(1971)	55652
CR	053	RESON PARAMS	EXPT-PROG	3		BNL-50298	173		5/71	RPI	STIEGLITZ+. SEE NP A163 592(1971)	55646
CR	053	STRNTH FNCTN	EXPT-PROG	3		BNL-50298	173		5/71	RPI	STIEGLITZ+. SEE NP A163 592(1971)	55640
CR	053	N,GAMMA	EXPT-PROG	3		BNL-50298	173		5/71	RPI	STIEGLITZ+. SEE NP A163 592(1971)	55634
CR	054	TOTAL XSECT	EXPT-PROG	3		BNL-50298	173		5/71	RPI	STIEGLITZ+. SEE NP A163 592(1971)	55651
CR	054	RESON PARAMS	EXPT-PROG	3		BNL-50298	173		5/71	RPI	STIEGLITZ+. SEE NP A163 592(1971)	55645
CR	054	STRNTH FNCTN	EXPT-PROG	3		BNL-50298	173		5/71	RPI	STIEGLITZ+. SEE NP A163 592(1971)	55639
CR	054	N,GAMMA	EXPT-PROG	3		BNL-50298	173		5/71	RPI	STIEGLITZ+. SEE NP A163 592(1971)	55633
FE		DIFF ELASTIC	EXPT-PROG	1.8 6	3.0 6	BNL-50298	1		5/71	ANL	SMITH+.ANAL TO BE COMPLETED,NO DATA	55578
FE		DIFF ELASTIC	EXPT-PROG	3		BNL-50298	172		5/71	RPI	ZUHR+.TOF. TO BE COMPLETED.NO DATA	55667
FE		NONEL GAMMAS	EXPT-PROG	8.6 5	1.7 7	BNL-50298	77		5/71	GA	ORPHAN+.LINAC.GE(LI) DET.CURVS.	55489
FE		TOT INELASTC	EXPT-PROG	1.8 6	3.6 6	BNL-50298	159		5/71	ORL	PEREY+. CURVE	55681
FE		DIFF INELAST	EXPT-PROG	1.8 6	3.0 6	BNL-50298	1		5/71	ANL	SMITH+.ANAL TO BE COMPLETED,NO DATA	55577
FE	056	N,PROTON	EXPT-PROG	TR	4.5 6	BNL-50298	1		5/71	ANL	MEADOWS.EXCITATION FNCT,ANAL TBC,NDG	55580
CO	059	TOTAL XSECT	EXPT-PROG	NDG		BNL-50298	110		5/71	LOK	FISHER+.DEFORMATION EFFECT.NO DATA	55493
CO	059	TOTAL XSECT	EXPT-PROG	NDG		BNL-50298	110		5/71	LOK	FISHER+.SPIN-SPIN EFFECT,TBP IN NP	55494
CO	059	DIFF ELASTIC	EXPT-PROG	1.8 6	3.0 6	BNL-50298	1		5/71	ANL	SMITH+.ANAL TO BE COMPLETED,NO DATA	55576
CO	059	DIFF INELAST	EXPT-PROG	1.8 6	3.0 6	BNL-50298	1		5/71	ANL	SMITH+.ANAL TO BE COMPLETED,NO DATA	55575
NI		DIFF ELASTIC	EXPT-PROG	1.8 6	3.0 6	BNL-50298	1		5/71	ANL	SMITH+.ANAL TO BE COMPLETED,NO DATA	55574
NI		DIFF ELASTIC	EXPT-PROG	3		BNL-50298	172		5/71	RPI	ZUHR+.TOF. TO BE COMPLETED.NO DATA	55666
NI		DIFF INELAST	EXPT-PROG	1.8 6	3.0 6	BNL-50298	1		5/71	ANL	SMITH+.ANAL TO BE COMPLETED,NO DATA	55573
NI	058	N,PROTON	EXPT-PROG	TR	4.5 6	BNL-50298	1		5/71	ANL	MEADOWS.EXCITATION FNCT,ANAL TBC,NDG	55581
NI	060	TOTAL XSECT	EXPT-PROG	3		BNL-50298	173		5/71	RPI	STIEGLITZ+. SEE NP A163 592(1971)	55650
NI	060	RESON PARAMS	EXPT-PROG	3		BNL-50298	173		5/71	RPI	STIEGLITZ+. SEE NP A163 592(1971)	55644
NI	060	STRNTH FNCTN	EXPT-PROG	3		BNL-50298	173		5/71	RPI	STIEGLITZ+. SEE NP A163 592(1971)	55638
NI	060	N,GAMMA	EXPT-PROG	3		BNL-50298	173		5/71	RPI	STIEGLITZ+. SEE NP A163 592(1971)	55632
CU		DIFF ELASTIC	EXPT-PROG	1.8 6	3.0 6	BNL-50298	1		5/71	ANL	SMITH+.ANAL TO BE COMPLETED,NO DATA	55568
CU		DIFF INELAST	EXPT-PROG	1.8 6	3.0 6	BNL-50298	1		5/71	ANL	SMITH+.ANAL TO BE COMPLETED,NO DATA	55563
CU		SPECT NGAMMA	EXPT-PROG	1.4 7		BNL-50298	73		5/71	COL	STAMATELATOS+. NO DATA GIVEN	55467
CU	063	N,GAMMA	EXPT-PROG	1.4 7		BNL-50298	73		5/71	COL	STAMATELATOS+. VALUE GIVEN	55464
SR		TOTAL XSECT	EXPT-PROG	5.0 4	8.8 5	BNL-50298	182		5/71	DKE	NEWSON+. NO SIG GIVEN	55608
SR		RESON PARAMS	EXPT-PROG	1.1 5	2.2 5	BNL-50298	182		5/71	DKE	NEWSON+. J PI WN FOR 10 RESON GIVEN	55607
Y	089	INELST GAMMA	EXPT-PROG	1.4 7		BNL-50298	102		5/71	LRL	DIETRICH+.GE(LI) DET.GAMMA SPEC+SIGS	55499
Y	089	N2N REACTION	EXPT-PROG	1.4 7		BNL-50298	102		5/71	LRL	DIETRICH+.GE(LI) DET.GAMMA SPEC+SIGS	55498
ZR		SPECT NGAMMA	EXPT-PROG	1.4 7		BNL-50298	73		5/71	COL	STAMATELATOS+. NO DATA GIVEN	55466
ZR	096	N,GAMMA	EXPT-PROG	1.4 7		BNL-50298	73		5/71	COL	STAMATELATOS+. VALUE GIVEN	55463
NB	093	DIFF ELASTIC	EXPT-PROG	1.8 6	3.0 6	BNL-50298	1		5/71	ANL	SMITH+.ANAL TO BE COMPLETED,NO DATA	55571
NB	093	DIFF INELAST	EXPT-PROG	1.8 6	3.0 6	BNL-50298	1		5/71	ANL	SMITH+.ANAL TO BE COMPLETED,NO DATA	55566
MO		N,GAMMA	EXPT-PROG	1. 3	1. 6	BNL-50298	76		5/71	GA	FRICKE. ANAL TBC, NO DATA GIVEN	55458
MO	092	RESON PARAMS	EXPT-PROG	NDG		BNL-50298	183		5/71	DKE	DIVADEENAM+. ANAL TBC, NO DATA GIVEN	55606
MO	098	RESON PARAMS	EXPT-PROG	NDG		BNL-50298	183		5/71	DKE	DIVADEENAM+. ANAL TBC, NO DATA GIVEN	55605

ELEMENT S	A	QUANTITY	TYPE	ENERGY MIN	ENERGY MAX	DOCUMENTATION REF	VOL	PAGE	DATE	LAB	COMMENTS	SERIAL NO.
TC	099	N,GAMMA	EXPT-PROG	PILE		BNL-50298	85		5/71	MTR	SCOVILLE+.ACT.SPEC-AVGD SIG REL AU	55476
RH	103	RESON PARAMS	EXPT-PROG	1.3 0	9.9 2	BNL-50298	74		5/71	GA	CARLSON. WG 2G*WN J FOR 64 RESON	55460
RH	103	RES INT ABS	EXPT-PROG	5. -1	1.0 6	BNL-50298	74		5/71	GA	CARLSON. VALUE GIVEN	55459
RH	103	N,GAMMA	EXPT-PROG	0	1. 6	BNL-50298	74		5/71	GA	CARLSON. NO DATA GIVEN	55461
RH	103	N,GAMMA	EXPT-PROG	1. 3	1. 6	BNL-50298	76		5/71	GA	FRICKE. ANAL TBC, NO DATA GIVEN	55457
AG	107	N,GAMMA	EXPT-PROG	PILE		BNL-50298	85		5/71	MTR	SCOVILLE+.ACT.SPEC-AVGD SIG REL AU	55475
AG	109	N,GAMMA	EXPT-PROG	PILE		BNL-50298	85		5/71	MTR	SCOVILLE+.ACT.SPEC-AVGD SIG REL AU	55474
CD	111	SPECT NGAMMA	EXPT-PROG		1.3 3	BNL-50298	19		5/71	BNL	CHRIEN+. NO DATA GIVEN	55547
IN	113	RESON PARAMS	EXPT-PROG	2.2 1	2.0 3	BNL-50298	35		5/71	COL	CAMARDA+.G*WN FOR 39RESON,WG FOR 3	55685
IN	115	RESON PARAMS	EXPT-PROG	2.3 1	2.0 3	BNL-50298	35		5/71	COL	CAMARDA+.G*WN FOR MANY RESONANCES	55591
IN	115	N,GAMMA	EXPT-PROG	PILE		BNL-50298	85		5/71	MTR	SCOVILLE+.ACT.SPEC-AVGD SIG REL AU	55473
SN	120	RESON PARAMS	EXPT-PROG		6.2 4	BNL-50298	152		5/71	ORL	CARLTON+.PARAMS FOR 90RESON,NO DATA	55697
SN	120	STRNTH FNCTN	EXPT-PROG		6.2 4	BNL-50298	152		5/71	ORL	CARLTON+.SO AND S1 MEASD,NO DATA GVN	55696
SB		SPECT NGAMMA	EXPT-PROG	1.4 7		BNL-50298	73		5/71	COL	STAMATELATOS+. NO DATA GIVEN	55465
SB	123	N,GAMMA	EXPT-PROG	1.4 7		BNL-50298	73		5/71	COL	STAMATELATOS+. VALUE GIVEN	55462
XE	124	SPECT NGAMMA	EXPT-PROG	5.2 0		BNL-50298	33		5/71	BNL	KANE+. XE125 LEVEL SCHEME SHOWN	55592
CS	133	N,GAMMA	EXPT-PROG	PILE		BNL-50298	85		5/71	MTR	SCOVILLE+.ACT. SPEC-AVGD SIG REL AU	55504
BA		TOTAL XSECT	EXPT-PROG	5.0 4	8.8 5	BNL-50298	182		5/71	OKE	NEWSON+. NO SIG GIVEN	55609
LA	139	RESON PARAMS	EXPT-PROG	2.4 1	1.0 4	BNL-50298	35		5/71	COL	CAMARDA+.G*WN FOR 81 RESONANCES GIVN	55590
PR	141	N,GAMMA	EXPT-PROG	PILE		BNL-50298	85		5/71	MTR	SCOVILLE+.ACT. SPEC-AVGD SIG REL AU	55678
ND	143	RESON PARAMS	EXPT-PROG	5.5 1	8.4 2	BNL-50298	132		5/71	NRL	STOLOVY+. J FOR 20 RESONANCES GIVEN	55624
ND	145	RESON PARAMS	EXPT-PROG	4.3 0	6.6 2	BNL-50298	132		5/71	NRL	STOLOVY+. J FOR 36 RESONANCES GIVEN	55623
SM	147	TOTAL XSECT	EXPT-PROG	1.0-2	1.2 3	BNL-50298	172		5/71	RPI	EILAND+.TRANS. LINAC. NO SIG GIVEN	55664
SM	147	RESON PARAMS	EXPT-PROG	1.0-2	1.2 3	BNL-50298	172		5/71	RPI	EILAND+. AVG D AND AVG G*WN GIVEN	55662
SM	147	STRNTH FNCTN	EXPT-PROG	1.0-2	1.2 3	BNL-50298	172		5/71	RPI	EILAND+. SO GIVEN	55660
SM	147	RES INT ABS	EXPT-PROG	5. -1	1.2 3	BNL-50298	172		5/71	RPI	EILAND+. VALUE GIVEN	55658
SM	149	RESON PARAMS	EXPT-PROG	6.5 0		BNL-50298	30		5/71	BNL	BRUNHART+. J TO BE MEASD,POLAR EXPT	55595
SM	150	TOTAL XSECT	EXPT-PROG	1.0-2	1.2 3	BNL-50298	172		5/71	RPI	EILAND+.TRANS. LINAC. NO SIG GIVEN	55663
SM	150	RESON PARAMS	EXPT-PROG	1.0-2	1.6 3	BNL-50298	172		5/71	RPI	EILAND+. PARAMS 127RESON,AVG GIVEN	55661
SM	150	STRNTH FNCTN	EXPT-PROG	1.0-2	1.6 3	BNL-50298	172		5/71	RPI	EILAND+. SO GIVEN	55659
SM	150	RES INT ABS	EXPT-PROG	5. -1	1.6 3	BNL-50298	172		5/71	RPI	EILAND+. VALUE GIVEN	55657
SM	152	RESON PARAMS	EXPT-PROG	1.5 3	5.1 3	BNL-50298	35		5/71	COL	CAMARDA+.WN FOR 61 RESONANCES GIVEN	55589
SM	154	RESON PARAMS	EXPT-PROG	2.5 3	4.1 3	BNL-50298	35		5/71	COL	CAMARDA+.WN FOR 13 RESONANCES GIVEN	55588
GD		N,GAMMA	EXPT-PROG	1. 3	1. 6	BNL-50298	76		5/71	GA	FRICKE. ANAL TBC, NO DATA GIVEN	55456
DY	160	TOTAL XSECT	EXPT-PROG		3	BNL-50298	35		5/71	COL	CAMARDA+.GOOD DATA TO 50C0EV.NDG	55542
DY	161	TOTAL XSECT	EXPT-PROG		3	BNL-50298	35		5/71	COL	CAMARDA+.GOOD DATA TO 5000EV.NDG	55541
DY	161	RESON PARAMS	EXPT-PROG	1.3 1	1.7 1	BNL-50298	30		5/71	BNL	RORER+. TRANS,J FOR 2 RESON GIVEN	55596
DY	162	TOTAL XSECT	EXPT-PROG		3	BNL-50298	35		5/71	COL	CAMARDA+.GOOD DATA TO 5000EV.NDG	55540
DY	163	TOTAL XSECT	EXPT-PROG		3	BNL-50298	35		5/71	COL	CAMARDA+.GOOD DATA TO 5000EV.NDG	55539
DY	164	TOTAL XSECT	EXPT-PROG		3	BNL-50298	35		5/71	COL	CAMARDA+.GOOD DATA TO 5000EV.NDG	55538
HO	165	N,GAMMA	EXPT-PROG	PILE		BNL-50298	85		5/71	MTR	SCOVILLE+.ACT. SPEC-AVGD SIG REL AU	55677
ER	166	STRNTH FNCTN	EXPT-PROG	NDG		BNL-50298	35		5/71	COL	CAMARDA+.FINAL SO AND S1 VALUES GVN	55587
ER	167	RESON PARAMS	EXPT-PROG	6.0 0	2	BNL-50298	21		5/71	BNL	CHRIEN+. J FOR 14RESON FROM CAPT,TBC	55545
ER	167	STRNTH FNCTN	EXPT-PROG	NDG		BNL-50298	35		5/71	COL	CAMARDA+.FINAL SO VALUE GIVEN	55586
ER	167	SPECT NGAMMA	EXPT-PROG	0	2	BNL-50298	21		5/71	BNL	CHRIEN+. CURVES,ANAL TO BE COMPLETED	55546
ER	168	STRNTH FNCTN	EXPT-PROG	NDG		BNL-50298	35		5/71	COL	CAMARDA+.FINAL SO AND S1 VALUES GIVN	55585
ER	170	STRNTH FNCTN	EXPT-PROG	NDG		BNL-50298	35		5/71	COL	CAMARDA+.FINAL SO AND S1 VALUES GIVN	55584
TM	169	N,GAMMA	EXPT-PROG	PILE		BNL-50298	85		5/71	MTR	SCOVILLE+.ACT. SPEC-AVGD SIG REL AU	55676

ELEMENT S	A	QUANTITY	TYPE	ENERGY MIN	ENERGY MAX	DOCUMENTATION REF	VOL	PAGE	DATE	LAB	COMMENTS	SERIAL NO.
YB	170	SPECT NGAMMA	EXPT-PROG	8. 0	7.3 1	BNL-50298	139		5/71	NRL	RITTER+. GAMMA ES FOR 4RESON SHOWN	55618
YB	171	RESON PARAMS	EXPT-PROG	7.9 0	1.3 2	BNL-50298	23		5/71	BNL	CHRIEN+. J PI FOR 20RESON FROM CAPT	55598
YB	171	SPECT NGAMMA	EXPT-PROG	0	2	BNL-50298	23		5/71	BNL	CHRIEN+. RESONANCE CAPTURE,CURVES	55599
YB	172	SPECT NGAMMA	EXPT-PROG	1.4 2	2.0 2	BNL-50298	139		5/71	NRL	RITTER+. GAMMA ES FOR 3RESON SHOWN	55617
YB	173	RESON PARAMS	EXPT-PROG	4.5 0	1.1 2	BNL-50298	21		5/71	BNL	CHRIEN+. J FOR 14RESON FROM CAPTURE	55543
YB	173	SPECT NGAMMA	EXPT-PROG	0	2	BNL-50298	21		5/71	BNL	CHRIEN+. RESONANCE CAPT,CURVES SHOWN	55544
HF	179	SPECT NGAMMA	EXPT-PROG	THR		BNL-50298	16		5/71	ANL	BUSHNELL. NO DATA GIVEN	55548
TA	181	N,GAMMA	EXPT-PROG	1. 3	1. 6	BNL-50298	76		5/71	GA	FRICKE. ANAL TBC, NO DATA GIVEN	55701
TA	181	SPECT NGAMMA	EXPT-PROG	THR	2	BNL-50298	13		5/71	ANL	ERSKINE+. NO DATA GIVEN,TO BE COMPLT	55549
W		N,GAMMA	EXPT-PROG	1. 3	1. 6	BNL-50298	76		5/71	GA	FRICKE. ANAL TBC, NO DATA GIVEN	55700
W		SPECT NGAMMA	EXPT-PROG	THR	2. 3	BNL-50298	86		5/71	MTR	GREENWOOD+. 2ES. CURVES	55503
W	182	STRNTH FNCTN	EXPT-PROG	0.	2.6 3	BNL-50298	35		5/71	COL	CAMARDA+.PROBABLY NO P LVLS,NO DATA	55583
W	182	SPECT NGAMMA	EXPT-PROG	2. 3		BNL-50298	86		5/71	MTR	GREENWOOD+. NO DATA GIVEN	55502
W	183	SPECT NGAMMA	EXPT-PROG	THR	2. 3	BNL-50298	86		5/71	MTR	GREENWOOD+. 2ES. TABLES	55501
RE		N,GAMMA	EXPT-PROG	1. 3	1. 6	BNL-50298	76		5/71	GA	FRICKE. ANAL TBC, NO DATA GIVEN	55699
RE	185	RESON PARAMS	EXPT-PROG	0	2	BNL-50298	133		5/71	NRL	STOLOVY+. TOF+CAPT GAMMA SPEC SHOWN	55622
RE	185	SPECT NGAMMA	EXPT-PROG	0	2	BNL-50298	133		5/71	NRL	STOLOVY+. RESON CAPT,GAMMA INT SHOWN	55620
RE	187	RESON PARAMS	EXPT-PROG	0	2	BNL-50298	133		5/71	NRL	STOLOVY+. TOF+CAPT GAMMA SPEC SHOWN	55621
RE	187	SPECT NGAMMA	EXPT-PROG	0	2	BNL-50298	133		5/71	NRL	STOLOVY+. RESON CAPT,GAMMA INT SHOWN	55619
RE	187	SPECT NGAMMA	EXPT-PROG	THR		BNL-50298	122		5/71	LAS	SHERA.RE188 LVL SCHEME ONLY SHOWN	55506
AU	197	N,GAMMA	EXPT-PROG	NDG		BNL-50298	112		5/71	LAS	NO DATA.BOMB NEUTS.SEE 71KNOX	55492
AU	197	N,GAMMA	EXPT-PROG	1. 3	1. 6	BNL-50298	76		5/71	GA	FRICKE. ANAL TBC. NO DATA GIVEN	55679
AU	197	N,GAMMA	EVAL-PROG	1.0 4	5.4 6	BNL-50298	106		5/71	LOK	VAUGHN+.BEST FIT TO DATA,TBL+CURVES	55495
TL	205	RESON PARAMS	EXPT-PROG	4.4 1	2.1 4	BNL-50298	158		5/71	ORL	EARLE+. 13RESON ES FROM CAPT SPECTRA	55689
TL	205	SPECT NGAMMA	EXPT-PROG	1	2.0 5	BNL-50298	158		5/71	ORL	EARLE+.ORELA. RESON CAPT. 13RESON	55690
PB		DIFF ELASTIC	EXPT-PROG	3		BNL-50298	172		5/71	RPI	ZUHR+.TOF. TO BE COMPLETED.NO DATA	55665
PB		DIFF ELASTIC	EXPT-PROG	7.0 6	1.4 7	BNL-50298	143		5/71	NEL	BUCHER+.2.5-15DEG,TBC,NO DATA GIVEN	55613
PB	207	RESON PARAMS	EXPT-PROG	3.1 3	7.0 5	BNL-50298	153		5/71	ORL	ALLEN+. WN WG J PI G*WG*WN/WT GIVEN	55693
PB	207	N,GAMMA	EXPT-PROG	3.0 3	6.4 5	BNL-50298	153		5/71	ORL	ALLEN+. ORELA. NO SIG GIVEN	55695
PB	207	SPECT NGAMMA	EXPT-PROG	3.0 3	6.4 5	BNL-50298	153		5/71	ORL	ALLEN+. CURVES OF GAMMA YIELDS	55694
PB	208	N,GAMMA	EXPT-PROG	6.0 6	1.5 7	BNL-50298	117		5/71	LAS	DRAKE+.VDG.TO LVLS IN PB209.CURVES	55509
PB	208	SPECT NGAMMA	EXPT-PROG	6.0 6	1.5 7	BNL-50298	117		5/71	LAS	DRAKE+.VDG. PULSE-HEIGHT CURVE SHOWN	55510
BI	209	SPECT NGAMMA	EXPT-PROG	THR		BNL-50298	123		5/71	LAS	JURNEY.0.04-2.9MEV GAMS.BI210 LVLS	55505
TH	229	RESON PARAMS	EXPT-PROG	6.1-1	5.1 1	BNL-50298	66		5/71	COL	FELVINCI+.WF SIGO*WF SIGO 29RESON	55468
TH	229	FISSION	EXPT-PROG	3.6-2	1	BNL-50298	66		5/71	COL	FELVINCI+.TOF.SIG CURV 1-5.8EV	55469
TH	230	FISSION	EXPT-PROG	NDG		BNL-50298	112		5/71	LAS	NO DATA. BOMB SOURCE. SEE 71KNOX	55523
TH	232	TOTAL XSECT	EXPT-PROG	0	1.0 4	BNL-50298	57		5/71	COL	RAHN+. CURVE 18-42KEV SHOWN	55530
TH	232	RESON PARAMS	EXPT-PROG	0	1.0 4	BNL-50298	57		5/71	COL	RAHN+. ANAL TO BE COMPLETED.NO DATA	55529
TH	232	N,GAMMA	EXPT-PROG	NDG		BNL-50298	112		5/71	LAS	NO DATA.BOMB NEUTS.SEE 71KNOX	55491
PA	231	FISSION	EXPT-PROG	NDG		BNL-50298	112		5/71	LAS	NO DATA. BOMB SOURCE. SEE 71KNOX	55522
U	233	FISSION	EXPT-PROG	6.0-2	4.0 4	BNL-50298	61		5/71	COL	FELVINCI+.PRELIM CURVS.ANAL TBC	55471
U	233	NU	EXPT-PROG	NDG		BNL-50298	174		5/71	RPI	REED+. TO BE COMPLETED. NO DATA GIVN	55629
U	234	SPECT NGAMMA	EXPT-PROG	THR		BNL-50298	124		5/71	LAS	JURNEY.GAMS BELOW 2.5MEV.U235 LVLS	55672
U	235	TOTAL XSECT	EXPT-PROG	NDG		BNL-50298	30		5/71	BNL	BRUNHART+. J DEPEND TO BE MEASD,POL	55594
U	235	FISSION	EXPT-PROG		5.2 6	BNL-50298	2		5/71	ANL	MEADOWS.RATIO TO U238,ANAL TBC,NDG	55559
U	235	FISSION	EXPT-PROG	2.0 6	5.0 6	BNL-50298	2		5/71	ANL	POENITZ.RATIO TO U238,TBC,NO DATA	55557
U	235	FISSION	EXPT-PROG	3.0 4	1.5 6	BNL-50298	4		5/71	ANL	POENITZ.RATIO TO PU239,GAP 30-900KEV	55554
U	235	FISSION	EXPT-PROG	PILE		BNL-50298	85		5/71	MTR	SCOVILLE+.ACT. SPEC-AVGD SIG REL AU	55674

ELEMENT S	A	QUANTITY	TYPE	ENERGY MIN	ENERGY MAX	DOCUMENTATION REF	VOL	PAGE	DATE	LAB	COMMENTS	SERIAL NO.
U	235	FISSION	EXPT-PROG	1.0 2	1.0 5	BNL-50298	162		5/71	ORL	SILVER+. SCINT. CURVE	55671
U	235	FISSION	EXPT-PROG	1.0 6	1.5 7	BNL-50298	117		5/71	LAS	SMITH+. TO BE COMPLETED. NO DATA	55507
U	235	FISSION	EXPT-PROG	1.2 4	3.5 5	BNL-50298	95		5/71	LRL	BOWMAN+.LINAC. CURVES.MUCH STRUCTURE	55500
U	235	FISSION	EXPT-PROG	5.0-2	4.0 4	BNL-50298	61		5/71	COL	FELVINCI+.PRELIM CURVS.ANAL TBC	55472
U	235	ALPHA	EXPT-PROG	1.0 2	1.0 5	BNL-50298	162		5/71	ORL	SILVER+. SCINT. CURVE	55670
U	235	NU	EXPT-PROG		4.0 1	BNL-50298	174		5/71	RPI	REED+. ANAL TO BE COMPLETED,NO DATA	55630
U	235	SPECT FISS N	EXPT-PROG	NDG		BNL-50298	5		5/71	ANL	SMITH.TOF,UP TO 8.0MEV PROMPT NEUTS	55553
U	235	SPECT FISS G	EXPT-PROG	NDG		BNL-50298	66		5/71	COL	DERENGOWSKI+.ANAL TBC,NO DATA GIVEN	55470
U	235	SPECT FISS G	EXPT-PROG	THR	5.0 1	BNL-50298	27		5/71	BNL	CHRIEN+. TABLE+CURV,0.57-8.3MEV GAMS	55597
U	235	FISS PROD GS	EXPT-PROG	NDG		BNL-50298	105		5/71	LRL	JOHN. 20-1000NSEC GAMS. NO DATA GIVN	55496
U	235	SPECT NGAMMA	EXPT-PROG	0	1	BNL-50298	59		5/71	COL	DERENGOWSKI+.RESON CAPT. SOME DATA	55526
U	235	SPECT NGAMMA	EXPT-PROG	NDG		BNL-50298	60		5/71	COL	FELVINCI+. GAMMA MULTIPOL,ANAL TBC	55525
U	238	TOTAL XSECT	EXPT-PROG	2.1 3	3.3 3	BNL-50298	47		5/71	COL	RAHN+. TRANSMISSION. CURVE	55533
U	238	RESON PARAMS	EXPT-PROG		6.0 2	BNL-50298	158		5/71	ORL	WASSON+.DIST OF PARTIAL WG	55691
U	238	RESON PARAMS	EXPT-PROG	3.7 1	2.4 2	BNL-50298	112		5/71	LAS	SILBERT+.BOMB NEUTS.AVG WF FOR 8RES	55517
U	238	RESON PARAMS	EXPT-PROG	6.6 0	5.0 3	BNL-50298	47		5/71	COL	RAHN+. G*WN AND WG FOR MANY RESON	55532
U	238	STRNTH FNCTN	EXPT-PROG	0.	5. 3	BNL-50298	47		5/71	COL	RAHN+. SO VALUE GIVEN	55531
U	238	DIFF ELASTIC	EXPT-PROG	1.8 6	3.0 6	BNL-50298	1		5/71	ANL	SMITH+.ANAL TO BE COMPLETED,NO DATA	55562
U	238	DIFF INELAST	EXPT-PROG	1.8 6	3.0 6	BNL-50298	1		5/71	ANL	SMITH+.ANAL TO BE COMPLETED,NO DATA	55561
U	238	FISSION	EXPT-PROG		5.2 6	BNL-50298	2		5/71	ANL	MEADOWS.RATIO TO U235,ANAL TBC,NDG	55558
U	238	FISSION	EXPT-PROG	2.0 6	5.0 6	BNL-50298	2		5/71	ANL	POENITZ.RATIO TO U235,TBC,NO DATA	55556
U	238	FISSION	EXPT-PROG	1	5	BNL-50298	112		5/71	LAS	SILBERT+.BOMB NEUTS.AVG KEV SIGS GVN	55518
U	238	FISSION	EXPT-PROG	PILE		BNL-50298	85		5/71	MTR	SCOVILLE+.ACT. SPEC-AVGD SIG REL AU	55673
U	238	N,GAMMA	EXPT-PROG	PILE		BNL-50298	85		5/71	MTR	SCOVILLE+.ACT. SPEC-AVGD SIG REL AU	55675
U	238	N,GAMMA	EXPT-PROG	1. 3	1. 6	BNL-50298	76		5/71	GA	FRICKE. ANAL TBC. NO DATA GIVEN	55680
U	238	N,GAMMA	EXPT-PROG	5.0 0	1.0 5	BNL-50298	162		5/71	ORL	SILVER+. SCINT. CURVES	55686
U	238	SPECT NGAMMA	EXPT-PROG	THR	2	BNL-50298	13		5/71	ANL	BOLLINGER+.CURVES,U239 LVLS SHOWN	55550
U	238	SPECT NGAMMA	EXPT-PROG		6.0 2	BNL-50298	158		5/71	ORL	WASSON+. RESONANCE CAPT,NO DATA GIVN	55692
NP	237	SPECT NGAMMA	EXPT-PROG	NDG		BNL-50298	60		5/71	COL	FELVINCI+. GAMMA MULTIPOL,ANAL TBC	55524
NP	237	SPECT NGAMMA	EXPT-PROG	4.9-1	5.8 0	BNL-50298	31		5/71	BNL	KANE. 0.487EV RESON SPEC GVN, TBC	55593
PU	239	FISSION	EXPT-PROG	3.0 4	1.5 6	BNL-50298	4		5/71	ANL	POENITZ.RATIO TO U235,GAP 30-900KEV	55555
PU	239	ALPHA	EXPT-PROG	1.0 2	1.0 4	BNL-50298	115		5/71	LAS	FARRELL+.BOMB NEUTS.TBL,CFD LRL DATA	55514
PU	239	ALPHA	EXPT-PROG	2.0-2	4.0 5	BNL-50298	162		5/71	ORL	GWIN+. ORELA. SCINT. NO DATA GIVEN	55669
PU	239	SPECT FISS N	EXPT-PROG	NDG		BNL-50298	5		5/71	ANL	SMITH.TOF,UP TO 8.0MEV PROMPT NEUTS	55552
PU	239	PHOTO-FISSN	EXPT-PROG	4.5 6	7.0 6	BNL-50298	12		5/71	ANL	STUBBINS+. NO DATA GIVEN	55551
PU	240	RESON PARAMS	EXPT-PROG	2.0 1	5.0 2	BNL-50298	170		5/71	RPI	HOCKENBURY+. WN AND WG GVN FOR 35RES	55668
PU	240	DIFF INELAST	EXPT-PROG	2. 5	1.5 6	BNL-50298	1		5/71	ANL	SMITH+.CURVS FOR EXCITATN OF 5 LVLS	55560
PU	242	FISSION	EXPT-PROG	NDG		BNL-50298	112		5/71	LAS	NO DATA. BOMB SOURCE. SEE 71KNOX	55521
PU	244	FISSION	EXPT-PROG	NDG		BNL-50298	112		5/71	LAS	NO DATA. BOMB SOURCE. SEE 71KNOX	55520
CM	243	TOTAL XSECT	EXPT-PROG	1.0 0	3.0 1	BNL-50298	81		5/71	MTR	BERRETH+.TRANS. CURVE	55484
CM	243	RESON PARAMS	EXPT-PROG	1.5 0	2.6 1	BNL-50298	81		5/71	MTR	BERRETH+.TRANS. WN WF1 WF2 15 RESON	55480
CM	244	TOTAL XSECT	EXPT-PROG	THR	3	BNL-50298	81		5/71	MTR	YOUNG+.ORELA,TRANS,TO BE COMPLTD,NDG	55487
CM	244	TOTAL XSECT	EXPT-PROG	1.0 0	3.0 1	BNL-50298	81		5/71	MTR	BERRETH+.TRANS. CURVE	55483
CM	244	RESON PARAMS	EXPT-PROG	THR	2	BNL-50298	81		5/71	MTR	YOUNG+.ORELA,TRANS,TO BE COMPLTD,NDG	55486
CM	244	RESON PARAMS	EXPT-PROG	7.7 0	2.3 1	BNL-50298	81		5/71	MTR	BERRETH+.TRANS. WN FOR 3 RESONANCES	55479
CM	245	TOTAL XSECT	EXPT-PROG	1.0 0	3.0 1	BNL-50298	81		5/71	MTR	BERRETH+.TRANS. CURVE	55482
CM	245	RESON PARAMS	EXPT-PROG	2.0 0	2.9 1	BNL-50298	81		5/71	MTR	BERRETH+.TRANS. WN WF1 FOR 10RESON	55478
CM	245	FISSION	EXPT-PROG	SPON		BNL-50298	81		5/71	MTR	SIMPSON+. TO BE DONE	55485

ELEMENT S	A	QUANTITY	TYPE	ENERGY MIN	ENERGY MAX	DOCUMENTATION REF	VOL	PAGE	DATE	LAB	COMMENTS	SERIAL NO.
CM	246	TOTAL XSECT	EXPT-PROG	1.0 0	3.0 1	BNL-50298	81		5/71	MTR	BERRETH+.TRANS. CURVE	55481
CM	246	RESON PARAMS	EXPT-PROG	4.3 0	1.5 1	BNL-50298	81		5/71	MTR	BERRETH+.TRANS. WN FOR 2 RESONANCES	55477
CF	249	FISSION	EXPT-PROG	NDG		BNL-50298	112		5/71	LAS	NO DATA. BOMB SOURCE. SEE 71KNOX	55519
CF	252	RESON PARAMS	EXPT-PROG	2.5 1	9.8 2	BNL-50298	112		5/71	LAS	MOORE+.BOMB SOURCE.SIGO*WF WN WF GVN	55515
CF	252	FISSION	EXPT-PROG	2.0 1	5.0 6	BNL-50298	112		5/71	LAS	MOORE+.BOMB SOURCE.CURVE. TBP IN PR	55516

ARGONNE NATIONAL LABORATORY

A. FAST NEUTRON PHYSICS

1. (n, p) Reactions (J. W. Meadows, Jr.)

The excitation functions for the $Ni^{58}(n, p)Co^{58}$ and $Fe^{56}(n, p)Mn^{56}$ reactions have been measured to 4.5 MeV and the relative excitation function for the $Ti^{47}(n, p)Sc^{47}$ reaction has been measured to 4.4 MeV. Data evaluation is in progress. (Pertinent to requests #84, 125, WASH-1144).

2. Fast Neutron Scattering (A. Smith and P. Guenther)

The experimental program of scattering measurements is now in a production status at the new Fast Neutron Generator. Primary emphasis has been given to elastic and inelastic neutron scattering from Fe, Co, Ni, C, Nb, Ti, V, Cu and U-238 over the incident neutron energy interval 1.8—3.0 MeV. The results are partly analyzed and appear of excellent quality.

The analysis of the previously reported measurements of scattering from ^{240}Pu (see NCSAC-33) is now complete. The resulting inelastic scattering cross sections are summarized in Fig. A-1, a plot of the inelastic neutron excitation cross sections of ^{240}Pu. The crosses indicate the experimental values. The solid curve is derived from optical-statistical model calculations. Fluctuation corrections have been applied to calculated excitations of the first state.

3. Energy Dependent Ratio of the Fission Cross Sections of ^{235}U to ^{238}U*

Two independent measurements of this quantity are in progress. The techniques and the experimental personnel are different in order to provide independent checks of the measured values.

---

*(Pertinent to request #409, WASH-1144)

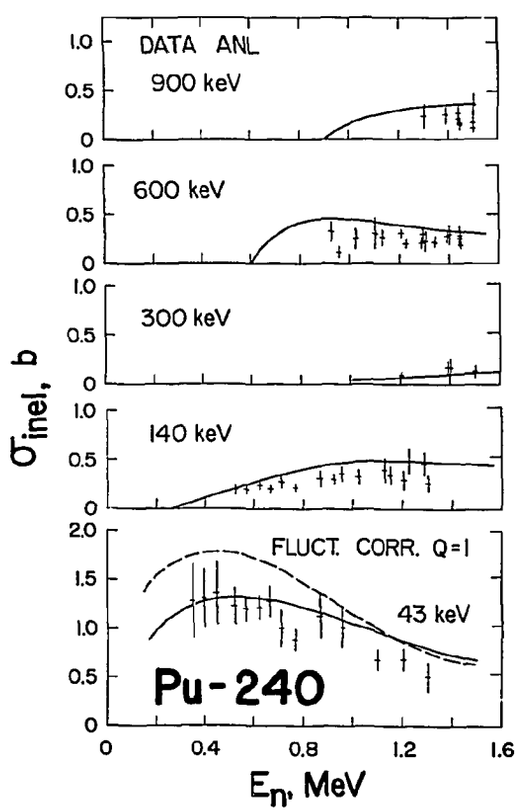

Fig. A-1

a. Program No. 1 (J. W. Meadows)

Measurements of the U-238/U-235 Fission cross section ratio to 5.2 MeV have been completed. The data are being processed and will soon be available in their final form.

b. Program No. 2 (W. P. Poenitz)

Some doubt has been cast on the procedure applied in the cross section evaluation[1] wherein the data measured by Lamphere[2] is multiplied by a factor of 0.94 as discussed previously.[3] However, preliminary results by Meadows,[4] above, indicate a deviation not only of the amplitude but also in shape from the highly accurate measurements by Stein et al.[5] Therefore, measurements have been carried out in the range from 2.0 to 5.0 MeV as well as at 2.5 MeV in order to determine the shape and the height of the plateau value of σ_f(U-238)/σ_f(U-235) ratio.

The present measurements have been carried out with a back-to-back gas scintillator fission counter. The time-of-flight method has been used for background suppression. Low mass arrangements have been used in order to reduce the corrections necessary for effects due to scattered lower energy neutrons. 25 $\mu gr/cm^2$ thick foils have been used in order to obtain a high efficiency and small corrections for total absorption of the fission fragments.

The present results support the difference in shape as observed by Meadows. They agree well with the original data by Lamphere;[2] however, a more accurate determination of the plateau

---

[1] W. G. Davey, Nucl. Sci. Eng., 32, 35 (1968).

[2] R. W. Lamphere, Phys. Rev. 104, 1654 (1956).

[3] W. P. Poenitz, Conf. on Nuclear Data for Reactors, Vol. II, CN-26/111, Helsinki 1970.

[4] J. W. Meadows, private communication, ANL, 1970.

[5] W. E. Stein et al., 2nd Conf. on Neutron Cross Sections and Technology, Vol. I, page 627, Washington 1968.

value is expected by an improvement of the mass assigment. Foils have been prepared for U-238 and U-235 material which had been spiked with U-234 in order to obtain very accurate mass ratios.

4. Measurement of the Fission Cross Section Ratio of Pu-239 and U-235 (W. P. Poenitz)

The ratio of σ_f(Pu-239)/σ_f(U-235) is rather well established in the energy range 200—1000 keV; however, major discrepancies exist at lower and higher energies. The data by Allen and Ferguson[1] and White et al.[2] diverge below 100 keV resulting in a difference of about 15 percent at 40 keV. Above 1 MeV the new data by Savin et al.[3] show strong fluctuations of the ratio not present in older data by Smirenkin et al.[4] and Netter.[5] In the present experiments, measurements have been carried out at 30 keV and in the range from 900—1500 keV. The experimental procedure has been described previously.[6] The σ_f(Pu-239)/σ_f(U-235) result at 30 keV is 0.79 ± 0.02, thus good agreement has been obtained with the data by Allen and Ferguson[1] and the more recent measurements by Szabo et al.[7] The present value is higher than that indicated by the data of Pfletschinger and Kaeppeler[8] though the difference is not outside combined errors. The present results closely follow those of Netter[5] and show no strong fluctuations of the nature reported by Savin et al.[3]

---

[1] W. D. Allen and A. T. G. Ferguson, Proc. Phys. Soc., London A70, 573 (1957).

[2] P. H. White et al., Proc. of Symposium on Fission Physics, IAEA, Vol. I, 219 (1965).

[3] M. V. Savin et al., INDC(CCP)-81U, 16 (1970).

[4] G. N. Smirenkin et al., Atomnaya Energiya 13, 336 (1962).

[5] F. Netter, CEA 1913 (1961).

[6] W. P. Poenitz, Nucl. Sci. Eng., 40, 383 (1970).

[7] I. Szabo et al., 3rd Conf. on Neutron Cross Section and Technology, Knoxville (1971).

[8] E. Pfletschinger and F. Kaeppeler, Nucl. Sci. Eng., 40, 374. (1970).

5. Prompt-Fission Neutron Spectra of ^{235}U and ^{239}Pu (A. Smith)

The prompt-fission-neutron spectra of ^{235}U and ^{239}Pu were experimentally studied using fast time-of-flight techniques. The ratio of the average-prompt-fission-neutron energy of ^{239}Pu to that of ^{235}U, deduced from measurements to 8.0 MeV, was $1.075 \pm \leq 2.0\%$. The ^{235}U spectrum, measured to 1.6 MeV, was consistent with a Maxwellian distribution having the "accepted" temperature of ~ 1.3 MeV. The ratio of the average prompt-fission-neutron energy of ^{239}Pu to that of ^{235}U deduced from the present work is in good agreement with values obtained from a number of other microscopic experiments, particularly those of Barnard et al. The present ratio is not consistent with some reported macroscopic results nor with the expression

$$E = 0.75 + 0.65\ \bar{\nu} + 1$$

deduced by Terrell from kinetic and equation-of-state considerations and comparisons with experiment. The equation leads to $d\bar{E}/d\bar{\nu}$ values approximately half those implied by the ratio resulting from the present experiments. The prompt-fission-neutron spectrum of ^{235}U to 1.6 MeV, is very similar to that obtained by Barnard et al. and from a number of other microscopic studies. The present results are not in reasonable agreement with spectra implied from fission-averaged-cross section measurements.

6. Neutron Flux Measurement with a Ge(Li) Detector (D. L. Smith)

Preliminary measurements indicate that Ge(Li) detectors offer promise for use as monitors of fast-neutron flux for $E_n > 1$ MeV. The detection mechanism is based upon excitation of the 694-keV 0^+ first excited state of ^{72}Ge (27.4% abundant in natural germanium) by neutron inelastic scattering. Gamma-ray de-excitation to the 0^+ ground state of ^{72}Ge is forbidden, however, internal conversion electrons are emitted which are detected with nearly 100% efficiency within the active region of the germanium diode. Among the desirable features observed for this detector are: i) insensitivity of low-energy background (detector threshold is $E_n = 694$ keV), ii) stability (detector efficiency not very sensitive to bias voltage), iii) good efficiency, and iv) the detected events appear in a single isolated peak

of the detector pulse-height spectrum. The energy dependence of the relative efficiency of this detector is currently under investigation.

7. A Study of the $^{48}Ca(p,n)^{48}Sc$ Reaction (A. J. Elwyn, F. T. Kuchnir, J. E. Monahan, F. P. Mooring, J. Lemming,* and W. G. Stoppenhagen**)

The reaction $^{48}Ca(p,n)^{48}Sc$ reaction has been studied at proton energies corresponding to the excitation of the $\frac{3}{2}^-$ ^{49}Ca ground state analog resonance in ^{49}Sc. The angular distributions of neutrons associated with final ^{48}Sc states at 0.131 (5^+), 0.252 (4^+), 0.624 (3^+), and 1.144 (2^+) MeV were measured at six angles in 4-keV steps from E_p = 1.95 to 1.99 MeV by time-of-flight techniques, with ^{48}Ca targets that were about 7 keV thick to 2 MeV protons. The results of these measurements are shown in Figs. A-2 and A-3 as the coefficients B_L in a Legendre polynomial expansion of the measured cross sections to each of the final ^{48}Sc states.

In a (p, n) reaction through a compound nucleus analog state the neutron decay proceeds primarily through those $T_<$ states that have the same spin and parity as the analog, namely $\frac{3}{2}^-$ in this case. However, the non-zero values of the coefficients B_1 and B_3, particularly in the excitation of the final states at 0.131, 0.252, and 0.624 MeV imply interference between such negative parity states in ^{49}Sc with those having positive parities (probably $\frac{3}{2}^+$ and $\frac{5}{2}^+$).

On the basis of previous experiments associated with this reaction[1] the $\frac{3}{2}^-$ analog state appears to be spread over several (about 8) $T_<$ -^{49}Sc states of the same spin and parity. In the present experiment, however, because of energy resolution, only two such components are seen—at approximately 1.965 and 1.975 MeV. Preliminary analysis of the present results based on the formalism of Mello[2] indicates that it is only the first of these $T_<$ -components (at 1.965 MeV) that contributes appreciably to the excitation of the four ^{48}Sc

---

*Also at Ohio University, Athens, Ohio.

**Ohio University, Lancaster, Ohio.

[1]See for example, P. Wilhjelm et al. Phys. Rev. 177, 1553 (1969).

[2]P. A. Mello, Annals of Physics (N. Y.) 45, 240 (1967).

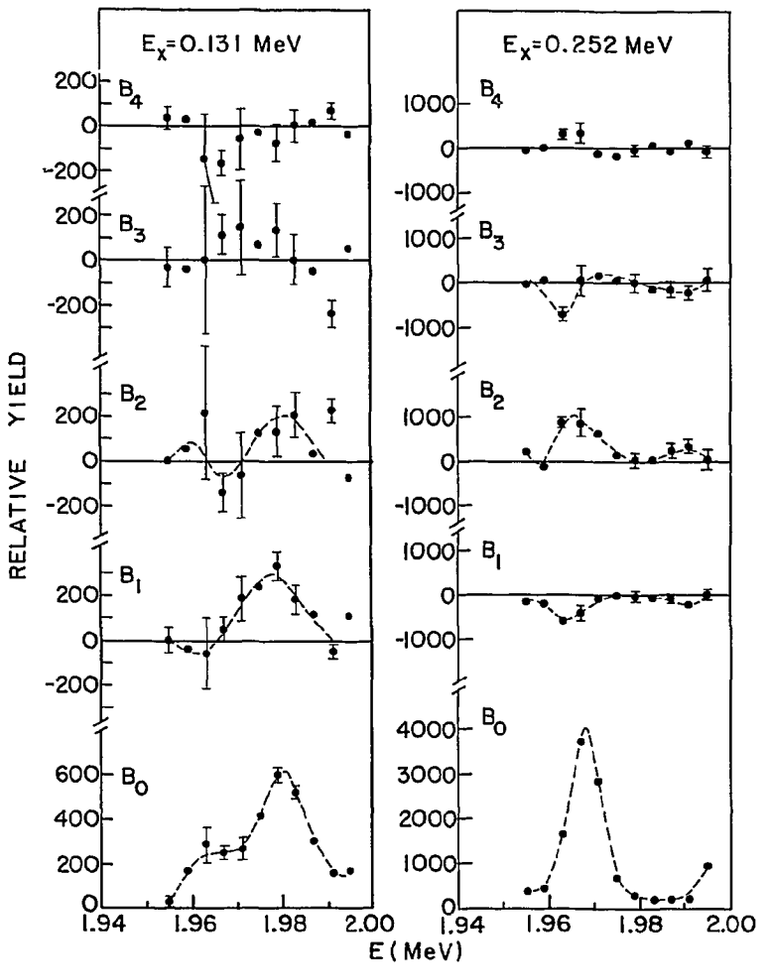

Fig. A-2

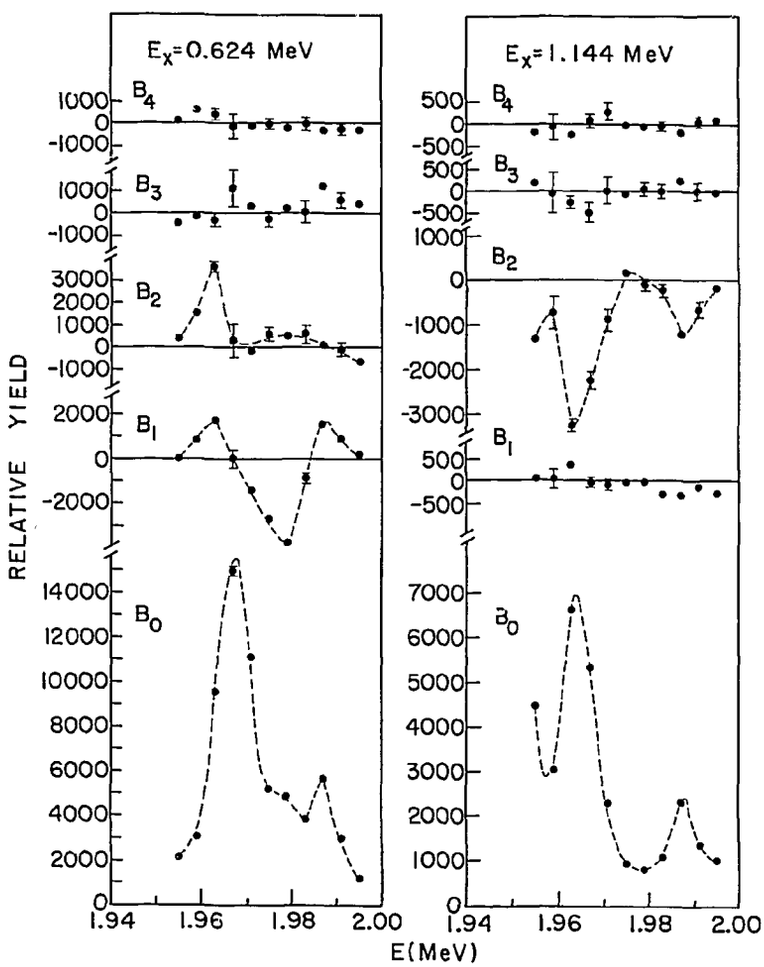

Fig. A-3

final states observed. Apparently the $T_<$-state at 1.975 MeV decays by neutrons predominantly to a negative parity state at about 1.4 MeV in ^{48}Sc. Further analysis is in progress to verify these preliminary conclusions. It is hoped that such an analysis might contribute to an understanding of the structure of the $T_<$-states that mix with the analog.

8. Polarization of Neutrons in (p, n) Reactions (A. J. Elwyn, F. T. Kuchnir, J. E. Monahan, F. P. Mooring, J. Lemming,* R. Finlay,** E. Sexton,† and R. Benenson†)

We are developing experimental techniques to measure the polarization of neutrons produced in charged-particle induced reactions. The method involves the measurement of the asymmetry in the scattering of neutrons by helium contained at high pressure in a gas scintillator. The recoils are detected in fast coincidence with scattered neutrons counted by two stilbene crystals placed at equal angles on either side of the beam incident on the helium cell. In our first measurements we have determined the neutron polarization in the $^{51}V(p, n)^{51}Cr$ ground state reaction at four angles for a value of proton energy (2.33 MeV) that corresponds to the excitation of an analog state in ^{52}Cr. Preliminary results indicate small values of the polarization (i.e. $\lesssim 10\%$) at all angles. In the neutron decay of an analog state the polarization is expected to be zero if statistical assumptions govern the distribution of the $T_<$ states. To the extent that the polarization is significantly non-zero, such a model breaks down. This technique might allow the determination of any background contribution to the (p, n) analog process. Further study of this and similar reactions on other targets is planned.

9. Facilities (Applied Physics Division)

A program to upgrade the pulsed source intensity of the Fast Neutron Generator has been implemented. Conservatively,

---

[3] G. Chilosi et al., Phys. Rev. Letters 20, 159 (1968).

*Also at Ohio University, Athens, Ohio.

**Ohio University, Athens, Ohio.

†SUNY, Albany, New York.

order of magnitude increases in peak pulsed intensity are expected to the 20—40 milliampere range. Such intensity will make a significant contribution to the studies of fast neutron cross sections.

10. Facilities (Physics Division)

During the past year a pulsed ion source (purchased from ORTEC) was installed in the terminal of the 4-MV Dynamitron. This beam-pulsing system consists of a duoplasmatron ion source followed by a beam pulser and a beam buncher. In typical operation proton beam pulses (without bunching) as short as 14 ns FWHM and with peak currents up to 800 μA have been readily accelerated. When these pulses are bunched they shorten to 1.3—1.5 ns FWHM with peak currents of 2—3 mA. The shortest pulses produced to date were 1.0 ns FWHM with a peak current of 1.6 mA. This source has been utilized in time-of-flight studies of some (p, n) reactions. For example, we are studying the ^{65}Cu(p, n)^{65}Zn reaction at incident proton energies that correspond to the excitation of various ^{66}Cu analog states in ^{66}Zn. In these preliminary experiments we have successfully separated those neutron groups corresponding to the excitation of the ground and seven excited states in ^{65}Zn. With flight paths of 2 meters we have resolved two neutron groups that differ in energy by 50 keV at a neutron energy near 1.2 MeV. Further study of this and other (p, n) reactions are planned. With the addition of a post-acceleration pulsing system (presently in the planning state) we expect to utilize the pulsed beam facility to study the properties of short-lived spontaneously fissioning isomeric states formed in neutron induced reactions.

B. CHARGED PARTICLE PHYSICS

1. (d, p) and (d, t) Studies of the Actinide Elements, ^{243}Cm, ^{245}Cm, ^{247}Cm, ^{249}Cm (T. H. Braid, R. R. Chasman, J. R. Erskine, and A. M. Friedman)

As part of a continuing study of the actinide nuclei, properties of states in ^{243}Cm, ^{245}Cm, ^{247}Cm, and ^{249}Cm have been determined by (d, p) and (d, t) reactions on targets of ^{244}Cm, ^{246}Cm, and ^{248}Cm. Excitation energies, differential cross sections, orbital assignments with confidence levels and ground-state Q values have been measured. Assignments of one-quasiparticle states have been made, and single-particle level schemes extracted from the data by

use of a pairing calculation. The extracted single-particle level schemes are compared with single-particle calculations, which include β_4 and β_6 deformations. Equilibrium values of β_2, β_4 and β_6 are estimated for the odd-mass Cm isotopes. A report of this work has been submitted for publication in the Physical Review.

2. Energy Levels in Cl^{34} from the $S^{33}(He^3, d)Cl^{34}$ Reaction (J. R. Erskine, D. J. Crozier, J. P. Schiffer, and W. P. Alford)

The energy levels of Cl^{34} have been studied with the $S^{33}(He^3, d)Cl^{34}$ reaction induced by the 14-MeV He^3 beam of the Argonne tandem Van de Graaff accelerator. An Enge split-pole magnetic spectrograph was used to record the deuteron spectra at scattering angles of 10—65° in 5° steps. An overall energy resolution width of 17 keV was achieved. Twenty-six levels up to an excitation energy of 4.6 MeV were observed and their spectroscopic factors were extracted. The results, when combined with previously known spin information, enable us to locate the major components of $(d_{3/2})^2$ and $(d_{3/2})(f_{7/2})$ configurations. The two-body matrix elements obtained here are compared with other two-body data in nearby nuclei and with calculated matrix elements.

C. PHOTONUCLEAR PHYSICS

1. Threshold Photoneutron Spectra for ^{53}Cr, ^{57}Fe, and Ni^{61} (H. E. Jackson and E. N. Strait)

The photoneutron cross sections for ^{53}Cr, ^{57}Fe, and ^{61}Ni have been measured near threshold with high resolution. Spins of resonances were assigned on the basis of angular distributions determined from the spectra for neutron emission at angles of 90° and 135°; the ground-state radiation widths $\Gamma_{\gamma 0}$ for most resonances were determined from the observed yields. Parity assignments were based on a comparison of data with total neutron cross sections of the daughter nuclei. The central feature of the results is an intense p-wave component whose integrated strength for all targets is greater than that of the s-wave component. In addition, an anomalous concentration of M1 strength is observed in an intense doublet with $J^\pi = \frac{3}{2}^-$ at $E_n = 230$ keV in the cross section for ^{57}Fe. The reduced widths for E1 and M1 radiation are consistent with the values $\bar{k}_{E1} = 0.0012$ and $\bar{k}_{M1} = 0.019$,

respectively. No evidence is found for the existence of doorway states proposed in reported measurements of the reactions $^{53}Cr(\gamma, n)$ and $^{57}Fe(\gamma, n)$ near threshold. The data were also tested for a correlation between the reduced neutron width for s-wave resonances in each target and the corresponding ground state radiation widths. In no case is there evidence for a significant correlation. Therefore the strong correlation reported between the reduced neutron widths and total radiation widths for s-wave resonances in even-even target nuclei in this mass region should not be attributed to the ground-state transition.

2. Study of Resonances in the Reactions $^{117}Sn(\gamma, n)^{116}Sn$ and $^{119}Sn(\gamma, n)^{118}Sn$ at Threshold (E. N. Strait and H. E. Jackson)

The threshold photoneutron spectra from enriched targets of ^{117}Sn and ^{119}Sn are currently under study at the ANL high intensity linac. Time-of-flight spectra have been observed for photoneutrons emitted at 90° and 135° to the incident photon beam. Data evaluation is in progress. Preliminary analysis suggests the presence of a dominant p-wave component excited by electric dipole absorption in the resonance structure.

3. Photofission of the Pu Isotopes in the "Subthreshold" Region (W. F. Stubbins* and H. E. Jackson)

Exploratory measurements of Pu isotope photofission yields for bremsstrahlung with end-point energies in the range 4.5—7.0 MeV are in progress. The objective is to determine the shape of the photofission cross sections in this low-energy region, and develop a capability for more extensive measurements of photofission. In initial studies of $^{239}Pu(\gamma, f)$ fission neutrons were detected by time of flight. The resulting data give information on both the shape of the fission yield curve, the energy spectrum of the fission neutrons, and angular distributions of fission neutrons relative to the photon beam.

---

*University of Cincinnati.

D. REACTOR NEUTRON PHYSICS

1. Excited States of ^{239}U from $^{238}U(n, \gamma)^{239}U$ (L. M. Bollinger and G. E. Thomas)

The excited states of ^{239}U have been studied by measuring both thermal-neutron-capture spectra and average-resonance-capture spectra. In these investigations, an effort was made to advance the technique of measuring thermal-capture spectra. Hence, results of exceptional statistical accuracy, signal-to-background ratio, energy resolution, and energy precision were obtained for a sample that contains only 6 ppm of impurities. A part of such a spectrum is given in Fig. D-1. The γ-ray lines from transitions in ^{239}U were positively identified by comparing the spectrum for the 6 ppm sample with a spectrum for a less pure sample. The parities of the final states observed in the thermal-capture spectra were determined from the intensities in the average-resonance capture spectrum. The results obtained for the states at excitation energies $E_x < 1000$ keV are given in Table D-I. Here the spins and parities given in the second column are those inferred from the observed intensities and those given in the last column are suggested assignments inferred from the previous work of Sheline et al. and from the rotational-band structure observed for the curium isotopes in recent experiments at the Argonne tandem (Braid et al.). This set of states is believed to be complete for $E_x \leq 890$ and $1 < J < 6$.

2. Excited States of ^{182}Ta (J. R. Erskine, L. M. Bollinger, and G. E. Thomas)

Both the (n, γ) and (d, p) reactions have been used in a study of excited states of ^{182}Ta. The (d, p) measurements were made with the new split-pole spectrograph at the FN tandem, and the nuclear emulsions exposed in the measurement were scanned by the computer-controlled automatic plate reader. In the (n, γ) study, both thermal-capture spectra and average-resonance-capture spectra were measured. In general terms, for the excitation energies < 800 keV, the (n, γ) data locate all states with spins $J = 2$, 3, 4, and 5, determine the parities, and set limits on the spins, whereas the (d, p) data detect states with $2 > J > 5$ and provide information about nuclear configurations for many of the states. The combined data give an exceptionally complete description of the level scheme of

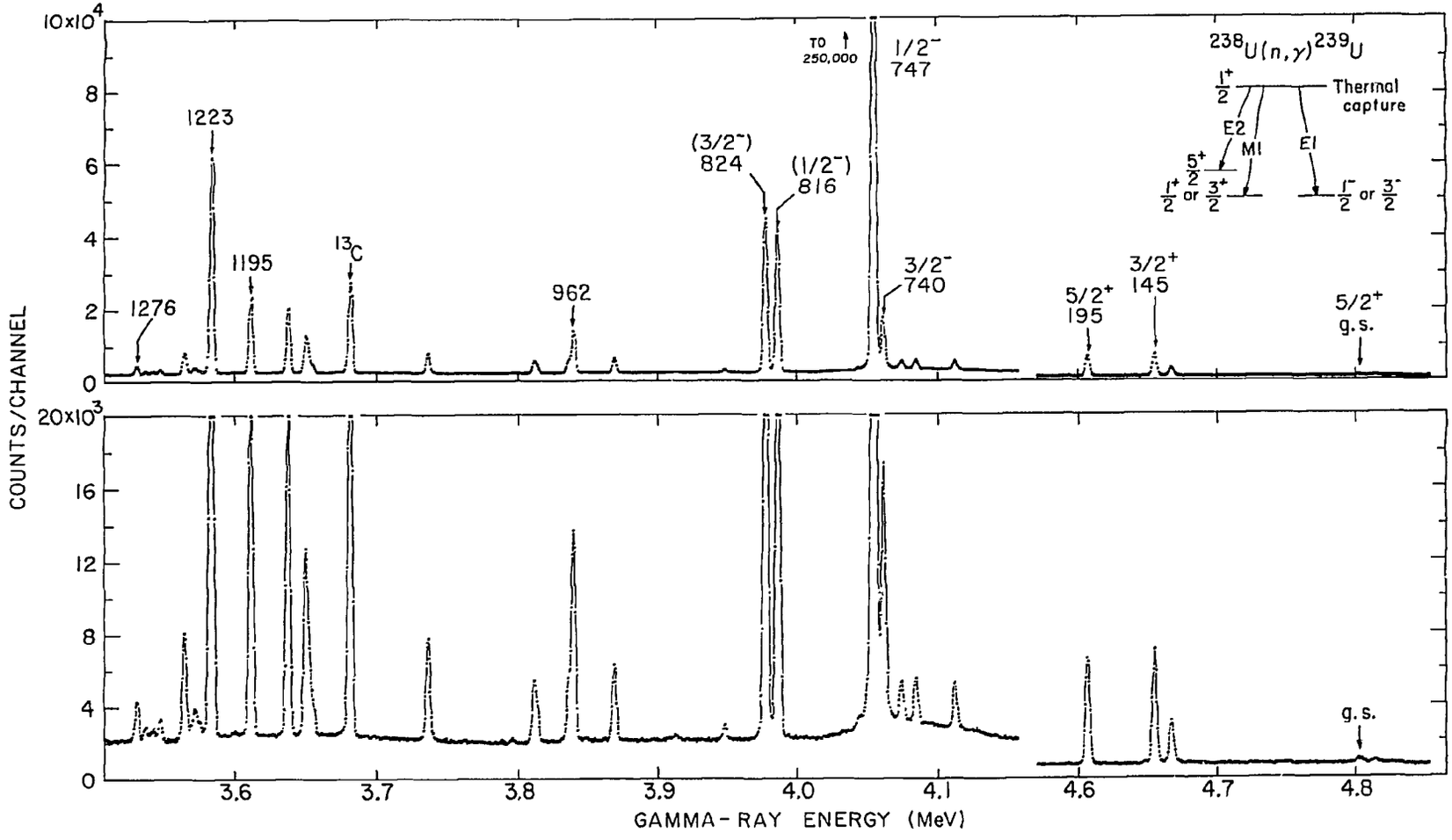

Fig. D-1

Table D-1. States of ^{239}U observed in $^{238}U(n, \gamma)^{239}U$.

E_x keV	J^π From Intensity	J^π From Band
0	$\frac{5}{2}^+$	$\frac{5}{2}^+$
134	$\frac{1}{2}, \frac{3}{2}^+$	$\frac{1}{2}^+$
145	$\frac{1}{2}, \frac{3}{2}^+$	$\frac{3}{2}^+$
195	$\frac{5}{2}^+$	$\frac{5}{2}^+$
688	$\frac{1}{2}, \frac{3}{2}^+$	$\frac{1}{2}^+$
716	$\frac{1}{2}, \frac{3}{2}^+$	$\frac{3}{2}^+$
727	$\frac{1}{2}, \frac{3}{2}^+$	$\frac{3}{2}^+$
735	$\frac{1}{2}, \frac{3}{2}, \frac{5}{2}^+$	$\frac{5}{2}^+$
740	$\frac{1}{2}, \frac{3}{2}^-$	$\frac{3}{2}^-$
747	$\frac{1}{2}, \frac{3}{2}^-$	$\frac{1}{2}^-$
757	$\frac{5}{2}^+$	$\frac{5}{2}^+$
816	$\frac{1}{2}, \frac{3}{2}^-$	$\frac{1}{2}^-$
824	$\frac{1}{2}, \frac{3}{2}^-$	$\frac{3}{2}^-$
853	$\frac{1}{2}, \frac{3}{2}^+$	$\frac{3}{2}^+$
890	$\frac{5}{2}^+$	$\frac{5}{2}^+$
933	$\frac{1}{2}, \frac{3}{2}^-$	
962	$\frac{1}{2}, \frac{3}{2}^-$	
966	$\frac{1}{2}, \frac{3}{2}^+$	
987	$\frac{1}{2}, \frac{3}{2}, \frac{5}{2}^+$	
991	$\frac{1}{2}, \frac{3}{2}$	

^{182}Ta. In most respects the results are in good agreement with those reported recently by Helmer et al., but are somewhat more extensive. The results are also in excellent agreement with the collective model of odd-odd nuclei. An effort to understand the states with excitation energies > 700 keV is still in progress.

3. Distribution of Intensities of Thermal-Neutron-Capture γ Rays (L. M. Bollinger)

In a short paper accepted for publication, the distribution of intensities of thermal-neutron-capture γ-rays is discussed within the framework of the statistical model. It is shown that, if initial states of only one spin and parity are involved, the γ-ray intensities for most nuclides approximately satisfy the Porter-Thomas distribution, independent of how many resonances contribute to the thermal-neutron-capture cross section.

4. Level Scheme of Hf^{180} (D. L. Bushnell*, R. K. Smither and D. J. Buss)

Thermal neutron-capture gamma-ray data from the reaction ^{179}Hf(n, γ)^{180}Hf have been combined with average resonance neutron-capture gamma-ray data for the same reaction to obtain energies, spins, and parities of states in ^{180}Hf. 25 levels have been found in the energy range 0–2.3 MeV and 20 spin and parity assignments have been made. An attempt is in progress to interpret the levels between 1 and 2 MeV as positive- and negative-parity rotational bands. The neutron binding energy for ^{180}Hf was found to be 7387.5 ± 0.5 keV.

5. Energy Levels in the Odd-A Sm Isotopes (R. K. Smither, D. J. Buss, and D. L. Bushnell*)

The level schemes of the odd Sm isotopes (145, 149, 151, 153, and 155) have been constructed by using the results of the "neutron average capture" technique in combination with the data from thermal (n, γ) experiments which make use of Ge(Li) detectors and the Argonne bent-crystal spectrometer. The ground-state J^π values are: ^{145}Sm, $\frac{7}{2}^-$; ^{149}Sm, $\frac{7}{2}^-$; ^{151}Sm, $\frac{3}{2}^-$; ^{153}Sm, $\frac{3}{2}^+$; and ^{155}Sm, $\frac{3}{2}^-$. This removes the uncertainty with regards to the ^{151}Sm

*Northern Illinois University.

and ^{153}Sm isotopes. Of special interest is a new first excited state for ^{155}Sm at 6.6 keV with $J^{\pi} = \frac{1}{2}^-$ or $\frac{3}{2}^-$. Also, the negative-parity states appear to follow a consistent pattern from isotope to isotope. The neutron binding energies are found to be 6762.7, 5872.5, 5591.7, 5869.1, and 5814.2 keV for the isotopes of mass 145, 149, 151, 153, and 155, respectively.

BROOKHAVEN NATIONAL LABORATORY

A. NEUTRON PHYSICS

1. Fast Chopper (R. E. Chrien, O. A. Wasson, G. W. Cole, R. G. Graves,* S. F. Mughabghab,** M. R. Bhat**

a) Instrumental Developments

An expansion of the ferrite core memory of the SDS-910 from 12K to 16K has been accomplished. Furthermore, time-sharing of the chopper SDS-910 has ceased since the recent (January 1971) termination of the slow chopper program at BNL. Accordingly the entire core storage of the 910 is now devoted to fast chopper programs and data. As a result a revision of the data accumulation programs is underway so that dead-time per event is reduced from 600 to 150 μsec and a wider variety of displays is available.

Recent experiments undertaken at high instantaneous counting rates (20,000 cps) show that a high proportion of events - up to 40% - can be shifted from the 2-escape peak to the continuum without appreciably increasing the FWHM of the 2-escape peak. In some time-of-flight experiments these instantaneous rates are reached, and a systematic error in γ-ray intensities may be introduced. A pile-up rejection circuit is being designed by V. Radeka, of the BNL instrumentation division, to eliminate this effect, and preliminary tests indicate that these errors can be made negligibly small.

b) Experimental

1) Evidence for valence neutron transitions in Mo isotopes. The decay of the compound nucleus by γ-ray emission is usually thought of in statistical terms. If the final state is of an especially simple form - e.g. that of a single particle excitation - the overlap integral in the matrix element selects a simple component of the complex initial state. The simplest such component is the single particle component, and the radiative strength is given by the following expression, taken from Lynn,[1,2]

---

* State University of New York, Stony Brook.

** Department of Applied Science, BNL.

[1] J. E. Lynn, "Theory of Neutron Resonance Reactions," Clarendon Press, Oxford 1968, p. 330

[2] There is, unfortunately, an error in Lynn's expression which can be traced to an error in A. R. Edmonds' "Angular Momentum in Quantum Mechanics", Princeton U. Press 1957. The above expression has been corrected.

$$\Gamma_{\lambda\mu} = \frac{16\pi}{9} k^3 \theta_\lambda^2 \theta_\mu^2 \left| \bar{e} \int_o^\infty \mu_\lambda \, r u_\mu \, dr \right|^2$$

$$\times \left(\frac{3}{4\pi}\right) (2J_\mu+1)(2j'+1)(2j''+1)(2\ell'+1) \; W^2(j' J_\lambda j'' J_\mu; I1)$$

$$\times W^2(\ell' j' \ell'' j''; \tfrac{1}{2} 1) C^2_{\ell' 1}(\ell'' 0; 00)$$

which describes an E-1 transition from a state $\{J_\lambda, j, \ell'\}$ with a dimensionless reduced width θ_λ^2 to the final state with $\{J_\mu, j'', \ell''\}$ and θ_μ^2.

A quantitative test of this "valence neutron" transition theory has been made to the P-wave resonance of Mo-92 and Mo-98. As shown in Fig.A-1, the measured and expected widths are in good agreement for those resonances[3] and final states with large reduced widths $\theta_\mu^2, \theta_\lambda^2$. The success of the model depends, apparently, on the fact that both Mo-92 and Mo-98 have closed neutron shells, so the probability of exciting the target nucleus core is not high.

Similar calculations are being carried out for p-wave resonances in Zr-96 and in the tin isotopes. Furthermore, recent reports[4] of correlations, in S-wave resonances, between the radiation widths and neutron widths are being examined in light of the agreement for the S-wave cases. Preliminary indications are that only about 1/3 of the total radiation widths for nuclides near the 3S giant resonance can be accounted for by the simple model. (Requests 199, 201, 202, 203, 204, 223, 224 WASH 1144)

2) Resonant Neutron Capture in ^{111}Cd(n,γ)^{112}Cd. (In collaboration with R. Moreh of the Nuclear Research Center-Negev, Israel) A previous experiment using the Cd-112(γ,γ')Cd-112 reaction yielded a correlation between the γ ray transition rates from a negative parity level near 7.6 MeV excitation to low-lying positive parity final states and the (d,p) spectroscopic factors of the final states.[5] The results were extended to higher excitation energies near 9.3 MeV by using the Cd-111(n,γ)Cd-112 reaction at the Fast Chopper. For the 6 resolved S-wave resonances below 300 eV neutron energy, the 10 γ rays

[3] Allen and Macklin (private communication) have shown that there are several p-wave resonances near 5000 eV in Mo-92. The remarks and measurements apply here in an average sense to this group of resonances.

[4] R. C. Block, R. G. Steiglitz and R. W. Hockenbury, NCSAC-33, p. 202.

[5] R. Moreh, private communication.

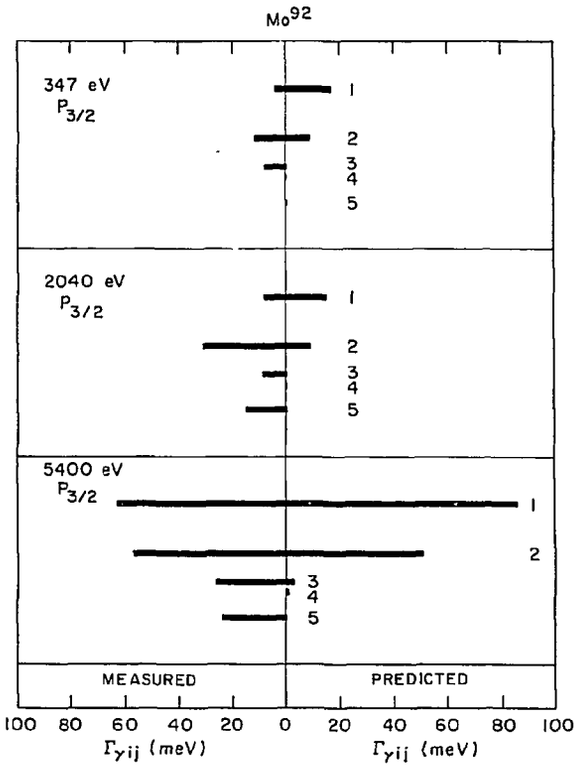

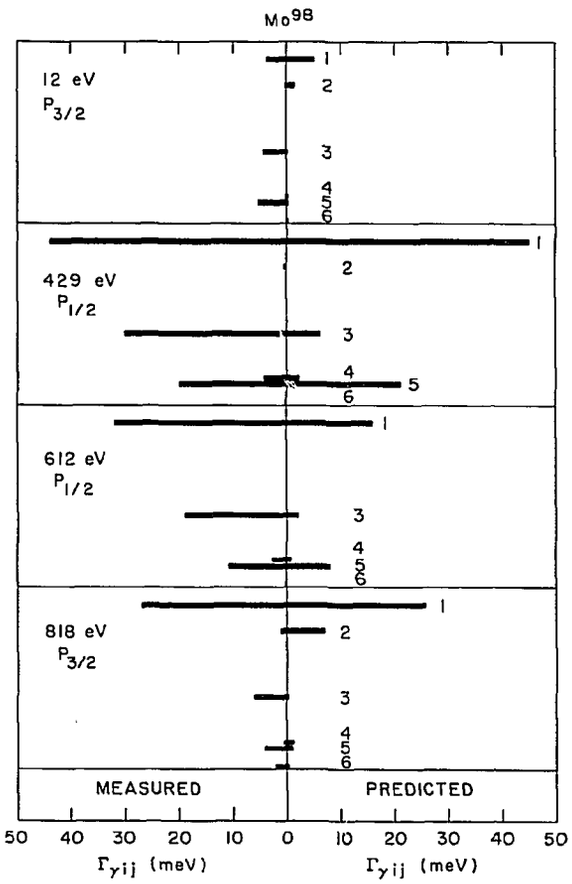

Figure A-1

with energies above 6.9 MeV have M1 multipolarity and their intensities show no correlation with the (d,p) spectroscopic factors. However, for the unresolved neutron region above 250 eV a significant correlation is observed. This confirms the (γ,γ') results and suggests that p-wave neutron capture is important for neutron energies between 250 eV and 1300 eV. There is also no evidence for a peak near 7.5 MeV in the M1 γ ray strength function.

3) Determination of the spins of neutron resonances of Er-167(n,γ)Er-168. Many previous experiments have demonstrated that the population of low-lying levels through multi-step cascades depends upon the spin of the initial state. The intensities of γ-rays depopulating these states are then a reliable indication of resonance spin. This technique has been applied to resonances in Er-167, and it is found that the γ-ray intensities of lives at 184.3 and 284.7 keV divide into two well-defined groups, as shown in Fig.A-2. The resonances at neutron energies of 5.98, 9.38, 26.1, 39.5, 42.3, 53.7, 62.3 (doublet), and 69.5 are assigned J=3, while the resonances at 7.9, 20.3, 27.4, 32.9, 37.7 and 50.3 have spins of J=4.* The high energy spectra for Er-167 in the neutron energy range to 100 eV have been recorded and are being analyzed. A comparison between the spin assignments based on high and low energy γ-rays will be made. (Request 295, WASH 1144)

4) Search for doorway states in the reaction Yb-173(n,γ)Yb-174. The recent discovery of correlations between radiative and neutron widths in Dy-163 has led to an attempt to map out systematically the occurrence of such effects in the region of the 4S giant resonance. The size as well as the detailed behavior of these correlations leads to the conclusion that they are probably due to doorway state components in the initial state wave functions. Based on the Dy-163 analysis the Yb-173(n,γ)Yb-174 would seem to be a plausible reaction to study for correlations because a) the average reduced neutron widths are large and b) the neutron binding energy is similar to that of Dy-163. As in the case of Dy-163, the target spin is $5/2^-$, leading to spins of 3 and 2. For the correlation analysis it is necessary to separate the resonances according to spin. This can be done reliably by combining high and low energy γ-ray spectral measurements.

A 230 gram sample of Yb_2O_3 was examined at both the 22 and 48-meter stations using 4cc and 20cc detectors. Spin 3 resonances are easily identified if the transitions to low-lying states of $J\pi = 4^+$ are observed. A state with $J\pi = 1^+$, tentatively assigned at $E_x = 1624.6$ keV by Greenwood,[6] can also be used to assign J = 2 resonances on a tentative

* The basis for the spin assignments to these groups lies in the previously established spin assignments for the 5.98 and 9.38 eV resonances, as indicated in BNL 325 2nd Edition, 2nd Supplement.

[6] R. C. Greenwood, C. W. Reich, J. J. H. Berlijn, Bull. Am. Phys. Soc. 15, 1668 (1970)

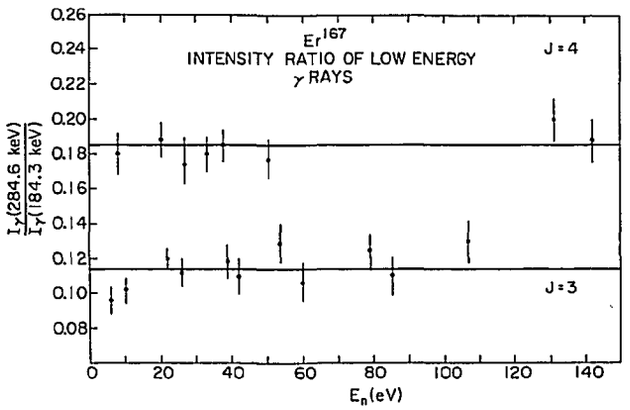

Figure A-2

basis. This 1^+ assignment is consistent with our observations.

The low energy γ-rays from the reaction Yb-173(n,γ)Yb-174 have been examined and found to fall into groups associated with initial state spin. A portion of the spectrum is shown in Fig.A-3 for 4 low lying resonances with J = 2 or 3. The pairs of γ-rays at (76.5, 176.6) keV and (272.9, 287.9) keV, assigned to transitions as in Fig. 3, show different ratios in the spin 2 and spin 3 resonances. These ratios can be plausibly understood in terms of the difference in population from the capturing state, where the population differences arise from the differences in angular momentum between the initial and final states in the cascade sequence. Based on the low energy ratios, we assign to 17.7, 31.3, 45.3, 69.1, 76.3, 106, and 111 eV resonances to J = 2, and the 4.5, 35.8, 53.6, 58.9, 66.3, 74.6, and 96.5 eV resonances to J = 3.

The correlation analysis shows a negligible correlation between reduced neutron width and partial radiative widths for J = 3 resonances. For J = 2 resonances, a correlation coefficient of 0.43 is obtained, at a significance level of 99.8%. This is a preliminary analysis, based on only 4 J = 2 resonances and 11 final states. The correlation arises principally because of the presence of strong transitions to the γ-vibrational band. The histogram of Fig. A-4 shows a Monte Carlo calculation for the significance of the correlation in Yb-173.

5) Resonant Neutron Capture in Yb-171(n,γ)Yb-172. The γ-ray spectra from a sample of 260 grams of 90.6% Yb-171 has been examined for comparison to the Yb-173 experiment. Neutron resonances from 7.5 eV to 130 eV were studied in the γ-ray energy regions of 70-1000 keV and 3 to 8 MeV. A resolution of 6.5 keV (FWHM) was achieved for the summed runs. Both high and low energy transitions were measured to form spin assignments for the resonances. Two typical spectra are shown in Fig.A-5,for the two possible spin states 0^- and 1^-.

In contrast to the Yb-173 case, the resonances in Yb-171 have a smaller average neutron width. There is an approximately 0.5 MeV difference in the neutron binding energy between Yb-172 and Yb-174. The correlations observed for Yb-173 are not seen in the Yb-171 spectra, which seem to show a statistical character. The assigned spins, based on the combination of high and low energy spectra, for resonances of Yb-171 are shown in Table I.

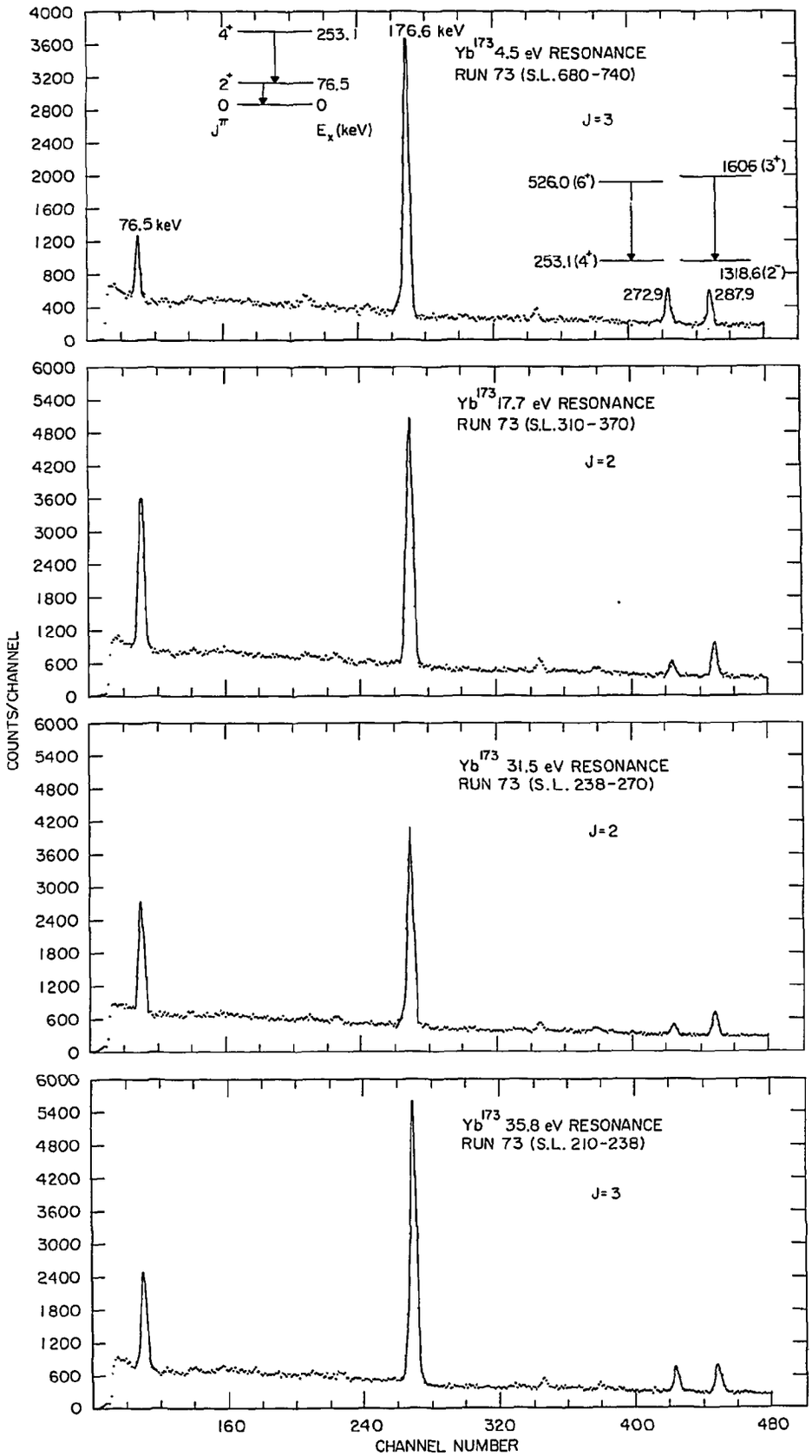

Figure A-3

DATA NOT FOR QUOTATION

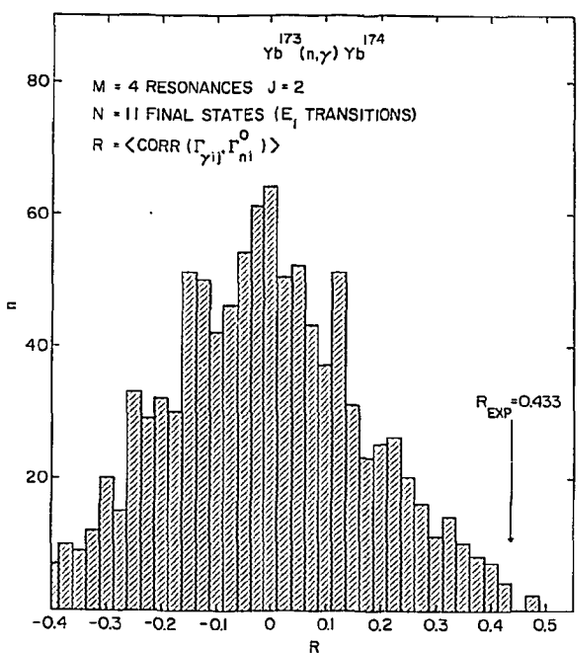

Figure A-4

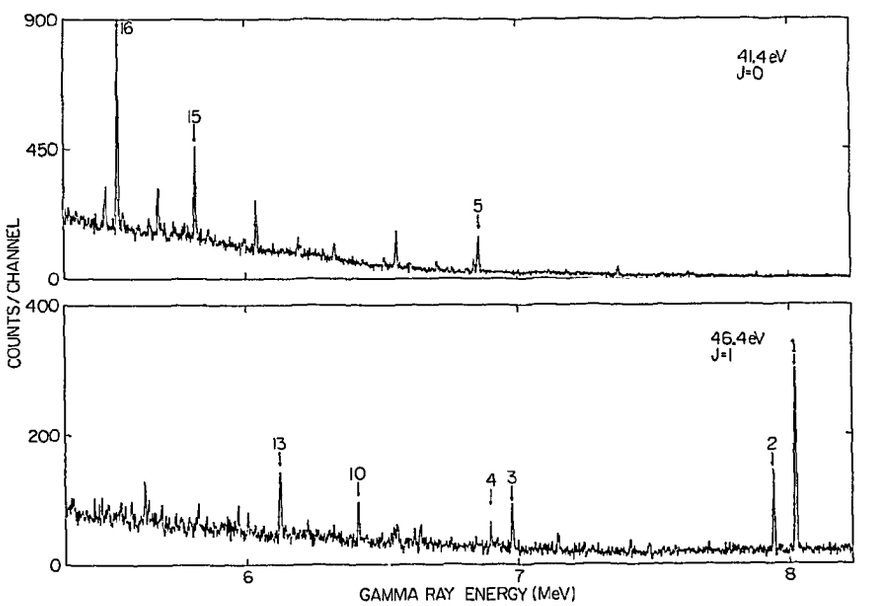

Figure A-5

Table I

Yb-171(n,γ) Spin Assignments

E_n(eV)	J^π	
7.93	(1^-)	unresolved
(8.1)	(0^-)	unresolved
13.1	0^-	
17.7	1^-	
21.8	1^-	
28.0	1^-	
34.5	1^-	
41.4	0^-	
46.4	1^-	
52.9	1^-	unresolved
54.2	0^-	unresolved
60.2	1^-	
64.8	1^-	
77.1	1^-	
81.8	1^-	unresolved
84.5	1^-	unresolved
95.3	0^-	
107.1	1^-	
111.9	1^-	
127.0	1^-	

6) Gamma rays following resonant neutron capture in U-235. The apparatus, described in previous NCSAC reports, for the detection of γ-rays in coincidence with neutron-induced fission events, has been used to study U-235 from thermal to about 50 eV neutron energy. Singles and coincidence spectra have been recorded for the γ-ray energy range from 570 to 1400 keV and from 4300-8300 keV. The coincidence resolving time in this experiment is about 140 ns. Table II lists the energies of the γ-rays found to be coincident with fission within the 140 ns resolving time. No corrections for possible background contamination due to fission neutron interactions with shielding material have been applied. No discrete peaks above 4300 keV are found in the prompt γ-ray spectrum, but the singles spectra show many peaks above 4300 keV which are associated with delayed γ-rays in the millisecond lifetime range. Figure A-6 shows a portion of the singles and coincident spectra in the low-γ-ray energy range. The data are being studied in a continuing attempt to assign fission and capture γ-rays in U-235. (Request #391, 392, 393, WASH 1144)

Table II

Low Energy "Prompt" Fission γ-Rays

Peak No.*	Energy, keV
	582.9 ± .0
	585.2 ± .1
	588.8 ± .3
	595.7 ± .0
	613.4 ± .5
	621.6 ± .1
1	631.5 ±1.5**
2	642.2 ± .7
3	706.9 ± .1
	774.9 ± .2
4	803.0 ± .1
5	815.3 ± .1
6	836.7 ± .1**
	868.4 ± .2
	912.7 ± .2**
	953.8 ± .3
	1013.8 ± .3
	1222.7 ± .2
	1278.8 ± .1

Peaks A (661.5 ± .0 keV) and B (765.8 ± .1 keV) are known not to be prompt fission γ-rays and indicate low accidental coincidence rate.

* Refers to Fig. 6

** Multiple peak

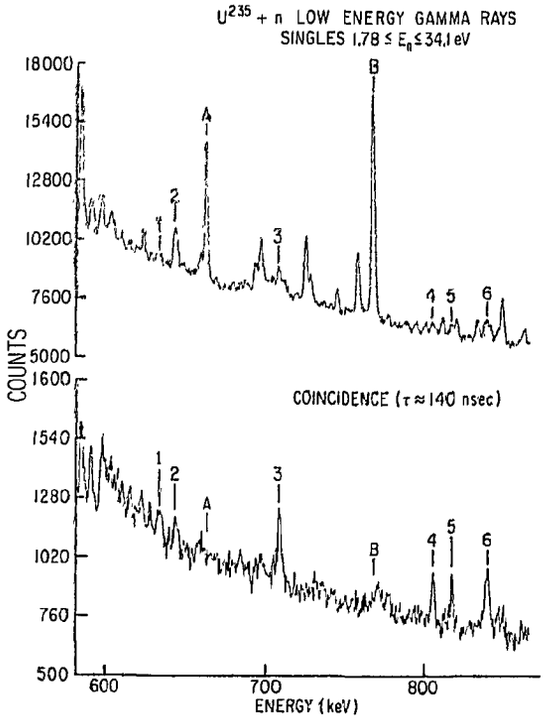

Figure A-6

2. Nuclear Cryogenics

a) Instrumental (G. Brunhart, D. C. Rorer, D. Potter)

An on-line computer system has been designed to utilize a surplus SDS 920 computer as controller and data acquisition unit for both neutron spectrometers at the H-1 beam of the HFBR. This system will greatly enhance the usefulness of the existing equipment. The construction of the necessary interfaces is in progress.

b) Experimental

1) Spin assignments of two weak resonances in Dy^{161} at 12.65 and 16.7 eV. (D. C. Rorer and G. Brunhart)

The total angular momentum, J, of the compound states corresponding to the weak resonances at 12.65 and 16.7 eV in Dy^{161} have been determined by measuring the transmission of polarized neutrons through polarized targets. While in general the spin assignments are made on the basis of the sign of the transmission effect in the case of unresolved resonances a comparison of the shape of the effect as a function of energy must be made with calculations. We have found our measurements to be consistent with the assignment $J = 3$ for both resonances.

2) Spin assignments of Sm^{149} neutron resonances by nuclear polarization. (G. Brunhart and D. C. Rorer)

Recent neutron resonance capture studies* of Sm^{149} have led to a disagreement with earlier spin assignments of the 6.48 eV neutron resonance.** We are preparing a Sm-Ho alloy target to do a polarization measurement in order to resolve the discrepancy. Due to the high vapor pressure of Sm special techniques have to be developed to produce the alloy. There is previous evidence that large nuclear polarizations of the otherwise antiferromagnetic samarium can be achieved in a Sm-Ho alloy.

* F. Becvar, Contributed paper at APS meeting, Houston, Oct. 1970.

** H. Marshak, H. Postma, V. L. Sailor, and C. A. Reynolds, Phys. Rev. 128, 1287 (1962)

3) Spin dependence of the U^{235} low-energy neutron cross section. (G. Brunhart and D. C. Rorer)

A target of anhydrous uranium lanthanum trichloride is being prepared for a polarization measurement. This effort is a

continuation of work begun at the BGRR several years ago.*

* R. I. Schermer, L. Passell, G. Brunhart, C. A. Reynolds, V. L. Sailor, and F. J. Shore, Phys. Rev. 167, 1121 (1968)

4) Magnetic moments of compound states corresponding to slow neutron cross section resonances. (G. Brunhart and D. C. Rorer)

A polarized neutron transmission method is used to determine the shift of the neutron resonance energies due to the hyperfine interaction of the compound states. The method has been tested successfully in the case of erbium.* Work is planned to continue with a series of rare earth elements and rare earth alloys.

* K. H. Beckurts and G. Brunhart, Phys. Rev. C1, 726 (1970)

B. NUCLEAR STRUCTURE

1) Gamma rays from resonance neutron capture in Np^{237}. (W. R. Kane)

Since Np^{237} is one of several nuclei which display clear evidence for subthreshold fission by slow neutrons, the gamma rays emitted after neutron capture in this nucleus are of considerable interest. It should be possible, through the study of these gamma rays, to establish enough features of the level structure of the product nucleus, Np^{238}, to measure, in turn, the spins of some of the low energy neutron resonances of Np^{237}. Furthermore, it would be of great interest to observe, if possible, transitions to or between the "Class II" states in the second minimum of the nuclear potential well.

At the crystal diffraction monochromator at the Brookhaven HFBR Ge(Li) gamma-ray spectra have been obtained for neutron capture in several resonances of Np^{237} with energies between 0.487 and 5.81 eV. A portion of the spectrum obtained for the 0.487 eV resonance is shown in Fig.B-1. While only a preliminary analysis of these results has been made, a number of these high energy gamma rays represent quite clearly transitions to levels of Np^{238} known from the alpha-decay of Am^{242}. The absolute values of the intensities of the high energy capture gamma rays on each resonance can be readily obtained by comparison with known decay gamma rays of Np^{238}. These results give a neutron separation energy of 5419 ± 3 keV for Np^{238}.

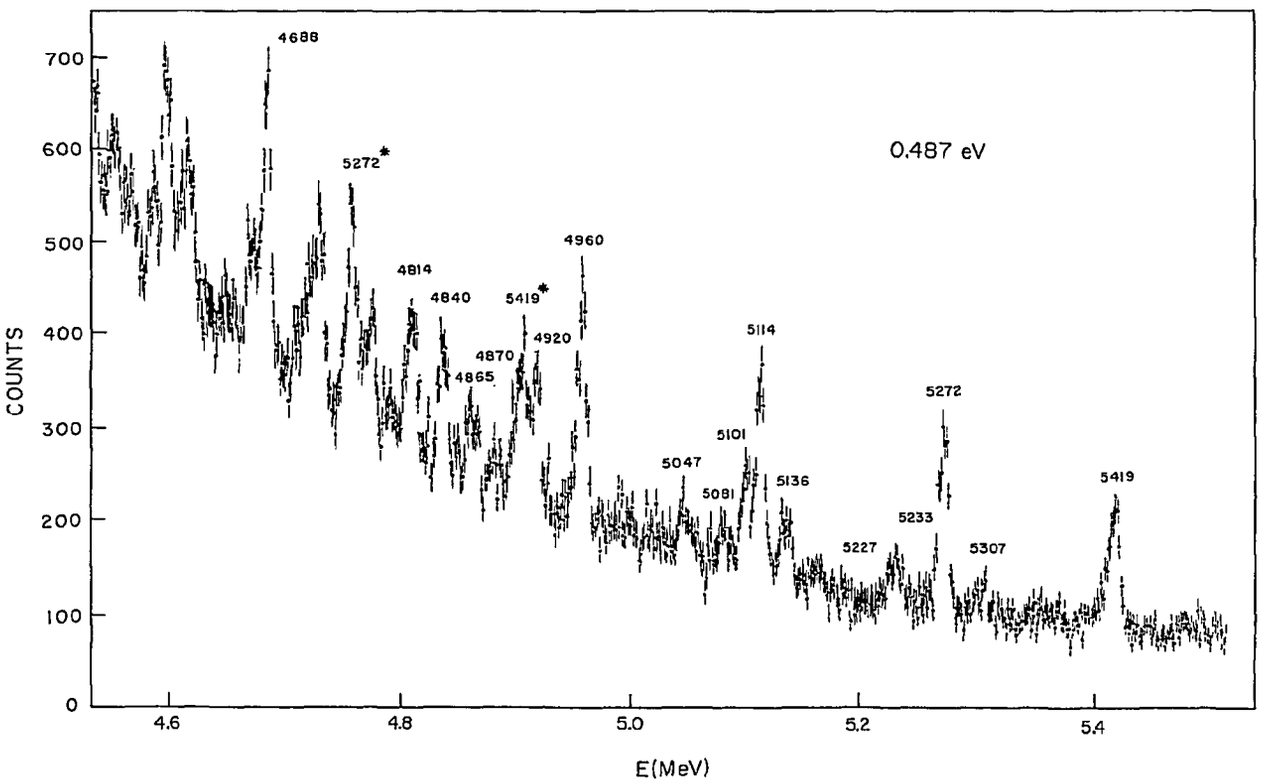

Figure B-1

2) Neutron capture in the 5.16 eV resonance of Xe^{124}.
(W. R. Kane, W. Gelletly, and D. R. Mackenzie)

In a continuation of work reported earlier (see status report to the NCSAC, Dec. 1970), the level structure of Xe^{125} has been investigated through studies of the gamma rays emitted after neutron capture in the 5.16 eV resonance of Xe^{124}. Xe^{125} is a particularly interesting nucleus since recent theoretical calculations have shown that nuclei in this region may not only have stable deformations, but that these deformations may be oblate, rather than prolate as in other known regions of deformation. Although Xe^{124} is only $\sim 0.1\%$ abundant in the normal Na_4XeO_6 target employed in this work, so that the target contains only ~ 2 mg of Xe^{124}, the sensitivity of the neutron monochromator is such that both Ge(Li) singles spectra and Ge-Ge coincidence results were obtained. In addition, further information was obtained on Xe^{125} from studies of the decay of 45 min. Cs^{125}. The latter activity was produced at the Brookhaven Tandem Van de Graaff accelerator via the $Cd^{113}(O^{16},4n)Ba^{125}$ reaction. Our present knowledge of the low-spin energy levels of Xe^{125} is summarized in the level scheme of Fig. B-2. While this information is as yet not complete enough to establish the existence of an oblate deformation in this nucleus, there are a number of features of the level scheme that are consistent with this hypothesis.

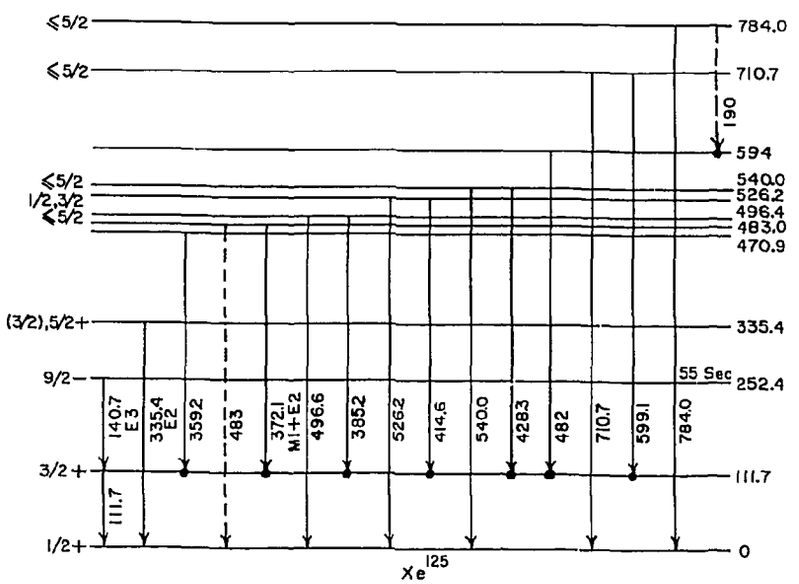

Figure B-2

COLUMBIA UNIVERSITY

I. NEUTRON SPECTROSCOPY

A. Neutron Resonance Cross Section Measurements (H. Camarda, G. Hacken, F. Rahn, H. Liou, W. W. Havens, Jr., J. Rainwater, M. Slagowitz, S. Wynchank)

Since the last reporting period, work in progress on the data obtained from the 1968 run for the mass regions $80 < A < 120$ and $139 < A < 186$ has progressed satisfactorily. The final resonance parameters have been obtained for the separated isotopes of In and La. Neutron widths for 39 levels in In^{113}, 227 levels in In^{115} and 81 levels in La^{139} are presented in Tables I.A.1, I.A.2 and I.A.3. Radiation widths have been determined for some of the stronger levels. The In^{115} and La^{139} data have been tested against the Porter-Thomas and Wigner distributions, and the $\ell = 0$ and $\ell = 1$ strength functions have been determined. For In^{115} the results are $S_0 = (.260 \pm .027)10^{-4}$, $S_1 = (2.0 \pm 0.5)10^{-4}$. For La^{139}, $S_0 = (.70 \pm .23)10^{-4}$ and $S_1 = (.50 \pm \overset{2.5}{2.0})10^{-4}$. For In^{115}, S_0 is estimated to be $(.85 \pm .20)10^{-4}$. Levels in In^{115} and La^{139} were assigned a probability for being p-wave, using Bayes' theorem in conjunction with known s-wave parameters. Both of these isotopes yielded a considerable number of observed p-wave levels.

The Porter-Thomas fit for In^{115} is excellent, while that for La^{139} is inconclusive or perhaps anomalous (as shown in Figs. I.A.1 and I.A.2). The $\ell = 0$ strength function of La^{139} exhibits a possibly non-statistical energy variation.

The analysis of the resonance parameters for the even-even isotopes Sm^{152} and Sm^{154} has been extended to 5100 eV. Resonance parameters for 60 additional levels in Sm^{152} and 13 levels in Sm^{154} previously unreported are presented in Tables I.A.4 and I.A.5. The analysis of these two separated isotopes show that relatively few levels have been missed below ~3000 eV. For nearest neighbor level spacing the Wigner distribution is expected to apply. More sensitive tests, devised by Dyson and Dyson and Mehta, suitable for single population ensembles of resonance levels, give evidence of longer range ordering of level positions (see last progress report). The Dyson and Mehta formulation predicted that the expected mean square deviation, Δ, between an observed level number of single population ($I = 0$, $\ell = 0$) resonances N(E) for $<E$ and a best fit straight line should have an expectation value of $<\Delta> = \frac{1}{\pi^2}[\ell n(n) - 0.0687]$ and a variance of $V_\Delta = 1.1690/\pi^4$. The small value of $<\Delta>$ for large n increasing only as $\ell n(n)$ implies a longer range ordering of level positions.

For Sm^{152}, 58 levels were observed below 3000 eV. The experimental

mean square deviation, Δ_{exp} = .431, compared to a predicted value of Δ = .404. In addition, the covariance of neighboring level spacings, $Cov(S_i,S_{i+1})$, was observed to be (-0.233 ± .106) in qualitative agreement with the expected covariance of (-0.25) for long range ordering of levels resulting from the treatment of random matrix models as obtained by Porter, Rosenzweig, Gunson, Kahn, and others. For an uncorrelated sequence of Wigner distributed spacings, the expected Cov = 0.0 ± $\sqrt{1/m}$ where m is the number of adjacent spacing pairs. The observed value of $(Cov + \Delta)_{exp}$ for Sm^{152} was found to be .198. This qualtity is more sensitive in testing the data. The probability of achieving less than this particular value of (Cov + Δ) for an uncorrelated Wigner distribution is .697, where this rather high value resulted from the fact that the size of the population (58) is somewhat too small to test the theory (better than 100 "clean" levels are required). In the case of Sm^{152} the theoretical predictions are used as a test of the reasonableness and completeness of the data.

We have previously cited in our last report our exceptionally good test case of Er^{166} which gives unambiguous, strong support for the almost crystal lattice type long range ordering of level positions. We have finished the analysis for the isotopes $Er^{166,167,168,170}$. The final s-wave strength functions for these isotopes are S_o=1.62x10^{-4}(Er^{166});1.84x10^{-4}(Er^{167});1.50x10^{-4}(Er^{168}) and 1.54x10^{-4}(Er^{170}). We have predicted the mean expected number of observed p-wave resonances for the even isotopes of Er and from this estimated the p-wave strength function for these isotopes. We have obtained values of S_1 = 0.60 x 10^{-4} (Er^{166});(0.70 ± 0.20)10^{-4} (Er^{168}) and (0.80 ± 0.25)10^{-4} (Er^{170}).

The data for Er^{168} was tested with a Bayes' theory criterion for establishing the s- and p-wave levels. Excellent agreement between the resulting spacing distribution and the Wigner distribution was obtained. We arrived at a value of $Cov(S_i, S_{i+1})$ of (-0.295 ± 0.138) and a Δ_{exp} of 0.287 (Δ_{Dyson} = 0.389 ± 0.110). The probability is 0.035 for obtaining a value of [Δ + Cov] = -0.0077 using an uncorrelated Wigner distribution. The Er^{168} gives conclusive evidence (although less so than the Er^{166} isotope) that the level spacing distribution agrees with the theory of Dyson and Mehta, but is not compatible with a theory having no long and short range correlations between spacings.

The data analysis for the even-even W^{182} isotope shows that the energy interval 0 to 2610 eV, containing 42 observed resonances, also provides a good test for single population statistical theories. The levels observed below 2610 eV are consistent with the Porter-Thomas distribution for the reduced neutron widths and the Wigner distribution for adjacent level spacings. In addition, a careful examination of the resolution of the measuring detectors enabled us to determine the expected number of observed p-wave levels and missing s-wave levels. We believe no p-wave levels were observed and approximately 2 s-wave levels were undetected. Another new statistic, termed the F-statistic, developed again by Dyson and Mehta, which is sensitive to the longer range correlations discussed in the previous paragraphs, was evaluated with the experimental data. This experimental value of the F-statistic was compared with the predictions of the random matrix model and

TABLE I.A.1

In^{113} RESONANCE PARAMETERS

E_o (eV)	ΔE_o (eV)	$g\Gamma_n$ (meV)	$\Delta g\Gamma_n$ (meV)	$g\Gamma^o_n$ (meV)	Γ_γ (meV)	$\Delta\Gamma_\gamma$ (meV)
21.547	.011	1.4	0.1	.30		
24.990	.014	4.65	0.10	.930	80	5
26.777	.015	.104	.023	.020		
32.243	.020	3.8	0.2	.67	72	10
44.714	.033	1.0	0.1	.15		
45.376	.033	0.84	0.01	.125		
70.291	.032	3.8	0.1	.45		
91.592	.048	15	5	1.56		
93.000	.049	2.12	0.04	.22		
103.95	.06	15	1	1.5	70	5
123.45	.08	6	1	.54		
203.36	.16	19	1	1.33		
228.50	.19	18.5	4.6	1.22		
234.48	.20	6.5	0.7	.42		
236.06	.20	3.5	0.9	.22		
241.73	.21	8.3	0.9	.54		
270.45	.12	4.4	0.7	.27		
304.26	.15	6.2	0.7	.36		
313.93	.15	3.5	0.9	.20		
325.83	.16	5.77	1.16	.32		
441.45	.25	6.9	0.9	.33		
511.56	.32	19.6	2.3	.865		
544.78	.35	41.6	2.3	1.8		
555.37	.36	11.8	1.2	.50		
582.87	.38	55.4	2.3	2.3		
593.02	.40	20.8	1.2	.85		
625.54	.43	34.6	2.3	1.39		
660.81	.47	37.0	2.3	1.44		
714.59	.52	46.2	4.6	1.73		
769.91	.59	37.0	2.3	1.34		
777.57	.59	15.9	0.7	.57		
785.35	.60	20.3	1.2	.725		
809.39	.63	19.2	1.2	.67		
912.01	.38	90.1	11.6	2.98		
1064.6	.48	23.1	2.3	.708		
1230.0	.59	55.4	4.6	1.57		
1254.6	.61	60	7	1.7		
1761.9	1.0	62	5	1.49		
2004.1	1.2	212	7	4.75		

TABLE I.A.2

In^{115} RESONANCE PARAMETERS

E_o (eV)	ΔE_o (eV)	$g\Gamma_n$ (meV)	$\Delta g\Gamma_n$ (meV)	$g\Gamma^o{}_n$ (meV)	$g\Gamma^1{}_n$ (meV)	Γ_γ (meV)	$\Delta\Gamma_\gamma$ (meV)
22.733	.012	.51	.02	.107		81	5
39.599	.027	2.1	0.1	.33		76	5
46.363	.035	.125	.005	.0184			
48.142	.037	.25	.05	.036		90	5
62.976	.027	.37	.05	.047		95	10
69.491	.032	.20	.05	.024			
73.082	.035	.006	.003	.0007	4.4		
80.874	.040	.75	.05	.083		70	10
83.276	.042	3.3	0.4	.36		73	5
86.355	.045	.026	.013	.0028	14.5		
94.341	.050	1.45	0.15	.149		90	10
100.83	.05	.022	.010	.0021	9.5		
110.90	.06	.024	.012	.0023	9.1		
114.43	.06	.052	.005	.0049	19.0		
120.71	.07	.004	.002	.00036	1.35		
125.89	.08	1.9	0.1	.17		65	20
132.81	.08	2.7	0.5	.23		180	50
144.04	.09	.073	.010	.0061	18.9		
145.76	.09	.03	.01	.0025	7.7		
150.29	.10	2.3	0.1	.19		85	10
158.59	.11	.073	.035	.0058	16.3		
162.38	.11	.063	.030	.0050	13.7		
164.67	.12	9.0	0.5	.70		82	10
168.08	.12	1.05	0.05	.081			
174.08	.13	0.10	0.04	.0076	19.5		
177.92	.13	1.5	0.3	.11		80	20
186.96	.14	10.0	1.0	.731		100	20
192.24	.15	.0160	.0004	.00115	2.69		
194.45	.15	.062	.030	.0044	10.2		
198.83	.15	.036	.020	.0026	5.80		
205.60	.16	11.5	3.0	.802			
211.88	.17	.26	.05	.018			
214.09	.17	.088	.005	.0060	12.6		
224.03	.18	16	3	1.07		60	15
226.81	.19	.66	.40	.044			
239.28	.20	.127	.060	.00819	15.3		
246.74	.21	.096	.050	.0061	11.1		
250.17	.22	30	2	1.9		85	10
266.96	.12	2.0	0.1	.12			
276.77	.12	.068	.030	.0041	6.64		
282.28	.13	.093	.040	.0055	8.77		
288.88	.13	10	1	.59			
294.33	.14	22	5	1.3			
302.52	.14	.052	.021	.0030	4.42		
308.37	.15	.063	.030	.0036	5.18		

TABLE I.A.2 (CONTINUED)

E_0 (eV)	ΔE_0 (eV)	$g\Gamma_n$ (meV)	$\Delta g\Gamma_n$ (meV)	$g\Gamma_n^0$ (meV)	$g\Gamma_n^1$ (meV)
319.49	.16	7.5	0.5	.42	
329.57	.16	0.10	0.05	.0055	7.48
336.73	.17	0.10	0.05	.0056	7.47
339.80	.17	0.95	0.05	.052	
345.18	.18	.15	.07	.0080	10.4
354.13	.18	3.14	1.00	.167	
360.60	.19	.10	.05	.0052	6.49
362.10	.19	5.44	.21	.286	
366.87	.19	.17	.08	.0086	10.5
370.94	.20	3.45	.21	.179	
379.10	.20	.314	.052	.0161	
382.97	.20	.61	.30	.031	
384.20	.21	2.93	.31	.149	
402.35	.22	15.7	3.1	.782	
411.56	.23	15.7	3.1	.772	
423.00	.24	5.23	0.52	.254	
431.21	.25	0.11	.05	.0053	5.55
437.16	.25	0.52	.05	.025	
448.90	.26	6.27	1.05	.296	
453.89	.27	10.5	2.1	.491	
456.82	.27	9.6	1.0	.45	
469.65	.28	2.72	0.31	.125	
473.58	.28	0.28	0.10	.013	12.0
477.55	.29	1.57	0.11	.0718	
488.01	.29	0.34	0.15	.015	14.2
493.67	.30	0.25	0.10	.011	10.4
498.20	.30	1.46	0.11	.0656	
501.88	.31	0.52	0.25	.023	
503.73	.31	12.5	2.1	.559	
506.21	.31	0.54	0.25	.024	
513.15	.32	.049	.025	.0022	1.88
515.38	.32	1.67	0.11	.0737	
525.46	.33	7.11	1.05	.310	
530.11	.33	0.47	0.05	.020	
547.92	.35	2.72	0.11	.116	
551.10	.35	0.84	0.05	.036	
559.70	.36	0.32	0.15	.013	10.7
562.61	.36	0.47	0.04	.020	15.8
569.62	.37	0.26	0.10	.011	8.57
571.86	.37	17.77	1.05	.743	
580.19	.38	3.97	0.21	.165	
589.09	.39	3.35	0.11	.138	
602.22	.40	1.05	0.21	.0426	
609.99	.41	0.42	0.03	.017	12.4

TABLE I.A.2 (CONTINUED)

E_0 (eV)	ΔE_0 (eV)	$g\Gamma_n$ (meV)	$\Delta g\Gamma_n$ (meV)	$g\Gamma_n^0$ (meV)	$g\Gamma_n^1$ (meV)
614.13	.42	18.82	1.05	.759	
619.59	.42	8.36	0.52	.336	
643.93	.45	2.40	0.11	.0947	
647.07	.45	1.86	0.10	.0731	
654.80	.46	4.50	0.10	.176	
674.03	.48	5.64	0.11	.217	
683.23	.49	1.57	0.11	.060	
694.62	.50	2.09	0.11	.0793	
699.15	.50	0.61	0.30	.023	14.8
704.75	.51	1.15	0.11	.0433	
707.83	.52	2.93	0.52	.110	
719.85	.53	1.57	0.11	.0584	
724.10	.54	0.50	0.25	.018	11.4
727.84	.54	1.67	0.11	.0620	
733.25	.54	6.17	0.11	.228	
752.66	.57	1.15	0.11	.0419	
760.06	.58	0.54	0.25	.0196	11.6
774.02	.59	10.45	1.05	.3757	
783.54	.60	7.94	0.21	.284	
789.58	.61	8.36	0.52	.289	
795.08	.62	2.9	2.0	.10	
800.63	.62	0.45	0.20	.016	8.9
812.55	.63	0.25	0.10	.0089	4.9
815.73	.64	1.67	0.31	.0585	
819.41	.32	4.18	0.52	.146	
829.79	.33	5.44	0.31	.189	
836.70	.33	8.88	0.31	.307	
853.52	.34	29.27	2.09	1.002	
861.08	.35	11.5	2.1	.392	
863.85	.35	9.4	2.1	.32	
869.44	.35	0.79	0.40	.027	13.8
875.09	.35	3.45	0.21	.117	
882.58	.36	0.38	0.20	.013	6.44
891.62	.37	7.94	0.21	.266	
898.96	.37	1.78	0.21	.0593	
906.76	.38	0.29	0.15	.0096	4.75
913.90	.38	6.9	0.3	.23	
923.43	.38	3.14	0.73	.103	
931.94	.39	1.14	0.50	.0375	
943.74	.39	0.55	0.25	.018	8.44
948.12	.40	26.1	1.0	.849	
956.57	.40	15.68	1.05	.5069	
973.81	.41	0.62	0.30	.020	9.2
977.99	.42	18.3	1.0	.585	
981.76	.42	1.45	0.21	.0463	
997.97	.43	16.7	1.0	.529	

TABLE I.A.2 (CONTINUED)

E_0 (eV)	ΔE_0 (eV)	$g\Gamma_n$ (meV)	$\Delta g\Gamma_n$ (meV)	$g\Gamma_n^0$ (meV)	$g\Gamma_n^1$ (meV)
1007.1	.44	0.41	0.20	.013	5.8
1019.5	.45	0.45	0.20	.014	6.25
1035.7	.46	3.45	0.52	.107	
1043.0	.46	26.1	2.1	.809	
1049.0	.46	2.61	0.31	.0807	
1055.1	.46	0.52	0.25	.016	6.8
1060.3	.47	6.48	0.31	.199	
1075.1	.48	17.8	2.1	.542	
1085.8	.49	16.7	1.0	.508	
1103.7	.50	0.71	0.30	.021	8.7
1111.7	.51	6.59	0.31	.197	
1140.2	.53	9.62	0.42	.285	
1170.3	.55	8.36	1.04	.244	
1179.7	.56	9.62	0.31	.280	
1188.0	.56	1.5	0.5	.044	
1190.8	.56	1.67	0.21	.0485	
1199.3	.57	0.41	0.20	.012	4.4
1213.1	.58	24.0	3.1	.690	
1216.6	.58	5.1	1.5	.146	
1224.2	.59	19.9	2.1	.568	
1237.8	.60	0.75	0.30	.021	7.77
1243.1	.60	10.45	1.05	.2965	
1270.0	.61	1.79	0.90	.0501	
1276.8	.62	2.76	1.40	.0772	
1281.2	.63	8.26	0.31	.231	
1304.7	.64	0.91	0.40	.025	8.66
1309.3	.65	7.11	0.31	.196	
1325.0	.66	5.75	2.09	.158	
1330.9	.66	6.48	0.42	.178	
1334.3	.67	3.97	0.31	.109	
1342.3	.67	4.08	0.31	.111	
1346.0	.68	7.1	0.3	.19	
1349.8	.68	14.6	2.1	.398	
1357.9	.69	3.66	0.31	.0993	
1367.6	.70	0.81	0.40	.022	7.15
1372.4	.70	1.42	0.70	.0382	12.5
1389.3	.71	5.12	0.42	.137	
1397.9	.72	6.48	0.52	.173	
1402.2	.72	3.66	0.21	.0977	
1415.9	.73	12.5	1.0	.333	
1421.0	.74	1.64	0.80	.0436	13.8
1430.6	.75	4.35	0.31	.115	
1441.8	.75	1.45	0.21	.0382	11.9
1448.6	.76	1.57	0.31	.0412	12.8
1460.7	.77	1.09	0.40	.0285	8.76
1468.4	.77	14.6	2.1	.382	

TABLE I.A.2 (CONTINUED)

E_0 (eV)	ΔE_0 (eV)	$g\Gamma_n$ (meV)	$\Delta g\Gamma_n$ (meV)	$g\Gamma_n^0$ (meV)	$g\Gamma_n^1$ (meV)
1480.0	.78	3.45	0.31	.0897	
1484.7	.79	0.26	0.10	.0068	2.07
1492.6	.80	2.16	0.70	.0559	
1520.6	.81	22.0	1.0	.563	
1546.1	.83	13.6	1.0	.346	
1554.4	.83	4.76	2.07	.121	
1562.9	.84	2.5	1.0	.063	
1567.1	.85	10.45	1.05	.2640	
1579.9	.86	1.5	0.5	.038	10.9
1595.5	.87	15.7	1.0	.393	
1614.0	.89	18.8	2.1	.468	
1619.3	.89	94.1	10.5	2.34	
1640.9	.91	23.0	1.0	.568	
1646.4	.91	1.23	0.50	.0304	8.28
1654.7	.92	1.2	0.5	.030	8.0
1664.9	.93	78.4	3.1	1.92	
1675.1	.94	0.8	0.3	.02	5.25
1679.8	.94	7.1	0.2	.17	
1688.4	.95	83.6	1.0	2.04	
1694.1	.96	6.0	1.5	.15	
1704.6	.97	1.06	0.50	.0256	6.77
1711.4	.97	29.3	3.1	.707	
1724.1	.98	4.5	0.2	.11	
1735.9	.99	36.6	5.2	.878	
1739.9	.99	4.4	1.5	.105	
1765.0	1.0	3.1	1.2	.073	
1780.3	1.0	2.6	0.2	.062	
1789.6	1.0	1.0	0.4	.024	6.12
1796.9	1.0	19.86	1.04	.4685	
1808.4	1.0	1.9	0.7	.044	11.0
1813.7	1.0	1.18	0.50	.0277	6.86
1826.4	1.0	1.8	0.8	.042	10.4
1833.9	1.1	2.3	0.8	.054	13.1
1843.6	1.1	3.2	1.0	.075	
1854.5	1.1	27.2	3.1	.631	
1865.5	1.1	6.8	0.5	.16	
1878.8	1.1	3.3	1.5	.077	
1891.1	1.1	64.8	3.1	1.49	
1904.7	1.1	8.3	2.1	.190	
1918.5	1.1	17.8	3.1	.406	
1925.4	1.1	1.35	0.6	.0307	7.16
1939.3	1.2	9.1	0.5	.21	
1946.4	1.2	16.7	1.0	.379	
1959.4	1.2	15.7	1.0	.354	
1967.7	1.2	8.36	2.09	.189	
1980.9	1.2	20.9	3.1	.470	

E_o (eV)	ΔE_o (eV)	$g\Gamma_n$ (meV)	$\Delta g\Gamma_n$ (meV)	$g\Gamma^o{}_n$ (meV)	$g\Gamma^l{}_n$ (meV)	E_o (eV)	ΔE_o (eV)	$g\Gamma_n$ (meV)	$\Delta g\Gamma_n$ (meV)	$g\Gamma^o{}_n$ (meV)	$g\Gamma^l{}_n$ (meV)
23.94	.013	.00067	.0007	.00014	2.25	4356.8	2.0	2500	300	37.9	
35.13	.023	.005	.005	.00084	9.46	4611.5	2.1	58	8	.85	73.8
35.93	.024	.004	.003	.00067	7.32	4646.0	2.2	1700	200	24.9	
39.00	.027	.017	.010	.0027	27.5	4729.5	2.2	70	5	1.0	85.8
42.18	.030	.007	.003	.0011	10.1	4810.7	2.3	70	10	1.0	83.7
72.167	.030	15.0	2.0	1.77		5177.6	2.6	60	10	.83	64.3
82.85	.041	.022	.010	.0024	11.5	5347.5	2.7	700	100	9.57	
99.29	.054	.035	.010	.0035	13.9	5517.4	2.8	110	10	1.48	
175.2	.13	.061	.020	.0046	10.4	5827.3	3.0	600	200	7.86	
243.8	.21	.107	.05	.00685	11.1	5839.5	3.1	80	40	1.05	71.7
247.6	.22	.09	.05	.0057	9.1	5854.8	3.1	70	40	.91	62.5
248.4	.22	.02	.02	.0013	2.0	5973.1	3.2	190	30	2.46	
339.3	.17	.16	.08	.0087	10.1	6329.6	3.5	80	10	1.0	63.6
617.06	.45	14	3	.56		6455.5	3.6	2100	100	26.1	
701.88	.26	4.0	0.5	.15	84.9	6552.5	3.6	900	100	11.1	
874.82	.35	9.2	1.0	.31		6856.8	3.9	1700	200	20.5	
904.24	.37	4.8	1.0	.16	69.7	6982.9	4.0	600	150	7.18	
961.06	.41	8.2	0.5	.26	109	7047.2	4.1	62	10	.74	42.0
1179.8	.56	900	100	26.2		7087.9	4.1	120	30	1.4	80.6
1207.5	.58	7	1	.2	66	7128.9	4.1	2000	200	23.7	
1255.4	.61	11	1	.31	98	7432.0	4.3	95	40	1.1	59.5
1425.4	.73	1.9	0.7	.050	13.9	7457.1	4.4	1300	200	15.1	
1431.5	.74	2.6	0.2	.069	19.0	7541.6	4.5	110	20	1.27	67.4
1634.8	.91	14	1	.35	83.8	7894.2	4.8	120	20	1.35	68.7
1649.4	.92	7.9	1.0	.19	46.7	8020.6	4.9	1300	200	14.5	
1824.4	.53	4.3	1.5	.10	21.7	8060.0	5.0	180	40	2.0	
1915.0	.57	9.2	1.0	.21	43.5	8165.1	5.1	110	25	1.2	59.9
1969.5	.60	4.5	0.5	.10	20.4	8350.0	5.2	250	50	2.74	
2116.0	.67	1500	200	32.6		8514.3	5.4	2400	200	26.0	
2149.7	.68	500	100	10.8		8661.4	5.5	800	400	8.6	
2175.2	.70	10.1	1.0	.217	39.4	8812.3	5.7	100	15	1.07	48.7
2379.5	.80	35	5	.72		8903.6	5.8	3500	300	37.1	
2467.7	.84	400	100	8.05		9210.4	6.1	50	10	.52	22.8
2663.2	.94	31	4	.60	89.4	9295.7	6.1	110	10	1.14	49.5
2854.6	1.0	200	50	3.74		9597.3	6.4	50	20	.51	21.5
2997.5	1.1	5500	500	100.5		9662.0	6.5	220	30	2.24	
3286.5	1.3	820	50	14.3		9873.5	6.7	700	100	7.04	
3420.8	1.4	10	2	.17	19.9	9981.8	6.8	1900	200	19.0	
3281.8	1.4	7000	100	118.6		10218	7.1	2300	200	22.75	
3726.0	1.6	110	20	1.80							
3749.5	1.6	2500	200	40.83							
4271.4	1.9	34	5	.52	48.5						

TABLE I.A.3 La^{139} RESONANCE PARAMETERS

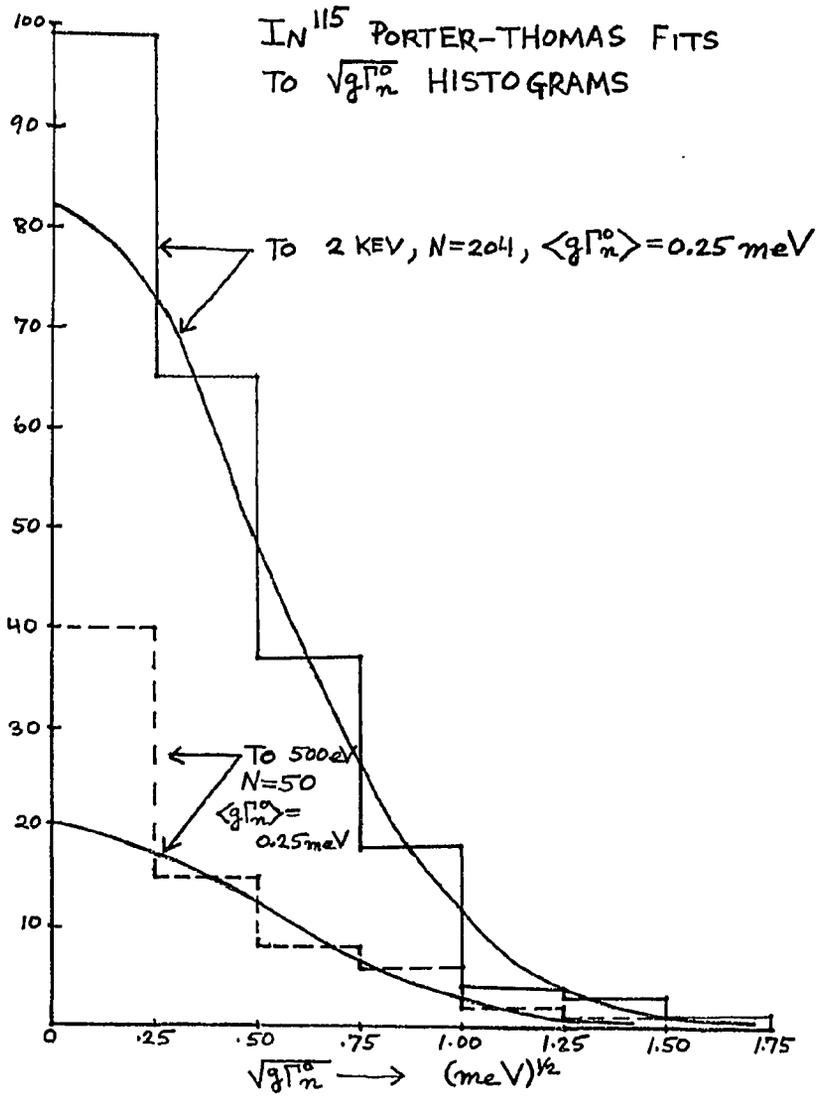

FIGURE I.A.1

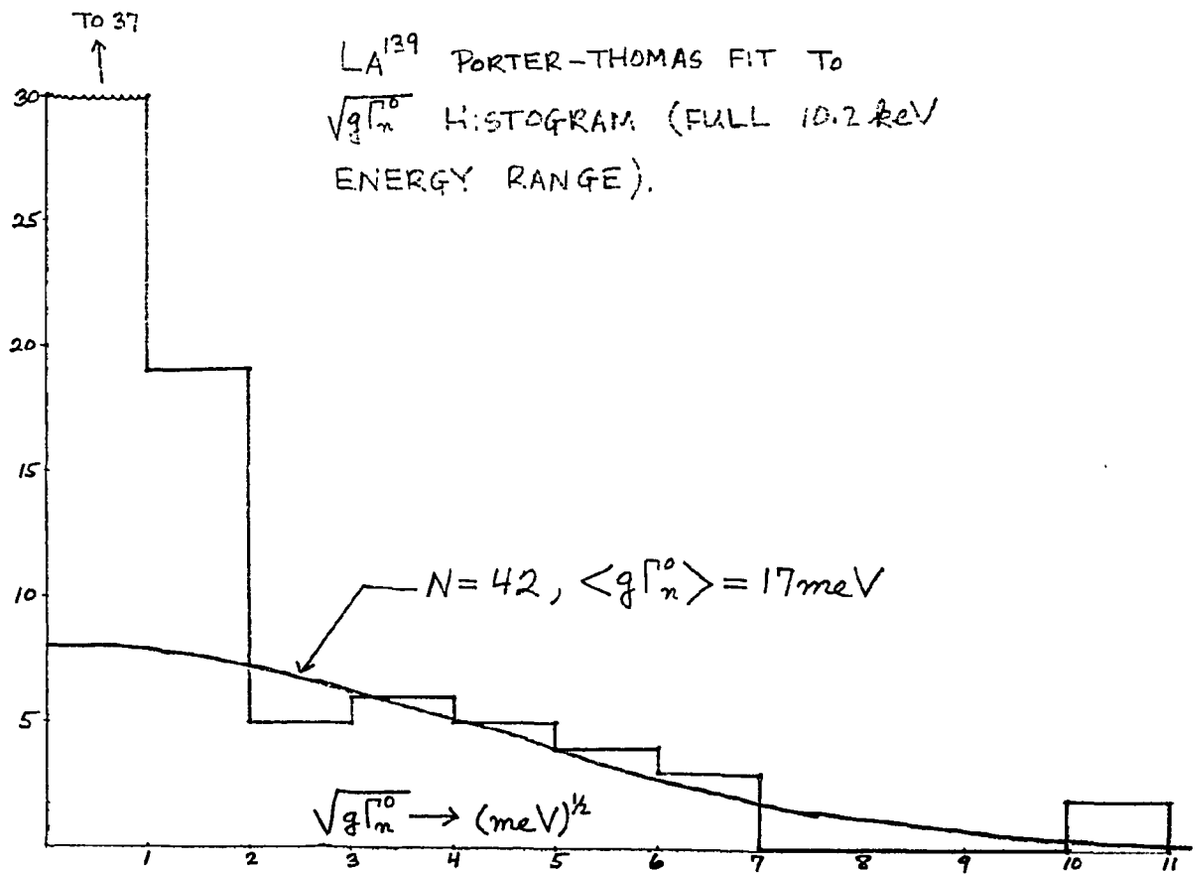

FIGURE I.A.2

TABLE I.A.4

NEUTRON RESONANCE PARAMETERS FOR Sm^{152}

Energy (eV)	Γ_n (eV)	Energy (eV)	Γ_n (eV)
1541.3 ±.8	.39 ± .08	3258.7 ± 1.3	.55 ± .07
1600.6 ±.9	.32 ± .05	3288.2 ± 1.3	1.09 ± .12
1691.8 ±.5	1.10 ± .09	3315.5 ± 1.4	.12 ± .03
1730.0 ±.6	.14 ± .05	3433.5 ± 1.4	1.14 ± .12
1748		3464.0 ± 1.4	.45 ± .07
1806.9 ±.6	.10 ± .04	3512.0 ± 1.5	.68 ± .09
1875.6 ±.6	.009 ± .005	3537.8 ± 1.5	2.43 ± .28
1954.8 ±.7	.39 ± .05	3609.4 ± 1.6	.13 ± .04
1987 ± 1	.013 ± .008	3665.0 ± 1.6	2.28 ± .26
2046.6 ±.7	.028 ± .009	3826.6 ± 1.6	.30 ± .04
2121.5 ±.7	.85 ± .09	3925.7 ± 1.7	.69 ± .09
2196.7 ±.8	.009 ± .006	4028.0 ± 1.7	.38 ± .05
2237.1 ±.8	.28 ± .04	4075.5 ± 1.8	.22 ± .05
2310.5 ±.9	.27 ± .04	4101.5 ± 1.8	.76 ± .10
2367.8 ±.9	.20 ± .03	4172.6 ± 1.9	4.05 ± .38
2392.5 ±.9	.18 ± .03	4215.3 ± 1.9	.57 ± .08
2456.3 ± 1.0	.40 ± .04	4320.3 ± 1.9	1.01 ± .13
2490.0 ± 1.0	.010 ± .006	4405 ± 2	.062 ± .025
2522.0 ± 1.0	.046 ± .020	4523 ± 2	.41 ± .06
2582.6 ± 1.0	.15 ± .03	4557 ± 2	.38 ± .06
2648.5 ± 1.1	2.29 ± .23	4590 ± 2	.28 ± .05
2656.9 ± 1.1	1.21 ± .13	4651 ± 2	.56 ± .06
2695.8 ± 1.1	.41 ± .06	4668 ± 2	1.54 ± .17
2854 ± 2	.033 ± .012	4725 ± 2	.066 ± .030
2912.1 ± 1.1	1.37 ± .15	4777 ± 2	.51 ± .07
2925.0 ± 1.2	.058 ± .019	4923 ± 2	.76 ± .11
2966.6 ± 1.2	.46 ± .07	4946 ± 3	.39 ± .06
2985.5 ± 1.2	1.21 ± .14	4985 ± 3	.164 ± .18
3030.7 ± 1.2	.61 ± .08	5073 ± 3	2.14 ± .25
3104 ± 2	.18 ± .04	5100 ± 3	.27 ± .07
3157.9 ± 1.3	.49 ± .06		

TABLE I.A.5

NEUTRON RESONANCE PARAMETERS FOR Sm^{154}

Energy (eV)	Γ_n (eV)	Energy (eV)	Γ_n (eV)
2529.5 ± 1.0	2.59 ± .75	4213.5 ± 1.8	3.39 ± .50
2834.1 ± 1.1	.19 ± .03	4415 ± 2	3.76 ± .51
2862.7 ± 1.1	.07 ± .01	4550 ± 2	.42 ± .07
2937.8 ± 1.2	1.42 ± .18	4757 ± 2	2.28 ± .31
3046.8 ± 1.2	1.46 ± .18	4920 ± 2	1.79 ± .22
3540.7 ± 1.4	.18 ± .09	4075 ± 3	1.23 ± .17
4060.5 ± 1.7	.59 ± .08		

with what would be expected from levels obeying only the Wigner distribution. The W^{182} data overwhelmingly favors the random matrix model and longer range correlations of level positions.

The preliminary processing of the $Dy^{160,161,162,163,164}$ separated isotope data has been completed. The data is presently being evaluated for the transmission measurements to obtain total neutron cross section [(τ,σ) values]. The energy range for which the data provides good results extends to greater than 5000 eV.

The analysis of the total neutron cross section for natural argon has been completed. Figure I.A.3 presents σ_{total} vs E for argon in the energy range 100 keV to 1 MeV.

The Nevis cyclotron coversion program is proceeding on schedule, with completion expected by the end of the year. This major modification retains the basic cyclotron magnet, with an additional iron band to lower the magnet reluctance. Pole pieces have been replaced by a new configuration N = 3 symmetry section iron with a small median plane gap. <B> = 18 kG near the center and 20 kG near the 80 inch radius. We expect to obtain ∿550 MeV proton energy beam with high extration efficiency for a 10 to 40 μA time average beam. The synchrocylotron will have a new R.F. system with a 300 Hz FM repetition rate.

B. Cross Section and Neutron Resonance Parameters of F and Al (U.N. Singh and J.B. Garg, SUNY, Albany, N.Y.; J. Rainwater, W. W. Havens, Jr. and S. Wynchank, Columbia University)

High resolution neutron total cross section measurements[1] in the energy interval of few keV to about 300 keV on natural samples of Fluorine and Aluminum made earlier have been analyzed with an elaborate multilevel R-matrix formalism with resolution correction. From this analysis it has been made possible to determine the energies and neutron widths of resonances and to make their L and J-value assignments. From these results the mean level spacing <D>, s-wave strength function (S_0) and p-wave strength function (S_1) have been determined. By combining these measurements with the known thermal data on the coherent scattering and capture cross section, it is possible to estimate the radiative capture widths of strong levels. Levels of Al^{28} and F^{20} are given in Tables I.B.1 and I.B.2.

C. Cross Section and Neutron Resonance Parameters of U^{238} (F. J. Rahn, H. Camarda, G. Hacken, W. W. Havens, Jr., H.I. Liou, J. Rainwater, M. Slagowitz, S. Wynchank, J. Arbo and C. Ho)

The transmission, self-indication and Moxon-Rae Data from the 1970 run were combined into a single package for the purpose of analysis. The U^{238} samples had thicknesses of 1/n = 8.47, 11.89, 27.1, 28.8, 36.0, 119, and 478 barns/atom and an isotope enrichment of greater than 99.99% in some samples. The transmission measurements at 40 and 200 meters were normalized separately. The first part of the run was used to obtain U^{238} normalization data utilizing

---

[1] J.B. Garg, J. Rainwater, S. Wynchank and W.W. Havens, Jr., International Conference on the Study of Nuclear Structure with Neutrons, Antwerp, Belgium (1965)

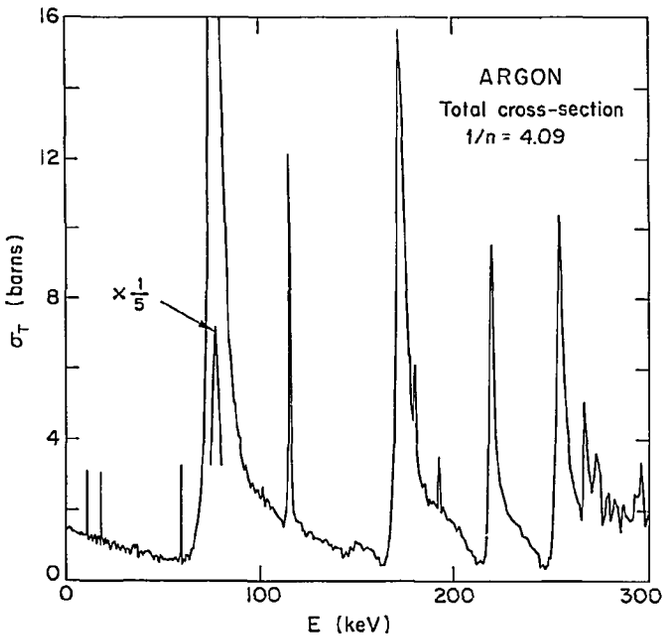

FIGURE I.A.3

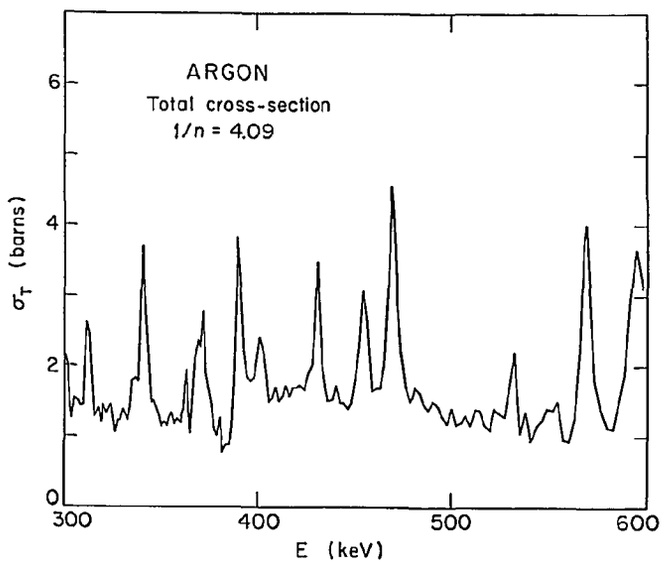

FIGURE I.A.3 (CONTINUED)

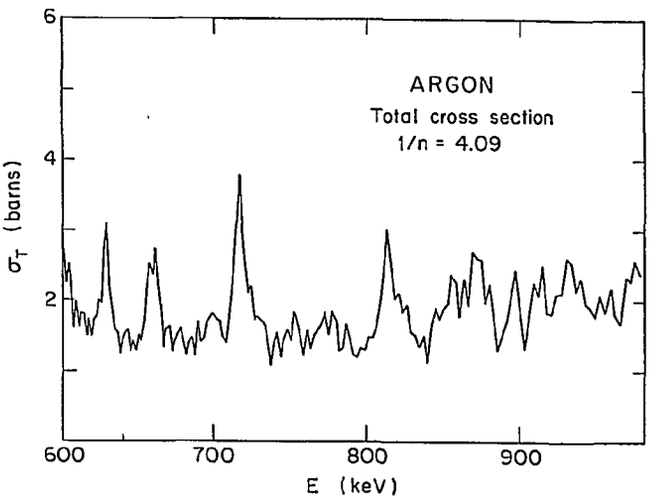

FIGURE I.A.3 (CONTINUED)

TABLE I.B.1

LEVELS OF AL^{28}

E_o (keV)	ℓ	J^π	Γ_n(keV)	$\Gamma^0{}_n$(eV)	$\Gamma^1{}_n$(eV)	Γ_γ(eV)
5.903 ± 0.006	1	1^-	0.01		26.68	5.0
34.70 ± 0.09	0	2^+	3.42	18.34		8.30
88.50 ± 0.36	1	3^-	11.28		547.56	9.0
120.0 ± 0.6	1	2^-	3.49		109.90	
145.0 ± 0.8	1	3^-	15.14		365.92	
159.0 ± 0.9	1	4^-	2.84		60.39	
204.8 ± 1.3	1	2^-	4.26		64.12	
208.1 ± 1.3	1	2^-	4.35		64.11	

TABLE I.B.2

LEVELS OF F^{20}

E_o (keV)	ℓ	J^π	Γ_n (keV)	$\Gamma^1{}_n$ (eV)	Γ_γ (eV)
27.02 ± 0.05	1	2^-	0.37	125.50	1.1
49.10 ± 0.15	1	1^-	1.31	185.19	1.6
97.00 ± 0.43	1	1^-	14.31	750.55	

Ta, Fe, Cu and Co reference samples. These reference samples have sharp structure in their cross sections, which makes it possible to determine the U^{238} transmission at the energies at which the structure occurs, without the need of determining the T=0 and T=1 points. The Moxon-Rae measurements were performed simultaneously at 33 meters on a different flight path. The D-only and D+T self indication experiments used a high effficiency plastic scintillation detector. With this detector we obtained extremely high count rates with excellent statistics. There was good agreement between the D-only and the Moxon-Rae data, even though only the Moxon-Rae detector is totally independent of the decay cascade from resonance to resonance. The D+T results for a number of different ratios of sample thicknesses provided additional data for the analysis of the resonance parameters.

The (T, σ_{tot}) values were obtained for U^{238} by the transmission of the difference technique. The total neutron cross section is presented in Fig. I.C.1. The experimental total neutron cross section has not been corrected for Doppler broadening, and is subject to the limitations of instrumental resolution and the choice of the (1/n) values of the samples. We ran extra thick samples in the transmission measurements to accurately measure the cross section between levels and in the level-potential interference dips. The quality of the data is demonstrated in Fig. I.C.1 by the large number of weak levels detected that have not been seen previously in transmission measurements. A portion of the data from 2 to 3.3 keV is shown in the figure.

To determine the resonance parameters, the assumption was made that the Breit-Wigner single level formula is valid, and we then determined the parameters most consistent with the experimental data. The curves of Γ_n vs Γ_γ from the areas obtained from the transmission data and the curves obtained from the capture and self-indication information which give other relations between Γ_n and Γ_γ are combined.

Table I.C.1 lists the resonance parameters $[E_o(eV), g\Gamma_n(meV), \Gamma_\gamma(meV)]$ for the 321 levels that we observed between 6 eV and 5 keV. In Fig. I.C.2 we show the values of Γ_γ as a function of energy, E, for 71 levels up to 2400 eV. We have assigned a systematic uncertainty of ±0.9 meV to account for the relative uncertainty in the normalization of the data. We find no evidence of a quasi-periodic variation of Γ_γ with neutron energy. Fig. I.C.3 shows the distribution of Γ_γ. The histogram is taken in intervals of 2 meV. The figure shows that the histogram can be suitably fit by a chi-squared function with 70±9 degrees of freedom, generated about the mean value of 22.9 meV.

The sum of the reduced neutron widths, $\Sigma(\Gamma^\circ_n)$ versus E for the 321 observed levels is plotted in Fig. I.C.4. The slope of the curve determines the ℓ=0 strength function. Our best choice $S_o = (1.02\pm.10)10^{-4}$ for the energy range 0-5 keV. This value is nearly independent of a few missing weak s-wave levels or the inclusion of p-wave or weak suprious levels. Fig. I.C.5 shows the distribution for values of $y=\sqrt{\Gamma^\circ_n}$ of U^{238}. The histogram is then taken in intervals of D_y=0.5 $meV^{1/2}$. The presently favored fit to the data, a chi-squared distribution of =1 degree of freedom (Porter-Thomas), is also shown. The Porter-Thomas distribution has been normalized to 208 levels in order to agree with the observed distribution for large y. The 113 excess levels are interpreted as p-wave levels or spurious resonances.

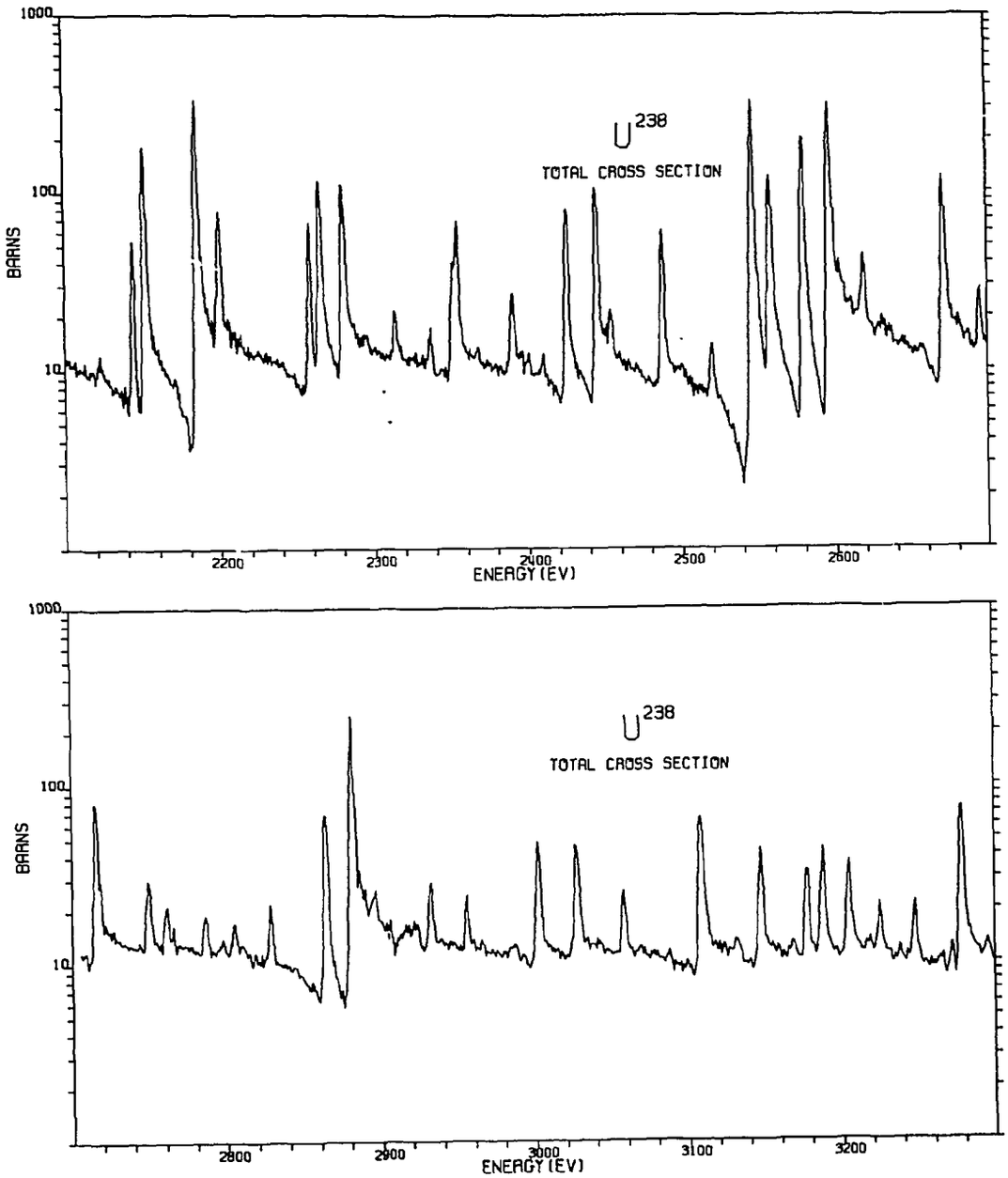

FIG. I.C.1

"MEASURED" TOTAL NEUTRON CROSS SECTION OF U^{238} VERSUS NEUTRON ENERGY (The peak values at resonance are limited by Doppler level broadening, experimental energy resolution, and the size of the 1/n value of our thinnest sample.)

TABLE I.C.1

NEUTRON RESONANCE PARAMETERS OF U^{238}

ENERGY(eV)	$g\Gamma_n$(meV)	Γ_γ(meV)
6.65±.10	1.40±.05	
10.22±.10	.0018±.0008	
19.50±.10	.0014±.0007	
20.90±.10	8.5±.8	24.±3.
36.80±.07	38.±2.	23.±2.
45.19±.07	.0020±.0015	
63.54±.07	.006±.003	
66.10±.15	28.±2.	21.±2.
72.46±.07	.001±.001	
74.67±.07	.001±.001	
80.70±.07	1.7±.2	
83.57±.07	.004±.002	
85.06±.07	.001±.001	
89.19±.07	.09±.01	
99.19±.07	.001±.001	
102.47±.09	73.±4.	28.±3.
111.27±.09	.001±.001	
116.82±.11	37.±3.	20.±2.
121.61±.11	.006±.003	
124.30±.12	.012±.005	
127.32±.13	.004±.002	
145.57±.15	.90±.05	
152.42±.17	.04±.02	
158.89±.18	.007±.003	
160.65±.18	.005±.003	
165.21±.19	3.1±.4	18.±5.
173.11±.21	.025±.012	
177.38±.22	.001±.001	
182.03±.22	.003±.002	
189.80±.23	188.±15.	27.±3.
196.14±.24	.001±.001	
198.57±.24	.003±.002	
200.54±.24	.008±.003	
202.30±.24	.04±.02	
208.49±.25	62.±6.	22.±4.
214.97±.28	.04±.02	
218.04±.28	.010±.005	
237.20±.16	35.±4.	24.±3.
242.60±.17	.15±.03	
253.88±.18	.10±.03	
255.37±.18	.06±.03	
257.10±.19	.02±.01	
263.91±.19	.23±.04	
273.56±.20	29.±3.	23.±3.
275.76±.20	.08±.06	
282.29±.21	.06±.03	
291.01±.21	17.±2.	22.±3.
294.96±.22	.03±.02	
311.13±.25	1.05±.10	
337.19±.26	.05±.02	
347.74±.28	89.±7.	28.±4.
351.75±.30	.08±.03	
354.66±.30	.03±.03	
377.03±.32	.90±.10	
397.39±.35	6.0±.5	22.±6.
407.64±.36	.08±.03	
410.18±.36	19.±2.	18.±2.
433.70±.40	8.8±1.0	20.±2.
439.7±.4	.16±.04	
454.1±.4	.40±.10	
462.8±.4	4.6±.5	
477.0±.4	3.0±.5	
485.4±.4	.03±.03	
488.2±.5	.45±.05	
498.9±.5	.08±.04	
518.27±.25	49.±5.	24.±2.
523.21±.25	.20±.07	
527.43±.25	.03±.03	
535.21±.25	45.±5.	23.±2.
542.34±.27	.05±.03	
555.90±.30	.80±.25	
579.87±.30	41.±4.	21.±2.
584.80±.31	.05±.04	
592.10±.31	.05±.04	
594.84±.31	85.±5.	20.±2.
606.12±.34	.25±.08	
619.75±.35	28.±3.	19.±2.
624.80±.35	1.0±.2	
628.29±.35	5.2±.5	
660.9±.4	138.±15.	29.±3.
668.4±.4	.25±.08	
677.5±.4	.70±.25	
692.9±.4	42.±5.	22.±2.
707.9±.4	19.±2.	21.±2.
712.4±.4	.25±.15	
720.9±.4	1.3±.2	
729.4±.4	.7±.2	
732.5±.4	1.0±.2	
743.2±.4	.3±.3	
756.0±.5	.45±.15	
764.8±.5	8.0±1.0	18.±2.
778.8±.5	1.8±.2	
790.4±.5	6.0±.4	
808.2±.5	.4±.2	
815.3±.5	.20±.10	
820.9±.5	62.±7.	20.±2.
832.4±.5	.25±.10	
846.9±.5	1.0±.3	
850.6±.5	55.±5.	23.±2.
856.1±.5	81.±7.	23.±2.
866.0±.5	5.0±.5	
888.6±.5	.15±.15	
890.6±.5	.8±.2	
904.5±.3	49.±3.	22.±2.
909.5±.3	1.3±.3	
924.5±.3	9.8±.8	28.±8.
932.3±.3	.3±.2	
936.6±.3	144.±12.	25.±2.

DATA NOT FOR QUOTATION

TABLE I.C.1 (CONTINUED)

NEUTRON RESONANCE PARAMETERS OF U^{238}

ENERGY(eV)	$g\Gamma_n$(meV)	Γ_γ(meV)
940.1±.4	.3±.2	
958.0±.4	203.±20.	21.±2.
964.9±.4	.20±.10	
976.8±.4	.6±.3	
985.6±.4	.3±.2	
991.4±.4	390.±25.	30.±5.
1000.5±.4	.10±.05	
1005.9±.4	.10±.05	
1010.5±.4	1.5±.5	
1014.4±.4	1.6±.5	
1022.9±.4	8.2±1.5	
1028.6±.5	2.5±1.0	
1031.1±.5	1.0±.6	
1054.0±.5	89.±8.	27.±2.
1062.3±.5	.7±.3	
1067.6±.5	1.0±.6	
1071.0±.5	.3±.3	
1081.1±.5	.7±.3	
1094.4±.5	1.3±.5	
1098.1±.5	17.±3.	22.±3.
1102.7±.5	2.0±.5	
1108.9±.5	27.±4.	24.±2.
1131.1±.5	1.8±.6	
1139.9±.5	220.±20.	23.±2.
1147.0±.5	.3±.2	
1154.8±.5	.4±.2	
1166.9±.5	85.±5.	23.±2.
1176.6±.5	60.±5.	22.±2.
1194.5±.5	89.±5.	19.±2.
1210.5±.5	7.0±.8	
1217.9±.5	.4±.2	
1237.9±.5	.4±.2	
1244.9±.5	280.±35.	24.±2.
1256.5±.6	.2±.2	
1266.8±.6	22.±3.	21.±2.
1272.7±.6	27.±3.	24.±2.
1298.1±.3	4.5±1.0	
1316.5±.3	4.0±.8	
1332.7±.6	1.6±.8	
1363.4±.6	1.1±.5	
1371.6±.6	.6±.4	
1381.6±.6	.6±.4	
1393.2±.3	182.±20.	28.±3.
1405.2±.3	70.±8.	25.±2.
1410.5±.6	.4±.3	
1416.3±.3	1.8±.5	
1419.2±.3	9.0±1.0	
1427.4±.4	33.±4.	26.±3.
1443.5±.4	18.±3.	22.±3.
1473.4±.4	121.±10.	28.±3.
1522.3±.4	240.±15.	30.±7.
1532.3±.4	.4±.3	
1545.8±.4	2.5±1.0	
1549.8±.4	1.2±.4	
1565.1±.4	4.5±1.5	
1597.5±.5	375.±25.	20.±4.
1622.3±.5	70.±14.	19.±3.
1637.4±.5	50.±8.	19.±3.
1646.1±.5	1.0±.5	
1662.0±.5	170.±20.	24.±4.
1688.3±.5	92.±10.	19.±3.
1709.0±.5	80.±8.	28.±5.
1722.2±.5	15.±2.	
1744.9±.5	2.0±.4	
1755.2±.5	90.±10.	27.±4.
1782.1±.5	655.±80.	
1797.5±.5	3.0±1.0	
1807.9±.5	14.5±3.5	17.±5.
1845.5±.5	13.±5.	15.±5.
1868.0±.5	4.±2.	
1902.4±.5	34.±4.	19.±4.
1912.6±.5	.5±.3	
1916.5±.5	25.±3.	19.±5.
1953.4±.5	3.0±1.0	
1968.6±.5	665.±120.	30.±10.
1974.3±.5	515.±80.	
2022.8±.6	220.±30.	20.±4.
2029.8±.6	61.±18.	18.±5.
2070.9±.6	.3±.2	
2088.1±.6	23.±5.	22.±4.
2095.9±.6	13.±3.	
2123.8±.6	3.0±1.5	
2144.6±.6	62.±8.	15.±5.
2152.2±.6	240.±35.	32.±8.
2175.2±.6	1.5±.7	
2186.0±.6	620.±80.	29.±7.
2200.6±.6	127.±17.	26.±5.
2229.3±.6	4.0±1.0	
2235.1±.6	4.7±1.0	
2258.8±.6	86.±15.	
2265.9±.7	210.±30.	20.±5.
2281.7±.7	135.±20.	18.±5.
2288.9±.7	.9±.5	
2314.5±.7	21.±4.	
2336.9±.7	8.±4.	
2352.8±.7	47.±10.	28.±5.
2355.3±.7	61.±10.	24.±5.
2391.4±.7	26.±4.	
2410.8±.7	4.±2.	
2425.7±.7	125.±18.	
2445.5±.7	195.±25.	
2454.8±.7	19.±3.	
2488.4±.7	88.±13.	
2520.7±.8	8.±3.	
2547.2±.8	550.±50.	
2558.5±.8	230.±30.	
2579.9±.8	315.±30.	
2596.5±.8	670.±45.	

TABLE I.C.1 (CONTINUED)

NEUTRON RESONANCE PARAMETERS OF U^{238}

ENERGY(eV)	$g\Gamma_n$(meV)	Γ_γ(meV)
2619.1±.8	45.±8.	
2631.7±.8	2.3±1.0	
2671.3±.9	240.±20.	
2695.6±.9	19.±4.	
2716.5±.9	145.±20.	
2728.4±.9	2.±2.	
2749.7±.9	45.±8.	
2761.6±.9	23.±5.	
2786.0±.9	12.±3.	
2798.1±.9	2.0±1.0	
2805.4±.9	4.±2.	
2828.4±.9	17.5±3.5	
2864.1±.9	175.±30.	
2881.8±.9	550.±40.	
2896.3±.9	12.±6.	
2907.1±.9	1.5±1.5	
2922.1±1.0	4.±2.	
2933.9±1.0	31.±4.	
2955.7±1.0	21.±5.	
2965.8±1.0	3.0±1.5	
2986.3±1.0	5.±2.	
3002.4±1.0	117.±15.	
3015.1±1.0	1.7±1.0	
3027.8±1.0	125.±20.	
3042.5±1.0	2.0±1.0	
3058.1±1.0	32.±8.	
3108.8±1.0	180.±30.	
3132.6±1.0	6.±3.	
3148.1±1.1	85.±14.	
3168.5±1.1	8.±3.	
3177.8±1.1	74.±13.	
3188.1±1.1	80.±14.	
3204.9±1.1	73.±13.	
3217.0±1.1	8.±4.	
3224.9±1.1	33.±8.	
3248.1±1.1	28.±6.	
3272.0±1.1	4.±2.	
3278.2±1.1	240.±30.	
3295.2±1.1	4.±2.	
3310.3±1.1	123.±20.	
3320.2±1.2	103.±20.	
3332.9±1.2	70.±10.	
3355.1±1.2	108.±15.	
3388.3±1.2	14.±4.	
3407.9±1.2	190.±30.	
3417.7±1.2	4.±3.	
3435.3±1.2	350.±40.	
3456.3±1.3	410.±50.	
3484.3±1.3	105.±25.	
3493.3±1.3	9.±4.	
3526.4±1.3	4.±3.	
3560.5±1.3	220.±30.	
3572.7±1.3	260.±30.	
3593.3±1.3	50.±6.	

ENERGY(eV)	$g\Gamma_n$(meV)	Γ_γ(meV)
3621.8±1.3	9.±4.	
3628.3±1.4	400.±40.	
3671.8±1.4	8.±5.	
3692.0±1.4	320.±40.	
3715.5±1.4	75.±25.	
3733.0±1.4	195.±40.	
3763.6±1.5	72.±12.	
3780.8±1.5	300.±60.	
3830.3±1.5	7.±4.	
3856.4±1.5	495.±100.	
3872.1±1.5	170.±50.	
3901.3±1.5	280.±60.	
3913.4±1.5	90.±15.	
3939.0±1.5	130.±20.	
3953.9±1.5	108.±15.	
4040.4±1.5	65.±10.	
4063.0±1.5	30.±8.	
4089.4±1.6	72.±15.	
4124.0±1.6	32.±8.	
4167.8±1.6	160.±35.	
4178.2±1.7	38.±9.	
4209.4±1.7	40.±9.	
4257.7±1.7	17.±7.	
4299.0±1.7	132.±18.	
4306.0±1.7	115.±17.	
4323.9±1.7	62.±10.	
4333.2±1.8	3.±2.	
4369.4±1.8	130.±15.	
4435.0±1.8	105.±25.	
4487.2±1.8	3.±2.	
4510.3±1.8	505.±80.	
4542.0±1.8	75.±12.	
4567.2±1.8	34.±8.	
4592.7±1.9	18.±6.	
4615.0±1.9	4.±3.	
4630.4±1.9	13.±6.	
4661.7±1.9	165.±40.	
4695.0±1.9	12.±6.	
4705.5±1.9	400.±60.	
4725.9±1.9	15.±6.	
4764.±2.	12.±6.	
4784.±2.	8.±4.	
4798.±2.	155.±35.	
4835.±2.	10.±5.	
4859.±2.	185.±30.	
4898.±2.	80.±15.	
4908.±2.	95.±15.	
4921.±2.	150.±40.	
4955.±2.	130.±30.	
4972.±2.	40.±15.	
5005.±2.	20.±10.	

DATA NOT FOR QUOTATION

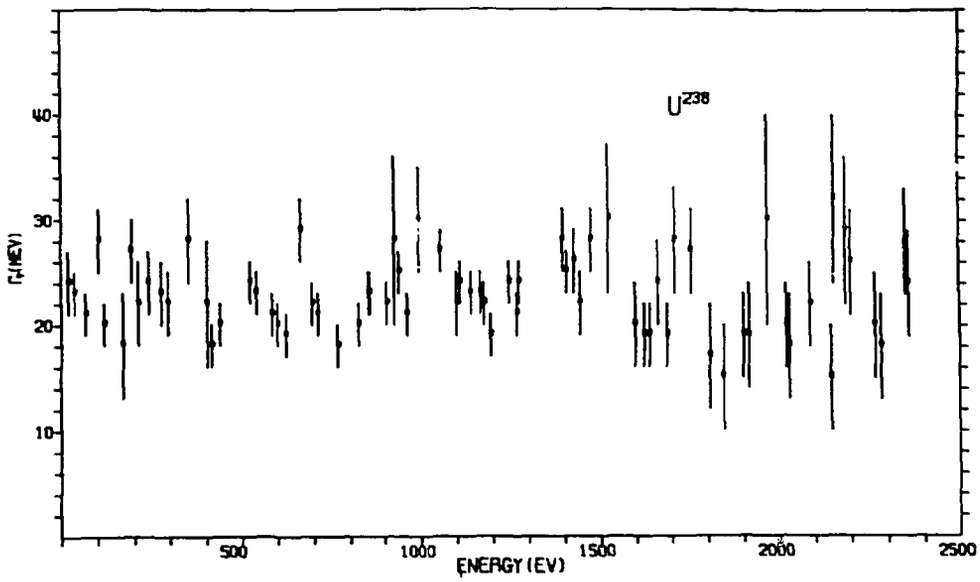

FIG. I.C. 2 RADIATION WIDTHS VERSUS NEUTRON ENERGY FOR 71 STRONGER LEVELS UP TO 2400 EV

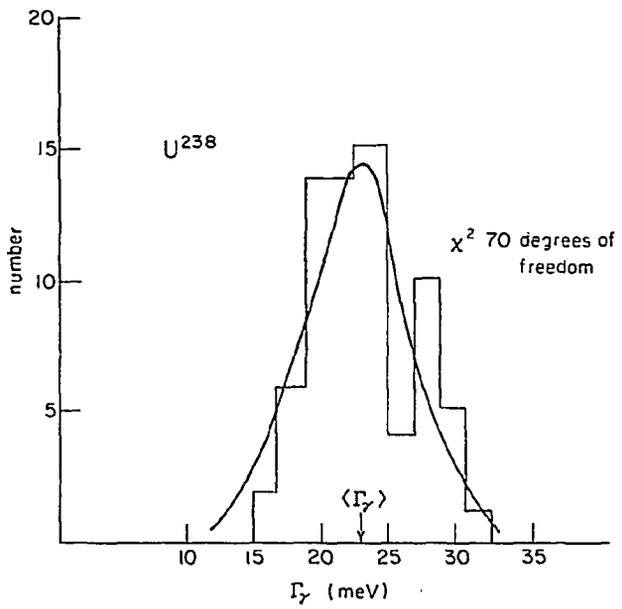

FIG. I.C.3

DISTRIBUTION OF RADIATION WIDTHS FOR THE 71 LEVELS OBTAINED IN THE ANALYSIS (The histogram is plotted in intervals of 2 meV. The curve is a Chi-squared distribution of 70 degrees of freedom about a mean of 22.9 meV.)

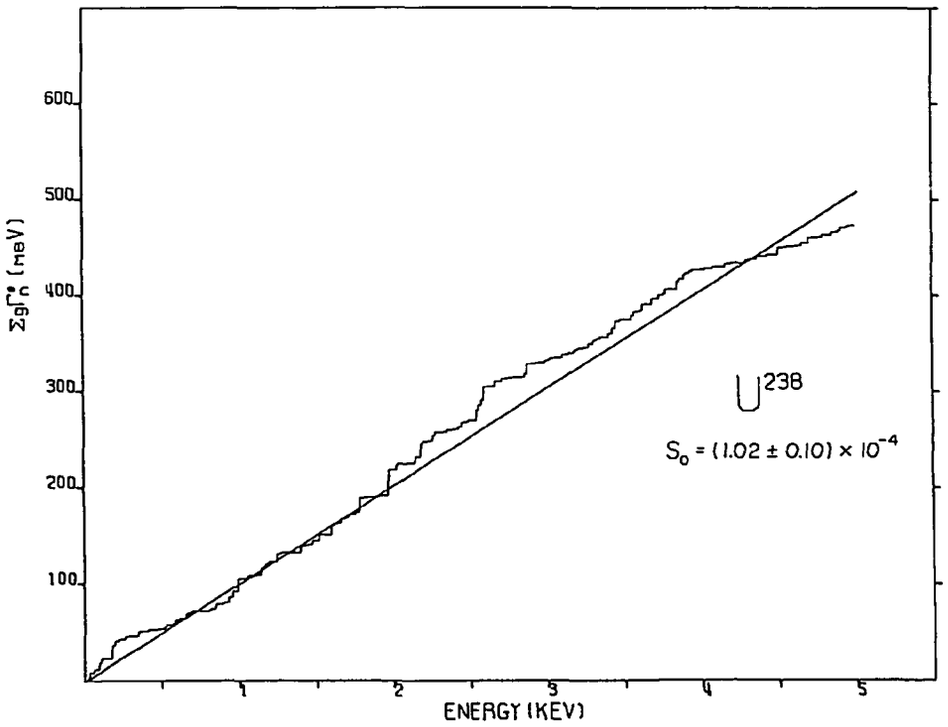

FIG. I.C.4

PLOT OF $\Sigma\Gamma^{\circ}_{n}$ VERSUS E. SLOPE OF THE CURVE DETERMINES THE ℓ=0 STRENGTH FUNCTION S_0

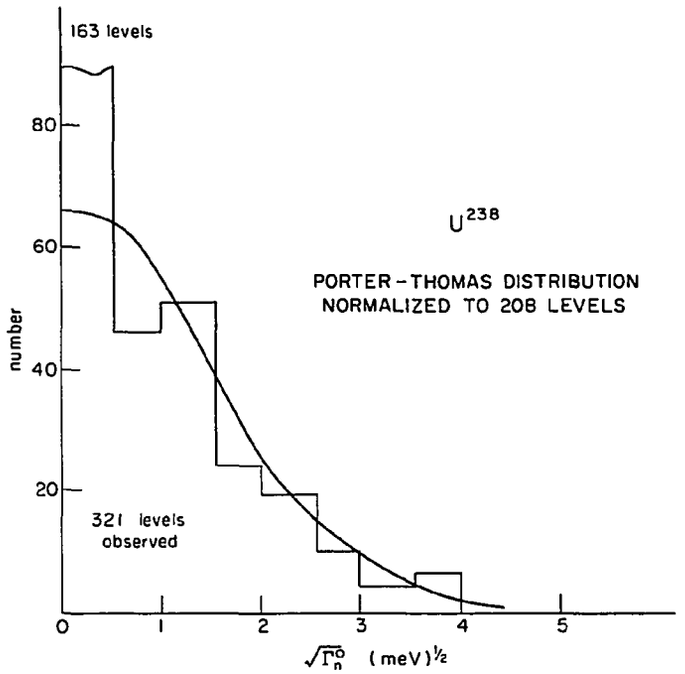

FIG. I.C.5

HISTOGRAM OF OBSERVED EXPERIMENTAL DISTRIBUTION OF $y=\sqrt{\Gamma^{\circ}_{n}}$ FOR U^{238} FOR INCREMENTS OF Δy=0.5 meV$^{1/2}$

(The curve is normalized to 208 levels. The excess levels of small y are interpreted to be ℓ=1 or spurious.)

D. Cross Section and Resonance Parameters of Th^{232} (F.J. Rahn, H. Camarda, G. Hacken, W.W. Havens, Jr., H.I. Liou, J. Rainwater, M. Slagowitz, S. Wynchank, J. Arbo and C. Ho)

The Th^{232} data taken during the last run are in the process of analysis. The data and method of analysis are similar to that of U^{238}. We have completed the analysis of (T, σ_{tot}) and the cross section in the region 0-10 keV. A portion of the results is shown in Fig. 1.D.1. We are presently in the process of obtaining the resonance parameters for these data.

E. Total Neutron Cross Section of ^{16}O at 2.37 MeV (J. Kalyna, I.J. Taylor, L.J. Lidofsky)

The minimum of the total neutron cross section of ^{16}O has been measured with a 5' long sample of liquid oxygen. The Van de Graaff Accelerator was pulsed to produce 5 nsec neutron bursts at 2 meters via the $^{7}Li)p,n)^{7}Be$ reaction and neutrons were detected with an 8" diameter by 1" thick NE213 organic liquid scintillator. Neutron-gamma ray discrimination was achieved by the time-zero cross over technique. A Monte Carlo simulation computer program corrected the data for inscattering from the cryostat. Isotopic concentrations of ^{17}O, ^{18}O and traces of Ar were analyzed by mass spectroscopic methods. Analysis of the data indicates that the cross section at the minimum is 85.3 ± 9 mb for ^{16}O and 96.7 ± 9 mb for natural oxygen.

A thesis entitled "Total Neutron Cross Section of Oxygen at 2.37 MeV" has been prepared and a paper with the same title will be submitted for publication as soon as the thesis is accepted.

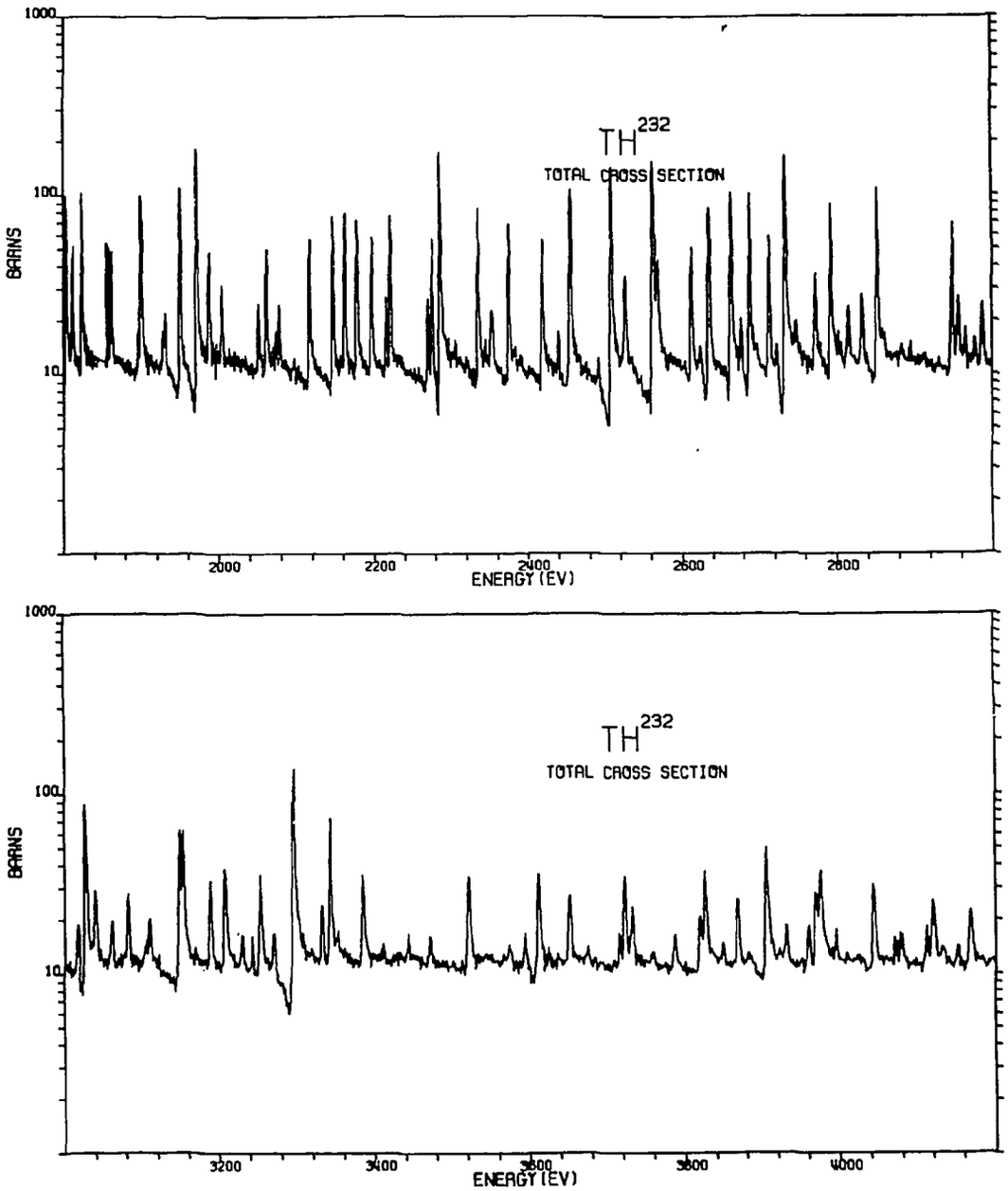

FIG. I.D.1 (CONTINUED)

THE "MEASURED" TOTAL NEUTRON CROSS SECTION OF TH^{232} *VS NEUTRON ENERGY*

F. Gamma Ray Spectra from Radiative Capture of U^{235} in the Resonance Region (M. Derengowski, J. Felvinci, C. Ho, E. Melkonian and W. W. Havens, Jr.)

The energies of gamma rays emitted by U^{235} after neutron absorption were recorded, along with the associated neutron time of flight data, from a thick ($\sim$1.5 g/cm^2) 2 by 8 inch U^{235} target in the neutron beam. The gamma ray energies were measured by means of a lithium drifted germanium detector. The purpose of the experiment was to identify neutron capture transitions from resonance energy neutrons. The experimental arrangement was described in last year's Progress Report.[1]

Roughly half the data taken during the four weeks of completely usable running time was taken with target out, to enable us to distinguish gamma ray lines associated with the U^{235} target from the background. Within the recorded gamma ray energy range of 1 to 8.5 MeV, the target-out counting rate was about two thirds the counting rate with the target in. This indicated that, even with the efforts we had made to shield the detector, background still remained a very great problem.

In the first stages of the analysis we found that the data tape contained very few tagged pulses from the pair spectrometer coincidence system, as compared with the observed coincidence rate during the run. Therefore, the coincidence could not be applied during the analysis, as had been planned.

The first analysis to be carried out was a comparison between the 8192 channel gamma spectra with target in and target out, summed over all neutron energies. There were several high energy lines which seemed to be target-connected, some of which corresponded to the capture lines from the 6.4 and 4.8 eV resonance levels reported by Kane.[2] In order to establish which, if any, of the gamma rays we observed could be attributed to capture, we examined the gamma spectra within sixteen neutron energy regions, including separate U^{235} resonances, and again compared the target-out spectra in each region. Here we encountered great difficulty because of poor statistics in the gamma spectra corresponding to single resonances, as well as high background. For lack of computer space, we used only 2000 channel analysis for these gamma spectra. However, in most of the neutron energy regions we examined, the number of counts per channel would not justify an expansion to the full 8000 channel resolution, even if it were otherwise feasible.

The peaks which were picked out by eye as being present in the target-in data and absent in the target-out data were very small, often less than 25 counts above background in area. This meant that some steps had to be taken to distinguish real peaks from statistical fluctuations. In the present analysis this was done arbitrarily by requiring a line to be present in more than one neutron energy group in order to be accepted as genuine. After subjecting all the observed gamma lines to this criterion, we then examined those

---

[1] Pegram Nuclear Physics Laboratories, NYO-73-243, UC-34 Physics, pp. 13-14.

[2] Walter R. Kane, Phys. Rev. Letters 25, 953 (1970).

that were left, to see whether they could be identified as capture gamma rays by their appearance in predominantly capture resonances and their non-appearance elsewhere. The results of this step were inconclusive. Most of the observed lines which appeared in one or more resonances also appeared at neutron energies between the resonances. The only lines which did not appear between resonances were those 1) at 5726 keV, observed in the 35 eV group and the 6.4 eV resonance; 2) a broad line between 5656 and 5659 keV, which appeared above 65 eV, as well as in the 35 eV group, the group containing the 12.4 and 11.7 eV resonances and possibly the 7.1 eV resonance, and 3) at 5437 keV, observed above 65 eV, in the 19.3 eV resonance, and possibly in the 12.4 and 11.7 eV resonance group. There are also suggestions of lines at 6488, 6227, 4970 and 4559 keV, but these are fairly doubtful at present.

G. Gamma-Ray Multipolarity Measurements for U^{235} and Np^{237} (J. Felvinci and E. Melkonian)

The multipolarity measurement planned and described in the 1969 Progress Report[1] was performed during the 1970 Nevis run. Two very well shielded 5" NaI detectors viewed a thick target in the neutron beam at 16 meters. A 500 mg/cm^2 U^{235} and a 230 mg/cm^2 Np^{237} sample were used for the experiments. Pulses from the two detectors and the TOF corresponding to them were recorded in two separate channels. The basic idea was to record the singles rate, leaving the coincidence rate to be determined by a subsequent program by requiring that the 2 different channels should have the same TOF value. In spite of heavy shielding, the background was very high and the counting rate limitation forced us to set the pulse height bias quite high, at around 3 MeV. Under these conditions we could not see any significant resonance structure in the Np^{237} experiment, although the U^{235} target gave the expected structure due to the higher γ energies. In the second part of the run, a hardware coincidence condition was imposed (30 nsec resolution) and this enable us to reduce the pulse height bias to around 1.5 MeV. Under these conditions both Np^{237} and U^{235} were run and both TOF and pulse height information were obtained. The Np^{237} data clearly shows most of the resonances determined by Asghar et al.[2] The yield of many of the resonances is not consistent with their previously measured Γ_n and Γ_γ values. At this point of the analysis it is not clear whether the differences are due to different spin states and consequently different cascades, or to the Porter-Thomas fluctuations of individual gamma rays between the different resonances. The latter effect would be magnified due to the limited γ-energy range measured.

The analysis of both Np^{237} and U^{235} data will continue and some information on the average γ-ray energies in individual resonances is expected.

---

[1] Pegram Nuclear Physics Laboratories, NYO-73-243, UC-34, Physics, pp. 14-15.

[2] Asghar et al., Phys. Letters 26B, 664 (1968).

H. Fission Cross Section of U^{235} (J. Felvinci and E. Melkonian)

During the 1970 Nevis run, the fission cross section of U^{235} was measured at 14 meters, using both a 200 mg/cm^2 and 7 mg/cm^2 third target. The range of neutron energies accepted was from 0.05 eV to 40 keV. In Fig. I.H.1 the fission yield between 10- 40 keV is shown and in Fig. I.H.2, the region between 17 eV and 22 eV can been seen. Efforts have been made to fit the fission yield in this region with a Doppler broadened single level Breit-Wigner formalism, and these fits are also shown on Fig. I.H.2. Analysis of the data continues and will be concentrated in the following three areas:

a. Normalizing the data to Deruyter's values between 7-11 eV[1]

b. Fitting the data with the Adler-Adler[2] multi-level formalism

c. Recalculating thick to thin ratios to identify differences between levels of different channels[3].

I. Fission Cross Section of U^{233} (J. Felvinci and E. Melkonian)

The fission cross section of U^{233} has been measured during the 1970 Nevis run. The target used was 120 μg/cm^2 thick U^{233} deposited on an aluminum foil. The TOF and the single fragment kinetic energy were both recorded event-by-event through the system described in the introduction. The target was located at 14 meters and the yield was obtained from 0.06 eV to 40 keV. There is considerable structure in the high energies (10- 40 keV) fission data, and this is reproduced in Fig. I.I.1. The yield was corrected by the known energy dependent neutron flux and normalized to Weston et al.'s data[4] at 2.3 eV to yield cross sections. The different resonances were fitted with single level Breit-Wigner formalism and a region around 15-30 eV is shown in Fig. I.I.2. It is planned that the cross section will be fitted by the Adler-Adler formalism, to yield the G and H values.

At the same time, the pulse height data was subdivided into 7 groups, as described in last year's report. The individual TOF spectra were plotted for each group and ratios were formed between the areas of resonances of the different groups. Any significant departure from equality would indicate the existence of channel effects. Detailed description of this method and the results will be presented at the Third Neutron Cross Sections and Technology Conference in March, 1971.

---

[1] A.J. Deruytter and C. Wagemans, Proceedings of the 2nd International Conf. on Nuclear Data for Reactors, Vol. I, p. 151. Vienna, IAEA, 1970.

[2] Adler & Adler, Proceedings of the 1st Conference on Neutron Cross Sections & Technology, Vol. II, p. 873. Washington, U.S.A.E.C., 1966.

[3] E. Melkonian and Mehta, Physics & Chemistry of Fission, Salzburg, IAEA, 1965.

[4] L.W. Weston et al., Nucl. Sci. & Eng. 34, 1 (1968).

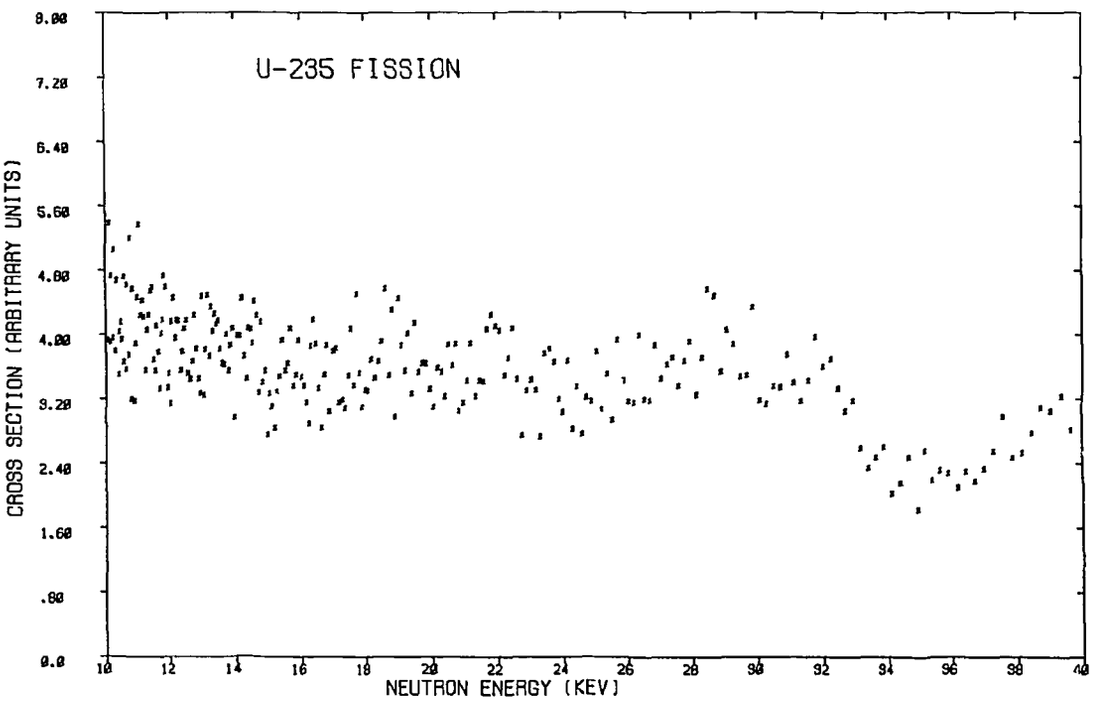

FIG. I.H.1 U^{235} FISSION CROSS SECTION (10 - 40 KEV)

(Dip at 35 keV due to aluminum in beam)

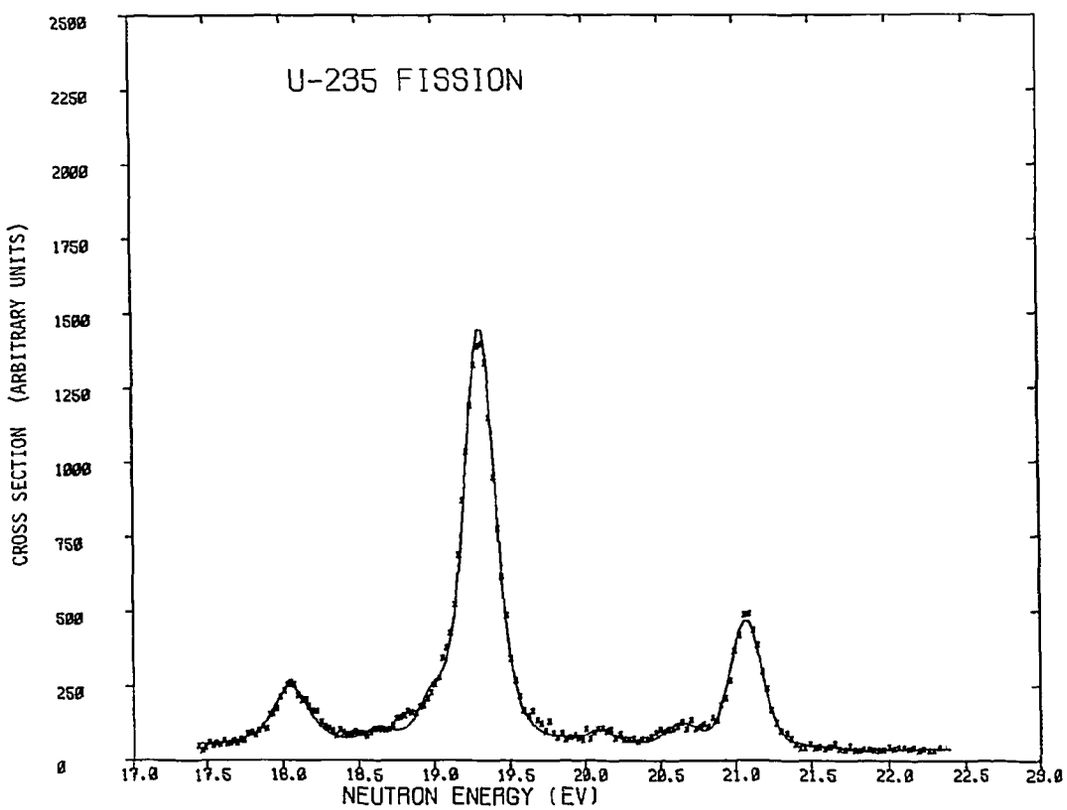

FIG. I.H.2 U^{235} FISSION BETWEEN 17 AND 22 EV

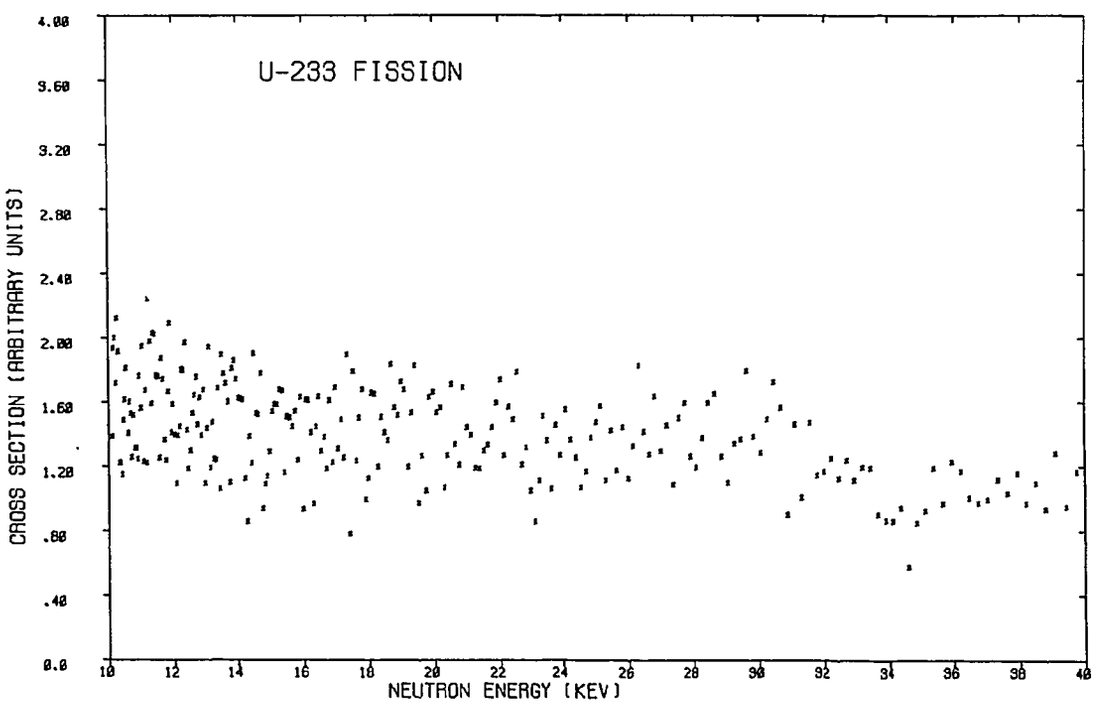

FIGURE I.I.1 U^{233} FISSION CROSS SECTION

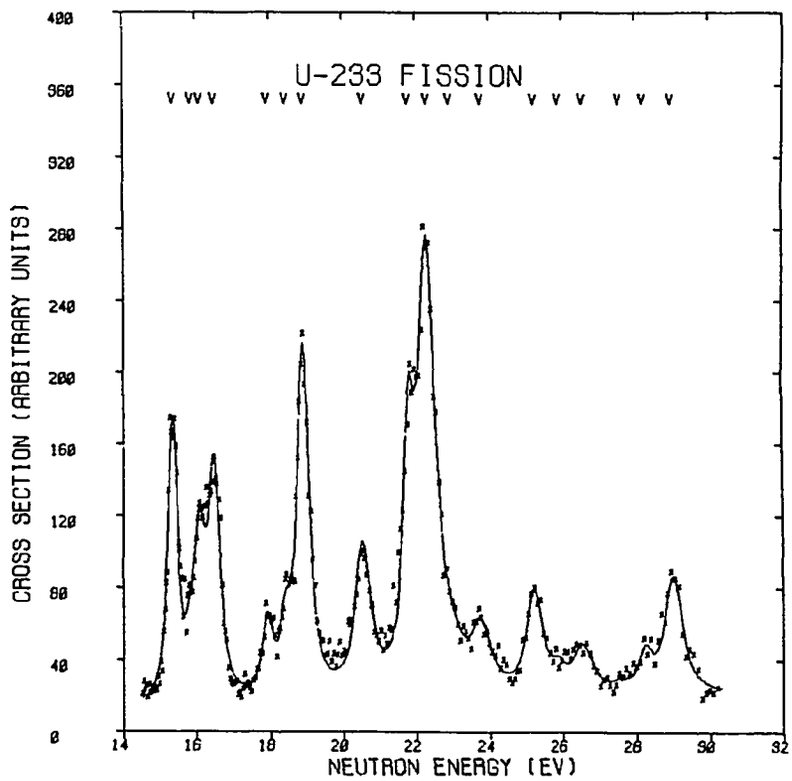

FIGURE I.I.2 U^{233} FISSION IN THE REGION 15 - 30 EV

J. Search for Delayed Fission Following Prompt Gamma Ray Emission in Fissile Nuclei (M. Derengowski, J. Felvinci and E. Melkonian)

The experiment so described in the previous progress report was performed in spring, 1970. The block diagram of the system is shown in Fig. I.J.1. The energies of the U^{235} fission fragment, the coincident γ-ray, the TOF of the neutron initiating fission and the time elapsed between the fission and γ-event were recorded. During the first part of the experiment, the time-to-amplitude converter (TAC) channel width was 3.7 nsec, while later it was reduced to 1.0 nsec (300 nsec full scale).

The prompt peak (i.e. fission and gamma ray coincident within the resolution time of the system (30 nsec) was seen and so was the expected flat background. There was an excess of events in the higher channels of the TAC, corresponging to delayed fissions (see Fig. I.J.2).

According to measurements by Elwyn and Ferguson[1] the lifetime of the U^{235} isomeric state is 67 nsec and has a $\sigma_{iso}/\sigma_{fiss} = 3 \times 10^{-4}$ at 2.2 MeV incident neutron energy. Their measurements on U^{233} indicate that this ratio is increasing for lower neutron energies.

The excess events in the TAC would correspond to a $\sigma_{iso}/\sigma_{fiss} = 0.15$ and a seemingly larger lifetime than that measured. At this point of the analysis, it is not certain whether these excess counts indicate an isomeric state or they are of spurious origin.

During the experiment all the γ-rays emitted up to 2 μsec after the fission event were also recorded on a 256 channel ADC. The ratio of these "coincident" fissions to all fissions was calculated and small differences were observed between several levels. As the gamma rays recorded were mostly prompt fission gamma rays, the spectrum of these could depend on a) the type of fragments being formed, b) the excitation energy being available. The gamma ray multiplicity as a function of the mass division shows a sawtooth dependence and has a small value at closed shell nuclei. Thus, changes in the mass distribution due to different fission channels could be reflected in the spectrum or yields of gamma rays.

The detailed analysis of this facet of the experiment is still in progress.

K. Slow Neutron Fission Cross Section of Th^{229} (J. Felvinci, J. Toraskar, and E. Melkonian)

The fission cross section of Th^{229}, one of the lightest of fissile nuclei, was measured during the 1970 Nevis run. The spin of Th^{229} is $5/2^+$ and thus, the compound nuclear states are expected to have spins 2^+ and 3^+ and the fission spectra should resemble U^{233} and Pu^{241}. Previous work on this isotope included the total cross section measurements of Coté et al.[2] and the

---

[1] Physics & Chemistry of Fission, IAEA, Viena, 1969, p. 457.

[2] R.E. Coté, H. Diamond and G.A. Gindler, BAPS 6, 417 (1961).

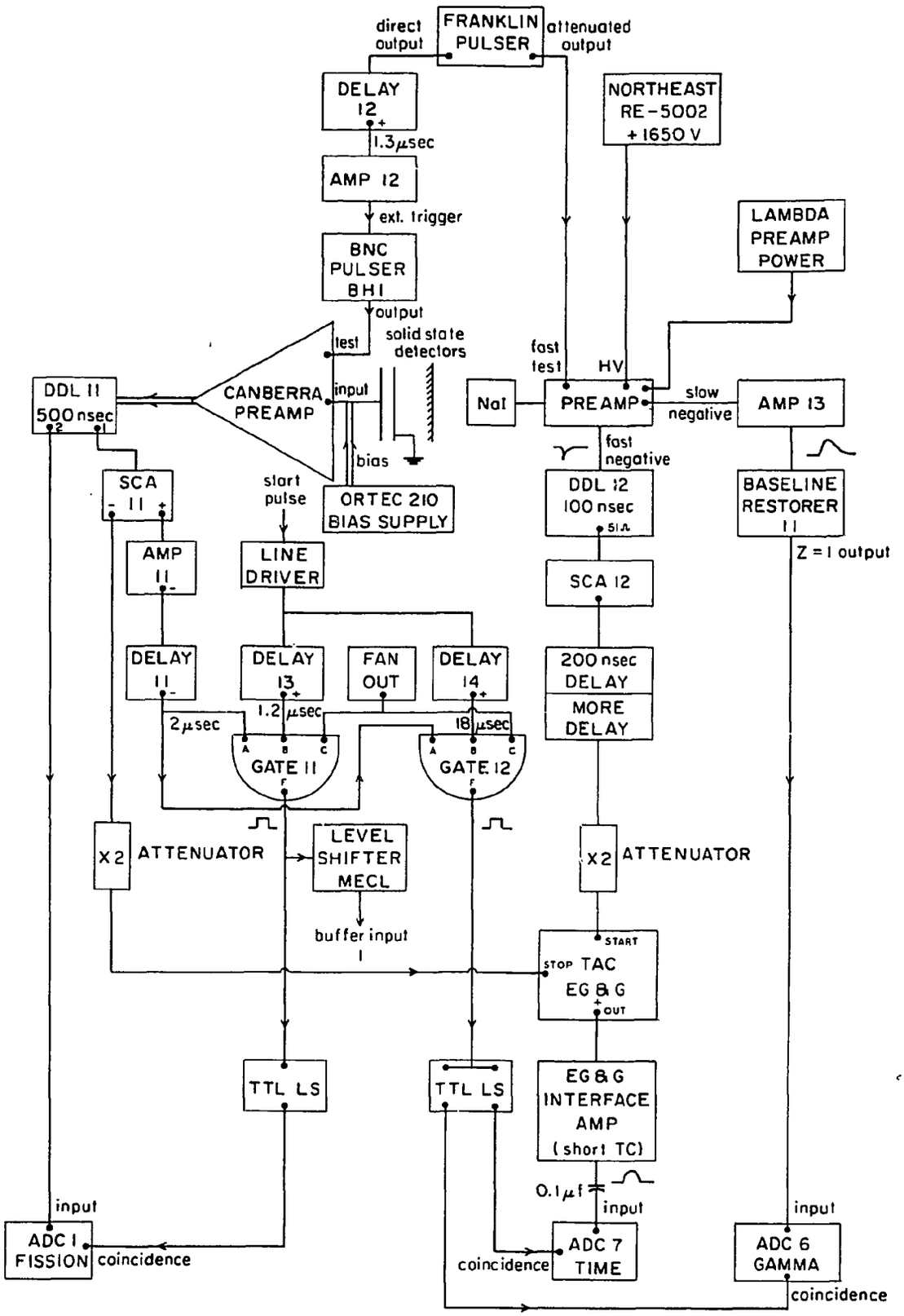

FIG. I.J.1

BLOCK DIAGRAM OF ISOMERIC STATE EXPERIMENT

DATA NOT FOR QUOTATION

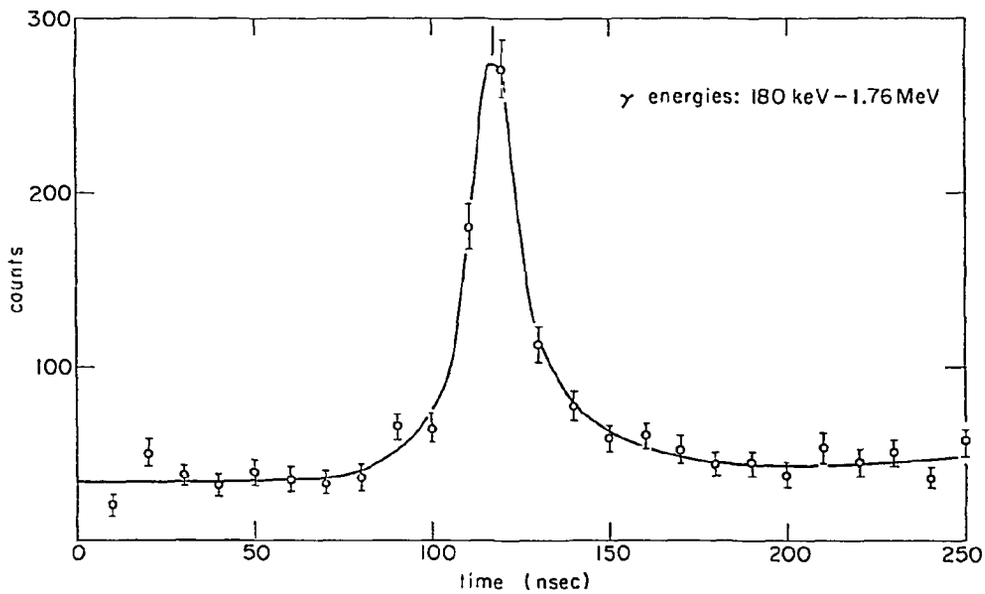

FIG. I.J.2 TIME DIFFERENCE BETWEEN GAMMA RAYS AND FISSION FRAGMENTS IN U^{235}

TABLE I.K.1

Parameters for Th^{229} fission

E_o(eV)	$\sigma_o\Gamma_f$(eVb)	σ_o Barns†	Γ(mV)$^+$	Γ_f mV
0.610	26.1 ± 2.4	6000 ± 460	47 ± 4	4.35
1.26	133.0 ± 7.1	4600 ± 1800	41 ± 16	29.0
1.44	16.8 ± 2.6			
1.72	24.7 ± 3.5	1500 ± 950	40 ± 25	16.5
1.96	54 ± 5	2150 ± 850	60 ± 25	25.1
3.18	52 ± 6			
4.16*	496 ± 21.2	3200 ± 830	140 ± 40	155
5.58	30 ± 6			
5.95	20 ± 5			
6.95	39 ± 7			
8.27	10 ± 4			
9.15	50 ± 9			
9.60	35 ± 8			
10.4	35 ± 8			
10.8	18 ± 6			
12.6	48 ± 10			
13.3	19 ± 7			
14.6	41 ± 10			
15.4	83 ± 15			
16.8	57 ± 13			
23.3	55 ± 14			
25.9	56 ± 15			
29.7	152 ± 26			
35.0	81 ± 20			
39.3	166 ± 30			
43.2	149 ± 30			
46.5	114 ± 27			
48.5	98 ± 25			
51.0	41 ± 16			

*Several resonances?

†BNL 325

fission measurements by Bollinger et al.[1]

The experiment, which was located at 12.05 meters on the B1 flight path had a thin 21 $\mu g/cm^2$, 99.95% pure Th^{229} target opposite a heavy ion solid state detector. The assembly was in a specially constructed thin-windowed fission chamber. In the second part of the run, a very thin, 14 $\mu g/cm^2$, 97.4% pure U^{235} target was mounted in place of the Th^{229} target and counted for purposes or normalization.

The TOF spectrum and the single fragment energy distribution were recorded for both of the targets with the system described in the introduction.

The neutron flux was determined by a Li^6 detector in the beam and also by the yield in the known U^{235} resonances. Fig. I.K.1 shows the cross section in arbitrary units from 1 eV to 5.8 eV. All the fission resonances seen by Bollinger et al. have been observed, and we have determined the position and $\sigma_o\Gamma_F$ values for 12 more resonances from 5 eV up to 51 eV (the low energy resonances below 1 eV reported by Konakhovich and Pevsner[2] were not seen). The $\sigma_o\Gamma_F$ values were determined from the relation

$$(\sigma_o\Gamma_F)_{Th} = (\sigma_o\Gamma_F)_U \left(\frac{N_{Th}}{N_U}\right)\left(\frac{E_{Th}}{E_U}\right)^{0.78} \frac{(\rho dx)_U}{(\rho dx)_{Th}} \cdot \frac{T_U}{T_{Th}}$$

where N is number of counts in the peak, E is the energy of the resonance, (ρdx) is the thickness of the target and T is the running time for normalized flux. For the levels where σ_o was known, Γ_F was calculated. Table I.K.1 shows these values.

The resonance at 4.16 eV is a complex system consisting probably of more than two levels. Single-level Doppler-broadened Breit-Wigner fits could not satisfactorily reproduce the experimental data. Multi-level fits were not yet implemented.

The TOF circuit cut off at 4.6 msec so that the cross section measurements extended down to only 0.036 eV. The ratio of the Th^{229} to the U^{235} cross section was determined at every channel and extrapolated down to 0.0253 eV assuming a 1/V dependence in Th^{229}. This procedure yielded 41 ± 5 barns. Calculations of the contribution from the higher lying levels (using the $\sigma_o\Gamma_F$ values from Table I.K.1) to the cross section at 0.0253 eV resulted in 28 barns. These results are not in serious disagreement with those of Gindler et al[3], who measured 30.5 ± 1.5 barns at thermal energies.

---

[1] L.M. Bollinger, H. Diamond and J.F. Gindler, BAPS 8, 370 (1963).

[2] Y.Y. Konakhovich and M.J. Pevsner, J. Atomic Energy 8, 39 (1961).

[3] J.E. Gindler, R.F. Flynn and J. Gray, Jr., J. Inorg. Nucl. Chem. 15, 1 (1960).

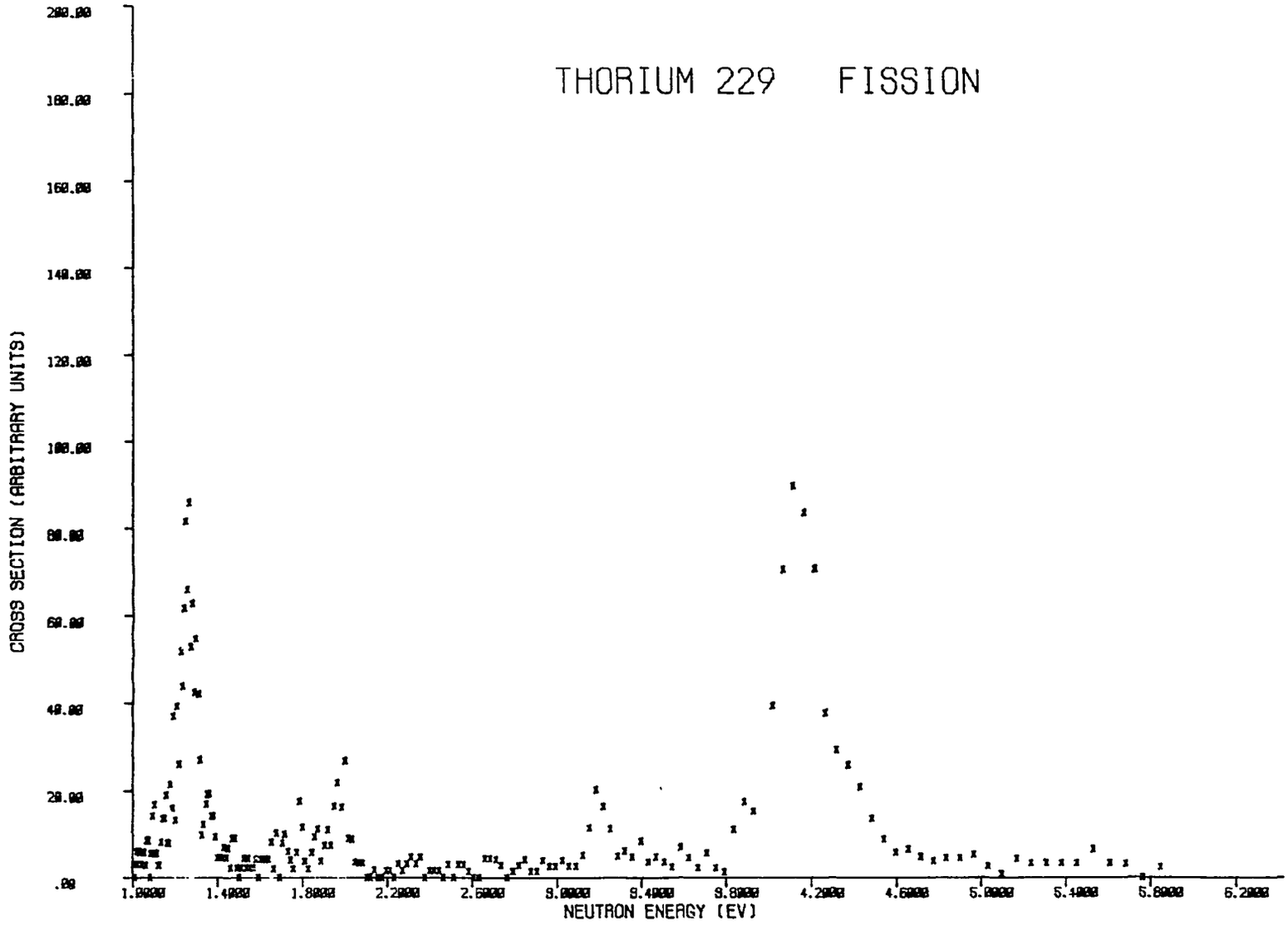

FIG. I.K.1 Th^{229} FISSION CROSS SECTION (1 - 6 EV)

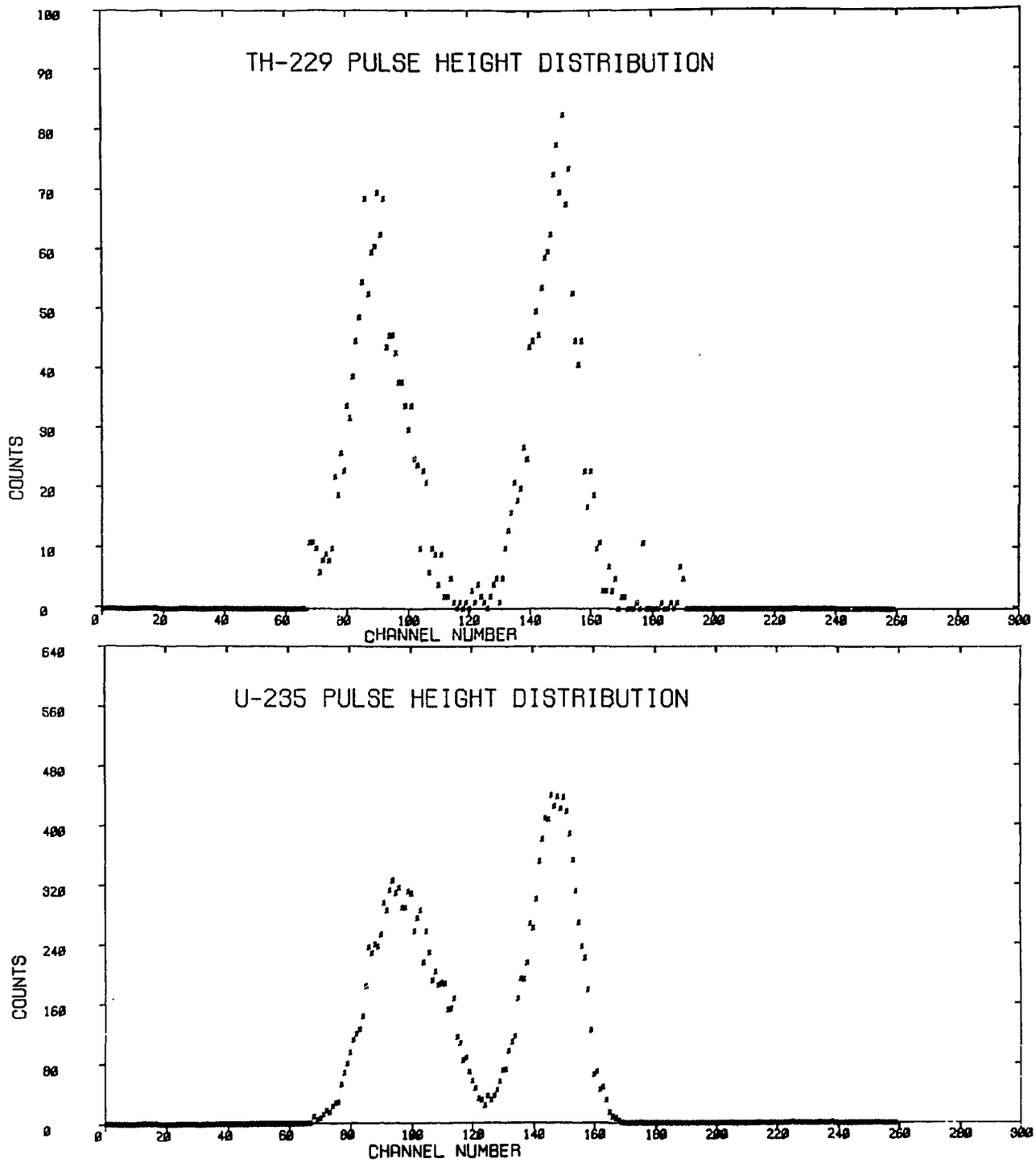

FIG. I.K.2

Th^{229} AND U^{235} PULSE HEIGHT DISTRIBUTION

The single fragment energy distribution is reproduced in Fig. I.K.2 for both Th^{229} and U^{235}. This shows a considerable tightening of the distribution of Th^{229} and a slight shift to lower average energies. The peak to valley ratio is increased over U^{235}. It should be pointed out that these spectra represent all the data, for all neutron energies. The average total kinetic energy for Th^{229} is approximately 160 MeV, which agrees with the trend among fissile nuclei.

II. KINETICS OF NEUTRON AND PHOTON GASES

A. Radiative Capture of 14 MeV Neutrons in Cu, Zr and Sb (M. Stamatelatos, L.J. Lidofsky, B. Lawergren)

14 MeV (n,γ) cross sections and high energy gamma ray spectra were measured for Cu, Zr and Sb. A coincidence-anticoincidence telescope-pair-spectrometer was used to detect and determine the energy of capture gammas. The resultant gamma spectra were compared with theoretical model predictions. Calculations using the semi-direct (collective) capture model yielded reasonable agreement in shape and magnitude. Cross sections obtained by integrating the gamma spectra for energies E_γ>14 MeV agreed with the values from previous activation measurements. It was concluded that a significant portion of the gamma spectrum following radiative capture of 14 MeV neutrons corresponds to decays directly to bound levels.

Element	Partial	Activation	For (Isotope)
Cu	2.4 ±.6 mb	2.56±.38 mb	Cu^{63}
Zr	2.8 ±.7 mb	≤4	Zr^{96}
Sb	5.1± 1.4 mb	15±3 mb	Sb^{123}

GULF RADIATION TECHNOLOGY
A Division of Gulf Energy and Environmental Systems Incorporated
San Diego, California

A. NEUTRON CROSS SECTIONS

1. Rhodium Resonance Parameters and Average Capture Cross Section (A. D. Carlson)

Measurements of the rhodium capture cross section up to 1 MeV have been completed. Below 1 keV, neutron resonance parameters have been obtained from capture and self-indication measurements. These parameters are shown in Table A-1. Most of the resonance parameters were obtained from area analysis. At low neutron energies shape analysis was used to determine the radiation widths for a number of weak resonances. Shape analysis was also used in conjunction with area analysis on the stronger resonances in order to permit spin determinations. The neutron width parameters obtained in this investigation are generally in agreement with those obtained by Ribon.[1] However, the average radiation width obtained here, 153 meV, is significantly smaller than that of Ribon, 171 meV. The results of both investigations indicate that there is no apparent dependence of the radiation width on the spin or parity of the level.

In addition to the resonances shown in Table A-1, a number of levels were observed which were either very weak or obscured by stronger resonances so that meaningful results could not be obtained. The generally small effects of these levels on the resonance parameter determinations for nearby resonances were calculated using the parameters of Ribon.

From 1-1000 keV measurements have been made of the average neutron capture cross section. These measurements are in satisfactory agreements with calculations of the capture cross section using $S_0 = 0.44 \times 10^{-4}$, $S_1 = 5.6 \times 10^{-4}$, $D_0 = 27$ eV and $I_\gamma = 153$ meV.

---

[1] P. Ribon, J. Girard and J. Trochon, "Statistical Properties of the Parameters of the Levels of ^{104}Rh," Nucl. Phys. A143, 130 (1970).

TABLE A-1

RHODIUM RESONANCE PARAMETERS

E_o(eV)	Γ_γ(MeV)	$2g\Gamma_n$(MeV)	J
1.259	154 ± 3	0.774 ± 0.01	
34.5	147 ± 18	0.024 ± 0.001	
44.6	-	0.005 ± 0.001	
46.8	145 ± 16	0.79 ± 0.04	
68.35	183 ± 46	0.30 ± 0.02	
83.5	-	0.012 ± 0.002	
95.75	154 ± 15	3.5 ± 0.2	
98.8	181 ± 90	0.09 ± 0.015	
110.9	167 ± 60	0.245 ± 0.015	
114.0	171 ± 70	0.17 ± 0.01	
125.6	142 ± 20	11.0 ± 0.5	
154.3	148 ± 10	105.0 ± 9.0	0
179.5	-	0.27 ± 0.02	
187.1	145 ± 12	57.0 ± 4.0	1
199.7	-	0.09 ± 0.02	
205.2	-	0.14 ± 0.02	
253.9	149 ± 15	51.0 ± 4.0	1
263.2	-	2.0 ± 0.13	
272.2	159 ± 9	90.0 ± 8.0	1
289.9	188 ± 26	33.0 ± 5.0	0?
313.1	-	0.4 ± 0.1	
319.6	150 ± 15	132.0 ± 15.0	1
327.7	-	1.0 ± 0.1	
354.1	-	0.2 ± 0.04	
362.7	-	0.8 ± 0.15	
366.3	-	3.4 ± 0.2	
373.9	-	0.73 ± 0.1	
376.7	-	0.22 ± 0.03	
388.5	-	0.39 ± 0.06	
406.1	161 ± 30	21.0 ± 3.0	1
435.3	141 ± 15	278.0 ± 39.0	1
443.8	-	0.43 ± 0.1	
447.0	-	0.33 ± 0.11	
449.9	-	5.8 ± 0.4	
472.9	-	1.7 ± 0.15	
486.5	-	2.1 ± 0.2	
492.0	-	4.6 ± 0.3	
504.7	-	0.9 ± 0.1	
526.0	-	1.3 ± 0.1	
555.1	150 ± 15	135.0 ± 30.0	1
581.3	-	4.2 ± 0.4	
604.3	-	4.0 ± 0.3	
620.3	-	9.4 ± 0.6	
645.7	151 ± 18	107.0 ± 20.0	1
663.0	-	9.8 ± 0.7	
676.5	-	4.5 ± 0.4	
683.1	-	5.9 ± 0.4	
691.5	164 ± 18	124.0 ± 9.0	1
701.0	145 ± 15	460.0 ± 35.0	1
726.9	-	1.0 ± 0.3	
740.9	-	3.2 ± 0.2	
759.0	-	4.2 ± 0.5	
782.0	153 ± 70	31.0 ± 6.0	
796.1	-	5.2 ± 0.4	
830.0	-	4.6 ± 0.6	
844.5	161 ± 13	229.0 ± 40.0	1
866.6	-	0.8 ± 0.2	
884.9	-	0.8 ± 0.2	
894.2	-	14.0 ± 1.3	
913.0	135 ± 20	72.0 ± 10.0	0
928.3	190 ± 90	82.0 ± 16.0	1?
954.0	-	36.0 ± 7.0	
968.6	-	1.0 ± 0.2	
988.9	-	1.2 ± 0.2	

The present measurements yield an infinite dilution resonance integral (0.5 eV - 1000 keV) of 1032 ± 10b. (This work is pertinent to request No. 228 in WASH-1144.)

2. Analysis of Average Capture Cross Sections (M. P. Fricke)

Some additional analysis has been made of our capture cross sections for Mo, Rh, Gd, Ta, W, Re, Au and ^{238}U which were measured previously[2] in the neutron energy region 1-1000 keV. The capture data at lower energies for the three monotopes and ^{238}U have been represented in terms of strength functions.[3] At higher energies, some additional investigations have been made of the energy dependence of the effective capture width appropriate for Hauser-Feshbach calculations. A more detailed treatment of the Fermi-gas form of the level density (appropriate at high excitation energies of the compound system) was found to substantially enhance the probability for neutron re-emission after a gamma-ray transition to a state above the separation energy.[3] This, in turn, causes the effective capture width to begin to decrease with increasing compound excitation energy much sooner than is predicted by conventional calculations. The radiative strength function then increases more slowly with excitation energy, in agreement with previous phenomenological indications.[4] Finally, our capture data for $^{238}U(n,\gamma)$ were used to make comparisons[3] to results of integral experiments on the fast critical reactor ZPR-3, Assembly 48. The eigenvalue calculated with these data is 0.9846, and that obtained with the ENDF/B-II values for $^{238}U(n,\gamma)$ is 0.9735. (These measurements are pertinent to request Nos. 223, 228, 274, 318, 331, 413 and 414 in WASH-1144.)

3. Measurements of the $^{10}B(n,\alpha)$ Cross Sections (S. Friesenhahn)

A program has been initiated to measure the $^{10}B(n,\alpha_0 + \alpha_1\gamma)^7Li$ and $^{10}B(n,\alpha_1\gamma)^7Li$ cross sections with a precision of 1% from 1 to 100

---

[2] M. P. Fricke et al., "Second International Conference on Nuclear Data for Reactors," Vol. II, p. 265, IAEA (Vienna), 1970.

[3] M. P. Fricke et al., Third Conference on Neutron Cross Sections and Technology, March 15-18, 1971, Knoxville, Tennessee (to be published).

[4] M. P. Fricke et al., "Second International Conference on Nuclear Data for Reactors," Vol. II, p. 281, IAEA (Vienna), 1970; and Phys. Letters 29B, 393 (1969).

keV and 3% from 100 keV to 1 MeV. These reactions will be observed using ion chambers, proportional counters and a Ge(Li) gamma spectrometer. A method has been developed to produce large-area, self-supporting source plates for the ion chambers. These source plates allow both the α and ^{7}Li reaction products to be observed, thus permitting the use of summing and coincidence techniques to improve the accuracy of electronic bias corrections. An ion chamber with an active area of 6,400 cm^2 is now under construction. (These measurements are pertinent to request Nos 28 and 29 in WASH-1144).

4. Fe and Aℓ (n,xγ) Cross Sections from 0.86 to 16.7 MeV Neutron Energy (V. Orphan, C. Hoot and J. John)

The (n,xγ) cross sections for Fe and Aℓ have been measured using an electron LINAC pulsed neutron source. The γ-rays were detected with an 80-cm^3 Ge(Li) detector, and the neutron energy E_n was determined by the time-of-flight technique. The two-parameter data were accumulated using an on-line computer. Integrated cross sections were deduced from differential cross sections measured at $\sim$125°. The cross sections for the strongest lines have high neutron energy resolution ($\sim$ 1% at 1 MeV), and grouped data were obtained for other lines. Results of some high-resolution measurements were illustrated in our previous NCSAC contribution.

Figure A-1 shows typical broad-group cross sections obtained for several γ-rays from Fe. The differential cross sections for the 1408-1412 keV doublet, the 1811 keV line and the 2599-2604 keV doublet are compared to several previous Van de Graaff measurements. In general, the present results are in very good agreement with the Texas Nuclear Corp. (TNC) data,[5] the measurements of Dickens,[6] and two measurements[7,8] near 14 MeV. The 1408 keV and 1811 keV cross

[5]P. S. Buchanan, "A Compilation of Cross Sections and Angular Distributions of Gamma Rays Produced by Neutron Bombardment of Various Nuclei," Report No. ORO 2791-28, Texas Nuclear Corporation (1969).

[6]J. K. Dickens and F. G. Perey, ORNL-4592, Oak Ridge National Laboratory (Sept. 1970).

[7]G. Clayeux and G. Grenier, "Spectres de Venvoi des Gammas Produits par des Neutrons de 14.1 MeV," Report No. CEA-R-3807, CEN-Saclay.

[8]F. C. Engesser and W. E. Thompson, J. Nucl. Energy 21, 487 (1967).

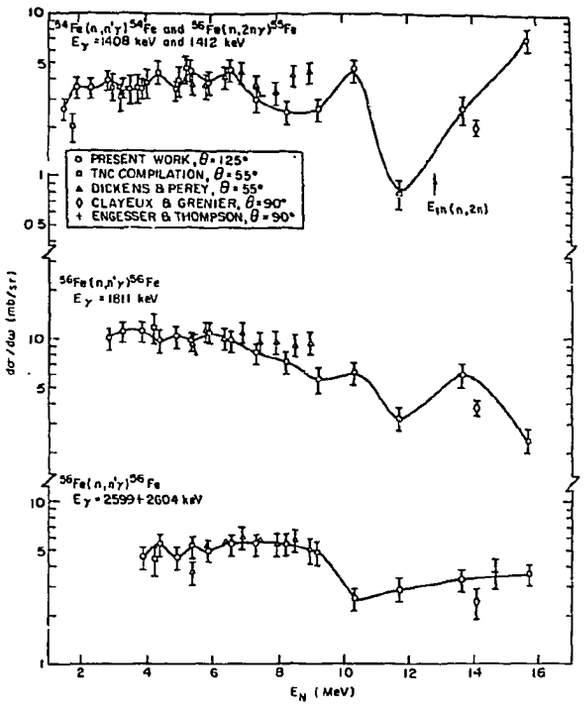

Fig. A-1. Differential gamma-ray production cross sections for neutron interactions with natural iron compared to previous data. The data points for the present work represent the average cross section over a neutron energy interval and are located at the midpoint of each interval. The solid line is simply a smooth curve connecting the present data points.

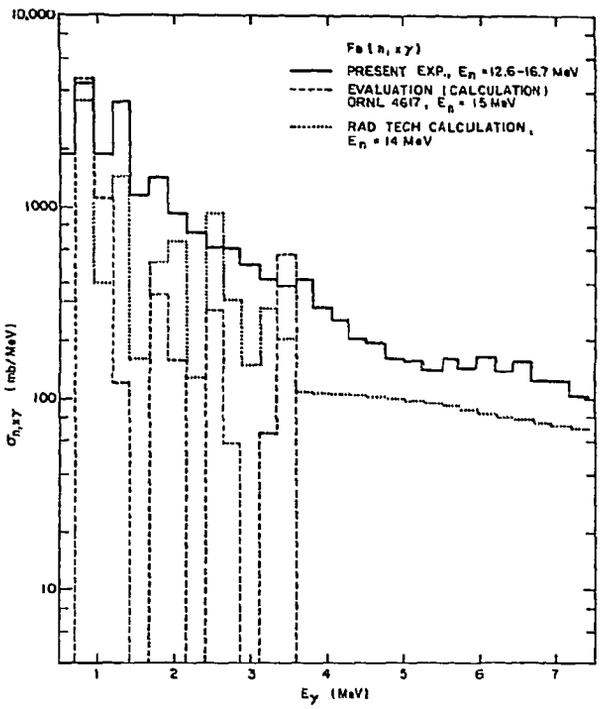

Fig. A-2. Total gamma production cross section for the neutron energy range 12.6 to 16.7 MeV compared to an evaluation and to a calculation including continuum.

sections are lower than the measurements of Dickens above about 8 MeV. The dip in the cross section for the 1408-1412 doublet near 12 MeV is a consequence of the threshold of the $^{56}Fe(n, 2n\gamma)^{55}Fe$ reaction at 12.85 MeV, above which there is a sharp increase in the yield of the 1412 keV γ-ray.

In some cases the γ-ray production cross sections measured for discrete lines represent only a fraction of the total γ-ray production cross section. The present results for Fe at the higher neutron energies illustrate this point. An examination of the Fe spectra reveals a significant number of weak γ-rays whose individual γ-ray production cross sections are too small to determine accurately but whose collective sum amounts to a significant fraction of the total γ-ray production cross section. Our γ-ray spectra corresponding to ten different neutron energy intervals have been unfolded using the MAZE1 code[9] in order to obtain the cross section for these weak γ-ray lines and continuum γ-rays. Figure A-2 shows the resulting total gamma-ray production cross section for Fe for the highest neutron energy interval, 12.6 to 16.7 MeV. The cross section for the sum of discrete and continuum γ-rays is given for 240 keV wide γ-ray energy intervals. These measured cross sections are compared with a calculated γ-ray production cross section which appeared in the most recent iron evaluation.[10] Also shown in this figure is the result of a Rad Tech calculation[11] using a simple statistical-model treatment. Contributions from (n, n') and (n, 2n) reactions and a limited amount of information on discrete level-excitation functions taken from Ref. 10 have been included in this calculation. As can be seen, the "continuum" contributions included in the calculation of Ref. 11 but absent in the evaluation constitute an important part of the total γ-ray production cross section. In fact, the experimental measurement shows that the continuum contribution to the cross section is about a factor of 3 greater than that from resolved lines for the neutron energy interval 12.6 to 16.7 MeV. (This work pertinent to request Nos. 64, 104, 105 and 106 in WASH-1144.)

---

[9]H. Kendrick and S. M. Sperling, "Numerical and Experimental Studies of Spectral Unfolding, Vol. II Unfolding with the MAZE1 System," Gulf Radiation Technology Report Gulf-RT-10486 (April 1, 1970).

[10]S. K. Penny and W. E. Kinney, "A Re-Evaluation of Natural Iron Neutron and Gamma-Ray Production Cross Sections," Oak Ridge National Laboratory Report ORNL-4617.

[11]M. P. Fricke, private communication, 1971. Calculations were made using the code SPECT10 of P. G. Young (unpublished).

5. Test of ENDF/B Cross Sections by Thermal Benchmark Calculations (E. L. Slaggie)

As a test of ENDF/B cross sections, thermal benchmark calculations have been performed[12] for eight water-moderated critical assemblies. Calculated reactivities for ^{235}U fueled systems are slightly low, differing from experiment by about one percent. Results for ^{239}Pu systems show calculated reactivities to be excessive, in one case by more than 2.5 percent. While the results for the ^{235}U systems can be regarded as satisfactory for this type of calculation, the disagreement in the case of the ^{239}Pu systems appears to be significant. A variety of checks were performed to reduce the likelihood that the discrepancies arise from inadequacies in the calculational methods. The possibility remains on the basis of these results that the ENDF/B ^{239}Pu thermal cross sections (both Version I and Version II) may be excessively reactive.

[12] E. L. Slaggie, "Thermal Benchmark Calculations for Water-Moderated Uranium- and Plutonium-Fueled Systems," USAEC Report Gulf-RT-10337, Gulf Radiation Technology, January 29, 1971.

IDAHO NUCLEAR CORPORATION

A. CROSS SECTIONS

1. Total Neutron Cross Section Measurement of ^{244}Cm (T. E. Young, F. B. Simpson and O. D. Simpson, INC; J. A. Harvey and N. Hill, ORNL; R. W. Benjamin, SRL)

Transmission measurements have been made on two samples of ^{244}Cm using the Oak Ridge Electron Linear Accelerator. The oxide samples used weighed approximately 34 and 6 mg and were prepared at ORNL. Measurements extended from the thermal energy region to several keV. Preliminary views of the data indicate that we will be able to obtain resonance parameters up to six or seven hundred eV. (Pertinent to Request 499, Priority II, Wash. 1144.)

2. Preparations for the ^{245}Cm Fission Cross Section Measurements (F. B. Simpson and L. G. Miller, INC; C. D. Bowman and J. Brown, LRL)

Checkout procedures have been completed on the gas scintillation chamber with alpha and spontaneous fission sources in preparation for the fission cross section measurement of ^{245}Cm. Good alpha discrimination has now been obtained. The next phase of the program calls for checking the fission chamber on the LRL accelerator using a ^{235}U fission foil in the presence of a high alpha background. (Pertinent to Request 506, Priority I, Wash. 1144.)

3. The Total Neutron Cross Sections of Curium 243, 244, 245 and 246 from 1-30 eV (J. R. Berreth and F. B. Simpson)

Analysis of the MTR fast chopper transmission data of three curium samples has been completed. The three samples contained high enrichments of ^{244}Cm (~94%) with varying amounts of curium 243, 245 and 246. Reich-Moore multilevel resonance parameters have been obtained for the 243 and 245 isotopes below 30 eV. Single-level parameters were determined for the 244 and 246 isotopes over the same energy region. The resonance parameters obtained are given in Table A-1. The theoretical total neutron cross sections calculated from these resonance parameters were Doppler broadened assuming an effective temperature of 320°K, and are shown in Figures A-1 - A-4. (Pertinent to Requests 496, 497, 499, 505, 506 and 509, mostly Priority I, Wash. 1144.)

TABLE A-1

Resonance Parameters of the Cm Isotopes

Isotope	E_o eV	Γ_n^o meV	Γ_γ meV	Γ_{f1} meV	Γ_{f2} meV
^{243}Cm	1.500	0.218	40	-100	350
	2.280	1.26	40	225	325
	3.095	0.42	40	-130	
	3.345	0.16	40	80	
	3.81	0.40	40	-110	
	5.40	0.35	40	150	
	5.97	1.57	40	-150	1.000
	8.80	0.31	40	-300	
	10.23	1.55	40	100	1400
	11.07	1.00	40	- 90	
	14.55	0.25	40	250	
	15.65	0.44	40	-250	
	21.68	1.11	40	250	
	24.44	0.56	40	-150	
	25.84	0.56	40	150	
^{244}Cm	7.67	3.57	35		
	16.77	0.40	40		
	22.76	0.17	40		
^{245}Cm	1.962	0.224	40	-285	
	4.68	0.96	40	375	
	9.17	0.22	40	-150	
	11.34	0.21	40	130	
	13.88	0.09	40	-170	
	16.01	0.32	40	400	
	21.34	0.64	40	-500	
	24.74	0.73	40	220	
	27.39	0.17	40	-230	
	29.35	0.70	40	400	
^{246}Cm	4.316	0.16	35		
	15.29	0.14	35		

NOTE: Γ_γ was assumed in all cases except for the 7.67 eV ^{244}Cm and 4.316 eV ^{246}Cm resonances.

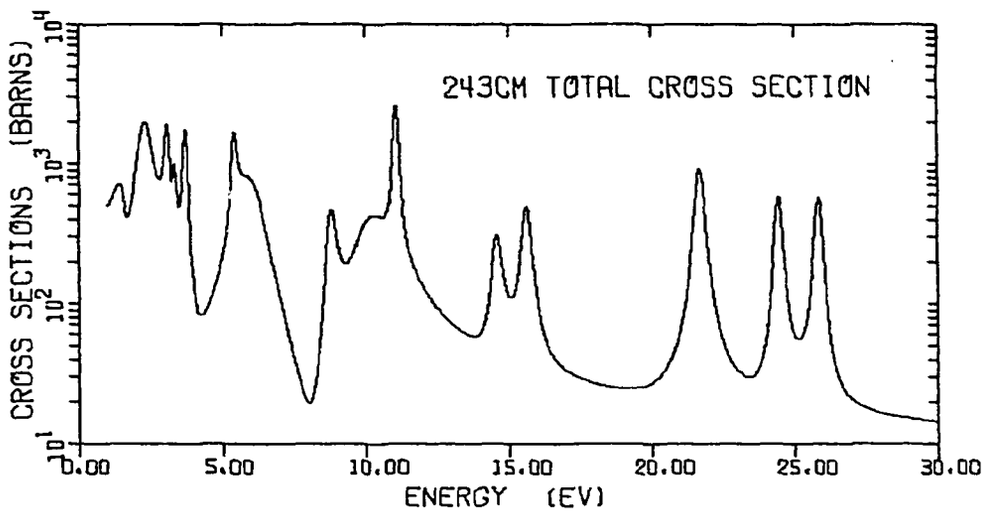

Figure A-1 The total neutron cross section as a function of neutron energy. This theoretical curve was calculated using the resonance parameters of Table A-1 and an effective temperature of 320°K.

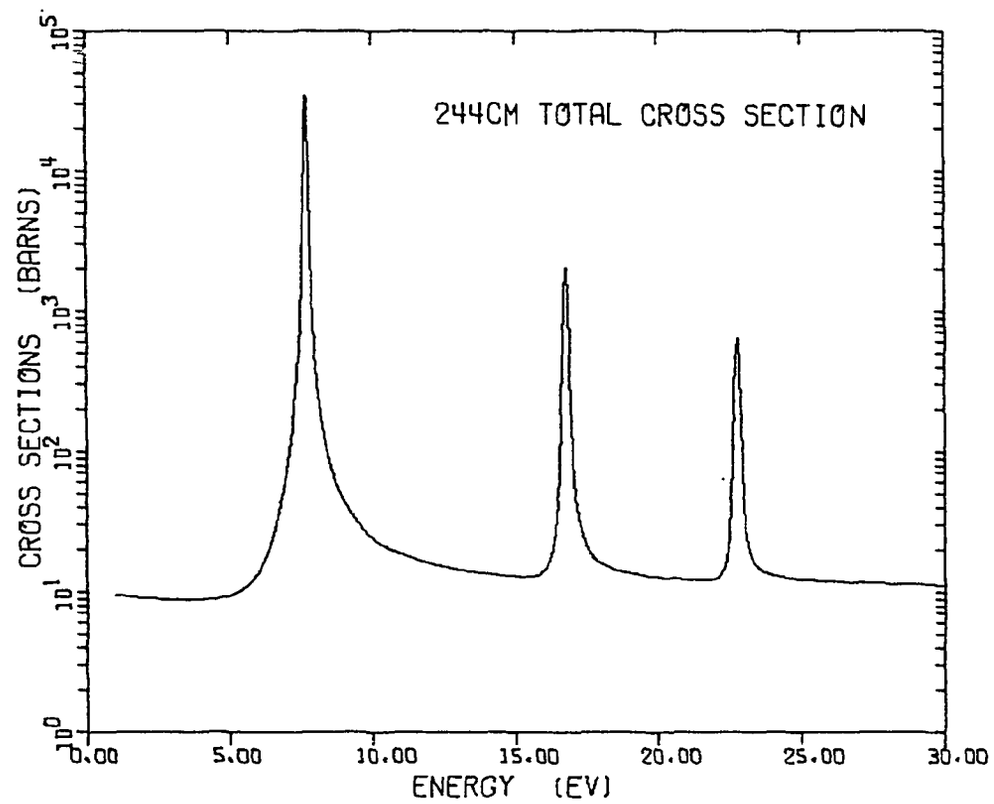

Figure A-2 The total neutron cross section as a function of neutron energy. This theoretical curve was calculated using the resonance parameters of Table A-1 and an effective temperature of 320°K.

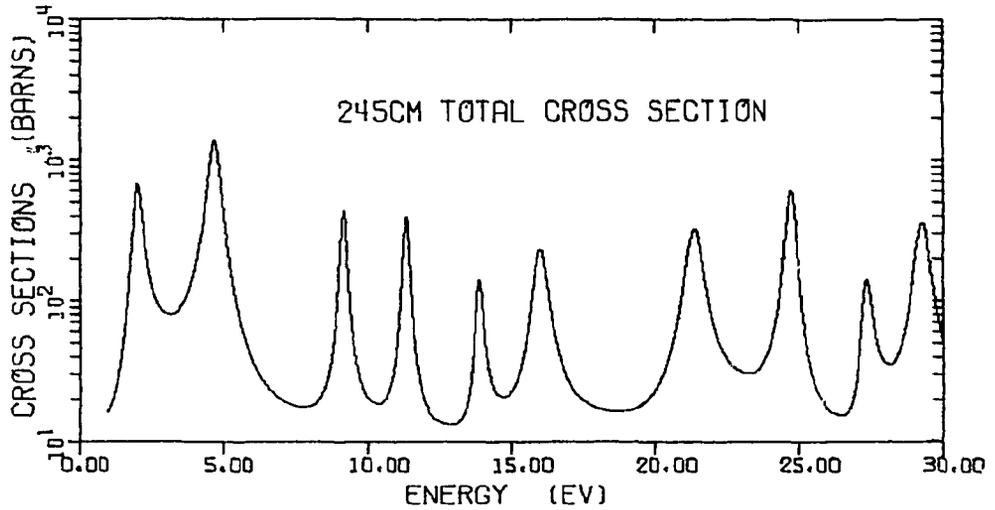

Figure A-3 The total neutron cross section as a function of neutron energy. This theoretical curve was calculated using the resonance parameters of Table A-1 and an effective temperature of 320°K.

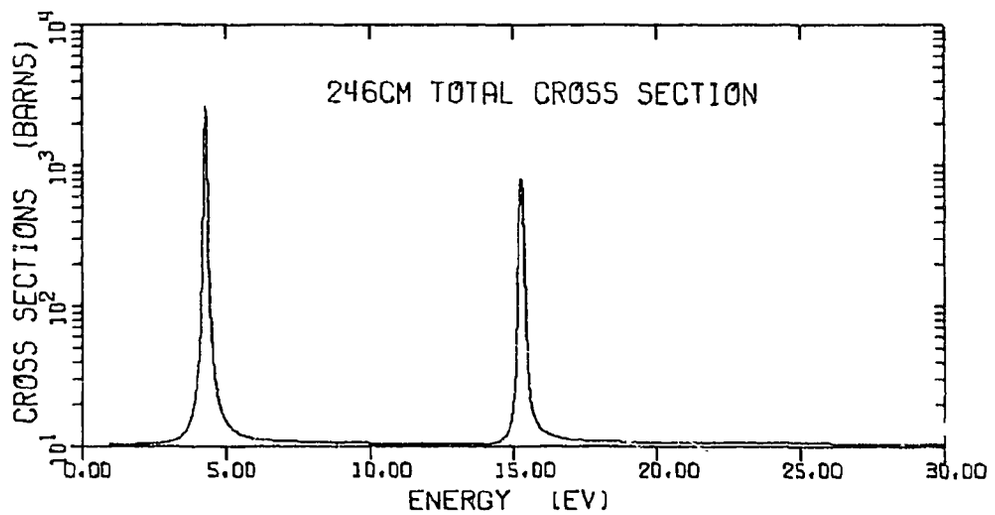

Figure A-4 The total neutron cross section as a function of neutron energy. This theoretical curve was calculated using the resonance parameters of Table A-1 and an effective temperature of 320°K.

B. CROSS SECTION FITTING TECHNIQUES (J. R. Smith, O. D. Simpson, N. H. Marshall and J. W. Codding, Jr.)

The Automated Cross Sections Analysis Program (ACSAP) is being prepared for general release. ACSAP has become a very versatile program. Its facility for handling and comparing large data sets with theoretical calculation is as valuable as its iterative fitting capabilities. A paper describing the versatility of ACSAP was presented at the Third Conference on Neutron Cross Sections Technology at Knoxville, March 15-17, 1971.

The capabilities of ACSAP are being utilized to derived resonance parameters for the fissile nuclei ^{235}U and ^{239}Pu for Version III of ENDF/B.

An area analysis routine is being added to ACSAP. When fully implemented this routine will give the user a choice of shape, area, or peak fitting techniques. These can be mixed, if desired, in one submission to the computer. (Pertinent to Request 449, Priority I, Wash. 1144.)

C. INTEGRAL CROSS SECTION MEASUREMENTS IN THE CFRMF (J. J. Scoville, Y. D. Harker, D. A. Pearson and R. G. Nisle)

Relative capture cross section integrals for a variety of materials have been measured in the Coupled Fast Reactivity Measurement Facility at Idaho. The spectral measurements and calculations are reported in the last NCSAC meeting[1] along with earlier activation and reactivity measurements. Listed in Table C-1 are the activation measurements completed since that meeting. The calculated ratios are derived from 1) semi-empirical calculations by Benzi, et al.[2], 2) experimental data listed in BNL-325[3], and 3) evaluated data as listed in ENDF/B Version II data file.[4] (Pertinent to Requests 382 and 414, Priority I, Wash. 1144.)

---

1. R. E. Chrien, "Reports to the AEC Nuclear Cross Sections Advisory Committee", Dec. 1, 1970, BNL 50276 (T-603), NCSAC-33.
2. V. Benzi and G. Reffo, CCDN-NW/10, ENEA Neutron Data Compilation Centre (December 1969) p. 6.
3. M. D. Goldberg, et al., "Neutron Cross Sections", BNL-325, 2nd ed. Suppl. No. 2 (1966).
4. ENDF/B Version II data file.

TABLE C-1

Spectrum Averaged Cross Sections

Reaction	$\bar{\sigma}/\bar{\sigma}$ Au(n,γ) Measured	Calculated	
$^{99}Tc(n,\gamma)^{100}Tc$	0.85 ± 0.14	0.83†	
$^{107}Ag(n,\gamma)^{108}Ag$	1.04 ± 0.13	0.90[2]	
$^{109}Ag(n,\gamma)^{110}Ag$	1.25 ± 0.18	1.12[2]	
$^{115}In(n,\gamma)^{116}In$	0.68 ± 0.06	0.42[2]	
$^{133}Cs(n,\gamma)^{134m}Cs$	0.096 ± 0.006	0.75[2]††	
$^{141}Pr(n,\gamma)^{142}Pr$	0.19	0.14[2]	0.16[3]
$^{165}Ho(n,\gamma)^{166g}Ho$	1.46 ± 0.21	2.04[3]	
$^{169}Tm(n,\gamma)^{170}Tm$	0.70 ± 0.04		
$^{238}U(n,\gamma)^{239}U$	0.625 ± 0.12	0.574[4]	
$^{235}U(n,f)$	3.21 ± 0.48	3.79[4]	
$^{238}U(n,f)$	0.130 ± 0.020	0.147[4]	

†Value determined from this work based upon calculated cross sections on odd-even nuclei determined by Benzi.

††One should note that the calculated cross section is for the general reaction $^{133}Cs(n,\gamma)^{134}Cs$ rather than one specified.

D. NEUTRON CAPTURE GAMMA-RAY STUDIES USING THE 2-keV NEUTRON BEAM FACILITY (R. C. Greenwood and C. W. Reich)

Analysis of the prompt gamma-ray spectra resulting from 2-keV neutron capture in natural tungsten, ^{182}W and ^{183}W and from thermal neutron capture in natural tungsten and ^{183}W has now been completed. Of particular interest to fast reactor shielding problems involving tungsten is the question of how the keV-neutron capture spectra compare with the thermal-neutron capture spectrum. In Figure D-1 are shown the higher-energy portions of the thermal and 2-keV neutron capture gamma-ray spectra obtained from a natural tungsten target. As is obvious from Figure D-1 there are gross differences in these spectra. A contributing factor to these spectral shape differences is that the thermal neutron capture spectrum from tungsten is principally composed of structure from

the $^{182}W(n,\gamma)$ and $^{186}W(n,\gamma)$ reactions, while the 2-keV neutron capture spectrum from tungsten is dominated by the $^{183}W(n,\gamma)$ reaction.

In order to obtain a quantitative comparison between these spectra, a method has been developed which will enable us to convert our 2-keV neutron-capture gamma-ray intensities into absolute intensities (e.g., in number of gammas produced per 100 neutrons captured). This will make it possible for the first time to make a direct comparison of the absolute intensities of the capture gamma radiation in 2-keV capture and in thermal-neutron capture. This method, as applied to the specific case of our data on tungsten, is described below.

First, considering the $^{183}W(n,\gamma)$ reaction, absolute thermal neutron capture gamma-ray intensities can be obtained by combining our data with Rasmussen's thermal-neutron capture data to obtain

For natural W

$I_\gamma(6144.1 + 6190.6) = 5.90$ γ's/100 neut. capt.
$I_\gamma(7299.9 + 7411.1) = 0.536$ γ's/100 neut. capt.

For ^{183}W

$I_\gamma(7299.9 + 7411.1) = 6.75$ γ's/100 neut. capt.

In order to obtain absolute intensity values for the primary 2-keV neutron capture gamma rays we note that, if all the transitions which populate the ground state band of ^{184}W were observed, it would be possible to obtain a conversion factor C to convert the relative I_γ values into absolute I_γ values as follows:

$$100\ \gamma\text{'s/100 neut. capt.} = C \sum_{\text{all}} \text{rel. } I_\gamma(\text{transitions which populate g.s. band}) \quad (1)$$

In this case, the vast majority of these transitions will be secondary transitions resulting from decay of levels in ^{184}W with energies between 900 keV and 3 MeV. It is generally not possible, from experimental considerations, however, to identify all of these secondary transitions Instead then, we choose to identify as many of the stronger of these transitions as is feasible. If enough of these secondary transitions are included, it seems a reasonable assumption to suppose that

$$\sum_{\text{many}} I_\gamma^{\text{thermal}} \text{ (second. trans. pop. g.s. band) = constant) =}$$

$$\sum_{\text{many}} I_\gamma^{\text{2-keV}} \text{ (second. trans. pop. g.s. band)} \qquad (2)$$

where the same transitions are involved in both sums. This procedure is illustrated in Table D-1. From Table D-1 we note that (1) 50% of all the secondary transitions populating the ground-state band are included in the sum, and (2) while there are significant changes in the individual thermal and 2-keV intensities of some of these secondary transitions, the overall intensity pattern is similar for both thermal and 2-keV neutron capture. This suggests that a reasonable conversion factor, from relative to absolute 2-keV neutron capture gamma-ray intensities, can be obtained using this technique. With this conversion factor we obtain, for capture of 2-keV neutrons in ^{183}W

$$I_\gamma^{\text{2-keV}} \text{ (7302.0 + 7412.9) = 4.00 } \gamma\text{'s/100 neut. capt.}$$

Absolute gamma-ray intensities for 2-keV neutron capture in natural tungsten are obtained from this $^{183}W(n,\gamma)$ data using the appropriate 2-keV neutron capture cross sections (from BNL-325). Thus we obtain for 2-keV neutron capture in natural tungsten

$$I_\gamma^{\text{2-keV}} \text{ (7302.0 + 7412.9) = 2.43 } \gamma\text{'s/100 neut. capt.}$$

With these conversion factors (from relative to absolute intensities) we are thus able to quantitatively compare the thermal and 2-keV neutron capture gamma ray spectral data. A comparison of the prompt gamma-ray intensities from the $^{NAT}W(n,\gamma)$ reaction down to an energy of 4.5 MeV is shown in Table D-2. (Primary capture gamma rays are however observed in these spectra down to 23.1 MeV.) From these data, the observed primary gamma rays observed in the thermal and 2-keV neutron capture spectra account for ≈38% and ≈28% of the primary capture gamma-ray intensity, respectively. (Pertinent to Request 322, Priority I, Wash. 1144.)

TABLE D-1

Intensities of low-energy capture gamma-ray transitions resulting from thermal- and 2-keV neutron capture in ^{183}W.

Gamma-Ray Energy (keV)	Thermal-neutron capture I_γ (γ's/100 neut. capt.)	Thermal-neutron capture rel. I_γ	2-keV neutron capture rel. I_γ
724	1.54	14.4	17.9
757	2.34	21.9	17.0
(763+769)	1.48	13.8	18.8
792	10.7	100	100
(891+894)	11.5	107.9	81.0
903	11.0	103	96.2
1010	3.09	28.9	26.4
1121	1.20	11.2	8.3
1275	2.74	25.6	11.2
(1313+1319)	1.82	17.0	15.7
1386	2.19	20.5	8.7
1430	0.91	8.5	9.5
SUM	50.5	472.7	410.7

TABLE D-2

Comparison of Prompt Gamma-Ray Intensities
Resulting from 2-keV and Thermal Neutron Capture in ^{183}W

Gamma-ray Energy (keV)[a]	Product Nucleus	I_γ (γ/100 neut. capt.) Thermal Neutrons	2-keV Neutrons	Gamma-ray Energy (keV)[a]	Product Nucleus	I_γ (γ/100 neut. capt.) Thermal Neutrons	2-keV Neutrons
7411.1	184	0.43	1.13	5124.1			0.09
7299.9	184	0.10	1.29	5116.6	184	0.10	0.14
6508.4	184	0.07	0.52	5089.0	185	0.09	0.14
6408.5	184	0.32	0.63	5042.9	183,4		0.33
6289.8	184	0.16	0.97	5023.1	184		0.24
6190.6	183	4.35	0.48	5016.0	184	0.12	0.15
6144.1	183	1.57	1.11	4994.3	184		0.18
6091.5	184		0.41	4986.8	185		0.29
6024.3	184	0.27	0.16	4973.0	184		0.10
5982.4	183,4		0.92	4952.9	184		0.11
5796.8	184	0.14	0.72	4930.3	185	0.08	
5784.8	184		0.46	4928.1	185		0.73
5753.8	185	0.05	0.26	4902.3	183,4		0.28
5731.5	185		0.29	4893.8	184		0.31
5700.3	184		0.24	4880.3	184	0.07	0.12
5661.6	185		0.58	4858.2	183,4		0.26
5637.9	184		0.33	4837.8			0.10
5604.0	184		0.20	4817.3			0.07
5551.7(?)			0.13	4797.5	184		0.07
5534.3	184		0.16	4782.4	184		0.25
5517.1			0.13	4757.6	183,4		0.24
5465.8	187	0.11	0.13	4747.2	187	0.12	0.30
5400.4	184		0.15	4719.6	183,4	0.20	0.39
5382.3	184		0.25	4706.0	183,4	0.04	0.24
5375.9	184		0.18	4689.7	184,7		0.29
5353.8		0.03		4684.5	187	1.29	
5349.9	184		0.08	4650.2	184,5,7	0.36	0.46
5320.8	187	2.77	0.49	4645.2	184		0.23
5315.4	184		0.30	4635.4	183	0.12	0.31
5308.4	184		0.17	4626.7	187	1.05	
5302.3	184		0.17	4611		0.04	0.25
5284.9	184	0.09	0.18	4597.7	184		0.20
5261.8	183,7	3.93	0.29	4574.5	187	0.81	
5256.3	183		0.21	4569.3	183,4		0.14
5243.3	184	0.06	0.35	4563.4		0.25	
5227.1	183(?)	0.03		4557.9	183	0.23	
5219.6	184		0.07	4534.2	183,5	0.11	0.24
5191.2	184		0.22	4525.9		0.05	
5164.5	183,4	1.80	0.46	4518.0	183,4	0.38	0.28
5142.2		0.04	0.12	4509.1		0.09	

a. In cases where the line is seen in both thermal and 2-keV neutron capture the thermal neutron capture line energy is given here, the 2-keV neutron capture lines have energies which are 2 keV higher than these.

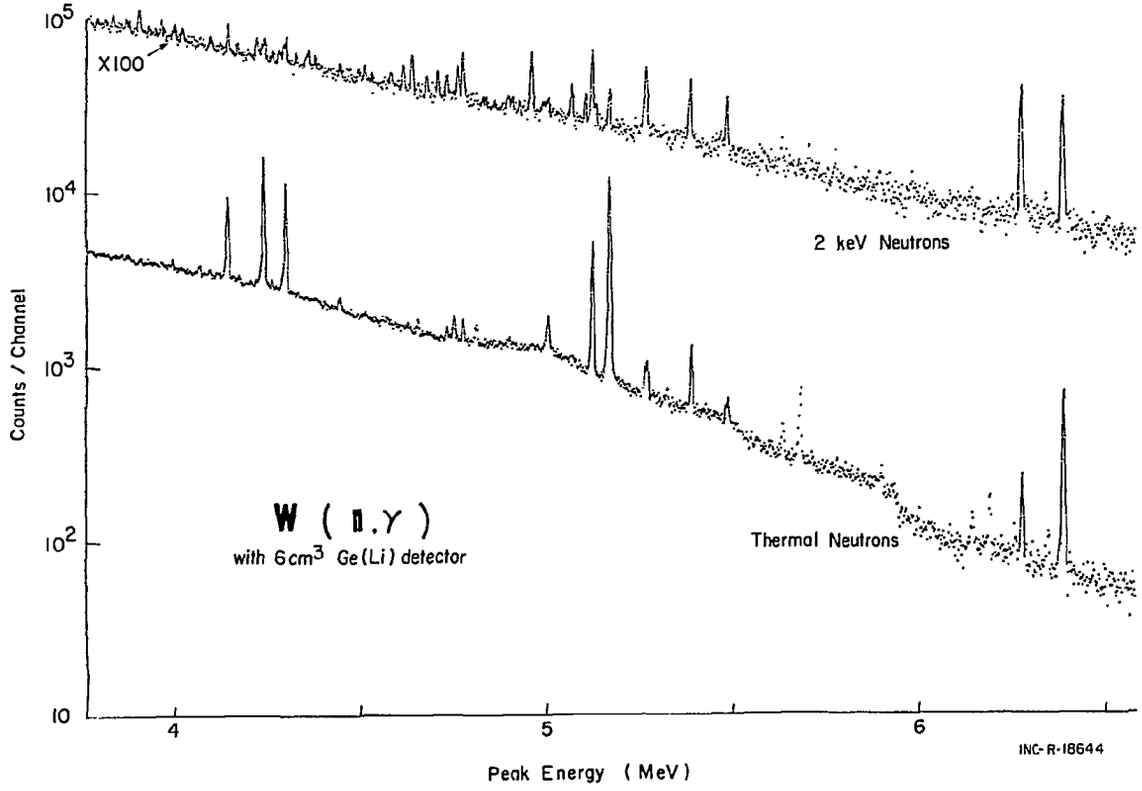

Figure D-1 The high-energy portions of the prompt gamma-ray spectra resulting from capture of thermal and 2-keV neutrons in tungsten. The peaks observed in this spectrum are principally double-escape peaks and hence the prompt gamma-ray energies are 1.022 MeV higher

LAWRENCE RADIATION LABORATORY

1. Photoneutron Cross Sections for ^{23}Na and ^{25}Mg in the Giant-Resonance Region (R. A. Alvarez, B. L. Berman, S. C. Fultz, D. R. Lasher, and T. W. Phillips)

^{23}Na and ^{25}Mg are among the deformed light nuclei whose photoneutron cross sections we have measured in recent years with the monochromatic-photon facility in LRL's 30 MeV linear electron accelerator. The structure in the giant resonance that we have been able to observe with the 200-keV resolution of the linac is qualitatively different from that in the neighboring even-A nuclei we have studied with the same technique (^{24}Mg, ^{26}Mg, and ^{28}Si). The latter nuclei exhibit strong intermediate structures with a number of peaks and shoulders in their excitation curves that have widths and spacings of a few hundred kilovolts. ^{23}Na and ^{25}Mg, on the other hand, exhibit smoother appearing giant-resonance shapes that have fewer and less pronounced peaks and shoulders. This is indicated by the total photoneutron cross sections shown in Figs. A-1 and A-2.

In this respect, ^{23}Na and ^{25}Mg more closely resemble the other neighboring odd-A nucleus that we have studied (^{27}Al). Although one might expect the additional unpaired nucleon in an odd-A nucleus to produce a richer structure than that in a self-conjugate nucleus, this is not apparent in the data. Such additional structure may be present, but it is not resolvable with the linac's 200-keV resolution.

In Figs. A-1 and A-2, the thresholds for the (γ,n), (γ,n), and (γ,np) reactions in ^{23}Na and ^{25}Mg are indicated by arrows. In both cases, the (γ,np) threshold is below the $(\gamma,2n)$ threshold. The $(\gamma,2n)$ cross sections for ^{23}Na and ^{25}Mg show that up to about 5 MeV above the threshold, the $(\gamma,2n)$ process is generally less than 10% of the total cross section.

The integrated cross sections up to the highest measured energies are 35% and 67% of the values predicted by the electric-dipole sum rule for ^{23}Na and ^{25}Mg respectively. However, it is evident from the data that ^{23}Na, at least, may have a significant contribution above the highest measured energy. Furthermore, the contribution from the (γ,p) reaction is expected to be significant in this region of the periodic table.

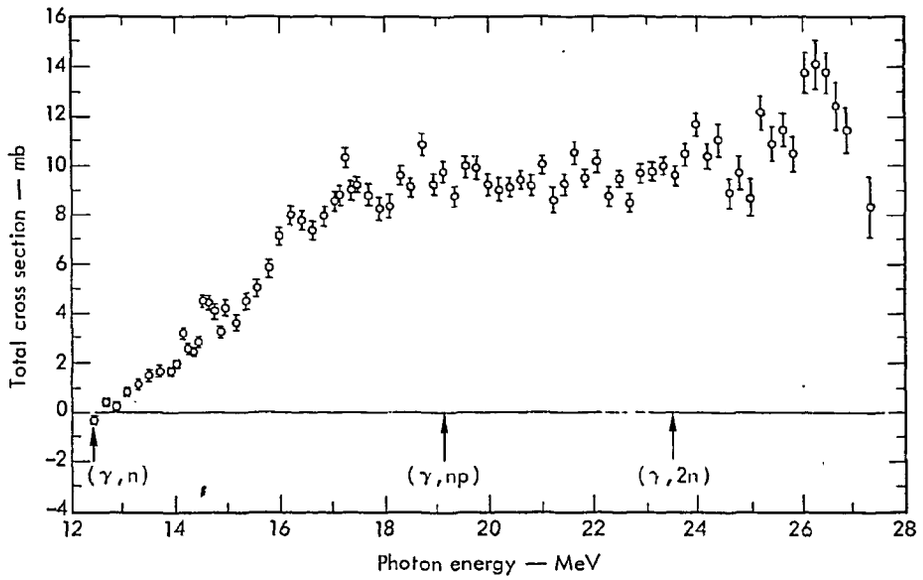

Fig.A-1 Total photoneutron cross section for ^{23}Na. The data shown represents the sum of the cross sections for the (γ,n), $(\gamma,2n)$, and (γ,np) reactions.

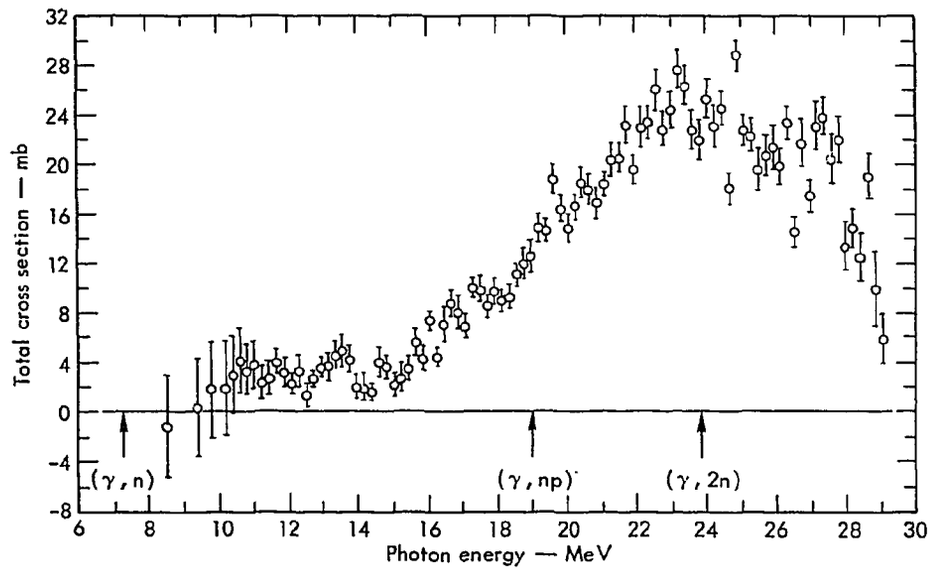

Fig.A-2. Total photoneutron cross section for ^{25}Mg. The data shown represents the sum of the cross sections for the (γ,n), $(\gamma,2n)$, and (γ,np) reactions.

2. The Use of Electrodeposition Methods to Prepare Actinide Targets for Cross Section Measurements and Accelerator Bombardments (J. E. Evans, R. W. Lougheed, M. S. Coops, R. W. Hoff, E. K. Hulet)

We have prepared targets of many of the actinide elements, e.g., U, Pu, Am, Cm, Bk, Cf, Es, and Fm for use in a comprehensive series of fission cross section measurements. Other experiments requiring actinide targets have involved accelerator bombardments, e.g., irradiation of ^{253}Es and ^{257}Fm at the HILAC, and symmetry studies of neutron-induced fission, e.g., recent studies of ^{257}Fm and ^{258}Fm fission. The experimental techniques require the targets be uniformly deposited in a thin layer on various backing materials such as Al, Ni, Pt, Be, Cu, and stainless steel. The backing materials ranged in thickness from 0.003 mil to 60 mil with target diameters ranging from 2 mm to 250 mm. In most cases the rarity of the nuclide required a deposition method that produces high yields, $\geq$ 90%.

The various methods developed to produce acceptable targets may be summarized as follows:

A. Electrodeposition technique.

1. Dilute nitric acid electrolyte: Useful for actinides on a tracer level where high yields and small target area are desirable (e.g., Es, Fm, targets on a Be backing plate).

2. Isopropyl alcohol-dilute nitric acid electrolyte: Useful for actinides from tracer to microgram levels where uniformity of deposit is critical (e.g., Bk, Cm, Es targets for Physics VIII cross section experiment).

3. Ammonium chloride electrolyte: Useful for deposition of massive amounts ($<$ 1 mg/cm^2) of actinides over large areas (180 cm^2). Also useful for deposition of actinides that are subject to hydrolysis in dilute acid (e.g., preparation of ^{232}U, ^{238}Pu, ^{242m}Am targets on Ni foils for fission cross section measurement).

B. Chemical replacement technique.

1. The method is useful for plating uranium on aluminum. The preparation of 1 mg/cm^2 deposits on 1 mil aluminum is typical.

Following deposition, it is usually necessary to determine the absolute amount of the actinide in the target. This quantity is most often determined by absolute alpha counting. In the case of targets with high activity levels (10^6 - 10^{11} α dpm) and large backing plates (8" diam), a new low geometry counter has been designed, built, and calibrated for this purpose. Uniformity of sample deposition has been monitored through alpha counter scanning techniques. (Pertinent to nearly all requests for heavy element cross section #'s 351 to 533).

3. Structure in the ^{235}U keV Fission Cross Section (C. D. Bowman, G. S. Sidhu, M. L. Stelts and J. C. Browne)

The structure in the keV fission cross section, which was reported at the Helsinki meeting, has been remeasured using the 250 meter flight path at the new Livermore 100 MeV electron linac.

The detector, which has been described elsewhere in detail,[1] permits the detection of fission events via a triple coincidence between the prompt fission gamma rays. The ^{235}U sample was a 0.125-cm-thick by 25-cm-diameter disk weighing 1300 g and containing 7% ^{238}U. The neutrons were produced by stopping the 100 MeV electron beam in a water-cooled tantalum target. The accelerator operated at 720 pps, with 30 nsec wide pulses and a peak current of 5 amps. Overlap was eliminated by means of a ^{10}B filter. The neutrons traversed a 1.25-cm-thick layer of water against the side of the tantalum target. The channel width was 32 nsec for the energy range above 35 keV and 64 nsec below. The time response of the detector was < 10 nsec. The resolution therefore was determined in the lower region almost entirely by the channel width and corresponded to 0.25 nsec/m. At higher energies the resolution was somewhat better; i.e. $\sim$ 0.15 nsec/m. The latter resolution is at least six times better than any previous fission measurement on ^{235}U in this energy region. Improvements in accelerator performance since this experiment was completed would permit a resolution which is at least three times that reported here and would allow a statistical precision above 100 keV of < 2%.

The neutron flux was monitored with a ^{6}Li-loaded-glass detector which was 0.1-cm-thick and 10 cm in diameter. The glass was mounted directly against the 0.6-cm-thick face of the photomultiplier tube. The flux monitor was located 2 meters behind the 0.125-cm-thick ^{235}U plate. The small corrections of the ^{6}Li data for the transmission of the plate were neglected. The backgrounds measured at 2 keV and 400 keV were 5 and 3% respectively; no attempt was made to correct the data for this effect.

[1] Van Hemert, Bowman, Baglan, Berman, Nucl. Instru. Meth. 89, 263 (1970)

The neutron spectrum was found to have significant fluctuations with energy owing to the 0.3-cm-thick iron can surrounding the tantalum target. Above 100 keV this caused no problems since the statistical precision of the flux monitor was adequate for a channel-by-channel division. However below this energy it was necessary to draw a smooth curve through the ^{6}Li data to average out statistical fluctuations but not to average out the effects of the iron resonances. The iron influenced the final cross section in only two places, which are discussed later.

After corrections were applied for the ^{6}Li (n,α) cross section using the Uttley and Diment[2] data the shape of the resulting ^{235}U fission cross section above 100 keV was found to differ considerably from the previously measured ^{235}U data. This was caused probably by scattering effects in the glass of the detector and the photomultiplier tube although possibly from persisting uncertainties in the ^{6}Li (n,α) cross section. The data below 100 keV was therefore normalized to Davey's[3] evaluated value of 1.64 barns at 100 keV. Above this energy the data was divided by the function required to give the average data the shape of Davey's evaluated curve.

Results

The results are shown in Figs. 1-4. No channels have been averaged in the data; each point is plotted. The standard deviation shown by the "wings" on the data points of Fig. 1 is much smaller than the scatter of the points and since the resolution function is almost square and determined by the channel width alone, one-point peaks are usually significant. A line has been drawn through the data of Fig. 1 to guide the eye. The average width and spacing of these structures is 60-80 eV compared with a resolution at 15 keV of 12 eV.

Fig. 2 shows the data from 20-40 keV. The channel width changes at 35.5 keV. The prominent peak near 22 keV is clearly a cluster of many narrow groups of structure.

Fig. 3 shows the data from 40 to 80 keV. Throughout this range, fluctuations of about 0.25 barns (corresponding to a standard deviation of about $\pm$ 6%) are clearly visible. The resolution at 60 keV is about 70 eV. The structure at 73.5 and 51.9 keV is caused by incomplete cancellation of the effects of the iron of the neutron-target can. These are the only places where iron was found to be responsible for structure.

Fig. 4 shows the data from 80 to 350 keV. At the higher energies the standard deviation is less than the point size. It is clear that real structure has been detected throughout the full range of the

[2] C. A. Uttley and K. M. Diment (unpublished work)
[3] W. G. Davey, Nucl. Sci. Eng. 26, 149 (1966)

data. The standard deviation in the data is about ± 3% at 200 keV.

In an experiment designed to obtain the highest resolution, compromises are required which reduce the absolute accuracy of the data. Therefore the data reported here should not be considered an attempt to reduce the present uncertainties in the ^{235}U fission cross section.

(Pertinent to requests 382, 384, 385 and 386).

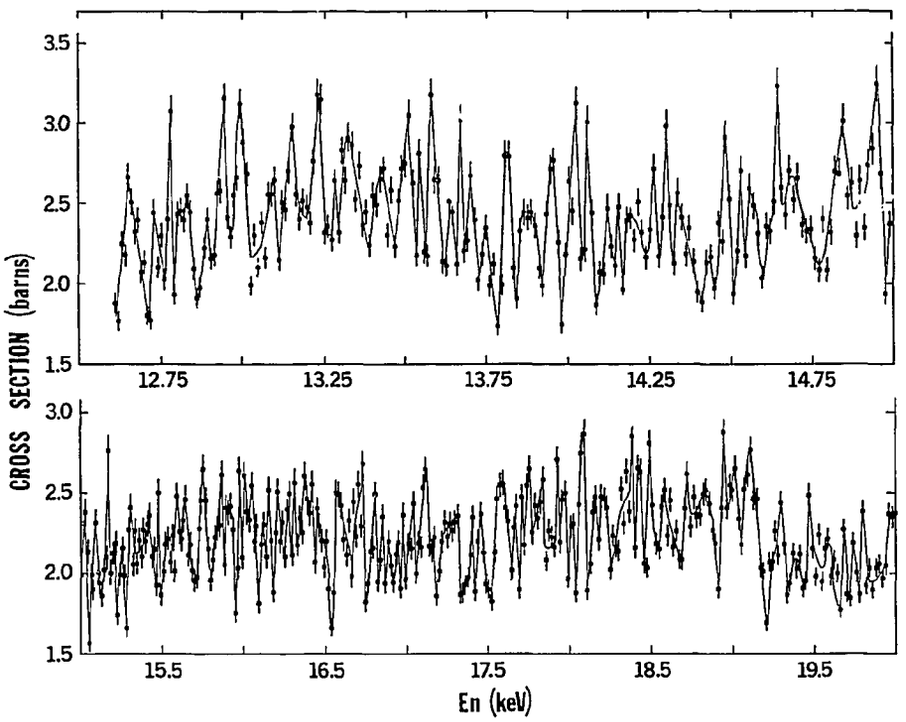

Fig. C-1 σ_f for ^{235}U from 12.5-20 keV

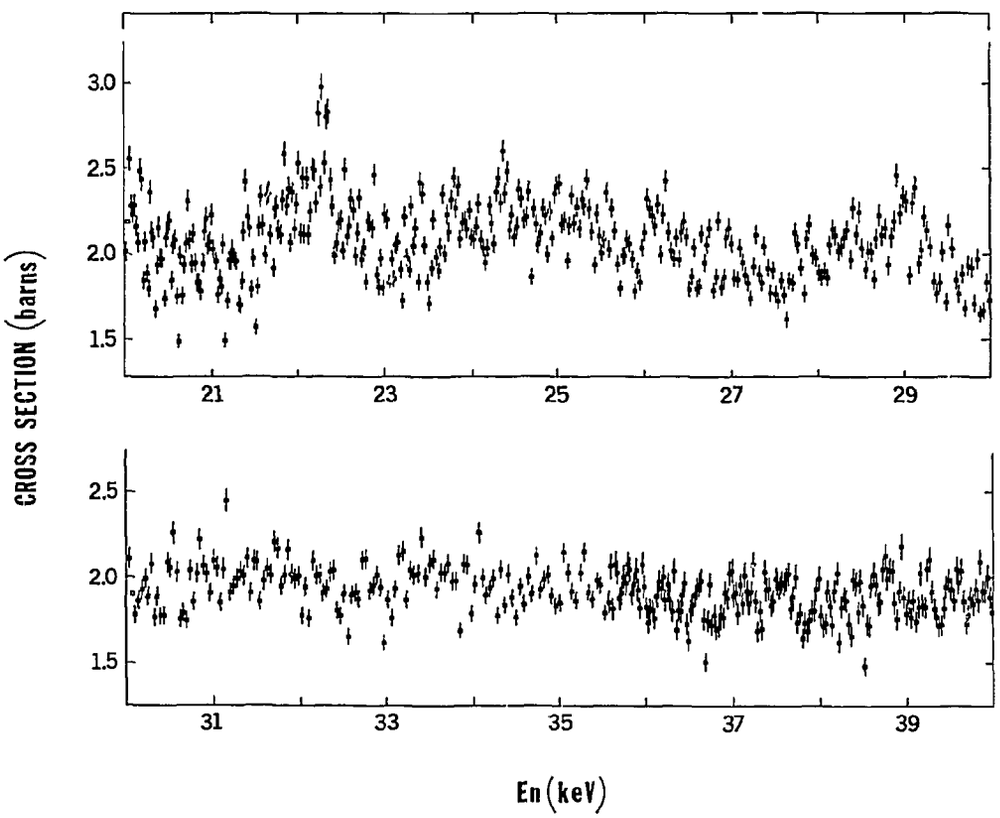

Fig. C-2 σ_f for ^{235}U from 20-40 keV

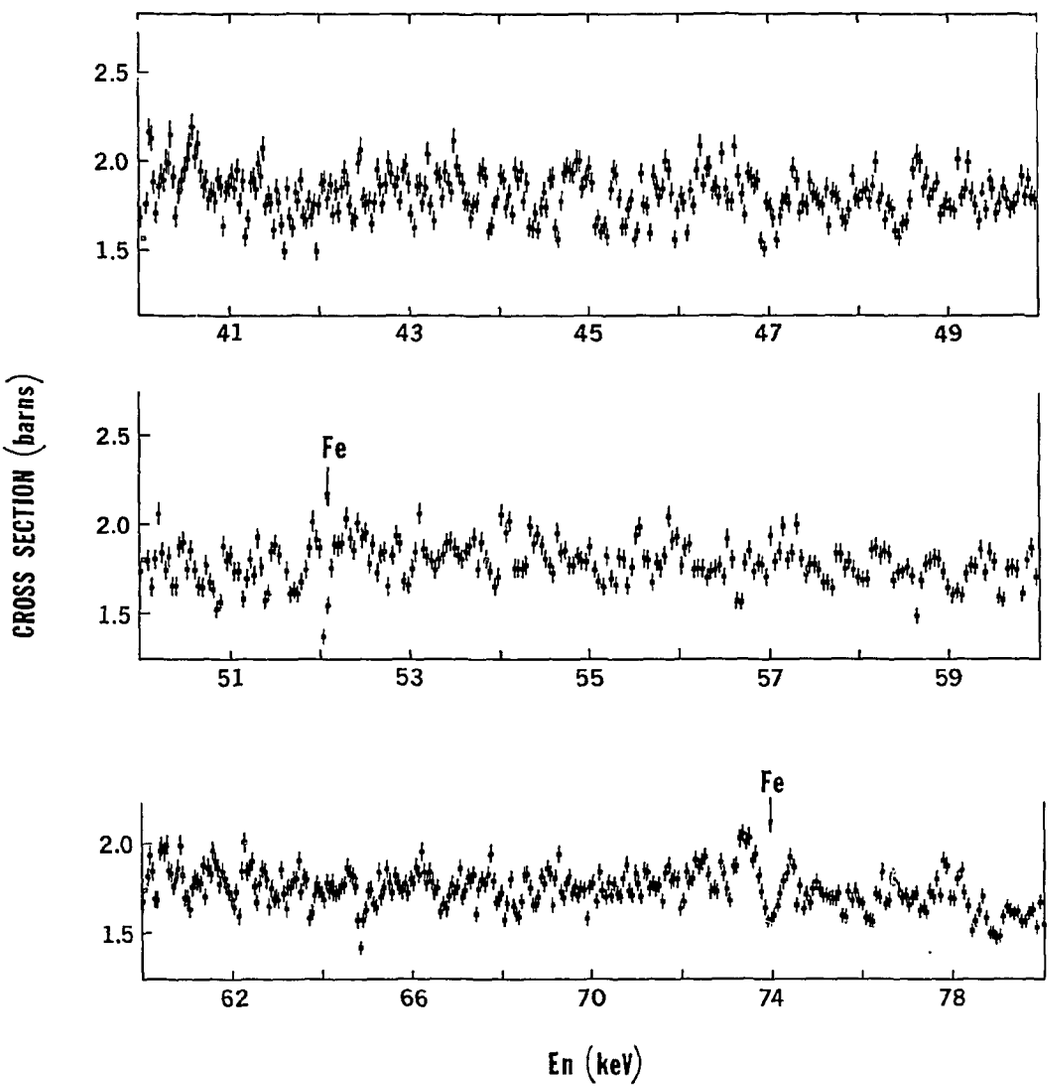

Fig. C-3 σ_f for ^{235}U from 40-80 keV

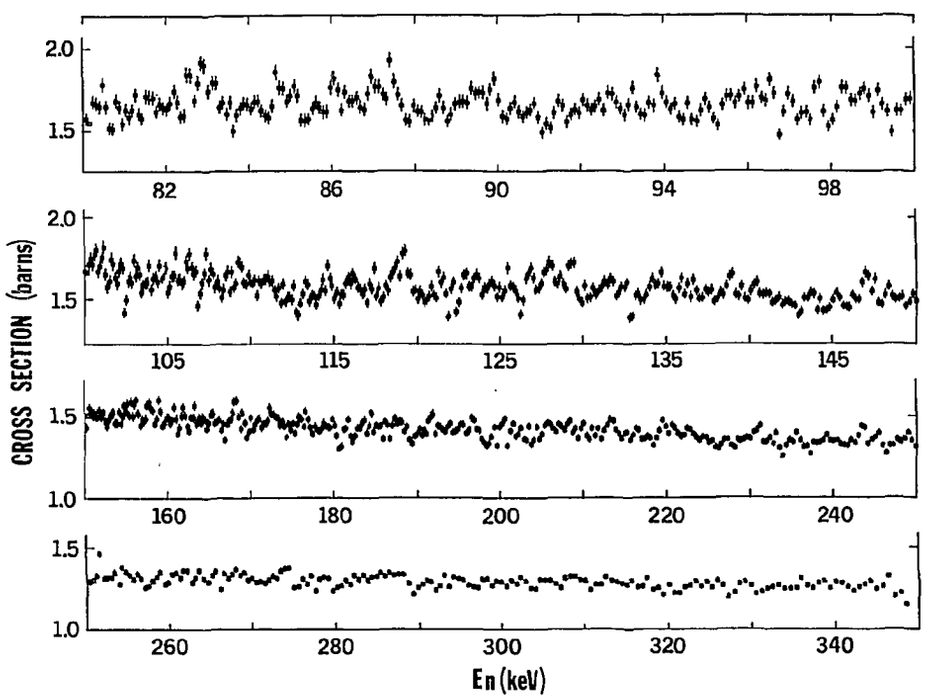

Fig. C-4 σ_f for ^{235}U from 80-350 keV

4. Investigation of Gamma Rays Produced in the $^{89}Y(n,n')$ and $^{89}Y(n,2n)$ Reactions (F. S. Dietrich, M. C. Gregory, and J. D. Anderson)

Gamma radiation has been observed following bombardment of natural (monoisotopic) yttrium metal with nominally 14.2-MeV neutrons from the ICT neutron generator. The gamma rays were observed with an 8-cm^3 Ge(Li) detector placed about 1 m from a scattering disc with a lead wedge to scatter out the direct neutron beam. Also, delayed radiation was investigated by pulsing the incident beam and gating off the counting apparatus during the beam bursts. Delayed radiations were observed having energies of 232, 393, 442, and 909 keV. The latter is ascribed to (n,n') excitation of the isomeric first excited state of ^{89}Y; the 442- and 232-keV delayed radiations presumably correspond to the decay sequence $8^+(674\text{ keV}) \rightarrow 5^-(232) \rightarrow 4^-(0)$ in ^{88}Y and the 393-keV radiation to the transition $1^+(393) \rightarrow 4^-(0)$ in ^{88}Y. We measured total cross sections for the prompt-plus-delayed yields to these levels with the Ge(Li) counter. Cross sections with 15% accuracy, are: 231 keV, 383 mb; 393 keV, 117 mb; 442 keV, 136 mb; 909 keV, 437 mb. Our work is summarized in Fig. 1 together with the spin-parity assignments of other investigators.

A Hauser-Feshbach calculation of the gamma yields was performed assuming a reaction sequence $^{89}Y + n \rightarrow {}^{90}Y^* \rightarrow {}^{89}Y^* + n \rightarrow {}^{88}Y^* + 2n$. By including the levels observed in the present experiment, and in addition a 7^+ level suggested by charged-particle reactions, we are able to obtain agreement with the observed cross sections within the present experimental accuracy. The results are extremely insensitive to the temperature and spin cut off parameters assumed for $^{89}Y^*$.

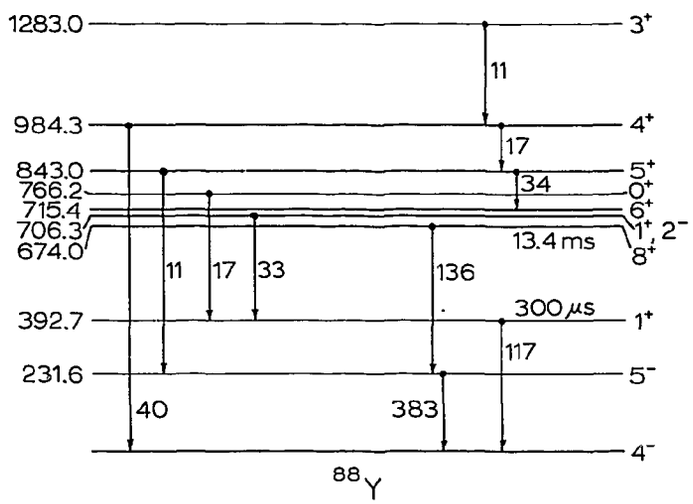

Fig. D-1. Gamma transitions observed following the $^{89}Y(n,2n)$ reaction. The numbers on the gamma lines represent the cross sections in mb; accuracy 15% for $\sigma > 100$ mb, and 30% otherwise.

5. EVALUATIONS (Robert J. Howerton)

The following neutron cross section evaluations have been revised in the LRL evaluated data library since the last report:

Total Evaluation: ^{1}H (received from L. Stewart, LASL);

Partial Evaluations: ^{6}Li, C, Al, Ti, ^{233}U, ^{235}U, ^{238}U, ^{239}Pu.

Several new volumes in the UCRL-50400 series, "An Integrated System for Production of Neutronics and Photonics Calculational Constants" have been published. These include a bibliography[1] for, and an index[2] to, the experimental neutron cross section data in the ECSIL system, and a tabulation of nuclear reaction threshold energies.[3]

A continuing effort is the checkout of neutron evaluations by calculation of appropriate parameters of critical assemblies and other integral measurements, e.g., pulsed spheres. The TART Monte Carlo code has been used for this purpose as it removes most of the numerical type restrictions. TART, for criticality analysis, operates in a batch neutron mode. The code currently utilizes 176 groups, 33 angular increments of equal probability for the differential distributions, a continuous neutron energy, and all of the physics available in the LRL Evaluated Nuclear Data Library.

---

[1] Howerton, Perkins, Altamirano, Hill, "A Bibliography of the Experimental Data of Neutron-Induced Reactions," UCRL-50400, Vol. 2 (1970).

[2] Howerton, Perkins, Altamirano, Hill, "An Index to the Experimental Data of Neutron-Induced Reactions," UCRL-50400, Vol. 3 (1970).

[3] R. J. Howerton, "Threshold of Nuclear Reactions Induced by Neutrons, Photons, Protons, Deuterons, Tritons, and Alpha Particles," UCRL-50400, Vol. 9 (1970).

6. EXPERIMENTS RELATED TO SAFEGUARDS

1. Delayed Fission Gamma Rays (Walter John)

Triple-coincidence experiments between two fission fragments and the delayed fission gamma-rays have been measured for gamma-ray half-lives in the range of 20 to 1000 nsec. The experiments were carried out on spontaneous fission of ^{252}Cf and neutron-induced fission of ^{235}U. By detecting the fission fragments, one learns the mass of the fragment emitting the γ-ray. Also, if the usual mass distribution is found in coincidence with a particular γ-ray, one knows that the γ-ray was emitted before the fission process.

2. Threshold Photoneutron Experiments (C. Bowman and B. Berman)

The threshold photoneutron technique holds some promise for identification of materials owing to the neutron spectra which are characteristic of a particular element or isotope. An attempt to discover a low energy (<10 keV) line in ^{235}U for this purpose was unsuccessful. However the technique might have application for other fissile or fertile elements and also for lighter materials of interest to the plowshare program.

3. ^{235}U Photofission Cross Section Measurements (R. Alvarez)

The photofission cross section of all fissile or fertile elements is of possible use to the Safeguards program. This laboratory has already carried out the first photofission cross section measurements on ^{235}U with monoenergetic γ-rays.[1] A program of this type is now planned for many other fissile isotopes.

4. Neutron and Photon-Induced Fission Isomers (J. Brown and C. Bowman)

Neutron or photon-induced fission isomers might find use in Safeguards applications. Since the half-lives are in the nsec to μsec range, the associated neutron or γ-rays are emitted much more quickly than in present systems where delayed neutrons are detected. This can mean a significant increase in signal-to-background ratio ($\gtrsim 10^3$) which might make up for the considerably smaller cross section for this process ($\sim 10^{-2}$), compared with that for delayed neutrons from prompt fission. Measurements are now underway to detect the 66 nsec isomer in the reaction $^{235}U + n$.

---

[1] Bowman, Auchampaugh, Fultz, Phys. Rev. 133, B676 (1964)

LOCKHEED PALO ALTO RESEARCH LABORATORY

A. NEUTRON PHYSICS

1. "Best-Fit" $^{197}Au(n,\gamma)^{198}Au$ Cross Section for Neutron Energies from 10 to 5400 keV (F. J. Vaughn and H. A. Grench)

The procedure employed in arriving at a "best-fit" cross-section curve was described in some detail in Reports to the AEC Nuclear Cross Sections Advisory Committee for the meeting of December 1-3, 1970 (Report no. BNL 50276). Since the submission of that report, the "best-fit" curve has been slightly revised because of the inclusion of another set of data in the analysis, and the curve has been compared with the results of experiments in which the cross section was measured at only one or a few energies.

The additional set of data included in the analysis was that of Kompe (complete reference given later on Fig. A-1). His measurements extended over the energy region from about 10 to 150 keV, and his results were therefore considered when extending the "best-fit" curve downward in energy from the 123-560 keV "standard" region.

Initially, the "best-fit" curve was obtained using only the results of fifteen sets of measurements which covered a significant range of neutron energy (the fourteen listed in BNL 50276 plus those of Kompe). However, many cross-section measurements have also been made at only one or a few neutron energies. References to these measurements are listed on Fig. A-2. To take these data into account, they were first renormalized as necessary to incorporate later information. They were then compared with the "best-fit" curve by calculating the "adjustment" factor by which all would have to be multiplied to attain the best agreement with the curve. A least-squares calculation in which these data were treated as one set, with each point weighted inversely as its quoted uncertainty, was performed. The adjustment factor was found to be 1.004 ± 0.044. Since this factor was not significantly different from unity, and since it was felt that there was no overwhelming evidence for the accuracy of any sub-set of these measurements at isolated energies, no alterations in the "best-fit" curve were made because of these additional results.

The "best-fit" cross-section curve is shown in Fig. A-1, together with the adjusted data from the fifteen sets employed. In the region below about 100 keV, some of the experimental results have been omitted from the plot for clarity, although all data were, of course, used in the analysis. The final adjustment factors for the various data sets are given in Table A-1, and numerical values of cross sections on the "best-fit" curve are given in Table A-2. The results of measurements made at only one or a few energies, together with the "best-fit" curve, are shown in Fig. A-2.

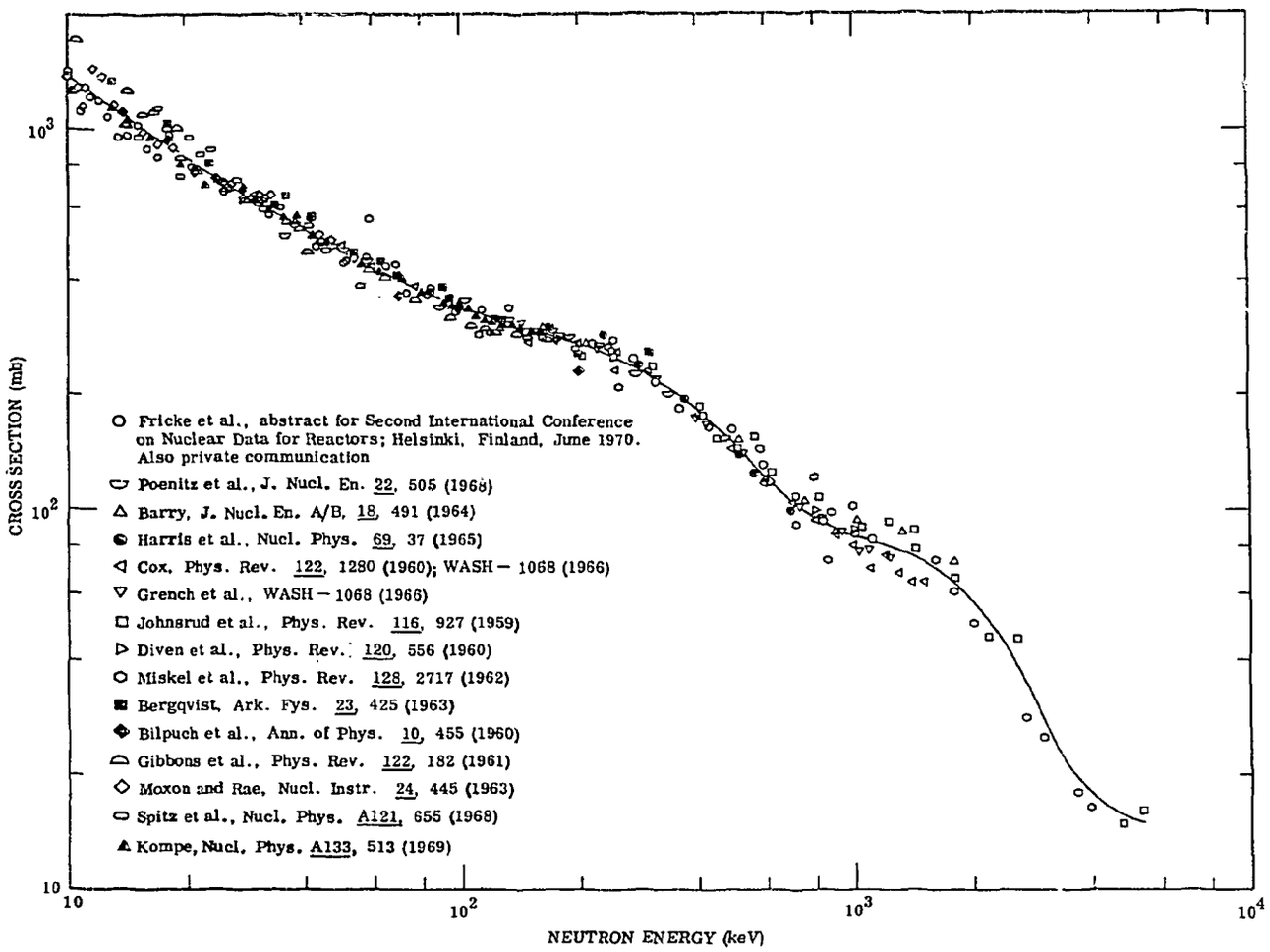

Figure A-1. "Best-fit" $^{197}Au(n,\gamma)^{198}Au$ cross-section curve with adjusted data used in obtaining the curve.

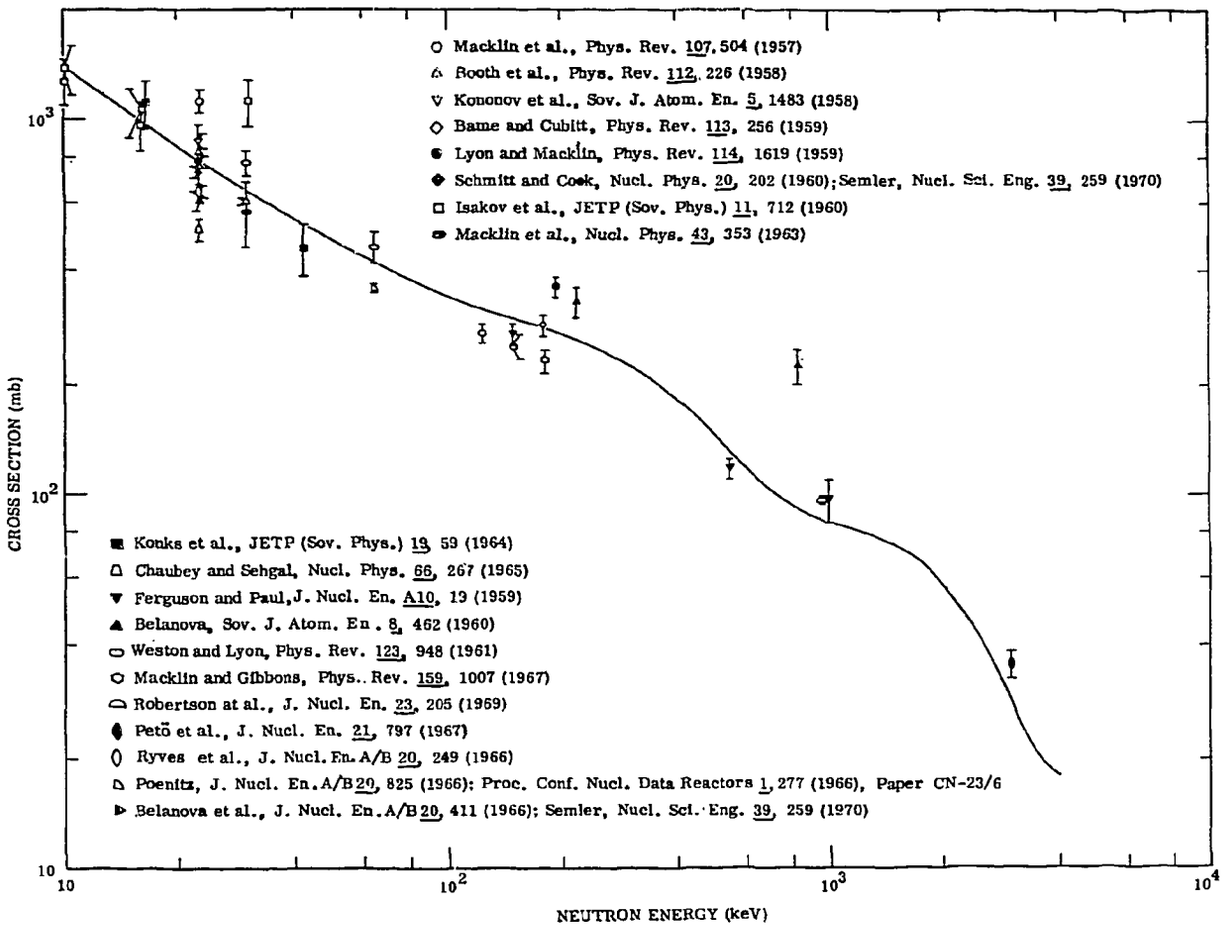

Figure A-2. "Best-fit" $^{197}Au(n,\gamma)^{198}Au$ cross-section curve with results of measurements made at only one or a few energies.

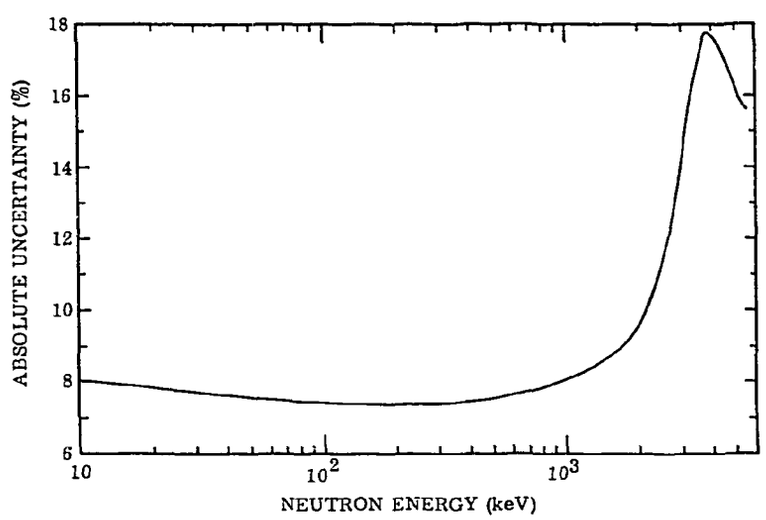

Figure A-3. Absolute uncertainty of "best-fit" $^{197}Au(n,\gamma)^{198}Au$ cross-section curve.

Table A-1. Adjustment factors for sets of cross-section data.

Experiment	Adjustment Factor
Fricke	1.01567
Poenitz	1.07871
Barry	0.93771
Harris	1.06969
Cox	0.82913 for E < 200 keV
	0.84796 for E ≥ 200 keV
Grench	0.93168
Johnsrud	0.99136
Diven	0.88967
Miskel	0.80488
Bergqvist	1.21152
Bilpuch	0.84956
Gibbons	1.22284
Moxon	1.19732
Spitz	1.28574
Kompe	1.11054

Table A-2. "Best-fit" $^{197}Au(n,\gamma)^{198}Au$ cross section.

E(keV)	σ(mb)	E	σ	E	σ	E	σ	E	σ
10	1393	42	527.8	190	275.7	600	119.9	2800	33.1
11	1299	44	513.7	200	270.8	650	111.0	2900	30.7
12	1219	46	500.8	210	266.1	700	103.8	3000	28.4
13	1150	48	488.8	220	261.5	750	98.16	3200	24.6
14	1090	50	477.8	230	256.8	800	93.71	3400	21.9
15	1038	52	467.5	240	252.2	850	90.27	3600	19.9
16	991.5	54	458.0	250	247.6	900	88.05	3800	18.7
17	950.1	56	449.1	260	243.0	950	86.08	4000	17.8
18	912.9	58	440.9	270	238.5	1000	84.45	4200	17.1
19	879.3	60	433.1	280	233.8	1100	81.73	4400	16.6
20	848.8	65	415.7	290	229.4	1200	79.53	4600	16.1
21	821.0	70	400.7	300	224.7	1300	77.53	4800	15.7
22	795.5	75	387.6	320	215.5	1400	75.20	5000	15.4
23	772.0	80	376.1	340	206.7	1500	72.61	5200	15.2
24	750.4	85	365.9	360	198.1	1600	69.80	5400	14.9
25	730.3	90	356.9	380	189.8	1700	66.81		
26	711.7	95	348.8	400	181.9	1800	63.68		
27	694.3	100	341.4	420	174.2	1900	60.46		
28	678.1	110	328.8	440	166.9	2000	57.17		
29	663.0	120	318.3	460	159.9	2100	53.86		
30	648.7	130	309.6	480	153.1	2200	50.56		
32	622.8	140	302.6	500	146.7	2300	47.30		
34	599.6	150	296.5	520	140.6	2400	44.09		
36	578.9	160	290.9	540	134.8	2500	40.98		
38	560.2	170	285.5	560	129.3	2600	38.00		
40	543.3	180	280.6	580	124.3	2700	35.50		

The inclusion of Kompe's data in the analysis also had a small effect on the estimated uncertainty of the "best-fit" curve in the low-energy region. As described in BNL 50276, the absolute uncertainty of the "best-fit" curve as a function of energy was obtained by quadratically combining the uncertainties arising from differences between reasonable fits, "error band" of the final fit, and absolute normalization. The resulting curve of absolute uncertainty as a function of energy is shown in Fig. A-3.

2. Gross-Fission-Product Gamma-Ray Spectroscopy (W. L. Imhof, L. F. Chase, Jr., R. A. Chalmers, and F. J. Vaughn)

Recent work on this program has been in areas which do not yield any new results to report. More data reduction and analysis remains to be done and will be reported on later.

3. Spin-Spin Effect in the ^{59}Co + n Total Cross Section (T. R. Fisher, H. A. Grench, D. C. Healey,* J. S. McCarthy,* and D. Parks*)

The calculation described in the last report has been completed, and the experimental results together with the theoretical calculation have been submitted for publication in Nuclear Physics. It is concluded that the large values of the spin-spin effect σ_{ss} at neutron energies less than 1 MeV are probably due to doorway states rather than the spin-spin term in the optical potential. Measurements at higher neutron energies should clarify this question; such measurements are in progress.

4. Deformation Effect in the ^{59}Co + n Total Cross Section (T. R. Fisher, D. C. Healey,* J. S. McCarthy,* and D. Parks*)

A DWBA calculation of $\Delta\sigma_{Def}$ has been completed and compared with the experimental results presented in the last report. If the deformation of ^{59}Co is taken as $\beta = 0.18$, the calculated values of $\Delta\sigma_{Def}$ are lower than the experimental ones by about a factor of three. The discrepancy may be due to doorway states in the compound nucleus. An experiment is in progress to obtain data on $\Delta\sigma_{Def}$ at higher neutron energies, where effects of doorway states should be less important. The nuclear alignment of the ^{59}Co target will be increased by the use of a single crystal and an improved dilution refrigerator. It is hoped that an alignment of 15-20% can be achieved.

5. Proton Scattering from Aligned ^{165}Ho (T. R. Fisher, B. A. Watson,* and S. I. Tabor*)

Preliminary data have been obtained on the elastic scattering of 10-MeV protons by aligned ^{165}Ho. The difference in the scattering cross section for an aligned vs. an unaligned target can be used to measure the

* Stanford University, Stanford, California.

nuclear quadrupole moment. The target was a single crystal of Ho metal and was operated at a temperature of 0.150°K. The nuclear alignment $B_2/B_2(\max)$ was -0.40. The aligned cross section at 180° is greater than the unaligned cross section by about 4%. This difference, however, has the opposite sign from that expected from the quadrupole-moment contribution, indicating that the nuclear potential tail may be contributing. Further measurements are in progress.

6. Radiation Damage Effects on Superconducting Microwave Cavities (T. R. Fisher and I. Ben Zoi*)

An experiment is in progress to study the effects of proton irradiation on the Q of superconducting Nb cavities. X-band cavities will be irradiated, while superconducting, with 3-MeV protons from the Lockheed Van de Graaff accelerator until a degradation in the Q of the cavities is observed. Annealing and recovery rates will then be studied.

LOS ALAMOS SCIENTIFIC LABORATORY

A. TIME OF FLIGHT WITH NUCLEAR EXPLOSIONS

1. New Results Reported at the Third Conference on Neutron Cross Sections and Technology. Relevant to Requests 336, 347, 348, and 528 of NCSAC-35.

New results from nuclear explosion measurements on the scattering and capture cross sections of ^{197}Au, on the capture cross section of ^{232}Th, and on the fission cross sections of ^{230}Th, ^{231}Pa, ^{242}Pu, ^{244}Pu, and ^{249}Cf will be reported in the proceedings of the Knoxville Conference on Neutron Cross Sections and Technology. Titles and authors of the papers are included in the Appendix.

2. Fission Cross Section of ^{238}U (M. G. Silbert and D. W. Bergen)

In an attempt to observe subthreshold fission in ^{238}U, a sample with very low ^{235}U content was exposed to the intense neutron beam of the Physics 8 nuclear explosion. A high-sensitivity oscilloscope setting allowed individual fission fragment pulses from a semiconductor detector to be counted. In the region from 37 to 237 eV, the average fission width for eight resonances was determined to be $(0.03 \pm 0.05) \times 10^{-6}$ eV. In the keV region, the average fission cross section was measured to be (61 ± 24) microbarns from 10 to 30 keV and (36 ± 14) microbarns from 30 to 100 keV.

3. Fission Cross Section of ^{252}Cf (M. S. Moore, J. H. McNally; and R. D. Baybarz, ORNL) Relevant to Request 533, NCSAC-35.

The neutron-induced fission cross section of ^{252}Cf was measured from 20 eV to 5 MeV neutron energy, using neutrons from the Physics 8 nuclear explosion. Pronounced sub-barrier resonance fission is observed below a few keV neutron energy. The fission threshold is found to occur at ~ 900 keV. Analysis of the data indicates that the fission barrier is quite transparent, giving an average fission width comparable to the radiative capture width in the resonance region. Figure A1 shows the fission cross section of ^{252}Cf from 10 keV to 5 MeV. Parameters for resonances below 1 keV are listed in Table A1. A manuscript describing this work has been submitted to the Physical Review.

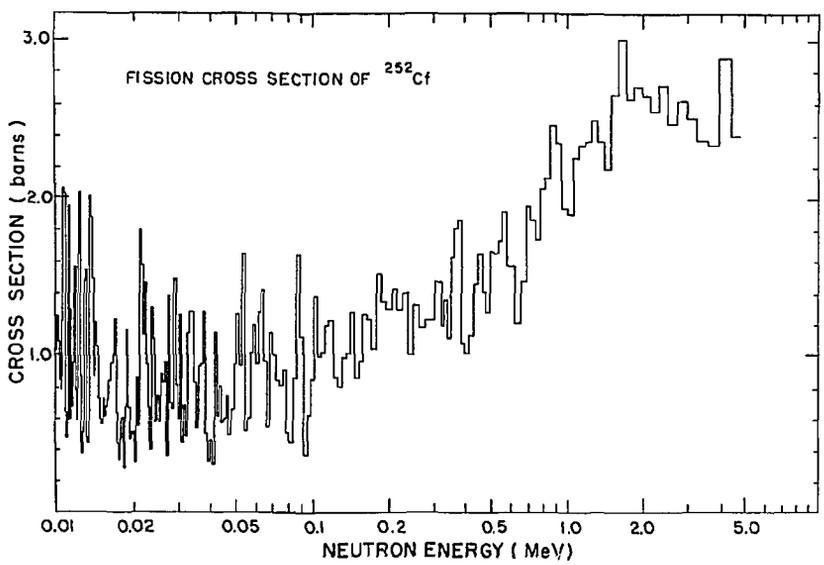

Fig. A1. Fission cross section of (^{252}Cf + n) for neutron energies between 0.01 and 5 MeV.

TABLE A1

Resonance Parameters for (^{252}Cf + n)

E_o(eV)	$\frac{\pi}{2}\sigma_o\Gamma_f$(barns-eV)	Γ_n(meV)[a]	Γ_f(meV)[a]
24.55	20.2 ± 5.1		
36.35	625 ± 49		
68.37	2137 ± 66	53.5 ± 3.0	180 ± 9
79.16	98 ± 8		
88.25	5.8 ± 1.6		
138.1	24.8 ± 4.2		
190.1	18.9 ± 4.7		
217.7	460 ± 38		
246.2	33 ± 8		
307.1	24.7 ± 3.6		
338.0	14.7 ± 3.8		
387.4	100 ± 11		
393.6	14.4 ± 3.8		
404.8	114 ± 12		
417.0	22.6 ± 5.1		
426.7	70 ± 9		
445.4	64 ± 10		
490.8	43 ± 10		
520.2	19 ± 5		
557.2	258 ± 26	≤ 370	≥ 42.5
561.9	78 ± 11		
606.4	117 ± 16		
626.4	10 ± 7		
643.7	13 ± 9		
674.2	32 ± 10		
706.2	31 ± 8		
726.1	404 ± 41	≤ 1250	≥ 82
754.1	41 ± 10		
771.1	43 ± 10		
813.5	9 ± 6		
833.1	186 ± 26	≤ 1300	≥ 44
841.0	18 ± 7		
877.6	31 ± 10		
931.8	16 ± 8		
983.5	10 ± 9		

[a] Since these values are determined from the product and the sum of the neutron and fission widths, it is possible that the entries in the table could be reversed.

4. Fission, Capture, and Scattering Cross Sections of ^{239}Pu (J. A. Farrell, G. F. Auchampaugh, and P. A. Seeger) Relevant to WASH-1144, Requests 442, 447, 449.

The comparison of alpha for ^{239}Pu reported in NCSAC-33 incorrectly quoted the Czirr and Lindsey results. Table A2 gives the comparison between LASL Physics-8 data and the correct LRL data.[1]

TABLE A2

^{239}Pu Alpha

Neutron Energy Interval (keV)	Physics 8	LRL[1]
9.0-10.0	0.74	0.62
8.0- 9.0	0.58	0.55
7.0- 8.0	0.68	0.62
6.0- 7.0	0.86	0.87
5.0- 6.0	0.93	0.87
4.0- 5.0	0.90	0.80
3.0- 4.0	0.95	0.88
2.0- 3.0	1.31	1.01
1.0- 2.0	1.17	0.85
0.9- 1.0	0.70	0.70
0.8- 0.9	0.79	0.64
0.7- 0.8	0.85	0.90
0.6- 0.7	1.68	1.6
0.5- 0.6	0.64	0.65
0.4- 0.5	0.57	0.45
0.3- 0.4	0.94	1.11
0.2- 0.3	0.67	0.86
0.1- 0.2	0.67	0.78

B. VAN DE GRAAFF NEUTRON STUDIES

1. Elastic Scattering and Polarization of Fast Neutrons by Liquid Deuterium and Tritium (J. D. Seagrave, J. C. Hopkins, A. Niiler (Edgewood Arsenal), R. K. Walter (EG&G), R. H. Sherman, and E. C. Kerr) Relevant to NCSAC-35, Request 4.

The draft and figures for this paper have been completed, and are now in the final editing stage. Preliminary integrals of the elastic distributions between 18 and 23 MeV permit inferences of the nonelastic

[1] J. B. Czirr and J. S. Lindsey, Nucl. Sci. Eng. 41, 56 (1970).

cross sections, with results substantially lower than earlier extrapolations of data at energies up to 14 MeV for D(n,2n)P, and a comparably rapid rise of T(n,2n)D above its threshold of 8.34 MeV. The "low" D(n,2n) values are consistent with values inferred from the elastic integrals at 36 and 46.3 MeV reported by the University of California, Davis Group (Romero et al., Phys. Rev. C2, 2134 (1970)) of 196 ± 5 and 146 ± 3 mb, respectively, if one uses total cross sections from Seagrave's spline fit curve and ignores the Davis ad hoc total cross sections. These σ_T values lie far above the curve, with variances of 71 and 39 from the curve, or even 29 and 19 from a curve computed with the inclusion of this data. Final integral values will be obtained from best spline fits to the elastic data with the program TRIPLØT.

2. Scintillation Measurement of D(n,2n) Cross Section (E. R. Graves and J. D. Seagrave)

Preliminary measurements taken with a deuterated scintillator yielded a spectrum of breakup protons in the scintillator. If this can be satisfactorily integrated over all energies a cross section for the breakup can be derived. The data will be reexamined promptly. The uncertainty will be introduced in determining the number less than 1 or 2 MeV. This measurement assumes new importance since the inelastic cross section obtained by subtracting the integrated elastic from the total seems to be much lower than previously thought.

The procedure is to plot the total proton spectrum. The elastic protons from hydrogen in the scintillator extend out to full neutron energy, sticking out past the breakup protons far enough so that an elastic spectrum may be normalized at the upper end. When the preliminary analysis was done it was assumed that the proton pulse height vs energy response in C_6D_6 was the same as in C_6H_6 which we had measured. During the summer of 1970 we obtained calibration data for both protons and deuterons in the C_6D_6 detector so that it should be possible to construct the elastic proton distribution curve without that assumption.

3. Elastic n-^{3}He Scattering (M. Drosg, D. K. McDaniels, J. C. Hopkins, J. T. Martin, J. D. Seagrave, and E. C. Kerr) Relevant to NCSAC-35, Request 7.

An investigation of the elastic scattering of neutrons from a 1/2-mole liquid ^{3}He sample has been started. The scattered neutrons are detected by means of time-of-flight techniques. So far, angular distribution measurements have been made at 7.9, 12.0 and 13.6 MeV covering angles between 19.4° and 118.5°. It is planned to take additional data up to 24 MeV with total errors near ±5%.

The absolute scale for the angular distributions is obtained by normalization to the well-known ^{1}H(n,n)^{1}H cross section. This is done in

an auxiliary scattering experiment with a hydrogen sample in the same geometry.

As a side product this study will lead to improved values for the total elastic cross section at these energies.

4. Fast Neutron Capture in ^{208}Pb (D. M. Drake, I. Bergqvist, D. K. McDaniels)

Gamma-ray spectra from $^{208}Pb(n,\gamma)$ reaction have been measured at several neutron energies between 6 and 15 MeV using the pulsed beam from the Los Alamos Scientific Laboratory tandem Van de Graaff. Figure B1 shows a gamma-ray pulse height spectrum from 11.2 MeV neutron bombardment of ^{208}Pb and its corresponding background spectrum. The peak near channel 126 corresponds to 15-MeV gamma rays emitted to the ground state of ^{209}Pb. Figure B2 shows the experimentally determined cross section to the $g_{9/2}$ state in ^{209}Pb and the semi-direct prediction.[1] The figure also shows similar experimental and predicted cross sections for levels which correspond to $j_{15/2} + d_{5/2}$ and $g_{7/2} + d_{3/2}$ in ^{209}Pb.

5. Gamma-Production Cross Sections (D. M. Drake, I. Bergqvist, and J. C. Hopkins)

We have remeasured the cross section for the production of the 1.78-MeV gamma ray from 7.5 MeV bombardment of Si. These measurements were made with a Ge(Li) center crystal and agree with our old measurements using NaI.

6. Absolute Fission Cross Section for ^{235}U (K. Smith, D. Barton, and G. Koontz)

An effort has been started to measure the neutron-induced fission cross section for ^{235}U from 1 to 15 MeV. The goal is to achieve the greatest accuracy compatible with a two-year program. It is expected that errors will be as low as 3% over most of the energy range. The fission cross section will be measured relative to the scattering cross section of hydrogen, using a neutron counter telescope with solid-state detectors to count recoil protons from a hydrogenous radiator that is located very near the ^{235}U fission foil. Fission fragments will be detected in nearly 2π geometry by a solid-state fission counter.

During the past 10 months, survey measurements of background problems in different detector systems have been made and the detailed counter system designed. The entire apparatus was completed in March 1971 and the entire measurement is expected to be completed a year later.

---

[1] C. F. Clement et al., Nucl. Phys. 66, 273 and 1293 (1965).

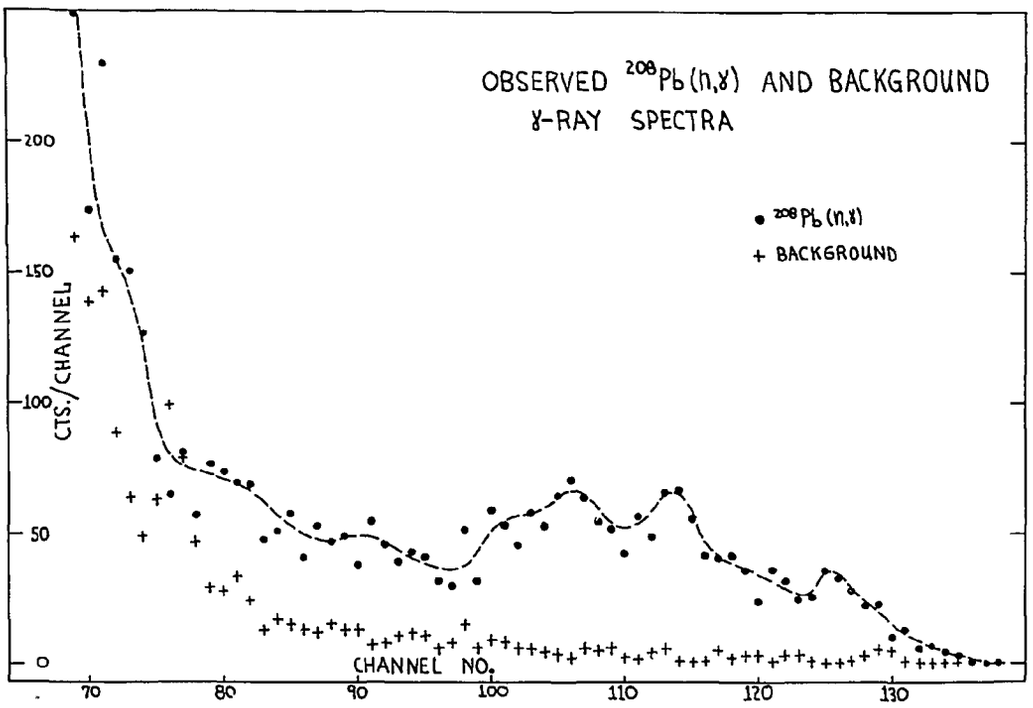

Fig. B1. Gamma-ray pulse height spectrum and background spectrum from 11.2 MeV neutron bombardment of ^{208}Pb.

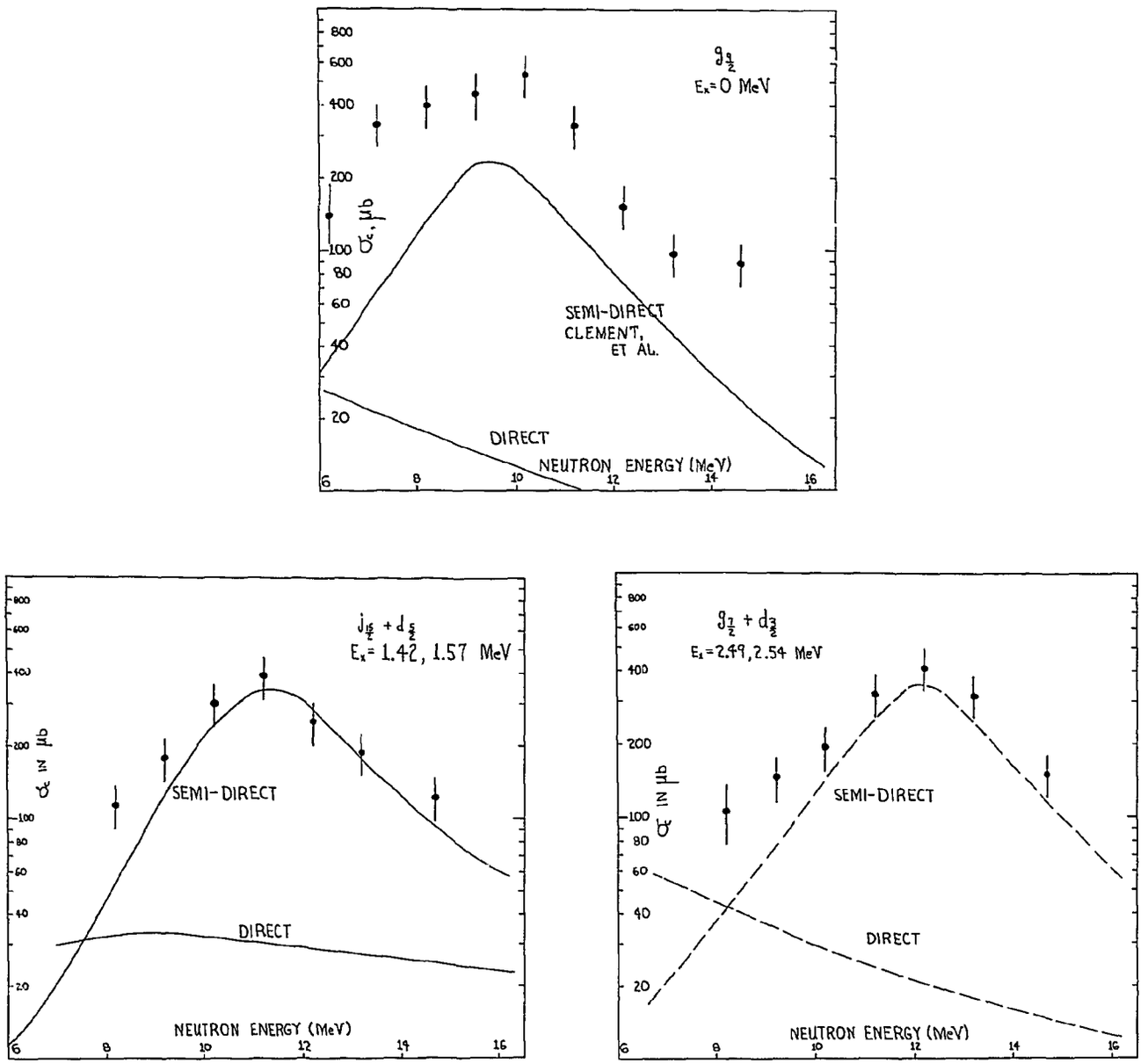

Fig. B2. Cross section for population of various levels of ^{209}Pb. Solid lines show the semi-direct and direct capture model predictions.

The neutron telescope flux monitor which will be used in the fission measurements has been tested with neutrons having energies between 1 and 7 MeV. The telescope consists of a CH_2 foil used as a source of proton recoils and a solid-state energy detector spaced some 10 cm away. One or more thin $\Delta E/\Delta X$ detectors may be placed between the foil and energy detectors if desired. The background with the CH_2 foil removed for two silicon detectors in series was 2 to 4% compared to the less than one percent background of an earlier test instrument. However, further attempts to clean the surfaces of the telescope may reduce the backgrounds. Further tests are needed to be able to determine the background source. At 1 MeV a 0.3 mil CH_2 foil was used and the foil-out background was about 7%. If operated at 7 MeV with a 4-mil CH_2 foil, a 0.5% background would result if it were entirely caused by hydrogen-contaminated materials other than the CH_2 foil. This emphasizes that at the lower energies extreme measures will have to be taken to reduce the organic contaminants on the walls of the telescope.

7. Angular Distribution and Absolute Cross-Section Measurements for the $T(p,n)^3He$ and $T(d,n)^4He$ Neutron Source Reactions (D. K. McDaniels, M. Drosg, J. C. Hopkins, J. T. Martin, and J. D. Seagrave)

Investigation of the neutron source reactions, $T(p,n)^3He$ and $T(d,n)^4He$, has begun, motivated by the lack of good angular distribution and absolute cross-section measurements above 11 MeV in both reactions, by serious uncertainties in the absolute yields at 0°, and by a possible 20% error in the $T(d,n)^4He$ angular distributions results in the 6-7-MeV region. The measurements utilize neutron time-of-flight techniques. Combining this latter technique with our carefully measured neutron detector efficiency permits relative yields to be established to better than 3%. Absolute cross sections will be obtained using an improved version of a counter telescope and will be compared to the results of measurements using the associated particle method.

Measurement of the angular distributions from 0°-140° laboratory angle at 10° intervals for the $T(p,n)^3He$ and $T(d,n)^4He$ reactions are essentially finished. Because of physical limitations, the back angle data were obtained with the neutron detector outside of its normal shielding. Data obtained at 90°, 100°, and 110° were used to normalize to the data previously obtained with the neutron detector in its shielded and collimated mount. Angular distributions have been measured for the $T(d,n)^4He$ reaction at E_d = 5.0, 6.0, 7.0, 10.0, 11.0, 12.0, 13.0, 14.0, 15.0, and 15.7 MeV. Measurements for the $T(p,n)^3He$ reaction were made at the same energies with the exception of E_p = 5.0 MeV. The 15.0 and 16.0 MeV data suffered from high counting rates and will be repeated.

A careful analysis of the measured $T(d,n)^4He$ angular distributions at 5.0, 6.0, and 10.0 MeV confirms that errors of the order of

20-30% do exist in the previously reported literature on this reaction. The disagreement is principally for angles greater than 60°. By contrast, our results agree, within error, with the work of Wisconsin and Livermore on the $T(p,n)^3He$ reaction over the energy range up to 12.5 MeV.

The goal of the investigation so far has been to obtain angular distribution data by the time-of-flight technique with relative errors of less than 3%. This objective was achieved except for the angular region from 120°-140° where the errors range between 3 and 7%. At the same time, rough estimates of the absolute yields were calculated. Comparison of our results with previous literature values for the 0° yields from these two reactions and with the precise results obtained from the associated particle measurements of Jarmie et al., for the $T(p,n)^3He$ reaction leads to the preliminary conclusion that the present literature values for the absolute yields from these two reactions are in error by about 20%. To establish the absolute cross sections more precisely a series of counter telescope measurements at 0° will be made. Combining this data with the results of similar measurements for the neutron detector will permit an absolute efficiency to be established over the neutron energy range of 5-33 MeV, covered by the present experiments.

C. FISSION ISOMER STUDIES (H. C. Britt, B. H. Erkkila, S. Burnett, and W. E. Stein)

The experimental portion of the fission isomer production experiments on the cyclotron have been finished. We have now reached the point where all isomers that can be formed from deuteron or alpha particle bombardment on available targets have been studied and detailed excitation functions have been measured for all feasible cases. We plan to start new experiments shortly to look at the feasibility of measuring characteristics of the protons emitted when isomers are produced by (d,p) reactions.

The final experiments involved an excitation function for isomers produced by deuteron bombardment of ^{243}Am. In this case, the isomers are produced predominantly by (d,p) and (d,pn) reactions and the results show that the $^{243}Am(d,p)^{244m}Am$ cross sections are roughly equal to those observed in the $^{235}U(d,p)^{236m}U$ reaction and the $^{243}Am(d,pn)^{243m}Am$ cross sections are close to those measured for the $^{239}Pu(d,pn)^{239m}Pu$ reaction. These results make it appear unlikely that the ^{236m}U isomer has as its major decay mode γ-ray de-excitation to the ground state in the first well as has been speculated previously by other authors.

A paper has been prepared for submission to The Physical Review with the following abstract:

Excitation functions have been measured for the production of fission isomers by (α,xn) reactions for bombarding energies of 20-29 MeV

and by (d,2n), (d,p), and (d,pn) reactions for bombarding energies of 9-14 MeV. Excitation functions for (α,xn) reactions were measured for targets of ^{233}U, ^{234}U, ^{235}U, ^{236}U, ^{238}U, ^{237}Np, ^{239}Pu, ^{240}Pu, ^{242}Pu, and ^{244}Pu. Excitation functions for deuteron reactions were measured for targets of ^{235}U, ^{237}Np, ^{239}Pu, ^{240}Pu, ^{242}Pu, ^{244}Pu, and ^{243}Am. New or more accurate half lives were determined for the following fission isomers: ^{235m}Pu, 30 ± 5 nsec; ^{238m}Pu, 6.5 ± 1 nsec; ^{240m}Pu, 3.8 ± 0.3 nsec; ^{241m}Cm, 15.3 ± 1 nsec; and ^{245m}Cm, 23 ± 5 nsec. New isomers in ^{242}Cm and ^{244}Cm were discovered but their half lives were too long for measurement with the present techniques. The results are analyzed with a statistical model using realistic level density expressions with many parameters fixed by comparison to experimental measurements of neutron fission cross sections, neutron to fission decay widths, spallation cross sections, and fission lifetimes. This model is applied to the presently measured excitation functions and the results obtained previously by other groups for (n,2n), (p,2n) and (γ,n) reactions. With this model fission barrier parameters are determined for Pu, Am, and Cm isotopes. Inconsistencies in the results obtained by applying this model to experimental isomer excitation functions indicate the directions for future refinements.

D. THERMAL NEUTRON CAPTURE GAMMA-RAY STUDIES

1. $^{187}Re(n,\gamma)^{188}Re$ (E. B. Shera)

A new measurement of the high energy (n,γ) spectrum has greatly improved the accuracy with which the low lying levels can be specified thus reducing ambiguities in the assignment of low energy gamma rays measured by the Risø bent crystal spectrometer. In addition, several questionable lines which appeared in earlier spectra but did not fit into the expected pattern of low energy ^{188}Re states can be positively eliminated by the new data.

The level scheme has been considerably extended by the recent effort and this has indicated the need for further experimental work. In particular, the (n,γ) data indicated the occurrence of a $K^{\pi} = 0^{+}$ band at 207 keV. No such state was seen in previous beta decay experiments and although there are theoretical reasons which suggest that beta decay to such a state should be hindered, such a level should be populated to an extent observable with present detectors. Since the experimental observation of beta decay to this state would represent an important confirmation of our interpretation of the ^{188}Re level structure, such experiments were undertaken. Happily, they yielded a positive result.

Confirmation of the existence of a $K^{\pi} = 0^{+}$ band in ^{188}Re is important because only a few such bands are known in odd-odd nuclei and the analysis of these bands can make a significant contribution to understanding the n-p interaction.

Identification of the K = 0 band has made it possible to make configurational assignments to levels which lie higher in the spectrum. At present the intrinsic configurations given in Table D1 have been identified. In most cases several rotational levels are known for each configuration.

TABLE D1

Intrinsic Configurations in ^{188}Re

Energy of band head (keV)	K^{π}	Configuration p		n
0	1^-	$5/2^+[402]\uparrow$	$\pm$	$3/2^-[512]\downarrow$
181	4^-			
169	3^-	$5/2^+[402]\uparrow$	$\pm$	$1/2^-[510]\uparrow$
256	2^-			
171	6^-	$5/2^+[402]\uparrow$	$\pm$	$7/2^-[503]\uparrow$
290	1^-			
205	2^-	$5/2^+[402]\uparrow$	-	$9/2^-[505]\downarrow$
230	3^+	$9/2^-[514]\uparrow$	-	$3/2^-[512]\downarrow$
207	0^+	$9/2^-[514]\uparrow$	-	$9/2^-[505]\downarrow$
439	3^+	$5/2^+[402]\uparrow$	-	$11/2^+[615]\uparrow$
(326)	4^-	$5/2^+[402]\uparrow$	+	$3/2^-[501]\uparrow$

2. $^{209}Bi(n,\gamma)^{210}Bi$ (E. T. Jurney)

The spectrum from the ^{210}Bi compound nucleus decay has been re-examined in the energy range 40-2900 keV, with particular emphasis on precise energy determination. Nearly 200 gamma rays are observed. Such a multiplicity of gammas increases the chance of accidental energy fits in the decay scheme, a situation which can be improved by determining the energies more accurately.

The observation of a 516.6-keV gamma is important in the establishment of the first excited 1^- level; the level is not directly excited by a primary gamma and can only be observed indirectly through its decay. Although the gamma is convincingly present in the data, extracting it

from the upper skirt of the very intense annihilation peak has proven to be difficult. The difficulty arises from the ratio of peak intensities (~500/1), from the complex shape of the annihilation peak, and from the uncertainty in the shape of the background under the annihilation peak. The most promising approach has been to subtract the annihilation peak produced in an external source made by sandwiching a radioactive positron emitter between two plates of Bi. Computer least-squares fitting of the region has been utterly unsuccessful, even by using two Gaussian functions with varying widths but with both centroids at 511 keV to approximate the shape of the annihilation peak.

In spite of the difficulty with the 1^- state, it has been possible to arrive at a level scheme of the states arising from the two lowest configurations. This part of the level scheme is given in Table D2, together with the theoretical predictions of Kim and Rasmussen (Nucl. Phys. 47, 184 (1963)).

TABLE D2

Configuration	J	E(keV)	Predicted E (K & R)
$\pi h_{9/2}\nu g_{9/2}$	0	46.5	22
	1	-0-	-0-
	2	319.7	283
	3	347.9	343
	4	502.8	459
	5	439.1	392
	6	544.9	510
	7	433.4	376
	8	582.4	532
	9	271.2	284

3. $^{234}U(n,\gamma)^{235}U$ (E. T. Jurney, H. C. Britt, and F. Rickey (Purdue))

The spectrum below 2.5 MeV has been re-examined with our present detectors. Over four hundred gammas have been measured. In the overall experiment, which incorporates data from four charged particle reactions in addition to the (n,γ) reaction, nearly one hundred levels below 1.5 MeV have been observed and arranged into 22 bands. It has been possible to identify many of these bands with particular Nilsson configurations on the basis of the charged particle intensity patterns, although it is apparent that much fragmentation of the pure Nilsson states occurs.

The new low-energy (n,γ) data include that part of the gamma-ray spectrum which corresponds to the de-excitation of the lower-lying levels. Incorporating these transitions into the level scheme has been a time-consuming proposition because of the enormous number of possible combinations generated by the large number of levels and transitions.

Figure D1 shows the de-excitation modes observed in the five lowest-lying bands (energies in keV). The energy loops found in this part of the decay scheme are generally precise to within the accuracy of the least squares fitting of the peak centroids, i.e., a few tens of eV. Work is progressing on the final version of the manuscript describing the experiment.

E. RESEARCH IN SUPPORT OF NUCLEAR SAFEGUARDS

1. Cross-Section Measurement of $^{9}Be(n,p)^{9}Li$ Leading to $^{8}Be + n$ (R. H. Augustson and H. O. Menlove) Relevant to Request No. 29, NCSAC-35.

We are in the process of measuring the cross section for the delayed neutron emission branch of the $^{9}Be(n,p)^{9}Li$ reaction at $E_n \sim 14.7$ MeV. Delayed neutrons result from the subsequent β^- decay of ^{9}Li to excited states of ^{9}Be which in turn decay by neutron emission. The measurement procedure for the cross section and β decay half life will closely parallel that used for similar determinations of the $^{17}O(n,p)^{17}N$ delayed neutron yields.[1]

F. FACILITIES AND TECHNIQUES

1. Liquid Fuel High Intensity Neutron Sources (L. D. P. King)

Work on the Kinetic Intense Neutron Generator (KING) reactor is continuing.

Recent calculations at LASL are checking Russian results which indicated that the performance index (ratio of power output to peak thermal flux) can be substantially increased over existing high flux reactors such as the HFIR or SM-2 if the dimensions of the central water island and annular fuel region can both be optimized.

The rapidly moving liquid core with no fuel elements used in the KING reactor concept permits such optimization for the first time. The uranyl sulfate fuel has a sufficient uranium solubility so that the annular fuel region can be adjusted in thickness to provide the best performance index. A thermal flux of about 3×10^{14} neutrons/cm^2/sec/MW appears to be achievable if the central flux island is about 10 cm in diameter and the annular fuel region about 3 cm thick.

---

[1] H. O. Menlove, R. H. Augustson, and C. N. Henry, Nucl. Sci. and Eng. 40, 136 (1970).

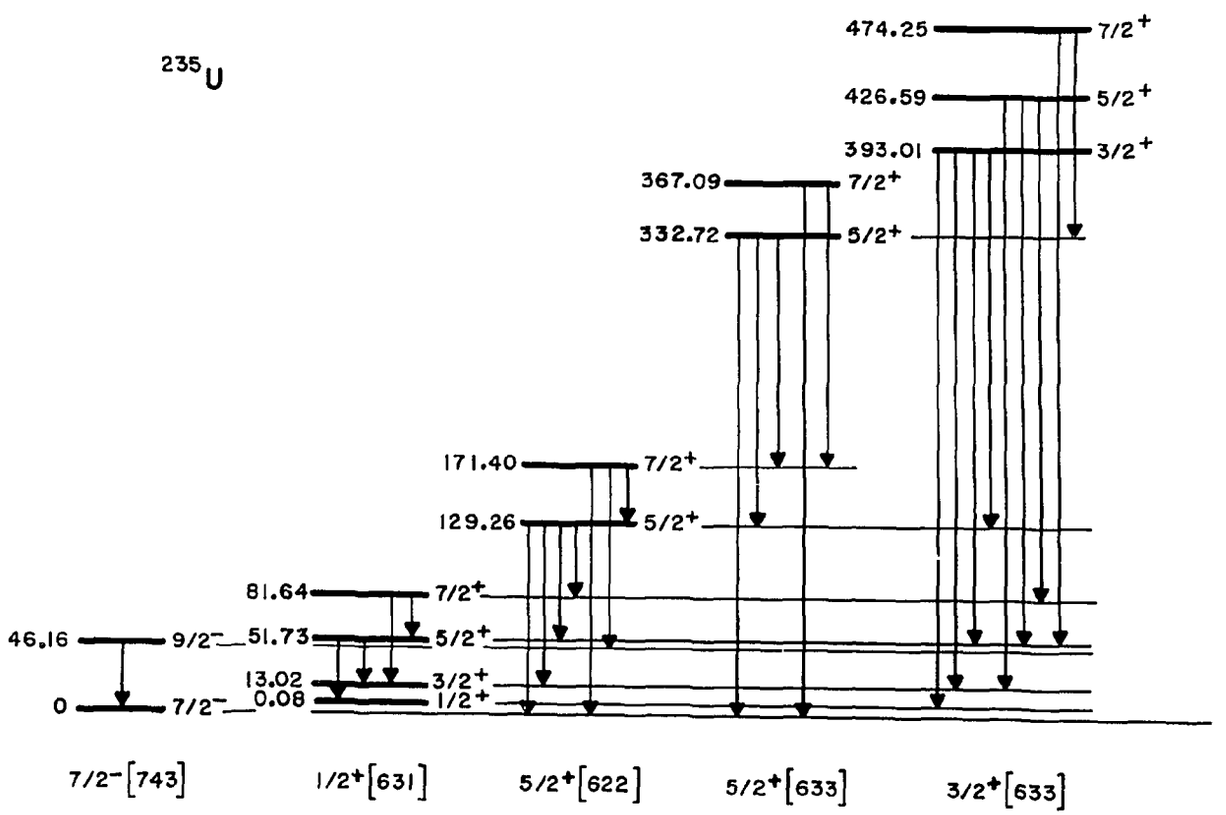

Fig. D1. Level scheme for the five lowest bands in ^{235}U populated by thermal neutron capture in ^{234}U.

Dynamic critical experiments to demonstrate the nuclear properties of the KING reactor are ready to commence in the near future. These tests are being carried out on a special facility known as Kinglet. All static neutronic calibrations have been completed at this time.

Consideration is being given to the construction of a 25 MW KING reactor at Los Alamos if the Kinglet experiments are successful. Such a device would serve the dual purpose of providing the world's highest steady-state thermal flux and at the same time serve as the test bed for determining total power output limitations of this concept.

2. Neutron Polarization Experiments by Time of Flight (G. A. Keyworth, J. R. Lemley, F. T. Seibel)

The LMN beam polarization system is progressing, but slowly. The superconducting coil is well along but the dewar and NMR system to map the field to permit inhomogeneity corrections are progressing slowly. Construction of the dewar has not yet begun, although the LASL shops have the completed drawings.

Pure ^{237}Np has been alloyed with palladium in an effort to find a suitable medium for a polarized Np target. The initial foil was 5 mils thick and contained 50 mg of Np. The initial attempt to obtain sizable polarization was successful. A large α-particle anisotropy was observed, indicating high polarization. We are now attempting to measure the γ-ray anisotropy for a strong 86-keV line in ^{237}Np decay. This information will permit the experimenters to correlate the α-particle anisotropy with degree of polarization.

An effort has been made to determine the feasibility of performing the Np fission experiment on a linac. The experiment does appear feasible, provided that a quite large sample is used and the fission neutron detected, rather than the fragments themselves, as previously intended on a bomb shot. It is hoped to make satisfactory arrangements to conduct the experiment at ORELA.

3. Neutron Polarization Experiments in the MeV Region (R. C. Haight, T. R. Donoghue (Ohio State), J. C. Martin, J. E. Simmons, and G. P. Lawrence)

The T(p,n)^{3}He reaction has been extensively studied. Three observables relating to the spin structure of the reaction have been measured, namely the polarization $P(\theta)$ of the neutrons produced with an unpolarized proton beam, the analyzing power $A(\theta)$ of the reaction when the proton beam is polarized, and the transfer of polarization. An excitation function of the polarization transfer was measured at 0° from 3 to 16 MeV. Corrections for finite geometry and multiple scattering are nearly finished. A contributed paper on the excitation function was given at the APS Washington meeting.

NATIONAL BUREAU OF STANDARDS

A. NEUTRON PHYSICS

1. MeV Neutron Total Cross Sections (R. B. Schwartz, R. A. Schrack, and H. T. Heaton II)

We have completed measurements of the total neutron cross sections of beryllium and silicon, and are presenting the results at the Washington Meeting of the American Physical Society. The following abstract has been submitted:

> We have measured the total neutron cross sections of beryllium and natural silicon from .5 to 20 MeV. The time-of-flight method was employed, using the NBS electron linear accelerator as a pulsed neutron source. The energy resolution varied from about .2 nsec/m at the low energy end to about .1 nsec/m at the high energy end. The statistical precision was made to be 2% or better everywhere; two sample thicknesses were employed with each element. Several low energy states in silicon and beryllium have been fit with a multi-level R-matrix code. Values of the width and energy for the fitted states will be given.

Figure A-1 shows our results for the beryllium cross section; and A-2 shows the silicon results. Figure A-3 compares our results for the 566 keV resonance in silicon with those from several other laboratories. In addition to the unfortunate discrepancies in the measured peak heights, it is interesting to note the difference in energy scales between the older Van de Graaff measurements (Saclay and Argonne) and the more recent time-of-flight measurements (Karlsruhe and NBS). This apparent systematic difference in energy scales has been noted before; more recent measurements seem to be in better agreement.

We have just completed measurement of the oxygen total cross section by measuring the transmission of single crystals of quartz (S_iO_2) relative to semi-conductor grade silicon. The results are generally in quite good agreement with the Karlsruhe data. Preliminary analysis indicates agreement with the results of Fowler et al. for the minimum at 2.35 MeV, in both cross section and energy. We plan to do further measurements and analysis in this energy region.

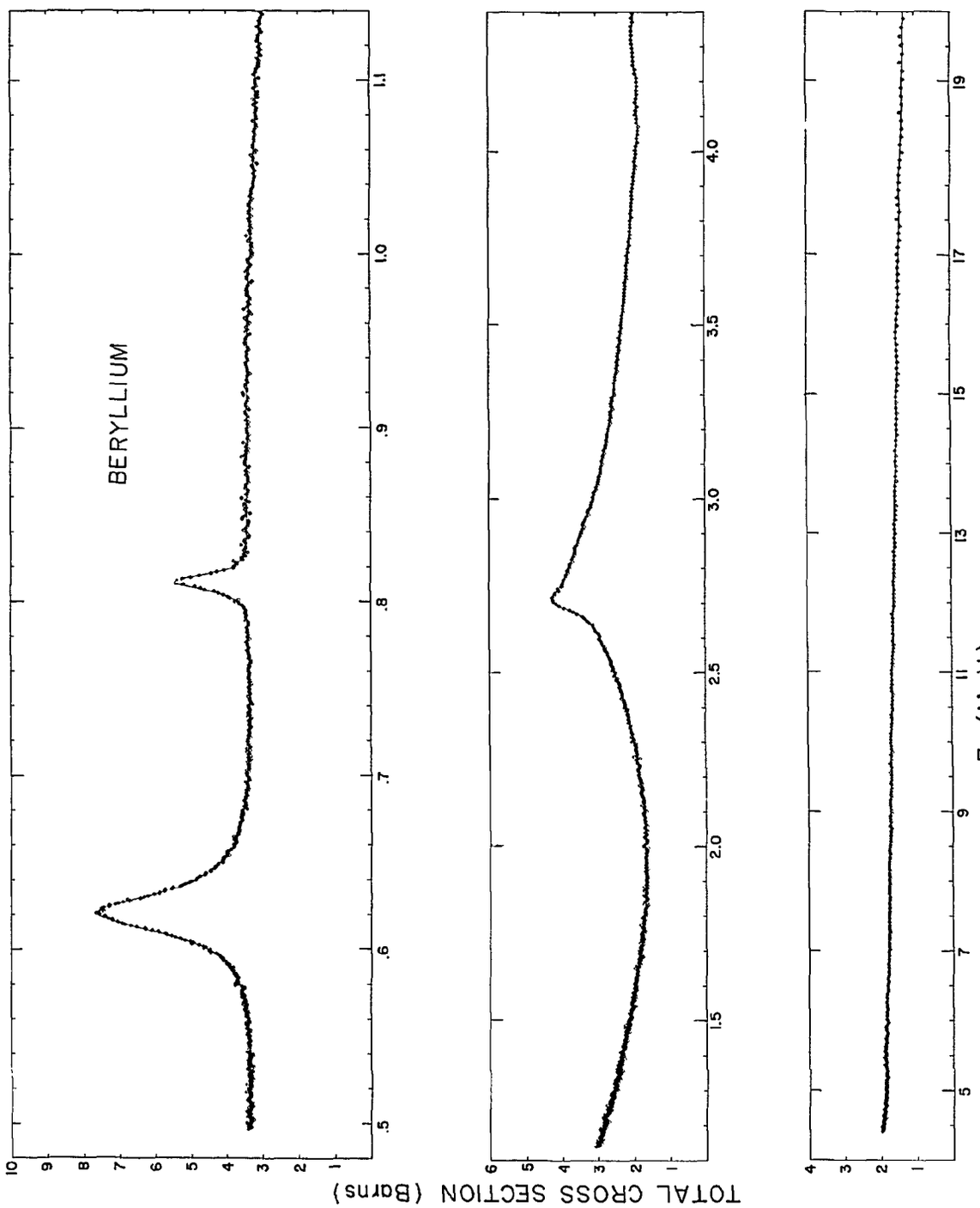

Fig. A-1

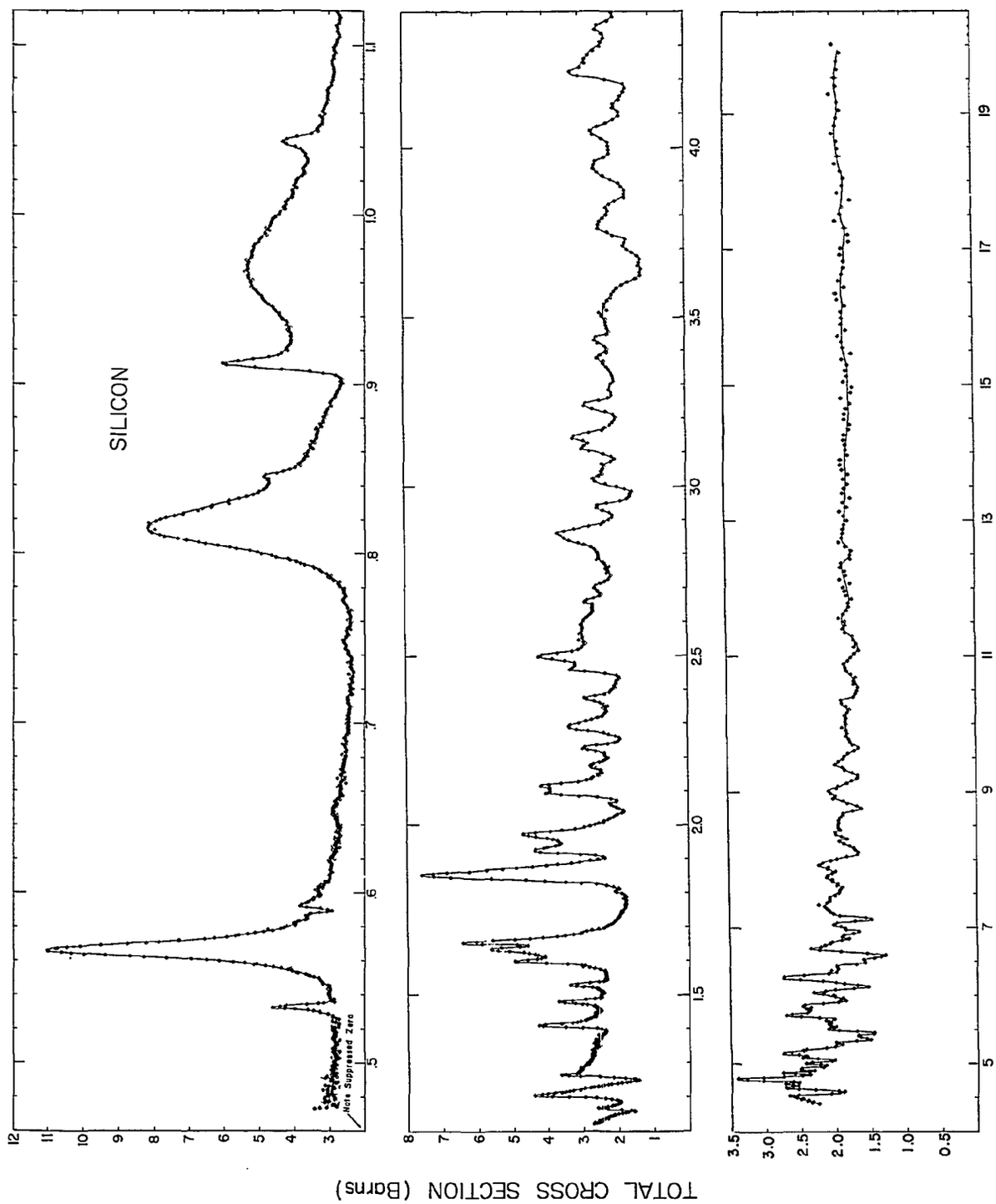

Fig. A-2

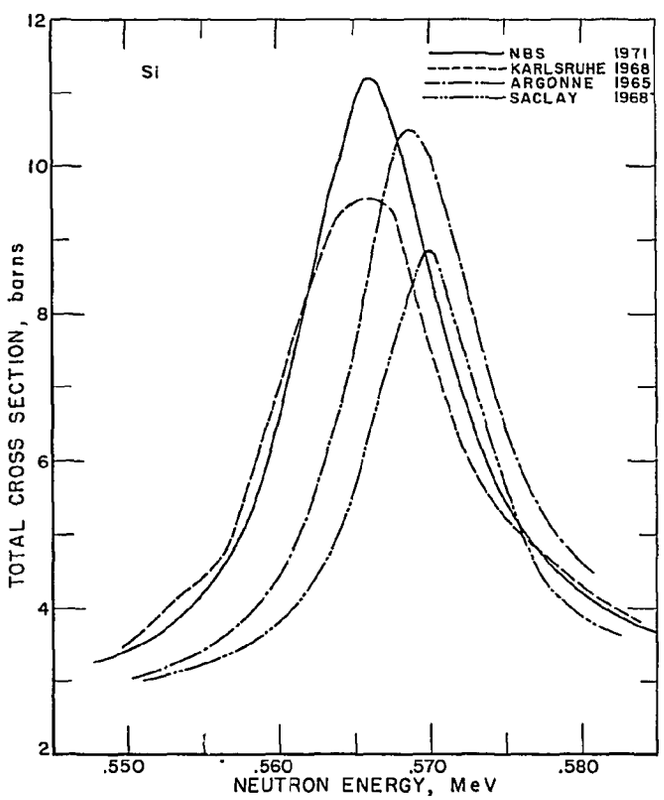

Fig. A-3

NAVAL RESEARCH LABORATORY

A. NEUTRON PHYSICS

1. Resonance Spin Determinations in Nd^{143} and Nd^{145} (A. Stolovy, T.F. Godlove, and A.I. Namenson)

The spin states of a large number of resonances in the targets Nd^{143} and Nd^{145} have been determined by the multiplicity technique used by Coceva et al.[1] and others. The cascade capture gamma-rays associated with the resonances were observed in coincidences and singles. Experiments were performed at the NRL Linac using 60 ns beam pulses with a peak current of 0.4 amp, a repetition rate of 360/sec, and a flight path of 10.7 meters. The capture gamma-rays are observed with four large NaI(Tl) detectors which surround the capture target. Single counts, double coincidences, and triple coincidences are sorted and stored according to time-of-flight as the data accumulates with an on-line computer. All time-of-flight and logic operations are performed by a system of fast integrated circuit cards[2]. Singles counts are taken with an integral bias level of 3 MeV, and coincidences are taken with a 0.55 MeV bias level. The ratio of coincidences to singles is a function of the spin of the capturing state, and the results generally fall into two groups. We have also taken data using a window from 0.55 MeV to 3 MeV for the coincidences instead of an integral bias level, in order to enhance the effect. The results are given in the following tables:

TABLE A-1

Resonance Spin State Determinations in Nd^{143}

E_o (eV)	J	E_o (eV)	J
55.4	4	403	(4)
127	3	409	(3)
135	3	446	(4)
159	(4)	509	3
180	(3)	527	4
187	(4)	557	4
307	4	661	(4)
325	4	710	4
339	4	780	4
351	3	845	(3)

[1]Coceva, Corvi, Giacobbe and Carraro, Nuclear Phys. A117, 586 (1968).
[2]Godlove, Smith and Namenson, Nuclear Instr. and Methods (Accepted for publication, 1971).

TABLE A-2

Resonance Spin Determinations in Nd^{145}

E_o (eV)	J	E_o (eV)	J
4.33	3	344	4
42.6	3	378	(4)
85.7	4	393	4
96.1	3	400	(3)
101.7	3	407	4
103.5	(4)	449	4
147	3	467	(3)
152	(4)	489	4
170	4	499	3
190	3	508	4
233	(4)	518	4
243	4	544	4
249	(3)	571	4
260	4	592	(4)
276	4	609	(3)
308	4	642	(4)
312	4	652	(3)
320	3	663	(3)

2. Evidence for Intermediate Structure from Resonance Capture in Re^{185} and Re^{187} (A. Stolovy, A.I. Namenson, and T.F. Godlove)

The neutron resonances in the target nuclei Re^{185} and Re^{187} have been studied up to 400 eV with a flight path of 10.7 meters, and using separated isotope targets. The observed time-of-flight spectra are shown in Figures A-1 and A-2. The neutron energies of a few arbitrarily selected resonances are labelled in eV. The discontinuities are produced by a computer "crunching" program which stores the first 512 channels at 1/16 μsec/channel, the next 224 channels at 1/8 μsec/channel and so on, so that the spectrum can be stored in a convenient number of channels without sacrificing resolution. Data were taken with high bias (gamma-rays above 4 MeV) and with low bias (gamma-rays above 1 MeV). The high bias data represent primary transitions from the capture states to low lying levels in the compound nucleus. The low bias data represent a sum over many cascade transitions, and is used to normalize the high bias data. An off-line computer program is used to obtain the integrated intensity under each resonance peak with the background removed.

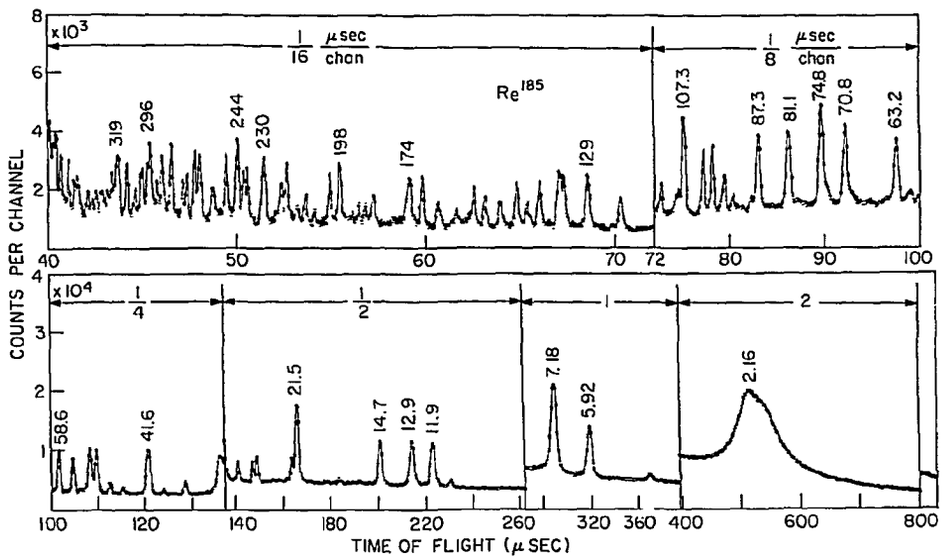

Fig. A-1. Neutron time of flight spectrum for Re^{185}.

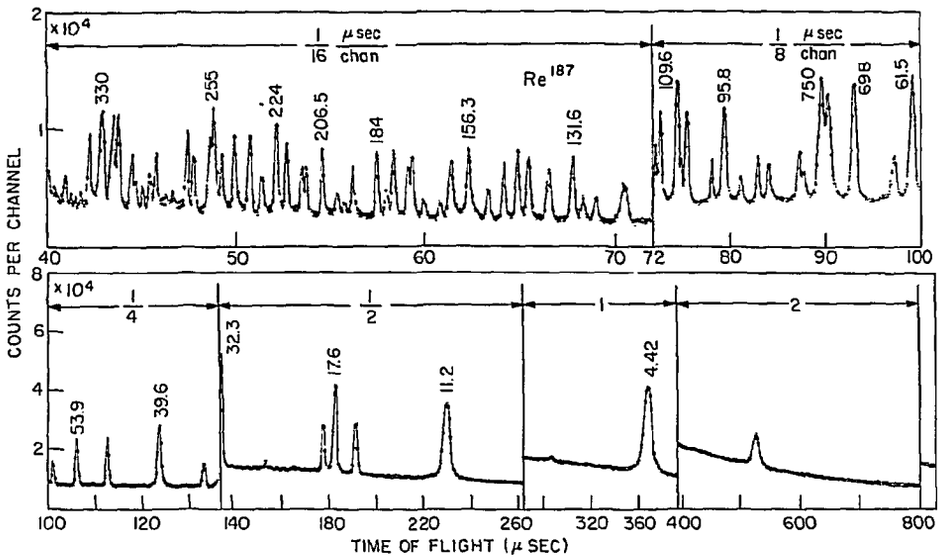

Fig. A-2. Neutron time-of-flight spectrum for Re-187.

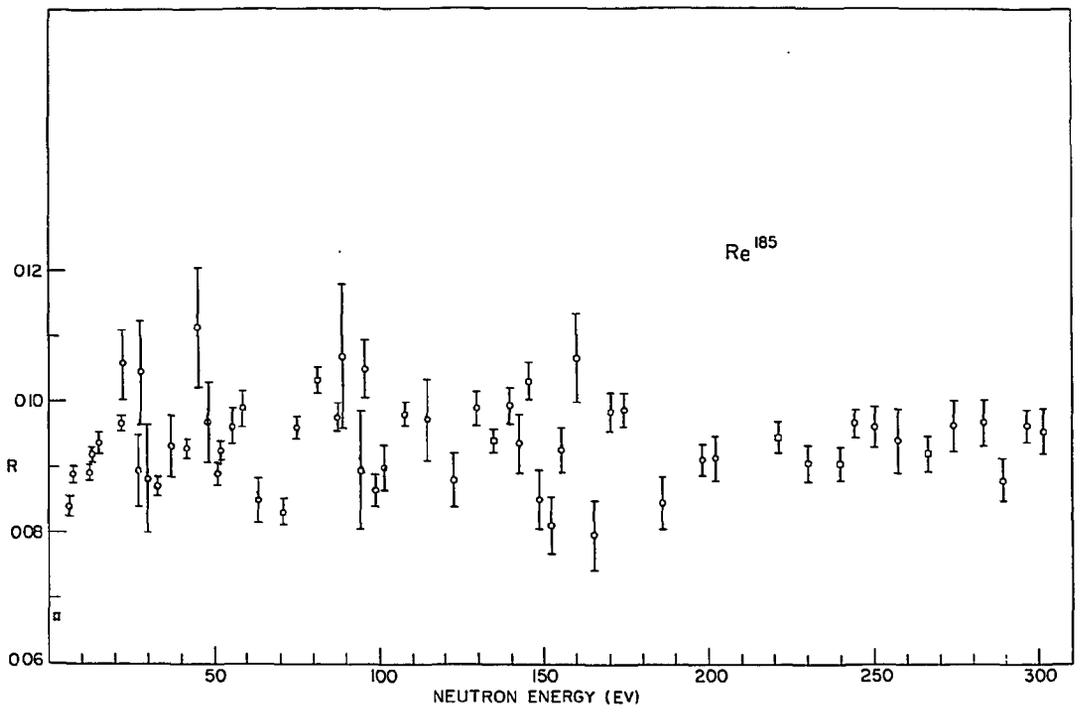

. A-3. Primary capture γ-ray intensities vs resonance energy for Re-185 and Re-187.

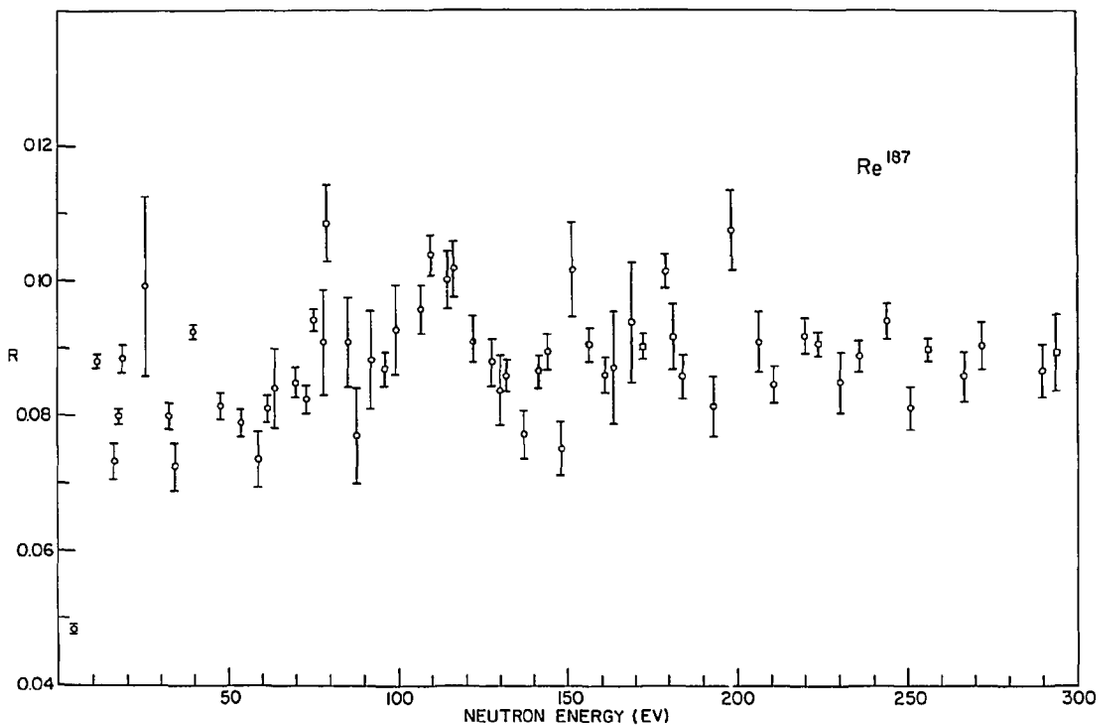

Figure A-4

The ratio R of the high bias data resonance intensity to that of the low bias data is the fraction of the total capture intensity due to gamma-rays above 4 MeV. In figure A-3, we have plotted R vs the neutron resonance energy for Re^{185} and Re^{187} respectively. Little if any structure is apparent in the Re^{185} data, but the Re^{187} data exhibits a bump between 90 eV and 140 eV. A statistical analysis of these data, in which we have looked for a correlation between adjacent points, as well as a χ^2 analysis, indicates that there is only about one chance in 300 that such a bump could occur by chance. We believe that this is evidence for the presence of at least one extremely narrow intermediate state, with a width of about 40 eV. This is even narrower than the intermediate structure found by Coceva et al[3] in In^{115}. Such a state must be highly complex, involving many particles and holes. It is perhaps just one rank lower than the narrow compound nucleus states (the resonances) in the hierarcy of possible intermediate states.

3. Monte Carlo Simulation of Multiplicity Experiment (A.I. Namenson)

A Monte Carlo simulation of the experiment of Stolovy et al (presented in this same report) was carried out for neutron capture by Hf^{177}, Hf^{179}, Nd^{143}, Nd^{145}, Re^{185} and Re^{187}. The method used was similar to that of Giacobbe et al[4]. Some of the differences are that the present calculation accounts for triple and quadruple coincidences and also considers improvements in the experiment such as using windows rather than base lines in counting the low energy lines.

To describe the nuclear levels in the energy region above the known decay scheme, a statistical model described in an article by Gilbert and Cameron[5] was applied. Weisskopf estimates were used for gamma ray transition probabilities from these levels to either known levels or to other levels in the region above the known decay scheme. For the purposes of calculation, only E1, M1 and E2 transitions were considered likely. (The error in neglecting M2 and higher order transitions is estimated to be less than 0.1%.) Once a gamma cascade reaches a known level, published data is used to complete the cascade to the point where it terminates in either the ground state or in an isomeric level.

---

[3]Coceva, Corvi, Giacobbe and Stefanon, Phys. Rev. Letters 25, 1047 (1970).
[4]Giacobbe, Stefanon, and Dellacasa, CNEN Report RT/FI (68) 20.
[5]A. Gilbert and A.G.W. Cameron, Can. J. Phys. 43, 1446 (1965).

For each possible spin, a number of gamma cascades were generated by this Monte Carlo process. For each cascade the number of gamma rays above a "singles" threshold (3.0 MeV for all cases) and a "multiples" threshold (550 keV for all cases) was counted. Analytic expressions were used to calculate the number of double, triple and four-fold coincidences which would result. The coincidence rates normalized to the singles rate should give a spin dependent ratio. The results in the following table show the percent by which the ratio for the larger spin exceeded that for the lower spin. An efficiency of 10% was used for all detectors.

TABLE A-3

Target Isotope	^{177}Hf	^{179}Hf	^{143}Nd	^{145}Nd	^{185}Re	^{187}Re
Doubles Effect	11 ± 4	5 ± 2	30 ± 10	29 ± 10	-8 ± 4	-10 ± 14
Triples Effect	14 ± 5	4 ± 3	46 ± 12	43 ± 15	-9 ± 5	-10 ± 16
Four-fold Effect	16 ± 6	5 ± 3	64 ± 16	55 ± 20	-10 ± 6	-16 ± 15

It is seen that the triples and four-fold coincidences give larger effects than the doubles. In practice, the counting rate for the four-folds was too small to be useful. For the triples however, the size of the effect compensated for the low counting rate. Because of the approximations made one would not expect these results to be exact. However, Hf^{179} is the only case where the computed effect is much smaller than measurements. The Nd isotopes give effects which are within statistics of our measurements. The calculation shows no significant effect for the Re isotopes which is also in agreement with experiment.

Some special studies were made on the Nd isotopes to investigate possible sources of error and possible improvements. These isotopes were chosen because they gave a large effect and also agreed well with experiment. Changes in the detector efficiency had little effect on the result as did moderate variations in the statistical distributions of nuclear levels.

The calculation indicated that significant improvements in the experiment could be obtained by imposing a low energy window condition on the multiples gamma lines rather than just a base line. For the doubles effect in Nd, the values shown in the above table would be increased by $63\% \pm 21\%$ by using a window from 550 keV to 2.00 MeV for multiple events instead of simply the 550 keV base line. Preliminary experimental results seem to support this.

Presently we are investigating how the results are affected by large deviations from the statistical model used, deviations from Weisskopf estimates, and the possible presence of anomalous bumps in the gamma spectra.

4. High Energy Gamma Rays Following Resonance Neutron Capture (J.C. Ritter, A.I. Namenson, G.L. Smith)

Experiments investigating the gamma ray spectra following slow neutron capture are underway using neutrons produced by the time-of-flight facility at the Naval Research Laboratory Linac. The motivation behind these experiments is to investigate the neutron capture mechanism as well as to obtain level energies, spins, and parities. Gamma rays are detected by a lithium-drifted germanium detector. Experiments on slow neutron capture by ^{170}Yb and ^{172}Yb have been completed and the results are presented in Tables A-4 and A-5 respectively. Calculations on these results are not complete but there does seem to be a hindrance of transitions to the $\frac{3}{2}^-$ $\frac{3}{2}$ [512] Nilsson band in ^{173}Yb, as was observed in thermal capture. Because of the small number of resonances, statistical fluctuations cannot be ruled out as an explanation.

There have been several improvements in the experimental arrangement since acquiring the Yb data. The experiment is now completely automated and under computer control. It is possible to accumulate two-dimensional data on magnetic tape in the form of 1024 time-of-flight channels by 4096 gamma-ray energy channels. The computer system is capable of reducing and analyzing this mass of data off-line by using the NASA IBM computer or a 7.2 megabyte disc memory. A new Ge(Li) detector with 48 cm^3 active volume has recently been installed.

Data on slow neutron capture by ^{168}Er, ^{185}Re and ^{187}Re have been accumulated with the new arrangement. The motivation behind the study of the Re isotopes was to assist with the spin measurements and to study in more detail the gamma rays in the region of the intermediate state proposed by Stolovy et al. (presented previously in this report).

TABLE A-4

Primary gamma rays from the $^{170}Yb(n,\gamma)^{171}Yb$ reaction. Energy uncertainty is ± 3-keV for intense transitions. The neutron separation energy is 6616 ± 3 keV[a]

Gamma Ray energy (keV)	Relative intensity Thermal[a]	Intensity (photons per 1000 captures) 8 eV resonance	40 eV resonance	67 eV resonance	73 eV resonance	Levels Populated Energy (keV)	Nilsson assignment
6616	100 ± 5	4.2 ± 0.6	23.1 ± 1.4	15.8 ± 3.1	1.8 ± 1.4	0	$\frac{1}{2}\frac{1}{2}^{-}$[521]
6549	15 ± 5	0.15 ± 0.45	2.9 ± 0.9	-0.9 ± 1.2	13.9 ± 2.3	67	$\frac{3}{2}\frac{1}{2}^{-}$[521]
5709		2.2 ± 0.9	5.9 ± 1.3	1.2 ± 2.3	0.2 ± 2.3	907	$\frac{3}{2}\frac{3}{2}^{-}$[521]
5628[b]	10 ± 5	11.9 ± 1.1	8.4 ± 1.4	0.9 ± 2.3	2.1 ± 2.5	988	$\frac{3}{2}\frac{1}{2}^{-}$[510]
5577		8.2 ± 1.0	-0.5 ± 1.0	-3.1 ± 2.0	22.8 ± 3.3	1039	
5288		0.9 ± 1.0	0.5 ± 1.1	3.6 ± 2.8	17.7 ± 3.0	1328	
5271		-0.7 ± 1.0	0.5 ± 1.1	-4.5 ± 2.2	12.6 ± 2.9	1345	
5082		5.6 ± 1.2	1.8 ± 1.3	-4.9 ± 2.7	-0.6 ± 2.6	1534	
4712		5.6 ± 1.4	0.3 ± 1.5	-1.1 ± 3.8	-0.8 ± 3.2	1904	

[a] A.I. Namenson and J.C. Ritter, Phys. Rev. 183, 983 (1969).

[b] Member of a doublet in thermal spectrum.

TABLE A-5

Primary gamma rays from the $Yb^{172}(n,\gamma)Yb^{173}$ reaction. Energy uncertainty is ± 3 keV for intense transitions. The neutron separation energy is 6365 ± 3 keV[a]

Gamma ray energy (keV)	Relative intensity per capture			Relative intensity Thermal[a]	Levels populated		
	140 eV	180 eV	202 eV		This experiment Energy (keV)	Burke et al[b] Energy (keV)	Nilsson assignment
5967	5 ± 3	39 ± 6	100 ± 9	97 ± 9	398	398	$\frac{1}{2}\frac{1}{2}^-[521]$
5904	10 ± 3	1 ± 2	32 ± 6	21 ± 10	461	~462	$\frac{3}{2}\frac{1}{2}^-[521]$
5336	34 ± 4	17 ± 4	7 ± 4	100 ± 9	1029	1031	$\frac{1}{2}\frac{1}{2}^-[510]$
5292	19 ± 5	29 ± 5	7 ± 4	74 ± 15	1073	1073	$\frac{3}{2}\frac{1}{2}^-[510]$
5136	40 ± 6	4 ± 3	2 ± 4		1229	1224	$\frac{3}{2}\frac{3}{2}^-[521]$
5025	1 ± 4	4 ± 4	2 ± 4		-	1340	$\frac{3}{2}\frac{3}{2}^-[512]$

[a] A.I. Namenson and J.C. Ritter, Phys. Rev. 183, 983 (1969).

[b] D.G. Burke et al., Kgl. Danske Videnskab. Selskab, Mat.-Fys. Medl. 35, No. 2 (1966).

B. SAFEGUARDS

1. Nondestructive Assay of Fissionable Materials (D.W. Jones, P.R. Malmberg, T.H. May, and C.V. Strain)[1]

A new technique for assaying uranium samples based upon the difference in the fission cross sections of uranium isotopes has been studied. In a test of this method, samples of uranium containing both ^{235}U and ^{238}U were bombarded with a beam of 0.5-MeV neutrons obtained from the $^{3}H(p,n)^{3}He$ reaction. The 0.5-MeV neutrons caused the ^{235}U nuclei to fission but failed to activate the ^{238}U because of its high fission threshold. Fission neutrons from ^{235}U were detected by a recoil proton scintillation counter which used the technique of pulse-shape discrimination to reject pulses induced in the detector by gamma rays. The relative sensitivities of the apparatus to ^{235}U and ^{238}U were measured and the ability of this method to detect changes in the ^{235}U content of a sample of uranium containing only a few percent of ^{235}U was studied.

[1]Jones, Malmberg, May and Strain, Nuclear Applications and Technology, 8, 79 (1970).

NUCLEAR EFFECTS LABORATORY

A. SMALL-ANGLE ELASTIC SCATTERING OF FAST NEUTRONS (W. P. Bucher, C. E. Hollandsworth, R. D. Lamoreaux, A. Niiler, and R. R. Sankey)

Data for the scattering of 7.55 and 9.5 MeV neutrons from C, N (N_2H_4), O(H_2O), and Pb at 2.5°, 7°, 11°, and 15° have been obtained using the special-purpose collimator described in previous reports. The data have been reduced and final corrections are being applied. Cross sections are measured relative to Pb with the small-angle collimator.

To obtain absolute cross sections, the differential scattering cross sections for Pb and CH_2 in the angular range 3.5° to 15° were measured at 7.55 and 9.5 MeV using time-of-flight techniques. Because of the relatively low forward-angle scattering cross section for carbon and hydrogen, the results for CH_2 are more susceptible to systematic errors due to air scattering effects than are the data for Pb. The CH_2 results were used to correct the Pb measurements for these effects.

Measurements at other energies between 7 and 10 MeV are in progress. Measurements will be continued for these elements to 14 MeV neutron energy in future months. (Pertinent to Requests #31, #33, #39, #40, and #44; WASH-1144 - Draft Version).

B. DELAYED FISSION ISOMERS (D. Eccleshall, J. K. Temperley, J. A. Morrissey; S. L. Bacharach (Catholic Univ.))

The delayed fission isomers occurring in ^{237}Pu have been studied via the reaction $^{237}Np(d,2n)^{237m}Pu$, using a pulsed-and-bunched deuteron beam and a standard catcher foil geometry. The current work and a recently-reported study by Russo et al.[1] represent the first simultaneous observation of both ^{237}Pu isomers. We have presented a preliminary report on our results,[2] and a detailed paper is being prepared for publication.

The time spectrum obtained from delayed fission events following the $^{237}Np(d,2n)$ reaction at an incident deuteron energy of 12 MeV is shown in Fig. B-1. The curves are the result of a least-squares fit

[1] Russo, Vandenbosch, Mehta, Tesmer, and Wolf, Bull. Am. Phys. Soc. 16, 55 (1971).

[2] Bacharach, Temperley, and Morrissey, Bull. Am. Phys. Soc. 16, 56 (1971).

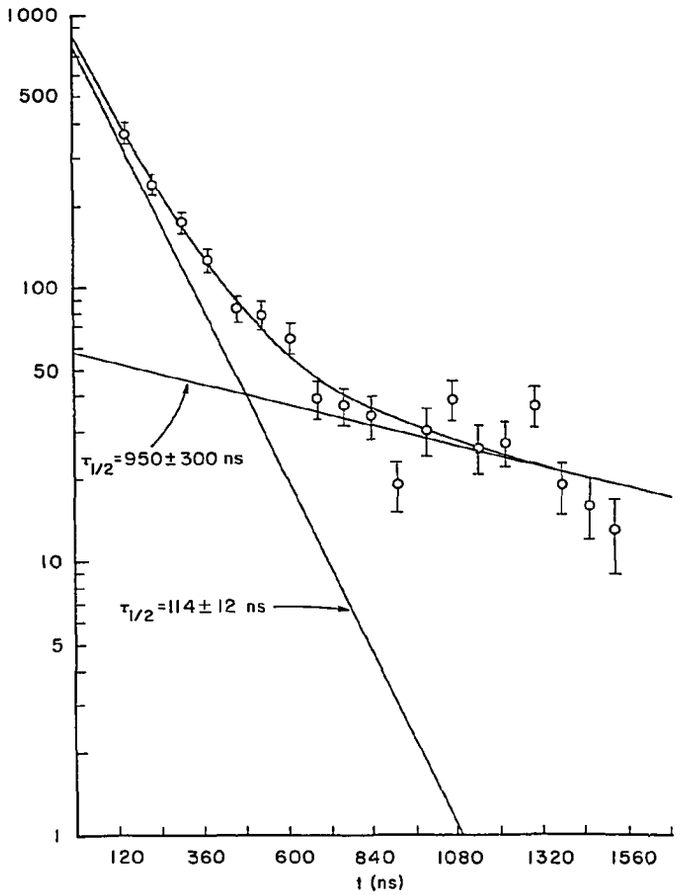

Fig. B-1 Delayed fission event rate following $^{237}N_p(d,2n)$ reaction at E_d = 12 MeV.

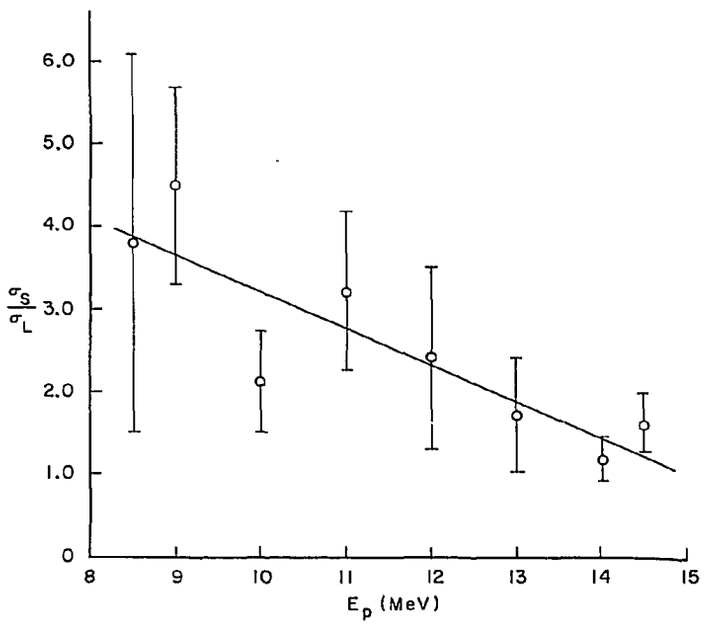

Fig. B-2 The ratio of short-lived to long-lived isomer production as a function of deuteron energy.

of the sum of two decaying exponentials to the data points. The half-lives obtained from this fit are $T^S_{1/2}$ = 114 ± 12 ns and $T^L_{1/2}$ = 950 ± 300 ns.

The ratio of the cross section for production of the short-lived isomer to that for the long-lived isomer is shown in Fig. B-2 for incident deuteron energies between 8.5 and 14.5 MeV. The straight line is the result of a least-squares fit to the data points. A chi-square test of this fit (6 degrees of freedom) yields a reduced chi-square value of 1.04 with a corresponding chi-square probability of 40%. A chi-square test applied to a horizontal line through the weighted average of the data points (7 degrees of freedom) yields a reduced chi-square value of 2.51 and a corresponding chi-square probability of 1.8%. While there is no theoretical justification for a straight-line fit to the data, these results strongly indicate that the production cross section for the long-lived isomer increases with respect to the cross section for production of the short-lived isomer as the deuteron energy is increased; certainly the converse is not true. We interpret this to mean that the 950-ns isomer lies at a higher excitation energy in the ^{237}Pu nucleus than does the 114-ns isomer.

Individual excitation functions for the production of each isomer have been obtained for incident deuteron energies between 8.5 and 14.5 MeV. The excitation function for the long-lived isomer peaks at $E_D \simeq 10$ MeV, that for the short-lived isomer somewhat lower. On the basis of these data an energy separation between the two isomers in the range of a few hundred keV to 1 MeV appears plausible. We have estimated the absolute cross sections for production of each isomer at a deuteron bombarding energy of 13 MeV to be $\sigma_S = 0.37^{+1}_{-0.05}$ μb and $\sigma_L = 0.25^{+1}_{-0.06}$ μb. The large positive uncertainties are due to target thickness, which precludes the precise determination of the fraction of ^{237m}Pu nuclides which recoil out of the target.

The single-fragment kinetic energy distributions for prompt and delayed events, obtained by summing the appropriate groups of data from a two-parameter analysis of energy versus time, at a deuteron bombarding energy of 13 MeV, are shown in Fig. B-3. The circles represent prompt events; the squares represent delayed events. The two distributions were obtained simultaneously with the same set of detectors; the prompt events are due to ^{237}Np(d,xf) reactions occurring at the catcher foil as a result of transfer of material from the target. From Fig. B-3 one finds a high-energy-peak/valley ratio of 1.9 ± 0.2 for the prompt events and 4.9 ± 1.2 for the delayed events. The higher ratio for the delayed events indicates that the delayed-fission process is more asymmetric than the prompt high-energy fission process.

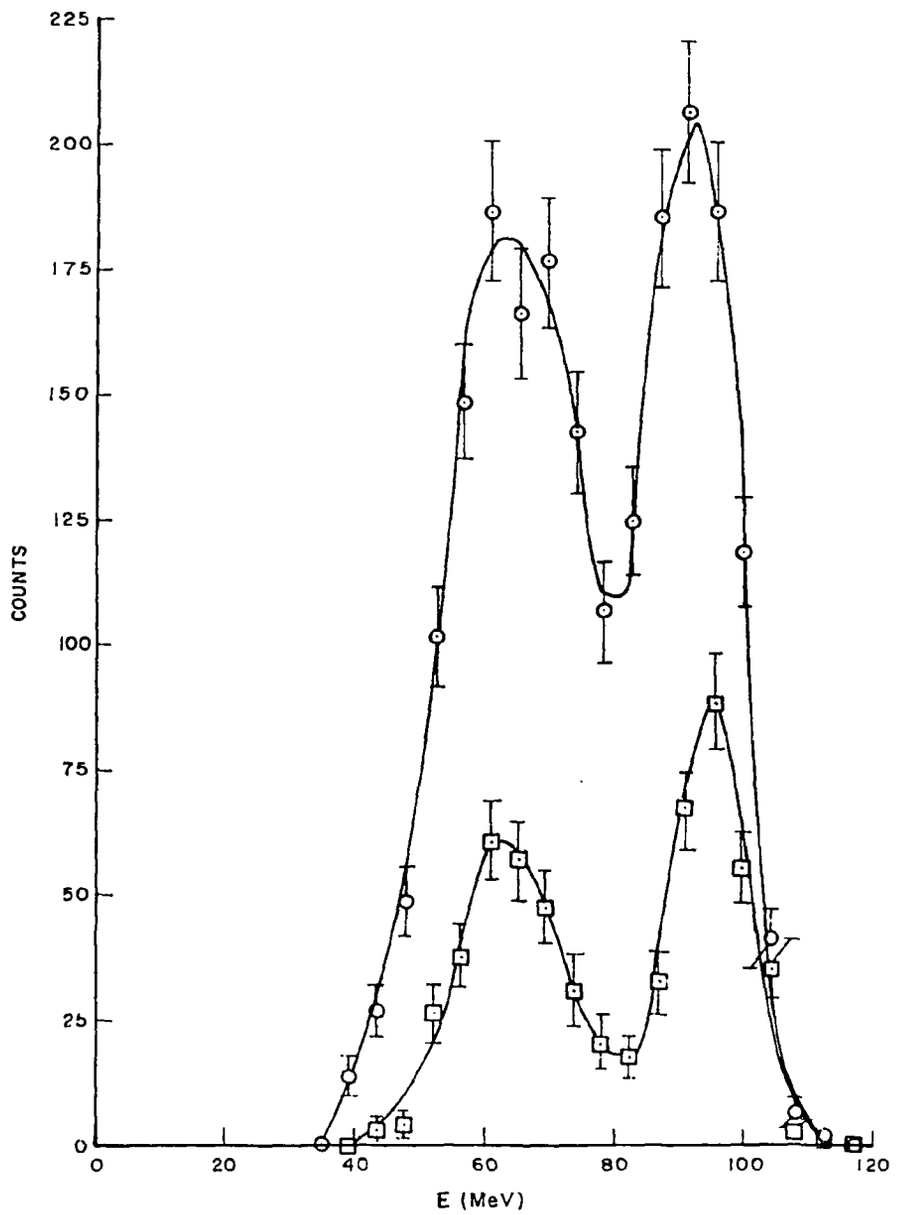

Fig. B-3 Single-fragment kenetic energy distributions for E_d - 13 MeV. Circles represent prompt, squares delayed events.

C. SENSITIVITY OF S_n CALCULATIONS TO FEATURES OF THE NITROGEN CROSS SECTION (R. S. Thomason)

A study of sensitivities of S_n neutron transport calculations to features of the nitrogen cross sections was formulated as a complementary effort to the experimental neutron cross section measurements. Specifically, it was of interest to determine what effect large errors in the small angle neutron elastic scattering cross section might have on one-dimensional flux solutions obtained using the S_n method.

Spherical geometry was selected for the problem and consists of a 1 m radius distributed source, a 100-percent nitrogen atmosphere at standard temperature and pressure from 1 m out to 2000 m, and a vacuum beyond 2000 m. One hundred spatial intervals and an S_{16} angular quadrature were used. Cross sections were obtained by collapsing the 100-group DLC-2B cross section tables for Nitrogen into 22 groups. (The DLC-2B Neutron Cross Section Library is available from ORNL.) The finest energy mesh was retained at the highest energies with most collapsing done on groups with energies less than about 1 MeV. This was done because energies above 1 MeV are of primary interest to this study and because most structure in the neutron cross section is found above 1 MeV.

To test the sensitivity of the S_n results to the goodness of the representation of the elastic scattering cross section angular distribution, calculations were made for P_0, P_3, and P_6 representations. P_l here indicates that the angular distribution of the elastic scattering is represented by an l^{th} order expansion in Legendre polynomials. The results were quite different in going from P_0 to P_3 as was to be expected. But the substantial change in the distribution obtained by going from P_3 to P_6 made very little difference in the resultant angular fluxes, much less the integrated flux. These results are in agreement with reports of other investigators and indicate the following, at least for the particular problem under study: information about the shape of the elastic scattering angular distributions need be no more detailed than is necessary to accurately determine the first several (3 to 5) terms in the Legendre polynomial expansion of the distribution.

In order to study the effects on the S_n results of various perturbations in the magnitudes of the input cross sections a computer routine was developed. This routine allows perturbations to be made on multigroup cross section sets which are equivalent to perturbations made on the original pointwise cross section data (e.g., ENDF data). Making the perturbation on the multigroup table rather than the basic cross section data results in a considerable savings of time, effort, and money.

Measurements of the nitrogen elastic scattering cross section at very small forward angles performed at the NEL Tandem Accelerator

Laboratory have indicated that accepted values of the integrated elastic scattering cross section may be low. To see what effect a 20% increase in the total elastic cross section would have on the S_n-calculated fluxes, and certain integrated quantities, a multigroup set was produced by applying the following perturbations to the original multigroup set: the elastic scattering cross section above 6 MeV was increased by 20%, the perturbation going to zero at 3 MeV with an energy dependence linear in lethergy; to maintain the total cross section unchanged, one-half of the value of the elastic cross section increase was taken from the absorption cross section and the other one-half was taken from the inelastic scattering cross section. The cross section decrease was divided equally between the absorption and inelastic scattering cross sections in an attempt to second-guess the cross section evaluator who somehow has to make up the original discrepancy between the total and partial cross sections.

An S_{16}-P_3 calculation using the 20%-elastic perturbed multigroup set yielded the following changes relative to the results using the unperturbed (original) set: total flux increased by 50%; tissue dose increased by 80%; and silicon damage increased by 92%. In addition, the scalar flux in some high energy groups increased by almost a factor of three.

D. NEUTRON PRODUCED GAMMA RAYS IN NITROGEN (C. M. Cialella)

Measurements of the gamma ray energy spectra and intensities produced by 15 MeV neutrons interacting with liquid nitrogen have been performed. Cylindrical samples of 15 cm diameter and 30 cm diameter were used. The complete spectrum was measured in two parts, from 0.5 to 2.5 MeV and from 2.0 to 10.0 MeV. A lithium-drifted germanium detector was used to detect the gamma rays. Time-of-flight analysis, with flight paths of 130 and 220 cm, was used to eliminate neutrons scattered from the sample into the detector and to suppress background. The results are being analyzed for differences from previous experiments.[1] Even though this analysis is preliminary, it appears that a closer examination of the high energy gamma rays (above 7 MeV) produced by 15 MeV neutrons in nitrogen is warranted.

[1] V. J. Orphan and C. G. Hoot, Measurement of Gamma Ray Production Cross Sections for Nitrogen and Oxygen, DASA Report No. 2267, GA-8006, January 31, 1969.

E. NITROGEN CROSS SECTION SENSITIVITY STUDIES USING THE SAMCEP CODE

N. E. Banks and W. B. Beverly; S. Hui (MAGI)

A correlated-sampling, neutron transport code (SAMCEP) has been written under contract for NEL by Mathematical Applications Group Inc. (MAGI). This code permits the calculation to a high statistical accuracy with minimum computer time, of the changes in the radiation field in a complex geometry which would be caused by perturbations in the input cross sections or in the neutron source. SAMCEP has been tested for operation on a CDC 6600 computer by running a standard Benchmark Problem of ORNL (i.e. the transport of neutrons in an infinite homogeneous atmosphere). This checks the code in the unperturbed mode.

One problem set has also been run for a point, isotropic 9.0 MeV source in an infinite, uniform, nitrogen atmosphere. The base cross sections used where the ENDF/B, round-1 evaluated data. A set of experimental total and partial nitrogen cross sections[1-4] was compiled over the energy range 5.25 to 9.0 MeV and plotted and a smooth curve was drawn through each set. The experimentally measured total cross section[1] was about 20% higher than the total of the experimentally measured non-elastic and elastic cross sections over most of this energy range.

This "missing partial cross section" was then added in turn to the various partials in order to make the total and partials consistent over the entire energy range. These perturbed cross section sets were: 1. Base set ENDF/B - Round 1; 2. Total and inelastic scattering cross section from ENDF/B - Round 1, absorption as given in Reference 2 with the discrepancy taken up by the elastic scattering cross section; 3. Total and elastic scattering cross section from ENDF/B - Round 1, total absorption as given in Reference 2 with the discrepancy taken up by the inelastic scattering cross section; 4. Total cross section given by Reference 1, inelastic cross section and absorption given by Dickens and Perey[2], elastic scattering from Bauer, et al.[3] and Chase, et al.[4]. The discrepancy is taken up by the elastic scattering; 5. Same as Case 4, except the discrepancy is absorbed by the inelastic scattering cross section.

These cross section sets were used as input for a problem set with each cross section set being the input for one perturbation. The fluence was calculated for each perturbed problem out to 2 mfp as well

1 A. D. Carlson, et al., DASA Report No. 2289 Vol 2 (1969), "High Resolution Measurements of the Total Neutron Cross Sections of Nitrogen and Iron".

2 J. K. Dickens and F. G. Perey, Nucl. Sc. & Eng. 36, pp 280-290 (1969), "The $^{14}N(n,x\gamma)$ Reaction for 5.8 $\leq$ En $\leq$ 8.6 MeV."

3 R. W. Bauer, et al., Nuc. Phy. A 93, pp 673-682, (1967), "Elastic Scattering of 7 to 14 MeV Neutrons from Nitrogen."

4 L. F. Chase, et al., LMSD-895076 (1961) "Fast Neutron Cross Sections of Oxygen and Nitrogen."

as the fluence differences between the various problems. These differences were calculated with a standard deviation one fifth or better than would have been the case when calculating the differences by independent runs for each of the five perturbations. Also, these five problems were run with a time approximately one and a half times that of a one-problem, independent run.

These results are now being analyzed and it is hoped that they will provide the effect of the nitrogen cross section discrepancy upon neutron transport results.

OAK RIDGE NATIONAL LABORATORY

A. NEUTRON PHYSICS

1. Total Cross Sections

a. Measurements and R-matrix Analysis of the Neutron Total Cross Section of ^{16}O*

(J. L. Fowler, C. H. Johnson and R. M. Feezel†)

We have used the $^{7}Li(p,n)$ neutron source with 2 to 3 keV resolution in order to clear-up a discrepancy or anomoly in the literature regarding the 3.765 MeV resonance in the neutron total cross section of ^{16}O. Earlier measurements,[1,2] which were made with T(p,n) neutrons produced by bombarding tritium absorbed in zirconium, gave peak cross sections corresponding to a J = 5/2 resonance. Differential cross sections, however, indicated the presence of a J = 7/2 resonance.[1,3] A possible explanation, suggested in an analysis of the data,[1] was a reduction of the cross section by an interference dip due to a narrow $d_{3/2}$ resonance postulated to be at 3.772 MeV. The present data give a peak cross section corresponding to J = 7/2 with a laboratory width of 18 keV. Thus there is no need for the narrow $d_{3/2}$ resonance to explain the low cross section.

Also we have fit our total cross sections and the cross sections from Wisconsin[2,4] up to 4.6 MeV by use of the two-channel multi-level R-matrix theory. For the off-resonance scattering we use the phase shifts for a real diffuse-edge potential.

The analysis shows that the narrow $d_{3/2}$ resonance at 4.18 MeV actually has a large reduced width. Interference with the 3.3 MeV resonance makes it appear narrow. Thus the single-particle $1d_{3/2}$ strength is divided about equally between this doublet and the well-known 1 MeV resonance.

The analysis shows further that the 4 MeV $p_{1/2}$ resonance observed from differential scattering[1,3] is not the same one as observed by several

---

*Material presented at Neut. Cross Sect. and Tech. Conf., Knoxville, Tenn., March 15-17, 1971.

†Undergraduate student from Auburn University.

[1]C. H. Johnson and J. L. Fowler, Phys. Rev. 162, 890 (1967).
[2]Fossan, Walter, Wilson and Barschall, Phys. Rev. 123, 209 (1961).
[3]D. Lister and A. Sayres, Phys. Rev. 143, 745 (1966).
[4]Striebel, Darden and Haeberli, Nucl. Phys. 6, 188 (1958).

groups[5] in the (n,α) reaction at 4 MeV. The latter is a resonance for $s_{1/2}$ neutrons. It is clear that both resonances have their effect in both the total and (n,α) reaction, but this fact was not detected previously.

---

[5]F. Ajzenberg-Selove and T. Lauritsen, Nucl. Phys. 11, 1 (1959).

b. The Neutron Total Cross Section of ^{16}O and ^{40}Ca*
(J. L. Fowler, C. H. Johnson, F. X. Haas,† and R. M. Feezel††)

The $^{7}Li(p,n)$ reaction produced by monoenergetic protons on thin lithium targets served as a neutron source to measure the cross section of ^{40}Ca (WASH-1144 No. 72) from 1.0 to 2.1 MeV with 4 keV resolution, and from 0.82 to 1.8 MeV with 2 keV resolution. In the common region from 1.0 to 1.8 MeV there were 45 peaks seen with 4 keV resolution and about twice as many with 2 keV. The ^{16}O cross section measured previously with $^{7}Li(p,n)$ neutrons was extended to 4.34 MeV with about 5 keV resolution. Since the correction for the second group of neutrons from the $^{7}Li(p,n)$ source becomes large at these higher energies, the ^{16}O cross section was remeasured with T(p,n) neutrons from 1.75 to 4.35 MeV with 30 keV resolution. Results for the two sources agree except near narrow resonances. In particular, the s-wave minimum at 2.35 MeV is 0.13 b for the $^{7}Li(p,n)$ source and, corrected for resolution, 0.134 b for the T(p,n) source. Recent $^{7}Li(p,n)$ data show the ^{16}O resonance at 3.765 MeV has J = 7/2.

---

*Submitted for publication in Proceedings Third Conf. on Neut. Cross Sect. and Tech., Knoxville, Tenn., March 15-17, 1971.
†Present address: Monsanto Research Corporation.
††Undergraduate student, Auburn University.

c. S- and P-Wave Neutron Strength Functions of ^{120}Sn*
(R. F. Carlton, J. A. Harvey, and G. G. Slaughter)

Neutron transmission measurements have been made upon a 2.67-in. thick sample of ^{120}Sn enriched to 98.39% utilizing the short burst, high-intensity Oak Ridge Linear Accelerator. Neutrons were produced by a Ta target using 6-nsec electron bursts at a pulse repetition rate of 700 Hz. The measurements were made at an 18-m flight station with a neutron energy resolution $\Delta E/E$ of $\sim 0.3\%$. The neutrons were detected by a $\frac{1}{2}$ in. by $4\frac{1}{2}$ in. ^{6}Li glass scintillator optically coupled to a RCA 4522 photomultiplier tube. Parameters have been obtained for 90 resonances up to 62 keV. From the shape of the resonances, ℓ-value assignments have

---

*To be presented at Washington, D.C., APS Meeting, April 26-29, 1971.

been made to many of the resonances. Observed level spacings and s- and p-wave strength functions based on these assignments are compared to earlier results.[1]

[1]Muradian, Shchepkin, Adamchuk and Arutyunov, Nucl. Phys. A147, 205 (1970).

2. Radiative Capture Cross Sections and Spectra

a. The Neutron Capture Cross Section of ^{207}Pb* (B. J. Allen† and R. L. Macklin)

Studies have continued on the neutron capture cross section of ^{207}Pb from 3 keV to 640 keV with total energy detectors at the Oak Ridge Electron Linear Accelerator. Two measurements were made at 40 meters with pulse widths of 5 and 40 nsec on 10.47 and 0.57 g cm^{-2} samples of separated ^{207}Pb. The capture cross section is obtained relative to that of gold. Shape analysis of the 41 keV resonance sets a new upper limit of 0.1 mb on the non-resonant capture cross section. Figures A-1, A-2, A-3 show the yield of neutron capture gamma rays vs neutron energy. Table I gives the corresponding derived parameters.

*Abstract, Third Neut. Cross Sect. and Tech. Conf., Knoxville, Tenn., March 15-17, 1971.

b. Program for Measuring Radiative Capture Cross Sections (R. L. Macklin and B. J. Allen*)

The neutron capture cross section facility at ORELA has operated well during the year. Samples run as of April 1971 include: ^{9}Be, ^{19}F, ^{24}Mg, ^{25}Mg, ^{26}Mg, ^{46}Ti, ^{47}Ti, ^{48}Ti, ^{49}Ti, ^{50}Ti, ^{50}Cr, ^{52}Cr, ^{53}Cr, ^{54}Cr, ^{86}Sr, ^{87}Sr, ^{88}Sr, ^{92}Mo, ^{94}Mo, ^{95}Mo, ^{96}Mo, ^{97}Mo, ^{98}Mo, ^{100}Mo, ^{134}Ba, ^{135}Ba, ^{136}Ba, ^{137}Ba, ^{138}Ba, ^{198}Hg, ^{199}Hg, ^{200}Hg, ^{201}Hg, ^{202}Hg, ^{204}Hg, ^{205}Tl, ^{206}Pb, ^{207}Pb, ^{208}Pb, ^{238}U (WASH-1144 Nos. 24, 53, 92, 223, 226, 339, 414). Data reduction to cross sections has been completed for some of these but a comprehensive computer program is still under development. The energy range covered is generally from 3 keV to 500 keV or the first inelastic threshold if higher. In cases of particular interest for capture, the first few hundred keV above the inelastic threshold can be covered by raising the bias (from .15 MeV) or correcting for the inelastic gamma yield where the inelastic cross sections are known (see Section E).

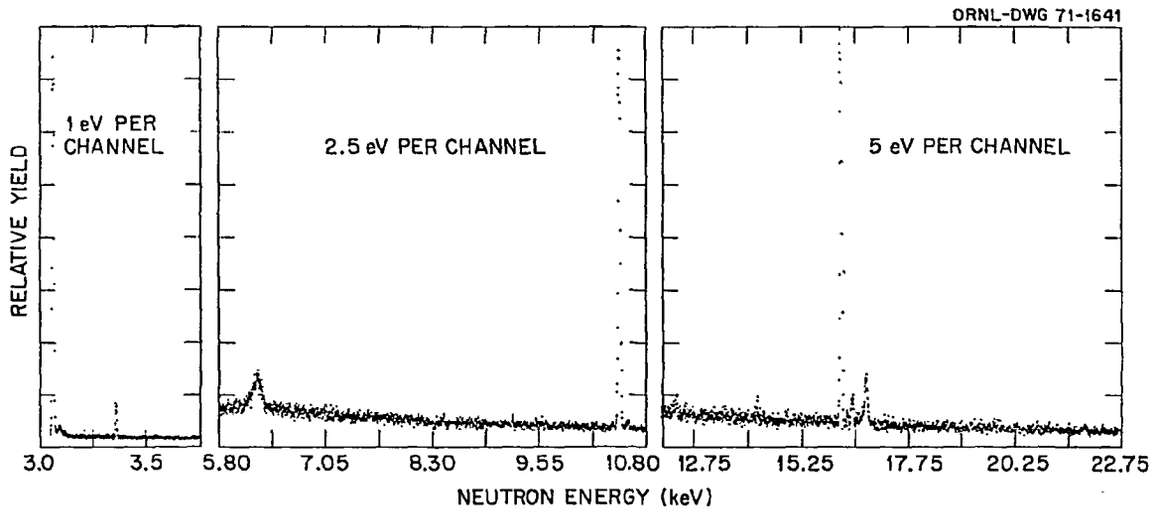

Figure A-1 Relative Yield $^{207}Pb(n\gamma)^{208}Pb$

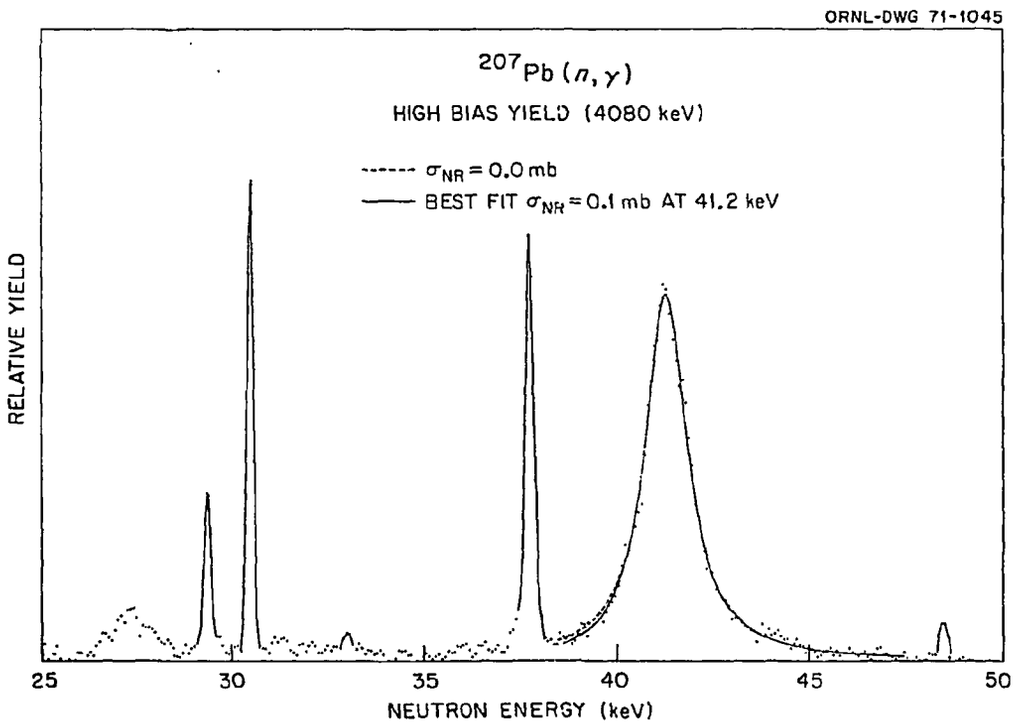

Figure A-2 Relative Yield $^{207}Pb(n\gamma)^{208}Pb$

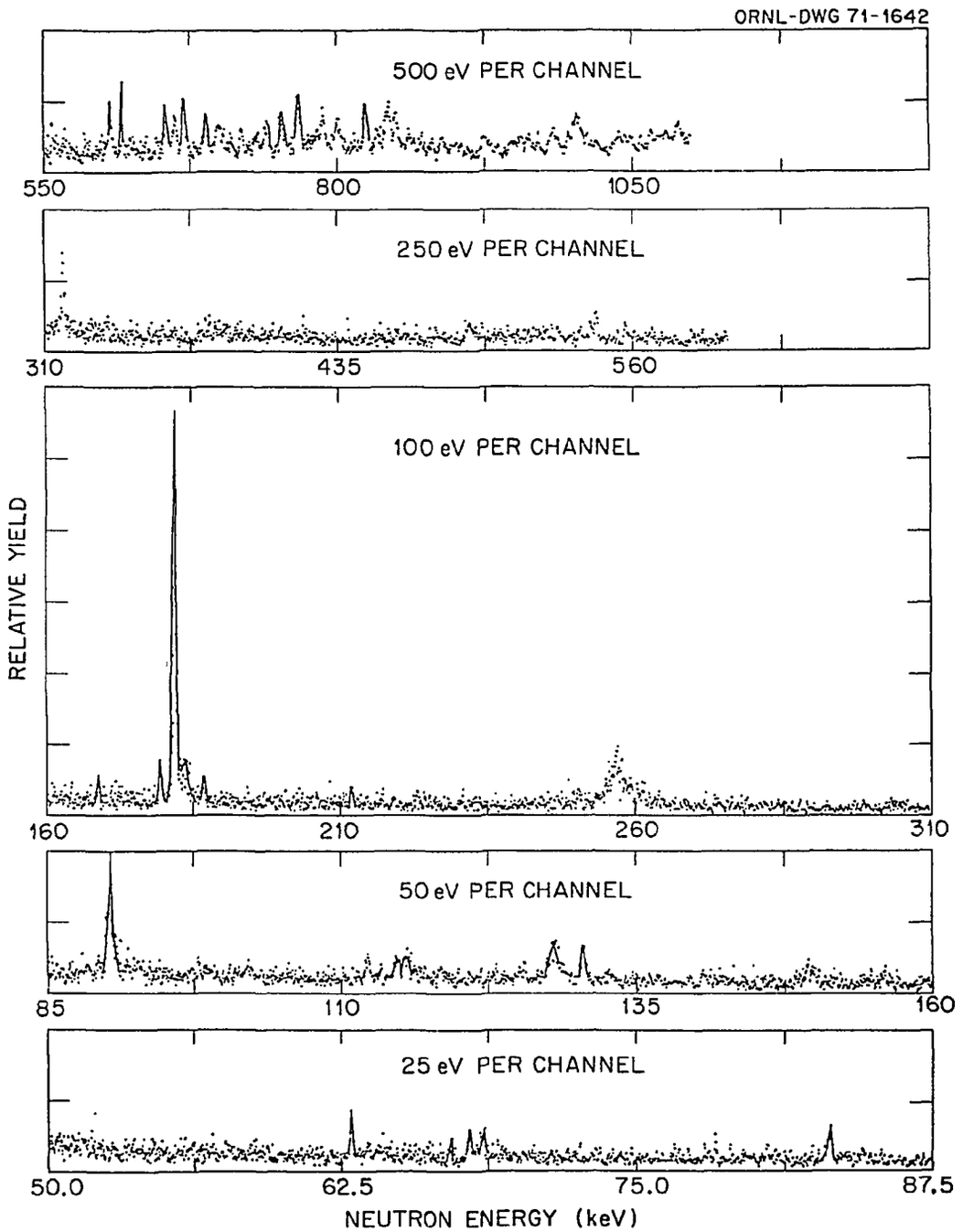

Figure A-3 Relative Yield $^{207}Pb(n\gamma)^{208}Pb$

Table 1. Resonance Parameters of ^{207}Pb

E_n(keV)	Γ_n(eV)	A(b.eV)	$g\Gamma_\gamma\Gamma_n/\Gamma$ (eV)	F (1)	J^π (2)	Γ_{γ_o} (eV)	Γ_{γ_o} (eV) (3)	E_n (keV) (3)	Γ_n (eV) (4)	Γ_γ(eV) (5)
3.071	~3	~86	.058	1.0	$1^\pm$	.06		3.0	0.2	
3.365	^{206}Pb									
5.99	Al(n',γ)									
10.21		47.3	.118	.6	2^+	(.06)		10.1		
(12.40)	50	1.2	.004	< 1						
14.26	^{206}Pb									
(14.94)	40	1.0	.004	< 1						
16.21		53.9	.224	.6	2^+	(.11)	.05	16.2		
16.47	^{206}Pb									} .24
16.81	60	11.1	.045	.3	2^+	.01				
21.90	^{206}Pb									
25.16	^{206}Pb									
25.48	^{206}Pb									
27.53	F(n',γ)									
30.54		31.0	.23	1.0	1^+	(.31)	.20	30.7		.47
33.04	60	4.9	.04	.6	2^+	.02				
37.82	100	62.3	.57	1.0	1^+	.76	.56	38.1	30	
41.17	1290	316	3.18	1.0	1^-	4.2	4.2	41.4	1250	} 5.5
44.35	390			~0						
48.51	50	10.1	.12	.7	1^-	.07			220	
62.93	100	10.2	.16	.6	2^+	.08				
67.10	220	3.6	.06	1.0	$1^\pm$	.08				
67.93	120	7.1	.12	1.0	1^+	.16			} 330	
68.50	220	7.3	.12	1.0	$1^\pm$	.16				
83.18	130	11.9*	.24	.5	2^+	.10				
90.40	680	69.9*	1.54	1.0	1^+	2.0	1.5	91.3		
93.15	730	6.4*	.15	.6	(2^+)	.10				
98.75	570	5.6*	.14	.6	(2^+)	.1				
102.25	570	10.3*	.26	1.0	$1^\pm$	.35				
112.30	340	12.4*	.34	.4	2^+	.11				
115.50	1230	41.4*	1.16	1.0	1^+	1.5	1.4	115		
118.8				~0						
125.0	440	16.5*	.50	.8	1^+	.5			(570)	
128.2	970	60.2*	1.88	.9	1^+	2.3	} 3.1			
130.6	230	27.0	.86	1.0	1^+	1.1		131	(640)	
133.0				~0						
149.8	1470	18.6*	.68	~0						
156.2				~0						
162.1	720	4.4	.18	1.0	$1^\pm$	.24	.57	158		

179.4	460	24.0	1.05		1.0	$1^{\pm}$	1.4	.53	168
181.9	310	231	10.2		1.0	1^{+}	13.6	11.0	184
187.0	570	12.7	.52 †		~1	$1^{\pm}$	.7		
257.1	4050	348*	20.4 †		1.0	1^{-}	28.4	15.3	260
299.7	1290	8.6	.5 †		~1	$1^{\pm}$	.7		
317.8	930	83.8	6.4 †		1.0	1^{+}	8.5	6.8	321
336.5	12470	38.3*	1.7 †		1.0	$1^{\pm}$	2.3		
360.0	8690	20.3*	0.8 †		~1	$1^{\pm}$	1.1		
490.8	2300	61.9*	7.1 †		.9	$1^{\pm}$	8.5	1.8	498
544.3		70.4	9.3		.9	$1^{-}(1^{+})$	(11.1)	7.2	553
578.5		6.7	.95		1.0	$1^{\pm}$	(1.3)	2.6	564
584.0		25.7	3.7		.7	$(1^{\pm})$	(2.1)		
593.8		8.8	1.27		.9	$1^{\pm}$	(1.5)		
607.5	3460	10.5*	1.55		.6	(2^{+})	.7		
617.5		53.5	8.0		.8	1^{+}	(8.5)	12.8	627
625.0	3410	44.8*	6.8		.8	1^{+}	7.2		
637.5	2770	12.7	2.0		.8	$1^{\pm}$	2.1		
647.0	1210	(25.6)	(4.0)		.4	2^{+}	(1.3)		
654.0	2020	(115)	(18.3)		.5	$2^{+}(1^{+})$	(7.3)	666	
661.5	1080	(97)	(15.6)		.3	2^{+}	(3.7)		
670.0	1930	(126)	(20.5)		.1	2^{+}	(1.6)		
686.5	2580	(107)	(17.9)		.2	2^{+}	(2.9)		
698.5	3180	(180)	(30.5)		.4	2^{+}	(9.8)		

Note: when F ≤ 0.1, $J^{\pi} = 0^{\pm}, 2^{\pm}, 3^{-}$

† Corrected for neutron sensitivity k = 1.1 x 10^{-4}

( ) Uncertain value or assume $\Gamma_n \gg \Gamma_\gamma$

* Not corrected for MS(~ 5%) and RSP(1-2%)

Resonance areas accurate to ± 15%

(1) F = Fraction of Transitions to Ground State ^{208}Pb

(2) Assignments Based Upon Combined Results of Several Investigators

(3) C. D. Bowman, R. J. Baglan, B. L. Berman, T. W. Phillips, Phys. Rev. Letters 25, 1302 (1970)

(4) E. G. Bilpuch, K. K. Seth, C. D. Bowman, R. H. Tabony, R. C. Smith, H. W. Newson, Ann. Phys. 14, 387 (1966)

(5) R. L. Macklin, P. J. Pasma, J. H. Gibbons, Phys. Rev. 136, 695 (1964).

The cross section standardization program has included measurements with $^{10}BF_3$ and ^{6}LiF ion chambers, $^{10}B(n,\alpha)\gamma$ and $^{7}Li(n,n')\gamma$ samples, 0.5 mm ^{6}Li glass scintillator and a thin foil proton recoil surface barrier detector.

---

*On assignment from Australian Atomic Energy Commission.

c. Distribution of Partial Radiation Widths in $^{238}U(n,\gamma)^{239}U$* (O. A. Wasson,† R. E. Chrien,†, G. G. Slaughter and J. A. Harvey)

The resonant neutron capture γ-ray spectra for 28 resonances below 600 eV neutron energy are measured in $^{238}U(n,\gamma)^{239}U$ with improved neutron and γ-ray energy resolution to allow an accurate test of the predictions of the statistical model of neutron capture. No convincing departures from these predictions are observed. The variation over 23 S-wave neutron resonances of the γ-ray transition probabilities to 15 final states is consistent with the Porter-Thomas distribution for both E1 and M1 multipoles. There is also no statistically significant correlation between the different decay modes of the neutron resonances. A large correlation coefficient of +0.91 is observed between the partial radiative widths of the 3991 and 3982 keV γ rays. This result, however, is not in violation of statistical independence for a sample size of 15 γ rays. The E1 and M1 γ-ray strength functions are $(2.6 \pm 0.4) \times 10^{-3}$ and $(8.1 \pm 1.6) \times 10^{-3}$ respectively, compared to 3×10^{-3} and 4×10^{-3} listed by Bartholomew as the median values of all nuclei. Three of the weaker resonances at 10.2, 89.5, and 263 eV are assigned to P-wave capture. The neutron binding energy is measured to be 4806.7 ± 2.0 keV which is 5.0 keV higher than the previously accepted value. Previously unobserved γ-ray transitions are reported.

---

*Abstract of paper submitted for publication in Phys. Rev.
†Brookhaven National Laboratory, Upton, New York.

d. Resonance Neutron Capture in ^{205}Tl* (E. D. Earle,† G. A. Bartholomew,†, M. A. Lone,†, B. J. Allen,†† J. A. Harvey, and G. G. Slaughter)

Gamma ray spectra following resonance neutron capture in ^{205}Tl have been recorded up to 200 keV neutron energy with the ORELA facility, extending work reported earlier.[1] Resonances at 0.0445, 1.445, 2.802, 3.053, 4.44, 5.11, 6.67, 8.45, 11.77, 13.29, 16.42, 17.45, and 20.80 keV are assigned to ^{205}Tl. Only the 0.0445, 2.802, 3.053 and 17.45 keV resonances were observed previously with the 3 keV doublet unresolved. The observed γ-rays above 3 MeV correspond to primary transitions to

known excited states[2] in ^{206}Tl. Primary transitions to all known states with J < 4 below 2 MeV and to at least 6 of the states between 2 and 3 MeV are observed.

---

*Abstract of paper to be presented at Washington, D.C., APS Meeting, April 26-29, 1971.
†AECL, Chalk River, Canada.
††On Assignment from Australian Atomic Energy Commission.
[1]Bartholomew, Earle and Lone, BAPS 15, 550 (1970).
[2]M. B. Lewis and W. W. Daehnick, Phys. Rev. C1, 1577 (1970).

3. Elastic and Inelastic Scattering Cross Sections

a. High Resolution Inelastic Cross Section Measurements for Na, Si, and Fe*
(F. G. Perey, W. E. Kinney and R. L. Macklin)

A program of inelastic scattering measurements has been initiated at ORELA. Data are obtained by detecting the de-excitation gamma rays in a 4π geometry with a flight path of 40 meters. The present detector is a hydrogen-free carbon fluoride liquid scintillator used in capture cross section measurements. The initial set of measurements was performed with only 0.125 nsec/meter resolution to investigate the technique. Data were reduced up to the threshold of the second excited state for ^{7}Li, C, Na, Si, and Fe (WASH-1144 Nos. 57, 101). The carbon data were used for background determination and the ^{7}Li data for flux determination. The data for Na, Si, and Fe will be presented. The cross sections show great resonance structure with peak-to-valley ratios larger than those found in the total cross section. The energy resolution is sufficient to identify all the resonances observed in the inelastic cross sections with resonances in the total cross sections. Various aspects of the experimental technique will be discussed.

Figures A-4, A-6, and A-5 show the results that were obtained.

---

*Abstract Third Neut. Cross Sect. and Techn. Conf., Knoxville, Tenn., 1971.

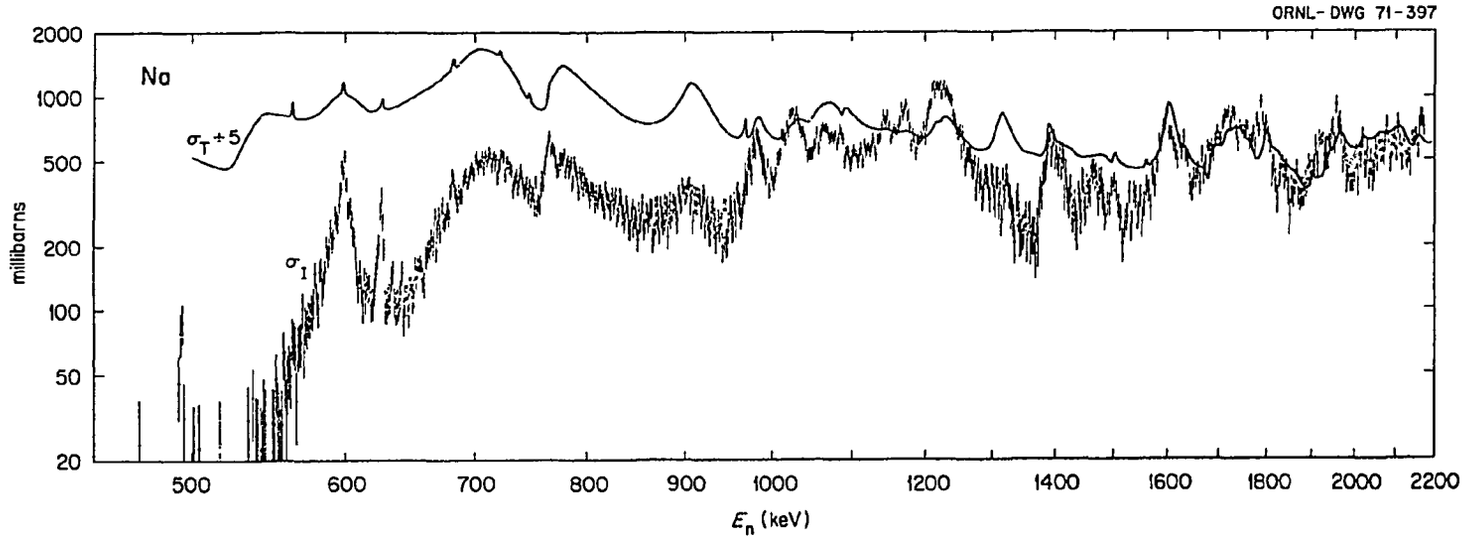

Figure A-4 Inelastic Cross Section of Sodium

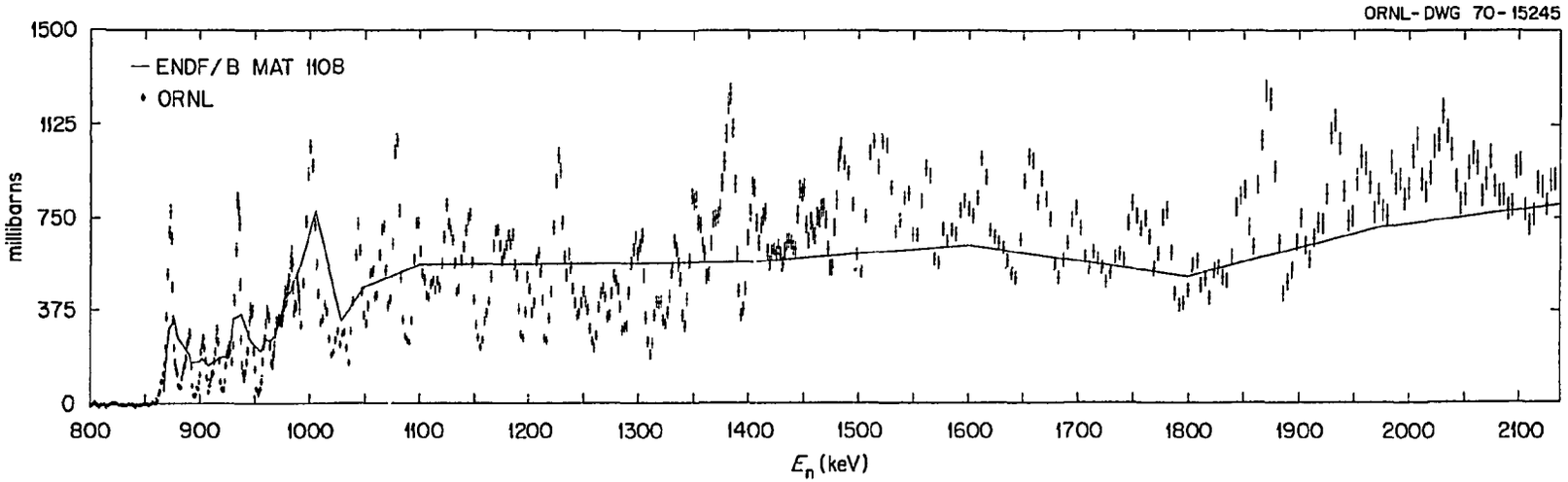

Figure A-5 Inelastic Cross Section of Iron

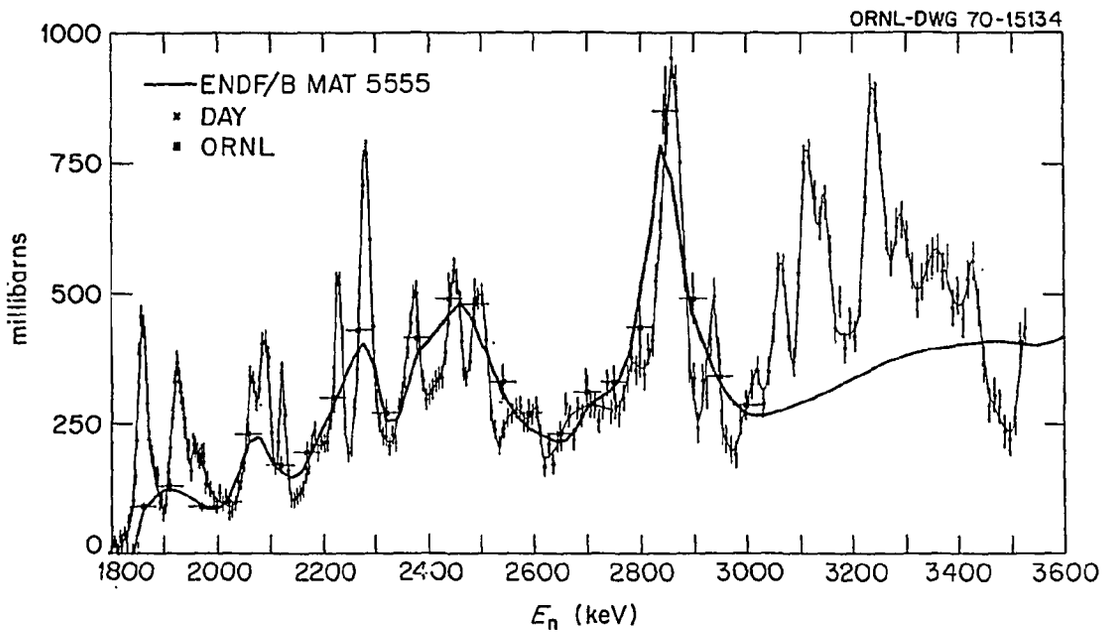

Figure A-6 Inelastic Cross Section of Silicon

4. Neutron Reaction and Gamma Ray Production Cross Sections

a. The Ca(n,xγ) Reaction at E_n = 5.9 MeV*
(J. K. Dickens and F. G. Perey

Gamma-ray production cross sections have been measured for 5.9 MeV neutrons interacting with calcium. Cross-section data are in reasonable agreement with previously reported neutron inelastic scattering cross sections.

*Abstract Third Neut. Cross Sec. and Tech. Conf., Knoxville, Tennessee, March 15-17, 1971.

5. Fission

a. Measurement of Neutron Cross Sections in ^{238}U and ^{235}U*
(E. G. Silver, G. de Saussure, R. B. Perez, and R. W. Ingle)

The $^{238}U(n,\gamma)$ and $^{235}U(n,f)$ cross sections have been measured using a large scintillation detector in a split-halves coincidence mode, up to 100 keV energy. Special care has been taken in making sample-thickness corrections to the observed $^{238}U(n,\gamma)$ data, with significant results. The $^{235}U(n,f)$ cross section has been measured both with a fission chamber and by the two-bias technique. Results are presented and compared with other work. Fission-to-capture ratio measurements are presented for ^{235}U including the gap hitherto found between 2 and 20 keV. Figure A-7 shows the measured apparent capture cross section (includes effects of resonance self-shielding and multiple scattering) $x\sqrt{E}$ ^{238}U and by comparison a prediction based upon the ENDF/B library. Figures A-8, A-9, and A-10 are respectively the average values of σ_c, $\sigma(nf)$ and α for ^{238}U, ^{235}U, and ^{235}U respectively.

*Abstract, Third Neut. Cross Sec. and Techn. Conf., Knoxville, Tenn., March 15-17, 1971.

b. Measurement of the Capture-to-Fission Ratio, α, for ^{239}Pu Over the Energy Region From 0.02 eV to 400 keV*
(R. Gwin, E. G. Silver, and R. W. Ingle)

Measurements of the neutron capture and fission cross sections of ^{239}Pu have been made at ORELA (WASH-1144 No. 447). A large liquid scintillator was used to detect the prompt gamma rays resulting from neutron absorption of ^{239}Pu and an ionization chamber containing 1.4 g of ^{239}Pu was used to define fission events. The primary goal of these experiments was to obtain data extending into the thermal energy region for normalization of the neutron cross sections. The initial reduction of the data shows that the values of α obtained are in good agreement

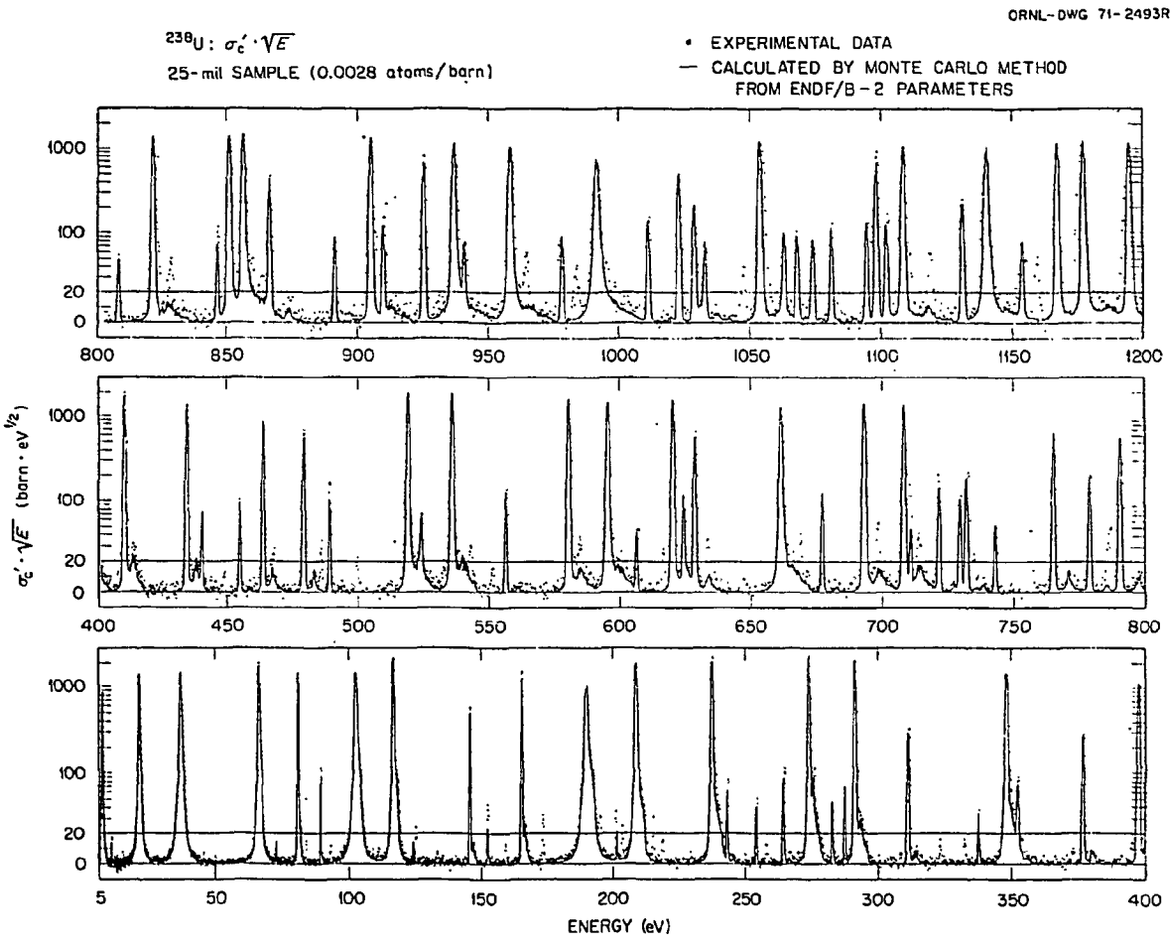

Figure A-7

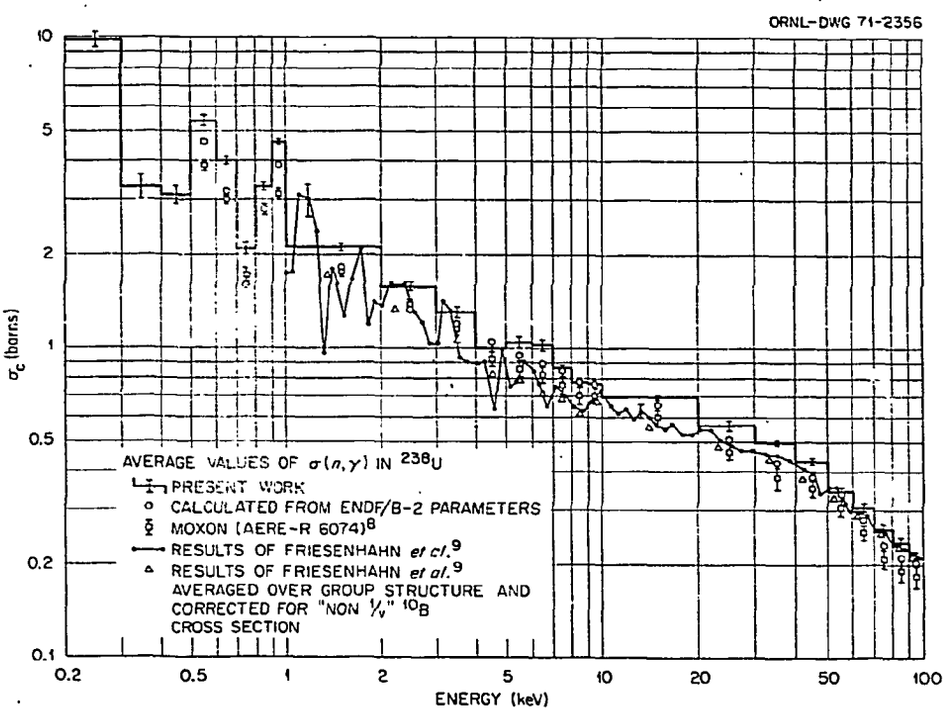

Figure A-8

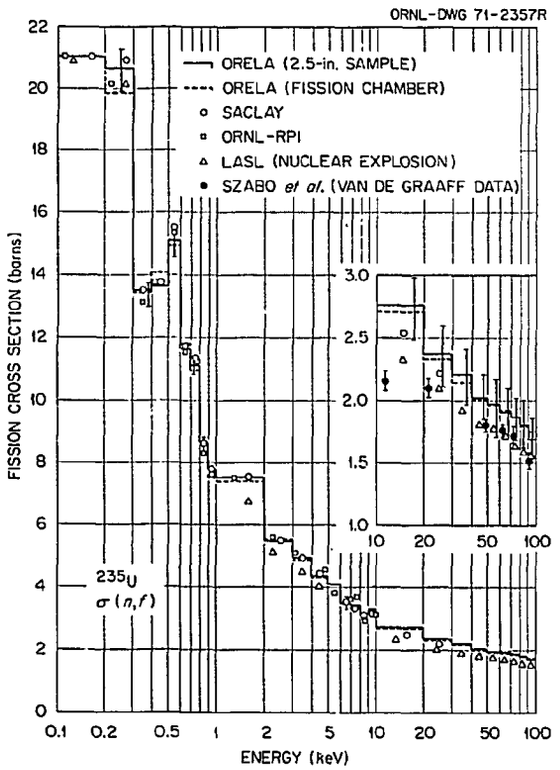

Figure A-9

DATA NOT FOR QUOTATION

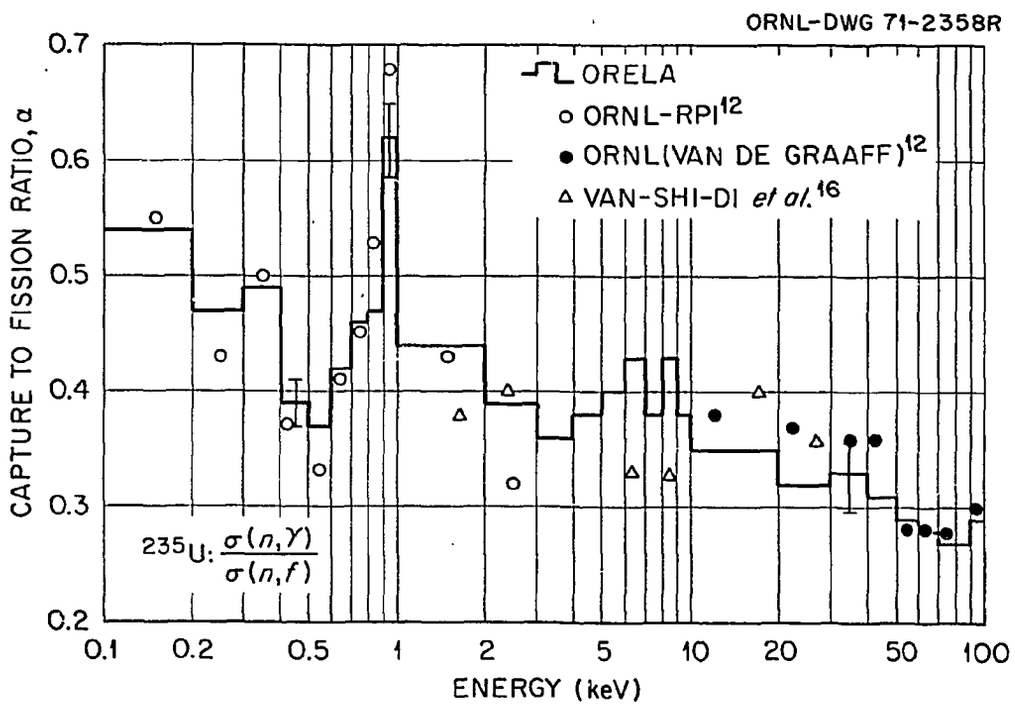

Figure A-10

both with those derived from the Oak Ridge National Laboratory-Rensselaer Polytechnic Institute experiments (1969) and with those measured in experiments at the ORNL Van de Graaff (1964, 1966) up to a neutron energy of 400 keV.

---

*Abstract, Third Neut. Cross Sect. and Tech. Conf., Knoxville, Tenn., March 15-17, 1971.

c. On the Influence of Fragment Shells in Nuclear Fission* (U. Mosel† and H. W. Schmitt)

The two center shell model has been used to calculate shell corrections to the liquid drop model following the Strutinsky procedure. The potential energy surfaces for heavy nuclei are obtained as functions of two degrees of freedom representing elongation and constriction. For lighter nuclei ($A < 226$) the fragment shells are found to dominate at the saddle point, so that the success of the liquid drop model can be understood in terms of the soft mid-shell character of the fragments formed. For heavier nuclei ($A > 226$), the saddle point properties are dominated by the structure of the compound nucleus, thus validating Bohr's channel concept in this region. Immediately following the saddle point, however, the minimum in the potential surface turns from the direction of almost pure elongation to one of almost pure constriction, and fragment shell structure dominates quickly, much before scission occurs.

---

*Abstract of paper to be presented at Washington, D.C., APS Meeting, April 26-29, 1971.
†University of Tennessee, Knoxville, Tennessee.

B. CHARGED PARTICLE PHYSICS

1. Comparison of States in ^{91,97}Nb Populated through the (d,n) and (^{3}He,d) Reactions* (J. L. Horton,† C. L. Hollas,† P. J. Riley,† S. A. A. Zaidi,† J. L. C. Ford, and C. M. Jones)

^{91}Nb and ^{97}Nb have been investigated as part of a systematic study of the (d,n) reaction in the A = 90 region. States of up to 6 MeV excitation have been observed using neutron time-of-flight techniques with a flight path of approximately 28 meters. Absolute differential cross sections have been measured and analyzed in terms of the distorted wave Born Approximation.[1,2] Good agreement between the two sets of

measurements is found for ^{91}Nb. For several low-lying states in ^{97}Nb there is disagreement between ℓ-value assignments reported for the (^{3}He,d) and those deduced in the present (d,n) measurements.

---

*Abstract of paper to be presented at Washington, D.C., APS Meeting, April 26-29, 1971.
†University of Texas at Austin, Austin, Texas.
[1]J. Piccard and G. Bassini, Nucl. Phys. A131, 636 (1969).
[2]Cates, Ball, and Newman, Phys. Rev. 187, 1682 (1969).

2. Spectroscopy of ^{93,95,97}Tc by the (d,n) Reaction*
(P. J. Riley,† C. L. Hollas,† J. L. Horton,† S. A. A. Zaidi,† J. L. C. Ford, and C. M. Jones)

The ^{92,94,96}Mo(d,n)^{93,95,97}Tc reactions have been studied by the neutron time-of-flight method, at an incident deuteron energy of 12 MeV and a neutron time resolution of less than 2 nanoseconds. Angular distributions of the outgoing neutrons have been measured at 5° intervals from 15° to 50° in the laboratory with flight paths of approximately 28 meters. Absolute differential cross sections have been measured and have been analyzed in terms of the distorted wave Born approximation. Spin and parity assignments and spectroscopic factors have been deduced. The experimental (d,n) results for ^{92}Mo(d,n)^{93}Tc are compared with previous (^{3}He,d) work;[1] overall, reasonable agreement between the two sets of measurements is found.

---

*Abstract of paper to be presented at Washington, D.C., APS Meeting, April 26-29, 1971.
†University of Texas at Austin, Austin, Texas.
[1]J. Picard and G. Bassani, Nucl. Phys. A131, 636 (1969).

3. Coulomb Excitation of ^{238}U*
(F. K. McGowan, W. T. Milner, R. L. Robinson, and P. H. Stelson)

Sixteen states in ^{238}U have been observed by direct E2 and E3 excitation with 5.5 MeV protons and 18 MeV ^{4}He ions. Reduced transition probabilities B(E2), B(M1), B(E3), and B(E1) have been deduced from γ-ray yield and angular distribution measurements. Level energies in keV (J^π, B(Eλ, 0 → J) in single particle units) are: 966 (2+, 0.13), 988(2+, 0.04), 1037.3 (2+, 0.69), 1060.2 (2+, 2.85), 1224 (2+, 0.19), 732.0 (3-, 23.2), 997.5 (3-, 9.9), and 1169 (3-, 5.4). The B(M1, 2' → 2) and B(E1) are 2 to 4 x 10^{-4} $(nm)^2$ and 3 to 8 x 10^{-5} $B(E1)_{sp}$, respectively. Interband B(E2) branching ratios for decay of the 1037- and 1060-keV states are not consistent with band mixing to first order. The B(E3, 0 → 3) are in good agreement with the microscopic description[1] of octupole vibrational states. The axially symmetric octupole deformation β_3 is about 0.08. B(E1) branching ratios for decay of the 3- and 1- states at 732-

and 680-keV are in excellent agreement with predicted values for K = 0.

---

*Abstract of paper to be presented at Washington, D.C., APS Meeting, April 26-29, 1971.

[1]K. Neegard and P. Vogel, Nucl. Phys. A149, 217 (1970).

4. Spin-Parity Assignments for the Low-Lying States in ^{95,97}Tc via the Neutron Decay of 0^+ and 2^+ Analogue States*
(H. J. Kim, R. L. Robinson, and C. H. Johnson)

Three low-lying excited states in each of the nuclei ^{91}Nb, ^{95}Tc, and ^{97}Tc were observed to be strongly populated by the neutron decay of the 2^+ resonances in the compound nuclei ^{92}Nb, ^{96}Tc, and ^{98}Tc. These resonances are the isospin analogues of the first 2^+ states of ^{92}Zr, ^{96}Mo, and ^{98}Mo, respectively. The neutron decay of the ground-state analogue of ^{98}Mo was also investigated. These decays of the analogue resonances were investigated via (p,n) reactions. The resonance energies (lab energy) and widths for the 2^+ resonances are: 4.154 ± 0.010 MeV and 33 ± 2 keV, 3.908 ± 0.010 MeV and 32 ± 2 keV, and 4.330 ± 0.010 MeV and 34 ± 2 keV for the compound nuclei ^{92}Nb, ^{96}Tc, and ^{98}Tc, respectively. The energy and width for the 0^+ resonance for ^{98}Tc are 3.505 ± 0.010 MeV and 25 ± 3 keV. The resonance yields to the individual states are compared to the expected yields based on the optical-model transmission coefficients. From these yields and the shapes of the off-resonance angular distributions, the following spin-parities are assigned: $3/2^-$ and $5/2^-$ for the 651 and 670 keV states of ^{95}Tc, respectively, and $3/2^-$ and $5/2^-$ for the 575 and 662 keV states of ^{97}Tc, respectively.

---

*Abstract of paper to be submitted for publication in Nuclear Physics.

5. Entrance Channel Interference Effect in the Neutron Decay of 2^+ Analogue Resonances*
(H. J. Kim and R. L. Robinson)

The angular distributions of the decay neutrons populating $1/2^-$, $3/2^-$ and $5/2^-$ states of ^{91}Nb and ^{95}Tc resulting from the s- and d-wave proton induced $J^\pi = 2^+$ analogue resonances are investigated. The experimental angular distributions show the interference effect arising from the coherence between the partial waves involved in the resonance. The analysis of the observation shows that it is necessary and sufficient that the interference be between the $s_{1/2}$ and $d_{5/2}$ partial waves in the entrance channel. The ratios of the spectroscopic factors and the relative signs of the reduced width amplitudes for the $s_{1/2}$ and $d_{5/2}$ protons

are deduced from the data. The ratios of the spectroscopic factors agree with the (d,p) results.

---

*Abstract of paper to be submitted for publication in Nuclear Physics.

6. Alpha-Neutron Total Cross Sections on ^{13}C, ^{17}O, ^{18}O, ^{21}Ne, and ^{22}Ne*

(F. X. Haas† and J. K. Bair)

The total neutron yields of the reactions $^{13}C(\alpha,n)^{16}O$, $^{17}O(\alpha,n)^{20}Ne$, $^{18}O(\alpha,n)^{21}Ne$, $^{21}Ne(\alpha,n)^{24}Mg$, and $^{22}Ne(\alpha,n)^{25}Mg$ have been measured in the alpha-particle energy range of 0.8 to 5.3 MeV using thin enriched targets. The total cross section of the $^{13}C(\alpha,n)^{16}O$ reaction was determined from measurements made on the 1.056 MeV resonance using infinitely thick targets of both enriched and natural elemental carbon. The ^{17}O, ^{21}Ne, ^{22}Ne targets were prepared by bombarding tantulum blanks with 24 keV ions in a magnetic separator. The $^{17}O(\alpha,n)^{20}Ne$ cross sections were obtained by normalizing to ^{17}O-^{18}O anodized target data and known ^{18}O cross section data. The ^{21}Ne and ^{22}Ne cross sections were obtained by measuring the total cross section with enriched gas targets. Data from these reactions will be presented.

---

*Abstract of paper to be presented at Washington, D.C., APS Meeting, April 26-29, 1971.
†Mound Laboratory, Ohio.

7. Observation of Nanosecond Isomers in ^{111}In and ^{113}In via the $(p,n\gamma)$ Reactions with a Pulsed Beam*

(H. J. Kim, R. L. Robinson, and W. T. Milner)

We searched for γ emitting nanosecond isomers in ^{111}In and ^{113}In by studying the time distributions of γ rays resulting from the $(p,n\gamma)$ reaction induced by a 3.8 MeV pulsed proton beam on ^{111}Cd and ^{113}Cd targets. The pulse height and time distribution of the γ rays detected by a 30-cc Ge(Li) detector were accumulated in a two-parameter analyzer operating in the 512 x 32 channel mode. The half-lives of the isomers were deduced by comparing the time distributions of delayed γ rays to that of prompt γ rays of similar energies. Both shape fitting and centroid shift were employed. The half-lives are 0.19 ± 0.06 and ≤ 0.2 nsec for the 652- and 662-keV transitions, respectively, in ^{111}In and 0.38 ± 0.05 and 0.60 ± 0.05 nsec for the 638- and 673-keV transitions, respectively, in ^{113}In. These transitions appear analogous to known nanosecond isomeric transitions in ^{115}In and ^{117}In.

---

*Abstract of paper to be presented at Washington, D.C., APS Meeting, April 26-29, 1971.

RENSSELAER POLYTECHNIC INSTITUTE

A. CROSS SECTION MEASUREMENTS

1. Resonance Parameters for ^{240}Pu from 20 to 500 eV*

(R. W. Hockenbury, J. D. Boice, W. R. Moyer and R. C. Block)

The following is an abstract of a paper presented at the March, 1971, Neutron Cross Section and Technology Conference:

Neutron absorption and transmission measurements were made on ^{240}Pu from 20 eV to about 1 keV as part of an experiment to measure the keV capture cross section. A high bias technique was used in the absorption measurements to separate the fission and capture components and upper limits can be set on the fission widths of these resonances. The capture data were normalized in two ways: (1) by the saturated capture method and (2) to transmission data where both capture and transmission give essentially the same result, $g\,\Gamma_n$. The normalizations agree within statistics. The advantages and sources of error of each method are examined. These data have been analyzed for resonance parameters. Our results for the radiation widths are 15-25% larger than previously reported values[2].

The resonance parameters obtained from the capture and transmission data are given in Table 1-1. The absolute normalization of the capture data to the transmission data has an uncertainty of ±3.8%.

---

* Pertinent to requests #459 and 461.

TABLE 1-1 ^{240}PU RESONANCE PARAMETERS

This Work			Ref. 1	Ref. 2
E_o (eV)	Γ_n (meV)	Γ_γ (meV)	Γ_n (meV)	Γ_γ (meV)
20.46	2.2 ± 0.6	(30)+	2.7 ± 0.3	-
38.37	17.0 ± 0.5	25.5 ± 0.8	19.2 ± 0.9	20.0 ± 2.0
41.79	14.2 ± 0.5	32.8 ± 1.0	16.8 ± 0.9	21.8 ± 2.0
66.71	53.2 ± 1.0	27.4 ± 0.6	55.9 ± 2.2	23.5 ± 2.0
72.82	21.5 ± 0.5	27.0 ± 0.6	22.0 ± 1.0	21.0 ± 2.0
90.81	12.7 ± 0.3	39.5 ± 1.0++	13.5 ± 0.6	19.5 ± 2.0
92.53	3.3 ± 0.1	-	3.0 ± 0.2	-
105.1	47.5 ± 1.5	37.5 ± 1.0++	45.5 ± 2.5	26.0 ± 2.5
121.7	15.0 ± 0.5	(30)	14.5 ± 0.9	21.5 ± 2.0
130.9	0.19 ± 0.03	(30)	0.15 ± 0.06	-
135.4	20.6 ± 0.5	(30)	18.5 ± 1.1	24.5 ± 2.5
152.0	13.8 ± 0.5	29.5 ± 1.1	14.2 ± 1.0	21.5 ± 2.0
162.8	9.0 ± 0.3	27.5 ± 0.9	8.6 ± 1.0	20.0 ± 3.0
170.2	17.5 ± 0.5	27.3 ± 0.9	13.7 ± 1.2	22.0 ± 2.0
185.9	18.8 ± 0.5	28.8 ± 0.9	16.3 ± 1.2	22.0 ± 2.0
192.2	0.3 ± 0.04	(30)	0.20 ± 0.12	-
199.8	1.0 ± 0.1	(30)	0.94 ± 0.1	-
239.3	13.8 ± 0.6	27.7 ± 1.0	12.2 ± 0.7	21.5 ± 2.5
260.4	25.0 ± 0.9	30.5 ± 1.0	23.2 ± 1.2	24.0 ± 2.3
287.1	137.0 ± 0.4	33.0 ± 1.1	138.2 ± 7.0	26.0 ± 2.0
304.9	7.4 ± 0.2	(30)	7.2 ± 0.7	-
318.5	6.0 ± 0.3	(30)	5.2 ± 0.5	-
320.8	20.0 ± 0.6	(30)	19.3 ± 1.0	21.0 ± 2.5
338.5	7.4 ± 0.3	(30)	5.7 ± 0.6	-
346.0	17.7 ± 0.5	(30)	16.5 ± 0.7	21.5 ± 2.5
363.8	30.4 ± 1.5	32.8 ± 1.7	32.5 ± 1.3	25.0 ± 2.5
372.1	16.0 ± 1.5	27.5 ± 0.3	13.8 ± 0.8	21.5 ± 3.0
405.1	102.6 ± 6.0	30.0 ± 0.2	108.5 ± 5.0	26.0 ± 2.3
419.2	6.2 ± 0.3	(30)	6.1 ± 0.7	-
446.2	2.2 ± 0.2	(30)	1.6 ± 0.3	-
448.7	18.7 ± 3.5	(30)	16.5 ± 1.2	26.5 ± 3.0
466.9	2.4 ± 0.2	(30)	3.1 ± 0.6	-
473.4	4.3 ± 0.3	(30)	4.2 ± 0.5	-
494.2	6.4 ± 0.3	(30)	5.8 ± 1.1	-
499.4	17.0 ± 2.2	33.5 ± 1.5	19.3 ± 1.4	21.5 ± 2.5

+ Set Γ_γ = 0.030 eV to determine Γ_n.
++ ^{239}Pu impurity at these energies.

1. W. Kolar and K.H. Bockhoff, Journ. of Nuc. Energy 22, 299 (1968).
2. H. Weigmann and H. Schmid, Journ. of Nuc. Energy 22, 317 (1968).

2. The Differential Elastic Scattering Cross Sections of keV Neutrons from Iron and Nickel* (R. Zuhr and K. Min)

The time of flight measurements of the differential elastic scattering cross sections of keV neutrons have continued, using a 26 meter flight path, a PDP-7 on-line computer, and associated equipment as described in the last report. Additional data has been accumulated for iron and lead at 45, 70, 90, 110, and 135 degrees, with 150 degree results being added to extend the range of angles covered. The gross features of the spectra obtained are similar to those included in the previous report, so further graphs are not presented. It is anticipated that extensive investigation of the differential elastic cross sections of nickel will be under way by early summer.

Sample thicknesses used thus far have ranged from 0.2 to 3.3 mean free paths at the energies under consideration. A Monte Carlo type analysis for the multiple scattering corrections is currently under development for the thicker samples. In addition the feasibility of using thinner samples, with a new high intensity electron gun in the Linac, will be tested. For energies away from the larger resonances, where multiple scattering corrections are less than 20%, an analysis based on the work of Lane and Miller[1] has been carried out. This work yielded results that agree statistically with tabulated cross-sections. As the analysis program is refined, it is expected that thick samples will also be adequately treated.

3. Transmission Measurements Upon Sm-147 and Sm-150 (H. M. Eiland*,* S. Weinstein**, and K. W. Seemann**)

The total cross sections of Sm-147 and Sm-150 from 0.01 eV to 1.2 keV have been determined by neutron transmission measurements upon oxide samples of high isotopic purity. The measurements were made at the RPI Linac with a Li-6 glass scintillation detector at 25 meters. Energy resolution in the resonance region varied from 2 to 10 nsec/m. Parameters have been extracted for 127 resonances of Sm-150 up to 1.6 keV. Some of the results of this meas-

* Pertinent to request #119

1 R. O. Lane and W.F. Miller, N.I.M. 16, 1 (1962).

urement are shown in the following table.

STATISTICAL PROPERTIES AND CROSS SECTIONS
FOR Sm-147 AND Sm-150

PROPERTY	VALUE FOR ISOTOPE SM-147	Sm-150
$\bar{D}$, eV	7.4 ± .7	68 ± 10
$g\Gamma_n^o$, mV/eV$^{\frac{1}{2}}$	3.47 ± .3	24.8 ± 2
So	4.6 ± .4 x 10^{-4}	3.6 ± .3x10^{-4}
Resonance Integral		
above 0.5 eV, b	714 ± 50	310 ± 15
(0.0253 eV), b	75 ± 6	133 ± 8

4. Total Neutron Cross Sections of Hydrogen and Deuterium Between 1 and 20 MeV (J. C. Clement, P. Stoler, C. G. Goulding, P. F. Yergin, and R. Fairchild)

The following abstract was submitted to the American Physical Society Meeting of April 26, 1971.

MeV total neutron cross sections for ^{1}H and ^{2}D have been measured by time of flight techniques using the Rensselaer electron Linac as a source of neutrons. The accelerator repetition rate was 500 PPS, with a beam width of 20 ns. The neutron flight path was 250 meters, and the minimum resolution was about 0.1 ns/m. The statistical accuracy per resolution width varies from about 1% to about 10%, depending on the neutron energy. The obtained cross sections will be compared with other recent measurements, and further discussed.

5. KeV Neutron Capture and Transmission Measurements on ^{50}Cr, ^{52}Cr, ^{53}Cr, ^{54}Cr, ^{60}Ni and V* (R. G. Stieglitz, R. W. Hockenbury, and R. C. Block)

This work is complete and has been published in Nuclear Physics A163 (1971) 592.

** Knolls Atomic Power Laboratory, Schenectady, N. Y.

* Pertinent to requests #84, 87 and 113.

6. Measurement* of $\bar{\nu}$ for ^{235}U and ^{233}U (R. L. Reed and R. C. Block)

The $\bar{\nu}$ measurements for ^{235}U below 40 eV have been completed and are now being analyzed. Based upon measurements relative to the thermal value, values of $\bar{\nu}$ for various isolated resonances will be calculated.

The work for the ^{233}U measurements is progressing. Fast current amplifiers for use with the 10 plate ^{233}U fission chamber have been built and are in the finishing stages. Gain shifts in the phototubes due to gamma flash and high instantaneous neutron capture in Gd are being investigated. Improvements in the logic system and the phototube bases will improve the neutron counting deadtime. It is envisioned to extend the measurements to the keV region.

7. Temperature-Dependent Transmission and Self-Indication Measurements Upon Ta in the Unresolved Region+ (T. Y. Byoun, R. C. Block and T. Semler (NASA))

A series of transmission and self-indication experiments have been carried out upon Ta below 100 keV to study the effects of resonance self-shielding in the unresolved neutron energy range. The ^{10}B-NaI detector at 27 meters and the 1.25-meter liquid scintillator capture detector at 25 meters were used respectively for the transmission and self-indication measurements.[1,2,3] The Rensselaer LINAC was operated at an electron energy of 70 MeV, a repetition rate of 480 pps, a peak electron current of 1.5 amperes, and with an electron pulse width from 50 to 250 nsec.

For both types of measurements a Ta sample, 0.0056, 0.0278, 0.0549, or 0.0802 atom/barn thick, was alternated in and out of the neutron beam with a 0.00147 atom/barn capture sample placed inside the capture detector for the self-indication measurements. A series of measurements were performed with the alternating sample maintained at 77° K, 295°K, or 1073°K.

---

* Pertinent to requests 261, 262, 289.

+ Work supported by NASA Grant NGR33-018-134.

The results of the transmission and the self-indication experiments are plotted in figures 7-1 and 7-2. The transmission and the SIR data are grouped into 10% wide energy bins. The high (or low) temperature transmission and SIR are calculated by normalizing the measured hot-to-room (or cold-to-room) ratio to the absolute room temperature results. No correction has been made for the sample thickness change resulting from thermal expansion; however, this causes less than a 1% change in the transmission or SIR. The accuracy (standard deviation) of the transmission measurements (room temperature, hot-to-room ratio, and cold-to-room ratio) is approximately 1% in the energy range 300 eV to 50 keV. However, in the self-indication measurements we have poorer counting statistics, 2% in the room temperature measurements and from 2% to 5% in the hot-to-room and cold-to-room ratio measurements. Fig. 7-1 shows (below 10 keV) that for a given sample thickness the transmission becomes smaller as the temperature increases. This is expected because of the Doppler broadening of the resonances. However, above 50 keV this effect disappears, indicating that the Ta resonance structure is highly overlapped and is effectively in the continuum region. Similar effects are observed in the SIR results of Fig. 7-2.

These measurements are interpreted by stochastically generating chains of "pseudo" resonances from the known distribution laws and fitting the room temperature data over the selected energy ranges and sample thicknesses used in this experiment.

The computer program DAISY[4] calculates the transmission and self-indication ratio from the Doppler broadened cross sections using the "pseudo" resonance parameters generated. The difference between the calculated and measured transmissions and SIR's are also computed from

$$\Delta T = \sum_{i=1}^{n} (T_c - T_m)_i$$

and

$$\Delta S = \sum_{i=1}^{n} (SIR_c - SIR_m)_i$$

where n is the number of samples thicknesses and the c and m subscripts are the calculated and measured values. ΔT and ΔS are minimized to some preset value by varying the initial input parameters and are tablulated in Tables 7-1 and 7-2. Analysis of the room temperature transmission and SIR show that the low energy Ta parameters[5] do fit the keV region within the errors quoted for these parameters. The 1073°K and 77°K data are being analyzed. The same experiment will

be carried out by using depleted uranium samples.

---

[1] R. W. Hockenbury, Z. M. Bartolome, J. R. Tatarczuk, W. R. Moyer and R. C. Block, Phys. Rev. 178, 1746 (1969).

[2] Z. M. Bartolome, R. W. Hockenbury, W. R. Moyer, J. R. Tatarczuk and R. C. Block, Nucl. Sci. and Eng. 37, 137 (1969).

[3] R. G. Stieglitz, R. W. Hockenbury, and R. C. Block, Nucl. Phys. A163, 592 (1971).

[4] The DAISY Program, NASA TN D-5837.

[5] J. G. Garg, J. Rainwater and W. W. Havens, Jr. (as quoted in BNL-325, 2nd Ed., Suppl. 2, 1966).

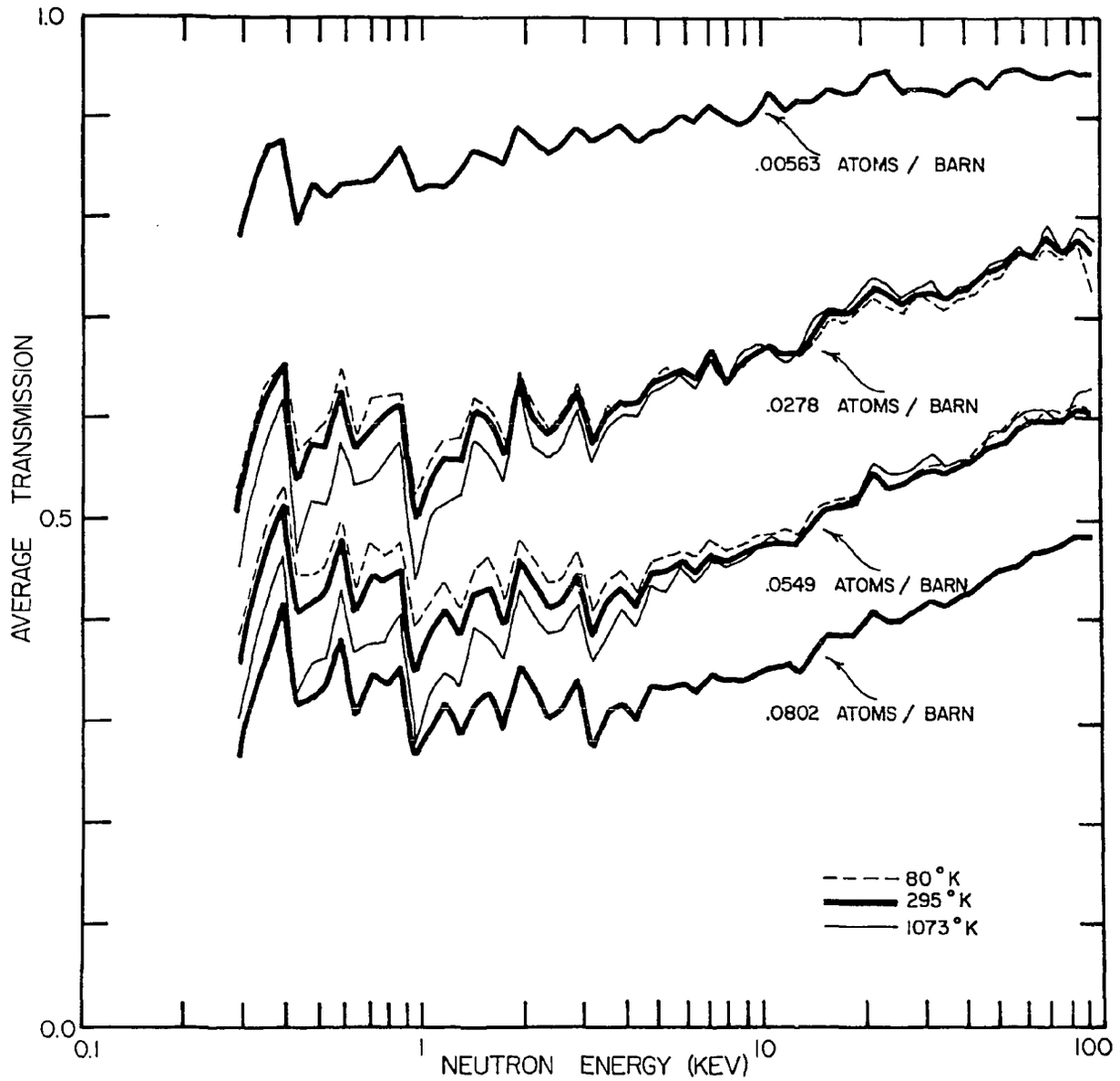

Fig. 7-1 Average Transmission vs. Neutron Energy

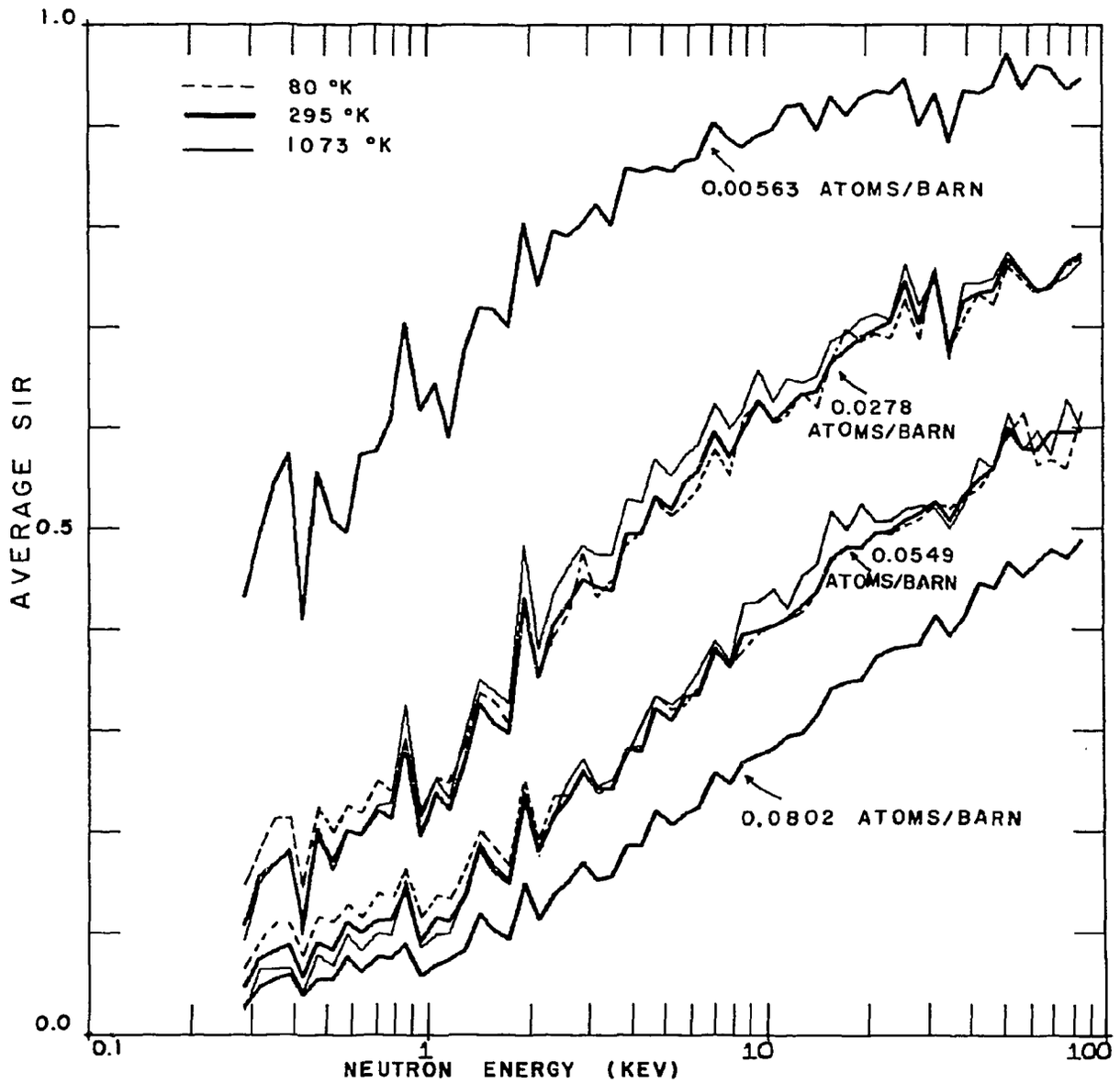

Fig. 7-2 Average SIR vs. Neutron Energy

Table 7-1 Energy Range from 3 to 4 KeV

Chain	$\overline{\Gamma_n^0}$ (meV)	σ_p (barns)	Γ_γ (meV)	D (eV)	ΔT	ΔS
L 1	1.62	8.500	56	4.5	+.0012	-.0079
L 2	1.62	8.000	56	4.5	+.0351	+.0129
L 3	1.80	8.500	56	4.5	-.0383	-.0543
L 4	1.62	8.425	56	4.5	+.0064	-.0047
L 5	1.62	8.500	50	4.5	+.0021	+.0021

Table 7-2 Energy Range from 10 to 11 KeV

Chain	$\overline{\Gamma_n^0}$ (meV)	σ_p (barns)	Γ_γ (meV)	D (eV)	ΔT	ΔS
H 1	1.62	8.5	50	4.5	-.0259	-.0024
H 2	1.62	8.2	50	4.5	-.0035	+.0165
H 3	1.62	8.3	50	4.5	-.0108	+.0100
H2+ p (p-waves)	1.62	8.2	50	4.5	-.0113	+.0159

B. INTEGRAL CHECKS OF CROSS-SECTION DATA

1. Fast Reactor Physics Studies (E. R. Gaerttner, M. W. Golay, N. N. Kaushal, B. K. Malaviya and M. Becker)

Integral checks of differential microscopic data, based on the study of fast neutron transport in bulk media, has been continuing. Time-of-flight-measured fast neutron angular flux spectra at different positions in simple, clean, homogeneous systems have been analyzed using transport-theory codes and standard data files. In addition, continuous slowing down theory has been developed to complement precise calculations. Most progress has so far been made for iron and depleted uranium.

In case of iron, data from KEDAK (Karlsruhe), ENDF/B-I and ENDF/B-II compilations have been checked. Some of the important conclusions of this evaluation are as follows:

(1) ENDF/B-I data appear to provide better general agreement with experiment than do Karlsruhe data because of better cross-section amplitudes in the 30-300 keV energy range. However, the ENDF/B-II data in this range are similar to Karlsruhe data.

(2) The capture cross section in ENDF/B-II is much more highly resolved over the entire energy range, and the average amplitude follows the Karlsruhe data more closely than ENDF/B-I.

(3) The total cross section in ENDF/B-II has a large number of very sharply resolved resonances at intermediate (hundreds of keV) energies with unreasonably deep minima. ENDF/B-I has insufficient resolution in most scattering resonances.

(4) The cross-section minimum for the 27-keV resonance in ENDF/B-I is much too low, causing unduly severe attenuation in energy compared with experiment. This minimum in ENDF/B-II, comparable to that for KEDAK file, is higher.

For depleted uranium, data from KEDAK, ENDF/B-I, ENDF/B-II and an old Argonne library (ANL set) have been

employed in the analysis and evaluation. The slope of the low-energy spectrum (below 40 keV) is found to be especially sensitive to capture data. The capture cross sections used, in turn, depend on basic data and on the unresolved resonance self-shielding (about a 30% effect at 10 keV). From these considerations, we infer that in the vicinity of 10 keV, the ANL set has about the right capture cross section; the ENDF/B-I (and also ENDF/B-II) capture is about 10% too high and the KEDAK capture value is about 25% too high; the recent ORNL measurements give even higher values. Conclusions are also obtained regarding the inelastic scattering cross section. At high energies (1-2 MeV), σ_{in} is too high in ENDF/B-I (as also in the ANL Set) but is about right in the new ENDF/B-II. In the energy range 40-500 keV, ENDF/B-I σ_{in} appears to be too high while the ANL Set seems to have the right value; the new ENDF/B-II data values are still somewhat high.

Studies for other materials are under way.

TRIANGLE UNIVERSITIES NUCLEAR LABORATORY

A. NEUTRON AND FISSION PHYSICS

1. Resonance Cross Section Measurements with Continuous Beam (J. Malan,* W. F. E. Pineo,** E. G. Bilpuch, H. W. Newson, R. L. Walter)

Neutron total cross sections of radio lead have been measured from 1.3 to 1.9 MeV neutron energy, a region in which some structure from an s-wave doorway state might be expected. These measurements were made using a new target chamber which permits the use of thin ($5\mu g/cm^2$) carbon foils as targets in the $C^{12}(d,n)$ reaction. A neutron energy resolution of less than 2 keV was achieved consistently over the entire energy range. These data are now being analyzed by J. G. Malan. The structure is complicated and only partially resolved, which renders the identification of a doorway state very difficult.

Neutron total cross sections of natural barium and strontium have been measured from 50 keV to 875 keV using a high resolution proton beam and the $^7Li(p,n)$ reaction as a neutron source. The target chamber mentioned above was used with thin LiF targets evaporated on the thin carbon foils. Since little heat was generated in the target or the foil, target deterioration was noticeably less than it had been when the targets were evaporated on thick tantalum backings. Targets of ~ 0.5 keV thickness were found to stand up for periods ranging from several hours to a few days to a proton beam of about 6 μA. The strontium data have been analyzed by R matrix curve fitting. In the following table preliminary results are compared to those of area analysis in our earlier published work:

160° Col.[1] E_0 KeV	20° Col. E_0 KeV	J^π	R-Mat. Γ_n (KeV)	Area[1] Γ_n (KeV)
105	109.0	$1/2^+$	0.150	0.150
110	113.0	$1/2^-$	0.080	0.240
122	129.5	$1/2^-$	2.000	1.875
142	144.5	$1/2^+$	0.230	0.180
151	151.0	$1/2^-$	2.500	0.850
153.5	156.7	$3/2^-$	0.150	0.290
171	169.0	$1/2^-$	2.500	0.470
196	198.0	$3/2^-$	1.350	1.300
200	202.0	$3/2^-$	0.200	0.310
212	216.5	$3/2^-$	0.250	0.790

Analysis is continuing. Apparent D-wave states complicate the analysis of the highest energy region. The barium data is not well resolved and may be suitable only for average cross section analysis.

An abstract describing this work has been contributed to the Washington meeting of the American Physical Society.

2. Average Total Neutron Cross Sections (W. F. E. Pineo)

Some of the above data are to be analyzed for strength functions by our average cross section technique.

3. Average Total Neutron Cross Sections and Strength Functions (W. F. E. Pineo, M. Divadeenam,+ E. G. Bilpuch, H. W. Newson)

Preparation of papers on this topic based on the theses of M. Divadeenam and W. F. E. Pineo is still in progress.

4. Analysis of Mo + n Resonances (M. Divadeenam, E. G. Bilpuch, H. W. Newson)

These data are being studied for signs of intermediate structure.

Assuming that the extra protons $[(1g_{9/2})^2]$ in the ground states of $_{42}Mo^{98}_{56}$ and $_{42}Mo^{92}_{50}$ are coupled to 0^+, a 2p-1h calculation is underway. In addition the particle + vibration model[2] will also be tested for the present case.

5. Shell Model Calculation of the Neutron Resonances and Intermediate Structure (F. T. Seibel,++ M. Divadeenam, W. P. Beres,‡+ H. W. Newson)

Calculations based on Feshbach, Kerman, and Lemmer's doorway-

* Now at the Atomic Energy Board of the Republic of South Africa, Pretoria
** Now at North Carolina A and T University, Greensboro, N. C.
\+ Now at North Carolina Central University, Durham, N. C.
++ Now at Los Alamos Scientific Laboratory, Los Alamos, New Mexico
‡+ Now at Wayne State University, Detroit, Michigan

1 Annals of Physics 14, 397 (1961)
2 W. P. Beres and M. Divadeenam, Physical Review Letters 25, 596 (1970)

state theory of intermediate structure are continuing. A basis of 2p-1h states is diagonalized via an effective two-body interaction. In the case of Sr^{89}, and Zr^{91}, the calculated p-wave escape widths are large compared to the s-wave widths in the low energy region. This is a manifestation of the single particle giant resonance phenomenon.

Preliminary estimates of the particle-vibration doorway escape widths in Sr^{89} indicate that the experimental data are in better agreement with the 2p-1h doorway predictions. Similar calculations are being done for the Ca^{49} case.

For comparison with low energy neutron scattering data, the sum rule $\Sigma\gamma_n^2 = \gamma_d^2$ has been employed, and the effect of doorway states on the local strength function and the fine structure observed is discussed. The widths of the s-wave resonances of Pb^{207} and Bi^{209} have been determined well enough to confirm the sum rule which should hold if the isolated $1/2^+$ resonance in Pb^{208} acts as a doorway state for Bi^{210}, Pb^{207} and Pb^{206}.

Two papers based on the investigations mentioned above have been accepted for publication in Annals of Physics. In addition a paper[1] entitled "Doorway Interpretation of Sr^{88} Neutron Resonances" is being presented at the forthcoming 1971 Spring American Physical Society meeting in Washington, D. C.

Neutron differential scattering cross sections of nuclei around A= 90 are being examined for p-wave doorway effects.

6. Fission Models (H. W. Newson)

A model of the fission products has been developed called the SLIP (Spherical Limit of the Independent Particle) Model which is in qualitative agreement with all known data on fission yields and predicts ν as a function of fragment mass quantitatively for asymmetric fission. No free parameters are necessary. A model of the whole process has also been devised which predicts a mechanism by which the fission products will be not distorted much more than in their ground states.

7. Charged Particle Induced Fission (F. O. Purser, J. R. Boyce, T. D. Hayward, E. G. Bilpuch, H. W. Newson, H. W. Schmitt*)

Total cross sections for proton induced fission of ^{233}U, ^{234}U, ^{235}U,

[1] M. Divadeenam, E. G. Bilpuch and H. W. Newson, Bull. Am. Phys. Soc. 16, 495 (1971)

^{236}U, and ^{238}U have been measured for proton energies from 6.0 to 30 MeV. Differential cross sections at 90° L have been measured at 250 keV intervals over this energy range, and complete angular distributions have been measured at maximum energy intervals of 2 MeV with more closely spaced measurements in those energy regions in which the anisotropy is not a slowly varying function of proton energy. Cross sections for which the analysis has been completed range from 1.6 barns for ^{235}U at 30 MeV to 1.3 barns for ^{238}U at this energy. All cross sections appear to be monotonically increasing functions of proton energy, dominated, below the coulomb barrier, by penetrability effects.

The angular distributions measured are consistent with the functional relationship

$$\sigma(\theta_{cm}) = \sigma_{90°}(1 + \epsilon \cos^2\theta_{cm})$$

even at the highest energies. Measured anisotropics ($\sigma_{0°}/\sigma_{90°}$) are considerably lower than those reported in the literature for neutron induced fission of the uranium isotopes. While the thresholds for opening of additional decay channels such as (p,nf), (p,2n), (p,3n) etc. appear to be reflected in the anisotropy measurements, they are not associated with the marked increases in anisotropy which are reported for neutron induced fission. More detailed measurements in these threshold regions are in progress.

The cross section measurements will be extended for proton energies less than 6.0 MeV. Since the fission channel makes the dominant contribution to the reaction cross section for these energies, accurate measurements should provide a test of the validity for the actinide nuclei of currently available proton optical model parameters. The proton elastic scattering program which has been delayed pending completion of the fission cross section measurements, will be resumed in conjunction with these experiments.

Fission fragment mass and kinetic energy distributions for several isotopes have been measured, principally to acquire a familiarity with the necessary techniques and to develop the appropriate computer programs. This capability is now operational and will be used in a detailed study of energy dependent effects at moderate excitation energies in the uranium isotopes. Accurate measurements for several isotopes over extended energy regions should provide adequate data to allow the unfolding of contributions to the fission process from competing channels, such as (p,nf), (p,2nf), etc.

Measurement of prompt neutron yields using the Cyclo-Graaff time-of-flight capability will be instituted following completion of the final shielding walls in the high-resolution target area.

8. Analysis of Nucleon-^{4}He Scattering below 20 MeV (Th. Stammbach, R. L. Walter)

An R-matrix analysis of all available n-^{4}He and p-^{4}He cross-section and polarization data has been made to give a new parameterization of these scattering processes. Phase shifts have been derived and polarization tables are compared to earlier reports. This work is being written for publication.

9. Polarization in (^{3}He,n) Reactions on ^{9}Be, ^{11}B and ^{13}C (R. S. Thomason, L. A. Schaller, Th. Stammbach, R. L. Walter)

A summary of the polarization in these reactions below 4 MeV is being prepared for publication.

10. Polarization of Neutrons from ^{6}Li(d,n) and ^{7}Li(d,n) (R. S. Thomason, G. Spalek, and R. L. Walter)

This work appeared in Nuc. Phys. A155, 659 (1970).

11. Neutron Polarization from (d,n) Reactions on ^{24}Mg, ^{28}Si, and ^{40}Ca (J. Taylor, Th. Stammbach and R. L. Walter)

A paper on this work is to be submitted to Nuclear Physics. The abstract of the thesis of J. Taylor follows:

> "Neutron polarizations from (d,n) reactions with unpolarized deuteron beams have been measured for several light nuclei. The ^{11}B(d,n_0) and ^{11}B(d,n_1) polarization angular distributions were measured at 7.6, 9.6 and 11.7 MeV. These reactions showed differences, as expected, between $p_{1/2}$ and $p_{3/2}$ stripping. However, characteristic j-dependent structure was hard to identify because the changes in the polarization were not systematic with increasing energy. Cross-section angular distributions and ^{11}B(d,d) elastic scattering data were also obtained. Numerous optical model parameter sets which reproduce the deuteron elastic scattering data were used in DWBA calculations. Modest agreement was found for the ^{11}B(d,n_0) reaction polarization distribution, but not for the ^{11}B(d,n_1) reaction.
>
> "Four neutron polarization angular distributions were measured for ^{28}Si(d,n_0) between 2.9 and 3.9 MeV. Compound

nucleus effects were apparent. A distribution was measured at 8.1 MeV for the $^{28}Si(d,n_0)$ and $^{28}Si(d,n_1)$ reactions. The 8.1 MeV results resembled previously reported data at 5.0 MeV. DWBA calculations were made at 5.0 and 8.1 MeV with existing optical potential parameters. They described the n_0 reaction reasonably well, but not the n_1 polarizations. Agreement with the (d,n) cross sections was reasonable for both groups.

"Polarization distributions were measured at six energies for the $^{24}Mg(d,n_0)$ and $^{24}Mg(d,n_1)$ reactions between 2.2 and 3.9 MeV, and polarization excitation functions were measured in about 100 keV steps at 20° and 40° (lab) from 2.0 to 3.9 MeV. The data showed some fluctuations with energy uncharacteristic of a smooth dependence expected from a direct reaction. No DWBA calculation will be attempted until higher energy polarization data are available.

"The $^{40}Ca(d,n_0)$ polarization distribution was measured at 3.8 MeV. DWBA calculations were made for ^{40}Ca with variations of existing potentials, and agreement was fair for the 3.8 MeV data and good for existing data at 6 MeV."

12. A DWBA Analysis of the Cross Section and Polarization Data for The $^{14}N(d,n)^{15}O$ Reaction at 3.5 MeV (M. M. Meier, R. L. Walter, T. R. Donoghue, R. G. Seyler, R. M. Drisko)

This work appeared in Nucl. Phys. A159, 273 (1970).

13. Polarization of Neutrons from ^{10}B, ^{11}B, and $^{13}C(d,n)$ Reactions (M.M Meier, R. S. Thomason and R. L. Walter)

These measurements were carried out for energies from 2.8 to 3.0 MeV. A report is being prepared for Nuclear Physics.

14. The j-dependence in the $^{11}B(d,n_0)$ and $^{11}B(d,n_1)$ Polarizations (J. Taylor, G. Spalek, Th. Stammbach, R. A. Hardekopf and R. L. Walter)

Optical Model analysis of the $^{11}B(d,d)$ data have been completed. DWBA calculations were compared to the (d,n) cross sections and polarizations

for the $p_{3/2}$ transfer ground-state reaction and (mostly) $p_{1/2}$ first excited state reaction. The work has been reported in the abstract of J. Taylor's thesis in Section 11. Some of the results were presented at the Madison Polarization Conference. A more complete report will be prepared for publication.

15. Remeasurement of the Neutron Polarization from the $^{7}Li(p,n)^{7}Be$ Reactions for 3 to 4 MeV Protons (R. A. Hardekopf, J. M. Joyce (ECU), G. L. Morgan ((ORNL)) and R. L. Walter)

A calibration of the $Li(p,n_0)$ and (p,n_1) polarization has been made and was reported at the Madison Polarization Conference. A more complete description has been submitted to Nuclear Physics.

16. Neutron-Helium Interaction II, Angular Distributions and Phase Shifts from 0.2 to 7.0 MeV (G. L. Morgan ((ORNL)) and R. L. Walter)

Differential cross section values have been extracted from previously published spectra recorded in a ^{4}He recoil scintillator. The data have been sent to the Neutron Cross Section Center at BNL and a short report of the data analysis has been published in Phys. Rev. C5, 2034 (1970).

17. Sources of Polarized Neutrons (R. L. Walter)

A review of the various sources of polarized neutrons has been made. Comparisons and advantages of different methods and reactions are listed. This paper will appear in the proceedings of the Madison Polarization Conference.

18. The $^{9}Be(d,n)$ Reaction from 3 to 4 MeV (G. Spalek, J. Taylor, R. A. Hardekopf, Th. Stammbach, R. L. Walter)

The polarization from the $^{9}Be(d,n)$ reactions for five neutron groups has been compared to DWBA calculations. As most of the reactions are 1p transfers, these reactions are a good test of the sensitivity to Q-value. Optical model fits were made to $^{9}Be(d,d)$ data obtained from 3 to 4 MeV. Preliminary results were presented at the Madison Polarization Symposium.

19. Polarization of Neutrons from the D(d,n) Reaction from 6 to 22 MeV (G. Spalek, R. A. Hardekopf, J. Taylor, Th. Stammbach, T. C. Rhea, J. Joyce, R. L. Walter)

A measurement of the D(d,n) neutron polarization was carried out from 6 to 14 MeV on the tandem and was reported at the Madison Polarization

Conference. A second phase, using the pulsed beam of the Cyclo-Graaff, extended these measurements to 22 MeV. The polarization at 45° c.m. was found to be around 0.35 above 16 MeV in disagreement with earlier values reported around 0.24. Thus the reaction is the most useful source of polarized neutrons for 16 MeV < E_n < 22 MeV and the only measured source between 18 and 22 MeV.

20. (p,n) Experiments with Chopped Beam (S. M. Shafroth, A. A. Jaffe, G. A. Bissinger, T. Dzubay, F. Everling, D. W. Miller, D. A. Outlaw, E. J. Ludwig, A. Watkins, P. Nettles)

a. The data on ^{80,82}Kr(p,n) and (p,nγ) have been prepared for publication and will be submitted after some minor details are cleared up, i.e., following the next run.

b. The ^{36}Ar(p,n)^{36}K threshold data have been accepted for publication, i.e., Physical Review Comments.

c. A study of the ^{36}Ar(p,n)^{36}K → β^+ ^{36}Ar*(γ) reaction has been made primarily to investigate the anomalous log ft in the ΔT = 0, ΔJ = 0 $2^+ \rightarrow 2^+$ transition from ^{36}K to ^{36}Ar(6.613). As a result it was found thai the log ft is normal (3.5). These data arebeing prepared for presentation at the Washington meeting of the American Physical Society and will be part of the Ph.D. thesis of D. W. Miller.

d. ^{12}C(p,nγ) experiments. The high-resolution magnet system is being used in conjunction with the Cyclo-Graaff proton beam to perform a study of isospin-forbidden resonances in the ^{12}C + p system. The study is being made by measuring the yield of β^+ particles produced in the (p,n) reaction. A computer-controlled electrostatic chopper has been installed and made operative for this purpose.

B. CHARGED PARTICLE REACTIONS

1. Fine Structure of Isobaric Analogue States in Medium-Weight Nuclei (N. H. Prochnow, D. P. Lindstrom, J. D. Moses, W. C. Peters, W. M Wilson, G. E. Mitchell, H. W. Newson, E. G. Bilpuch)

a. The Chromium Isotopes

A paper has been accepted for publication in Nuclear Physics on the question of the enhancement of neutron decay by analogue states in ^{65}Cu

and ^{55}Mn, entitled "A High Resolution Investigation of the (p,n) Reaction through Isobaric Analogue Resonances". The following is the abstract of that paper:

> "The ^{54}Cr(p,n)^{54}Mn and ^{64}Ni(p,n)^{64}Cu total neutron yields and the ^{54}Cr(p,p)^{54}Cr and ^{64}Ni(p,p)^{64}Ni differential cross sections were measured in the vicinity of the analogues of the third excited state of ^{55}Cr and the first excited state of ^{65}Ni. The total energy spread for these measurements is approximately 300-400 eV. The data are examined for an enhancement of the neutron widths of the fine-structure resonances associated with these analogue states. No enhancement of the neutron widths is observed."

A paper on the reactions ^{50,52,54}Cr(p,p), ^{50}Cr(p,p'), and ^{54}Cr(p,n) is in preparation.

Computer codes based on formulae of Robson and Lane have been written for the analysis of the fine structure distributions of analogue states. A systematic analysis of the available fine structure distributions is planned.

b. The Iron Isotopes

A paper has been accepted for publication in Nuclear Physics entitled "Fine Structure of Analogue States in ^{55}Co, ^{57}Co, and ^{59}Co". The following is the abstract of that paper:

> "Differential cross sections were measured at four angles for proton elastic scattering from ^{54,56,58}Fe at energies ranging between 1.8 and 3.3 MeV. Using the TUNL 3 MV Van de Graaff accelerator and high-resolution analyzer-homogenizer system, a total resolution of 300-400 eV was achieved for thin solid targets of enriched iron isotopes. Seven analogue states in ^{55}Co and ^{57}Co appeared as single resonances; three analogue states in ^{59}Co showed well-developed fine structure distributions. Spins, parities, and widths were determined for approximately 200 resonances. Spectroscopic factors and Coulomb energy differences were extracted for the analogue states."

Analysis of the resonances in ^{58}Fe above 2.6 MeV has now been essentially completed. The yield of gamma rays from the (p,p') reaction has been measured to aid in this analysis.

A multilevel, single channel computer code has been adapted to the DDP-224 α-computer. Utilization of this code in analyzing elastic resonances should reduce the time required to perform such analyses.

c. The Titanium Isotopes

The following excitation functions have been measured:

$^{48}Ti\,(p,p)^{48}Ti$; 1.8 MeV to 3.1 MeV at 160°, 135°, 105°, 90°
$^{48}Ti\,(p,p_1)^{48}Ti^*$; " " at 160°, 135°, 105°, or 90°
$^{46}Ti(p,p)^{46}Ti$; " 3.08 MeV at 160°, 135°, 120°, 90°
$^{46}Ti(p,p_1)^{46}Ti^*$; " " at 160°, 135°, 105°, or 90°

A total overall energy resolution of 250-350 eV was achieved.

A continuous fit to the ^{48}Ti + p data has been obtained, and resonance energies, spins, parities and elastic and reaction widths have been extracted for over 300 resonances. Two analogue states have been identified and Coulomb energies and spectroscopic factors have been extracted. Linear correlation coefficients have been determined for the elastic and reaction widths for both on-analogue data and off-analogue data. This aspect of the ^{48}Ti + p data will be presented at the 1971 Washington APS meeting.

Analysis of the ^{48}Ti + p data with regard to statistical properties of the nucleus such as spacing distributions and reduced width distributions has been practically completed. A more detailed discussion of this is included in Section 2.

The ^{46}Ti + p data has been analyzed from 1.8 MeV to 2.6 MeV and resonance energies, spins, parities and elastic and reaction widths have been obtained for 50 resonances. The data from 3.00 to 3.08 MeV are partially analyzed and the data from 2.6 to 3.00 MeV are currently being analyzed. Experiments are being planned to measure the $^{50}Ti(p,p)^{50}Ti$ and $^{50}Ti(p,p_1)^{50}Ti^*$ excitation functions over the energy range 1.8 MeV to 3.3 MeV.

d. The Calcium Isotopes

An excitation function in $^{40}Ca(p,p)$ was measured from 1.80 MeV - 2.90 MeV. These data were analyzed using the multi-level, multi-channel, R-matrix formalism code MULTI, and 5 broad levels were fit. An excitation function in $^{44}Ca(p,p)$ was measured from 1.60 MeV - 1.70 MeV and from 1.80 MeV - 2.94 MeV, and $^{44}Ca(p,p')$ was measured from 2.60 MeV - 2.94 MeV.

These data were analyzed from 2.00 MeV - 2.48 MeV and approximately 100 levels have been fit. Analysis of the rest of the data is in progress.

e. (p,γ) Reactions

Preliminary measurements on the decay of the fine structure states of the analog of the ground state of ^{55}Cr have been repeated, and relative widths from the ground state gamma decay have been compared with the elastic reduced widths of the fragments. Data reduction for other strong gamma rays is in progress. Analysis for possible channel-channel correlations will be made in the near future. A talk on this work will be presented at the 1971 Washington American Physical Society meeting.

2. Statistical Properties of Nuclei Via Proton Resonance Reactions
(E. G. Bilpuch, G. E. Mitchell, N. H. Prochnow, H. W. Newson, R. Y. Cusson and J. D. Moses)

For many years the statistical properties of excited nuclei have been studied extensively via neutron resonance reactions and very little statistical information has been obtained from charged particle resonance reactions.

At the present time our group is engaged in a systematic study of the medium-weight nuclei utilizing the high resolution techniques on the TUNL 3 MV accelerator. Using solid targets of 1 to 2 μgms thickness, our overall resolution is 300 eV over an energy range of E_p = 1.5 to 3.3 MeV. The two major aims of this extensive study (of essentially all the even-even targets in the A = 40-64 mass region) are:

1. To investigate thoroughly the fine structure of analogue states and

2. To determine level densities, spacing distributions, width distributions and proton strength functions for various ℓ and J values.

Recently we have observed that the local average s-wave spacing in ^{49}V has an exponential energy dependence at excitation energies of 8.5 to 9.8 MeV. After correcting for this energy dependence the experimental width and spacing distributions agree with the Porter-Thomas and Wigner distributions. A letter based on this work has been submitted to Physics Letters and the abstract follows:

"Proton scattering from ^{48}Ti has been measured from 1.8 to 3.1 MeV bombarding energy with an overall energy resolution of 300 eV. The statistical properties of 70 s-wave resonances are examined. The average s-wave spacing displays an exponential dependence $\langle D \rangle \sim \exp(-E_p/T)$. The spacing distribution (after correction for the exponential energy dependence) and the reduced width distribution are in good agreement with the Wigner and Porter-Thomas distributions."

C. DEVELOPMENT

1. Accelerator Improvements (F. O. Purser, T. D. Hayward, J. R. Boyce, H. W. Newson, R. L. Rummel, M. T. Smith, T. Dzubay, E. G. Bilpuch, J. D. Moses, G. E. Mitchell)

a. Tandem Accelerator

The terminal instability and sagging associated with the onset of high gamma fluxes in the region of the terminal have been eliminated. The accelerator was re-opened soon after the last report period and all components thoroughly re-checked, all vacuum seals leak tested and found to be tight, and the column resistor string completely overhauled to prevent recurrence of previously experienced intermittent open circuits due to faulty contact. In addition, the following steps were taken:

(1) The up-charge screen and the terminal charging screen were repositioned to place them in very firm contact with the charging belt.

(2) The second low energy accelerating tube exhibited light-to-moderate radiation darkening in two areas. Clamp-on magnets were installed 10 electrodes upstream from each of these areas with the magnetic fields aligned to reinforce the transverse gradient of the inclined field sections.

Following this overhaul, the tandem has run stably and routinely for a period of three months with no recurrence of the former problems. Terminal voltages up to 8 MV have been attained routinely during this period. A subsequent tank opening to replace stripper foils revealed no increase in the radiation darkening previously observed and that the charging screens were still correctly positioned.

Materials have been ordered and shop drawings completed for manufacture of a direct extraction negative ion source based on modification of an existing duo-plasmatron. This source will increase our heavy ion capability

and will be very useful in conjunction with our very high-resolution development work with the tandem.

b. The Injector Cyclotron

The new cooling-water system referred to in the last report has been placed in satisfactory full time operation. Component cooling and vacuum system operation has been markedly improved by the change over. The cleaner low-ion content water circulating in the all copper system is gradually re-absorbing the iron deposited in the cyclotron cooling passages by the previous system and by periodic recycling of the water supply it is hoped to continue this cleaning process.

Feed-back circuitry designed to stabilize the dee voltage by a signal derived from the extracted beam has been operationally tested. Ripple components in the dee voltage showed a reduction of 50% with this method of control. Operational use of this technique will be implemented upon installation of an improved deflection supply. The present deflector supply has sufficient 120 cycle ripple (1%) to give a substantial erroneous error signal to the feedback circuit.

The in-house designed deflector supply intended to replace this supply has encountered difficulties. We are presently investigating relative costs involved in re-design of the present circuit as opposed to purchase of a commercial supply with the required characteristics.

Use of the cyclotron injector continues to represent approximately 40% of total accelerator operating time with tandem-only operation filling the remainder. Deuteron operation has increased largely due to a requirement for 20-24 MeV deuterons for neutron polarization experiments. The cyclotron continues to operate reliably with routine delivery of beam currents in excess of those required experimentally.

c. Beam Transport System

The high resolution analyzing system has met its final acceptance tests by demonstrating an energy resolution of $\Delta E/E \leq 1/5700$ measured at 14.233 MeV using the $T = 3/2$ analogue resonance in ^{13}N. This exceeds the guaranteed resolution of 1/5400. With this resolving power for the system, the laboratory is guaranteed a capability of performing experiments with beam energy spreads of < 5.2 keV at 30 MeV. With appropriate magnet cycling, energy reproducibility has been found to be better than $\pm$ 0.5 keV at the 14.233 calibration

point.

Two experimental stations are in operation in the high resolution target area with three more programmed to be installed in the coming six months. With this addition, eight experimental stations will be in operation in the Cyclo-Graaff laboratory. Two of these stations will be served by large (24" diameter) scattering chambers.

d. Improved Beam Energy Resolution for The Tandem Accelerator

When a tandem Van de Graaff accelerator is operated using oxygen gas in the stripper canal, both a neutral H beam and a charged H^+ beam are produced. These two beams have been utilized on the TUNL FN tandem to obtain improved energy resolution. The H^+ beam is deflected by a magnet and focussed onto a target. At the O^0 exit port of this magnet the neutral beam passes through a biased carbon foil and emerges as an H^+ beam. This beam is transmitted to a high dispersion magnetic analyzer. An error signal obtained from the exit slits of this magnet is applied to the carbon foil stripper to keep the beam centered on the exit slits. After suitable amplification, this signal is also used to modulate the target potential. Preliminary measurements of known resonances in ^{50}Cr and ^{54}Fe near 3 MeV yield a resolution of $\sim$ 600 eV. Contributions to the resolution (particularly Doppler broadening of the HH^+ beam in the exchange canal of the ion source) are being investigated.

2. Pulsed Beams (F. O. Purser, T. D. Hayward, J. R. Boyce, D. E. Elliott, H. W. Newson, R. O. Nelson, R. A. Hilko, T. Dzubay, N.R. Roberson, P. Nettles, E. J. Ludwig, S. M. Shafroth)

a. Cyclo-Graaff Time-of-Flight System

Difficulties encountered with the design of the pulse-suppression system for the cyclotron appear to have been overcome. The inherent period of the extracted cyclotron beam is 40 ns with a pulse length varying from 0.4 to 2 ns dependent upon tuning conditions and internal slit locations. The pulse suppression system will allow TOF work with periods of 2^N(40 ns) with $0 \leq N \leq 4$. Suppression of the intermediate pulses for the longer periods involves switching 400 volts with a rise time ≤ 5 ns on a pair of deflection plates in the cyclotron source. The switching is accomplished by turning on a bank of parallel transistors coupled through finite cores. At the higher repetition rates, the cores initially chosen were heated past their curie points with subsequent switching failure. Substitute cores with larger heat capacity have proven workable on the bench and a full system test is scheduled for the near future.

b. Particle Identification by Time-of-Flight

Mass-identification using one detector and the TUNL Cyclo-Graaff was accomplished by measuring the time-of-flight (TIME) and energy (E) and then forming the product E and square of TIME. This product should be proportional to mass. Product was formed in an on-line computer digitally and displayed against E two-dimensionally. Particle groups corresponding to mass 1, 2, 3, 4 and 6 were seen for 21 MeV deuterons on ^{24}Mg. This method is being further investigated to replace ΔE-E solid-state telescopes.

c. Electrostatic Beam Chopper

The electrostatic beam chopper has been installed in the high resolution magnets system and has operated successfully. A 10 keV power supply is used along with a high voltage triode to supply voltage to the plates. The signal to the grid of the triode is of variable frequency and duration and is controlled by the DDP-224 on-line computer. Positron decay half-lives of 10 ms have been observed by chopping of a proton beam and measuring the β^+ yield from the residual nucleus during the beam-off period.

3. Polarized Beams (T. B. Clegg, R. A. Hardekopf, T. Trainor, G. A. Bissinger, E. J. Ludwig, A. C. Watkins, T. G. Dzubay)

a. Lamb Shift Polarized Ion Source

The Lamb-shift polarized ion source installed last summer on the TUNL tandem accelerator is now being used extensively for experiments. The ion source itself has required constant maintenance as problems in the initial design of the source have appeared.

It became clear that the diffusion pumps on the source could not be operated unbaffled, and freon cooled baffles were installed. The electrostatic mirror of Brookhaven design used in the first 90° deflection of the polarized beam was replaced by a gridded mirror which is a copy of the Wisconsin-designed electrostatic mirror. High voltage power supplies used for the mirrors and lenses have been found to drift and work is underway to regulate them.

The source has now produced beams on target of 8 nA of 82% polarized proton beam, 10 nA of purely tensor polarized deuteron beam with $P_{zz} = -1.4$. Data collection programs which allow the collection and analysis of polarization data on-line with the DDP-224 computer are in use.

b. Polarization Monitor for Polarized Proton Beams

The proton polarization monitor reported on previously has been modified to improve performance. It was found that the count rate using the "Venetian blind" slits to define the angular range for the scattered particles was too large with the beam currents available from the polarized ion source. Also the resolution in the detector peak corresponding to the elastically scattered protons was poor. Both problems were resolved by replacing the "Venetian blind" slits with a more standard two-slit geometry to define the scattering angle for the protons elastically scattered from the helium gas. The new geometry defines the scattering angle to be $\theta_{lab} = 112°$ where the p-^{4}He analyzing power is its maximum. The monitor now has an efficiency of about 60 counts/sec-nanoampere for a helium pressure of 6 atmospheres.

c. Large-Capacity Foil Stripper for The Tandem Accelerator

The design has been completed. Construction will begin when shop time becomes available.

4. Computers and Programming (C. R. Gould, S. E. Edwards, R. O. Nelson, R. J. Eastgate, R. A. Hardekopf, R. A. Hilko, J. M. Joyce, W. M. Wilson, T. G. Dzubay, D. P. Lindstrom, N. R. Roberson)

a. On-Line Acquisition and Analysis of Data

A third Northern Scientific 50 MHz, 8K analogue to digital converter will be acquired and interfaced to the 16 K on-line DDP-224 computer. An IBM Model 29 card punch is now interfaced to the 8K off-line DDP-224 computer and has proved reliable and useful for data output and card duplicating.

Both computers have generally been scheduled 24 hours a day during the last six months and have operated reliably with few main frame problems.

b. IBM 360 and DDP-224 Programming

The programs JIB 3, SNOOPY, BANDMIX, DWUCK, JUPITOR-2, M2, CORPAR and FTAU, mentioned in the last report, continue to be used at TUCC on the IBM 360. In addition, a single precision version of P. D. Kunz's new DWBA code DWUCK-2 has been recently implemented. This code is based on DWUCK but has provisions for the inclusion of microscopic form factors and for two nucleon transfer analysis.

Three programs are now available for analyzing the high resolution data from the homogenized tandem beam. The data taking program NUMUD is optimized for studying excitation curves in very small steps. Program MULTI is a multilevel, single channel R-matrix code for generating theoretical resonance shapes. Program SMEAR allows the results of program MULTI to be averaged over the effective beam width in order to determine the profile of the beam energy distribution.

The optical model code OPTICS which was chained to run in the DDP-224 has been modified and extended. A report on this code has been prepared for publication and a paper will be presented at the Washington meeting of the American Physical Society.

The system software supplied by Honeywell was modified to speed up the loading process for relocatable subroutines on the second files of systems tapes. By repacking the subroutines into 128 word records, the load time for the test programs has been cut by a factor of six. In addition the accuracy of a number of the floating point math subroutines has been improved.

YALE UNIVERSITY

A. NEUTRON TIME-OF-FLIGHT STUDIES (F.W.K. Firk, R.J. Holt, K. Nath, H.L. Schultz and F.D. Brooks*)

1. Polarization in n-p Scattering

Measurements of the polarization in n-p scattering in the energy range 5-25 MeV are now in progress. The neutron polarimeter, which uses the known direction-sensitive pulse shape discrimination properties of anthracene crystals, is working satisfactorily. The source of polarized neutrons is the reaction $D_2O(\gamma,n)$ at an angle of 45^o (both the deuterium and oxygen nuclei in the target contribute useful yields of polarized neutrons at these energies). The neutron energies are measured with a time-of-flight resolution of 0.3 $ns.m^{-1}$. This is a 3-parameter experiment and the necessary hardware and software associated with a PDP-7 computer is now developed fully (this aspect of the work was carried out in collaboration with G.W. Cole of B.N.L.).

2. Polarization of Photoneutrons from the Deuteron

The differential polarization of photoneutrons from the reaction $D(\gamma,n)p$ has been measured at reaction angles of 45^o and 90^o in the energy range 5-35 MeV. The polarization was measured by observing the elastic scattering of neutrons from a liquid helium target: the neutron energies were determined by the time-of-flight method. The neutron spins were precessed through measured angles using a 1.2 m long, 4KG solenoid (the neutron energy determination making it possible to deduce the angle of precession). Neutron multiple scattering corrections in the targets (CD_2, CH_2, D_2O and H_2O) are now being made, and the final polarization results will be available in the near future.

---

* On leave from University of Cape Town, South Africa.

APPENDIX: Recent Publications

ARGONNE NATIONAL LABORATORY

1. Average-Resonance Method of Neutron-Capture γ-Ray Spectroscopy: States of ^{106}Pd, ^{156}Gd, ^{158}Gd, ^{166}Ho, and ^{168}Er, L. M. Bollinger and G. E. Thomas, Phys. Rev. C2, 1951-2000 (November 1970)

2. Direct Reactions on ^{10}Be, D. L. Auton, Nucl. Phys. A157, 305-322 (23 November 1970)

3. ΛN Tensor Forces for Scattering and for the Λ-Particle Binding in Nuclear Matter, A. R. Bodmer, D.M. Rote, and A. L. Mazza, Phys. Rev. C2, 1623-1648 (November 1970)

4. Spin Dependence in Inelastic Scattering, J. C. Legg, D. R. Abraham, J. L. Yntema, R. C. Bearse, and H. T. Fortune, Phys. Rev. C2, 1733-1737 (November 1970)

5. Nuclear Structure of Sc^{48} from the $Ti^{49}(d,He^3)Sc^{48}$ Reaction, Hajime Ohnuma and J. L. Yntema, Phys. Rev. C2, 1725-1728 (November 1970)

6. $^{10}B(\alpha,{}^6Li)^8Be$ Reaction at 46 MeV and the Configuration of the ^{10}B Ground State, B. Zeidman, H. T. Fortune, and Achim Richter, Phys. Rev. C2, 1612-1616 (November 1970)

7. Gamma Rays from Thermal Neutron Capture in ^{28}Si, ^{29}Si, and ^{30}Si, G. B. Beard and G. E. Thomas, Nucl. Phys. A157, 520-528 (1970)

8. Gamma Rays from Neutron Capture in Resonances, L. M. Bollinger, Experimental Neutron Resonance Spectroscopy, Ed. J. A. Harvey (Academic Press, Inc., New York, 1970), Chapter IV, pp. 235-345

9. States in ^{12}B Observed in the Scattering of Neutrons by ^{11}B, R. O. Lane, C. E. Nelson, J. L. Adams, J. E. Monahan, A. J. Elwyn, F. P. Mooring, and A. S. Langsdorf, Phys. Rev. C2, 2097-2105 (December 1970)

10. Group Theory and Theoretical Physics, H. J. Lipkin, Proc. Conf. on Methods and Problems of Theoretical Physics, Birmingham, July 4-6, 1967, Ed. J. E. Bowcock (North-Holland Publ. Co., Amsterdam, 1970), pp. 381-399

11. The Quest for Superheavies, J. P. Schiffer, Comments on Nucl. Particle Phys. 4(2), 90 (1970)

12. Properties of ^{55}Mn, ^{56}Mn, and ^{57}Fe in the Unified Rotational Model, J. R. Comfort, P. Wasielewski, F. B. Malik, and W. Scholz, Nucl. Phys. A160(2), 385 (1971)

13. Ru$^{103, 105}$ States Observed in the Reactions Ru$^{102, 104}$(d, p), H. T. Fortune, G. C. Morrison, J. A. Nolen, Jr., and Paul Kienle, Phys. Rev. C3, 337-344 (January 1971)

14. An Apparatus for "Channeling" Experiments, D. S. Gemmell and J. N. Worthington, Nucl. Instr. Methods 91(1), 15-28 (1971)

15. Convergence of the Sasakawa Expansion for the Scattering Amplitude, Fritz Coester, Phys. Rev. C3, 525-529 (February 1971)

16. Coulomb Excitation of Levels in Pb^{105}, H. H. Bolotin and D. A. McClure, Phys. Rev. C3, 797-806 (February 1971)

17. On the Repulson of Slow Neutrons by Attractive Potentials, Murray Peshkin and G. R. Ringo, Am. J. Phys. 39, 324-327 (March 1971)

18. Lifetime of the 981-keV State in Li^{8}, M. J. Throop, D. H. Youngblood, and G. C. Morrison, Phys. Rev. C3, 536-543 (February 1971)

19. Proton Stripping Strengths for Levels of ^{11}C, J. R. Comfort, H. T. Fortune, J. V. Maher, and B. Zeidman, Phys. Rev. C3, 1086-1094 (March 1971)

20. Off-Shell Continuations of the Two-Particle Transition Matrix with Bound States, K. L. Kowalski, J. E. Monahan, C. M. Shakin, and R. M. Thaler, Phys. Rev. C3, 1146-1151 (March 1971)

21. ^{87}Y States Populated by Single-Proton Stripping, J. V. Maher, J. R. Comfort, and G. C. Morrison, Phys. Rev. C3, 1162-1168 (March 1971)

22. Regge Poles and Strong Absorption in Heavy-Ion and α-Nucleus Scattering, K. W. McVoy, Phys. Rev. C3, 1104-1118 (March 1971)

23. The DELPHI-SPEAKEASY System. I. Overall Description, Stanley Cohen, Computer Phys. Commun. 2, 1-10 (January 1971)

24. Measurements of the Ratios of Capture and Fission Neutron Cross Sections of ^{235}U, ^{238}U and ^{239}Pu at 130 to 1400 keV, W. P. Poenitz, Nucl. Sci. and Eng. 40, 383 (1970)

25. Recent Experimental Data for Heavy Nuclei, W. P. Poenitz, IAEA Conference on Nuclear Data for Reactors, Helsinki, June 1970, to be published

26. Comment on Resonance Averaging, P. A. Moldauer, Phys. Rev. C3, 948-949 (1971)

27. The Total Neutron Cross Section of Lithium-7 and Carbon from 100 to 1500 keV, J. W. Meadows and J. F. Whalen, Nucl. Eng. 41, 351 (1970)

28. Precision Thermal Cross Sections of Lithium and Boron, J. W. Meadows, EANDC Symposium on Neutron Standards and Flux Normalization, October 1970, Argonne National Laboratory, to be published

29. Experimental Studies of Polarization Produced by Elastic Scattering of Neutrons in the Vicinity of 1.0 MeV, S. A. Cox and E. D. Whiting, International Symposium on Polarization Phenomena in Nuclear Reactions, August 1970, Madison, Wisconsin

30. Performance of the ANL Tandem Dynamitron, S. A. Cox and P. Hanley, 1971 Particle Accelerator Conference, March 1971, Chicago, Illinois

31. Fast Neutron Cross Sections: Theory and Experiment, P. A. Moldauer and A. B. Smith, Invited Paper, Third Conference on Neutron Cross Sections and Technology, March 1971, Knoxville, Tennessee, to be published

32. Interpretation and Intercomparison of Standard Cross Sections, W. P. Poenitz, EANDC Conference on Neutron Standards and Flux Normalization, October 1970, Argonne National Laboratory

33. Measurements of the ^{235}U Fission Cross Section at 552 keV and 644 keV, W. P. Poenitz, EANDC Conference on Neutron Standards and Flux Normalization, October 1970, Argonne National Laboratory

34. Absolute Cross Sections of ^{197}Au and ^{238}U, W. P. Poenitz, EANDC Conference on Neutron Standards and Flux Normalization, October 1970, Argonne National Laboratory

35. ^{165}Ho Fast Neutron Cross Sections, J. W. Meadows, A. B. Smith, J. F. Whalen and T. D. Beynon, Zeits für Physik, accepted for publication

36. Note on the Prompt-Fission-Neutron Spectra of ^{235}U and ^{239}Pu, A. B. Smith, Nucl. Sci. and Eng., accepted for publication

37. Variation of the Intrinsic Efficiency of a Cylindrical Planar Ge(Li) Gamma-ray Detector with Source Distance, D. S. Smith, Nucl. Instr. and Methods, submitted

Abstracts of contributions presented at recent meetings:

1. Elastic and Inelastic Scattering of ^{14}N, ^{15}N, and ^{16}O from ^{28}Si, K. O. Groeneveld, Achim Richter, R. H. Siemssen, and W. G. Stoppenhagen, Bull. Am. Phys. Soc. 15, 1676 (December 1970)

2. Further Developments in the Energy-Level Statistic A(n), J. E. Monahan and Norbert Rosenzweig, Bull. Am. Phys. Soc. 15, 1668 (December 1970)

3. Gamma-Ray Transitions in $^{46,47}Ti$, H. E. Siefken, Luise Meyer-Schützmeister, J. W. Smith, G. Hardie, and P. P. Singh, Bull. Am. Phys. Soc. 15, 1673 (December 1970)

4. Identification and Distorted-Wave Analysis of Unnatural-Parity States in ^{58}Ni, M. M. Stautberg, Bull. Am. Phys. Soc. 15, 1681 (December 1970)

5. Lifetimes of Low-Lying Levels in ^{28}Al, J. V. Maher, G. B. Beard, G. H. Wedberg, and R. E. Segel, Bull. Am. Phys. Soc. 16, 58 (January 1971)

6. $^{12}C + ^{16}O$ Elastic Scattering, R. E. Malmin, R. H. Siemssen, and P. P. Singh, Bull. Am. Phys. Soc. 16, 100 (January 1971)

7. Calculations of Shielding for Large Cyclotrons, T. H. Braid, R. F. Rapids, R. H. Siemssen, and J. W. Tippie, Bull. Am. Phys. Soc. 16, 257 (February 1971)

8. Elastische und inelastische Streuung von ^{14}N, ^{15}N und ^{16}O an ^{28}Si, K. O. Groeneveld, A. Richter, R. H. Siemssen, and W. G. Stoppenhagen, Verhandl. Deut. Physik. Ges. 3, 237 (1971)

9. Die Reaktionen (^{6}Li, ^{7}Li) und (^{6}Li, ^{7}Be) an den Targetkernen ^{11}B, ^{12}C und ^{14}N und die Einnucleon-Parentage von Masse-7-Kernen, K. O. Groeneveld, A. Richter, U. Strohbusch, and B. Zeidman, Verhandl. Deut. Physik. Ges. 3, 238 (1971)

10. Der γ-Zerfall der tiefstliegenden isobaren Analogzustände in ^{33}S, ^{41}Ca und ^{47}Ti, K. T. Knöpfle, C. Mayer-Böricke, M. Rogge, D. S. Gemmell, L. Meyer-Schützmeister, H. Ohnuma, and N. G. Puttaswamy, Verhandl. Deut. Physik. Ges. 3, 130-131 (1971)

11. Symmetrien bei Kernreaktionen zur Erzeugung von Isospin Multipletts, A. Richter, H. T. Fortune, C. M. Vincent, B. Zeidman, and D. Robson, Verhandl. Deut. Physik. Ges. 3, 129-130 (1971)

12. Das Niveauschema von ^{233}Th, T. von Egidy, O. W. B. Schult, D. Rabenstein, R. E. Chrien, J. R. Erskine, H. A. Baader, and D. Breitig, Verhandl. Deut. Physik. Ges. 3, 248 (1971)

BROOKHAVEN NATIONAL LABORATORY

Recent Publications

M. R. Bhat, R. E. Chrien, D. I. Garber, and O. A. Wasson, Gamma rays from thermal and resonance capture in Sb-121 and Sb-123. Phys. Rev. C2, 1115-1125 (1970).

M. R. Bhat, R. E. Chrien, D. I. Garber, and O. A. Wasson, Low energy gamma rays from resonant neutron capture in Tm-169. Phys. Rev. C2, 2030-2033 (1970).

S. F. Mughabghab, R. E. Chrien, and O. A. Wasson, Evidence for non-statistical effects in the reaction Dy-163(n,γ)Dy-164. Phys. Rev. Letters 25, 1970-1673 (1970).

K. Rimawi, J. B. Garg, R. E. Chrien, and R. G. Graves, Resonance neutron capture in Rh-103. Phys. Rev. C2, 1793-1808 (1970).

O. A. Wasson and R. E. Chrien, Resonant neutron capture in Lu-175. Phys. Rev. C2, 675-689 (1970).

M. Beer, Doorway states and primary neutron capture gamma-rays. Annals of Phys. (in press)

R. E. Chrien, K. Rimawi, and J. B. Garg, Resonance neutron capture in Nb-93. Phys. Rev. (in press)

F. Becvar, R. E. Chrien, and O. A. Wasson, The study of neutron resonance capture in Sm-149. Bull. Am. Phys. Soc. II, 15, 1667 (1970).

M. Beer. Doorway states and the reaction mechanisms of primary neutron capture γ-rays. Bull. Am. Phys. Soc. II, 15, 548 (1970).

R. E. Chrien, P. Liaud, and O. A. Wasson, Neutron capture γ-rays from Sodium. Bull. Am. Phys. Soc. II, 16, 15 (1971).

R. G. Graves, C. Olmer, and R. E. Chrien, Resonant and thermal neutron capture gamma rays from Cesium. Bull. Am. Phys. Soc. II, 15, 548 (1970).

S. Mughabghab, R. E. Chrien, and O. A. Wasson, Spin assignments of neutron resonances of Dy-163 using the (n,γ) reaction. Bull. Am. Phys. Soc. II, 15, 549 (1970).

S. F. Mughabghab, R. E. Chrien, and O. A. Wasson, Nonstatistical effects in S-wave neutron capture in Dy-163(n,γ)Dy-164. Bull. Am. Phys. Soc. II, 15, 1667 (1970).

S. F. Mughabghab, R. E. Chrien, O. A. Wasson, and M. R. Bhat, Evidence for nonstatistical effects in P-Wave neutron capture in Mo^{98}. Bull. Am. Phys. Soc. II, 15, 1667 (1970).

O. A. Wasson, Nonstatistical effects in neutron radiative capture. Bull. Am. Phys. Soc. II, 15, 640 (1970).

O. A. Wasson, R. E. Chrien, G. G. Slaughter and J. A. Harvey, Distribution of partial radiation widths in U-238(n,γ)U-239. Bull. Am. Phys. Soc. II, 15, 1668 (1970).

O. A. Wasson and R. Moreh, Resonant neutron capture in Cd-111(n,γ) Cd-112. Bull. Am. Phys. Soc. II, 16, 15 (1971).

R. E. Chrien, O. A. Wasson, S. Dritsa, S. Bokharee and J. B. Garg, High energy γ rays following neutron capture in Pu-239 and U-235. Proceedings of 2nd Inter. Conf. on Nuclear Data for Reactors, Helsinki, Finland, June 15-19, 1970.

R. E. Chrien, S. Dritsa, R. G. Graves, W. R. Kane, and O. A. Wasson. High resolution capture γ-ray spectroscopy in fissile nuclides. Third Conf. on Neutron Cross Sections and Technology, Knoxville, Tenn. March 15-17, 1971.

S. F. Mughabghab, O. A. Wasson, and R. E. Chrien, Identification of parity of resonances from primary γ-ray transitions. Third Conf. on Neutron Cross Sections and Technology, Knoxville, Tenn. March 15-17, 1971.

S. F. Mughabghab, O. A. Wasson, G. W. Cole, and R. E. Chrien. The use of primary and low energy gamma rays for spin determination of S-wave resonances. Third Conf. on Neutron Cross Sections and Technology, Knoxville, Tenn. March 15-17, 1971.

O. A. Wasson and R. E. Chrien. Gamma rays from resonance neutron capture in Th-232. Third Conf. on Neutron Cross Sections and Technology, Knoxville, Tenn. March 15-17, 1971.

G. W. Cole, S. F. Mughabghab, O. A. Wasson, and R. E. Chrien, Resonant neutron capture in $^{171}Yb(n,\gamma)^{172}Yb$. Bull. Am. Phys. Soc. 16, 496 (1971).

R. G. Graves, D. I. Garber, and R. E. Chrien, Gamma rays from resonance neutron capture in U-235. Bull. Am. Phys. Soc. 16, 496 (1971).

S. F. Mughabghab, O. A. Wasson, G. W. Cole, R. E. Chrien, and M. R. Bhat, Search for doorway states in the reaction Yb-173(n,γ) Yb-174. Bull. Am. Phys. Soc. 16, 496 (1971).

O. A. Wasson, S. F. Mughabghab, and R. E. Chrien, Determination of spins of neutron resonances of Er-167. Bull. Am. Phys. Soc. 16, 496 (1971).

G. Brunhart, Hans Postma, D. C. Rorer, V. L. Sailor, L. Vanneste. Absolute spin assignments of Dy^{161} and Dy^{163} neutron resonances and the hyperfine coupling constants in Dy^{163}. Z. Naturforch. (in press)

D. C. Rorer and G. Brunhart. Spin assignments of two weak resonances in Dy^{161} at 12.65 and 16.7 eV. Bull. Am. Phys. Soc. 16, 518 (1971).

W. Gelletly, W. R. Kane, and D. R. MacKenzie. Neutron capture γ-rays from the 14.1 eV resonance in $^{131}Xe(n,\gamma)^{132}Xe$. Phys. Rev. C-3, 1678 (1971).

W. R. Kane. Gamma-ray spectra from capture of monochromatic Bragg diffracted neutrons. Invited Talk 1971 Spring Meeting of the American Physical Society 26-29 April 1971.

LOS ALAMOS SCIENTIFIC LABORATORY

The following recent journal articles may be of interest:

A. Hemmendinger	Neutrons from Nuclear Explosions	Am. Scientist 58, 622 (1970).
B. C. Diven	Nuclear Explosions as a Nuclear Physics Tool	Ann. Rev. Nucl. Sci. 20, 79 (1970).
H. T. Motz	Neutron Capture Gamma Ray Spectroscopy	Ann. Rev. Nucl. Sci. 20, 1 (1970).
J. H. McCrary L. D. Looney H. F. Atwater	Attenuation of 5.9 keV Photons by Helium and Hydrogen	J. Appl. Phys. 41, 3570 (1970).
R. R. Fullwood	Versatile Mercury Film Pulser	Nucl. Instr. Methods 87, 149 (1970).
M.-L. Andersen S. A. Andersen O. Nathan K. M. Bisgard K. Gregersen O. Hansen S. Hinds R. Chapman	Neutron Transfer Reactions on ^{204}Hg	Nucl. Phys. A153, 17 (1970).
D. W. Bergen R. R. Fullwood	Neutron Induced Fission Cross Section of ^{242}Pu	Nucl. Phys. A163, 577 (1971).
W. K. Brown D. R. Dixon D. M. Drake	Fission Cross Sections of ^{237}Np from Pommard	Nucl. Phys. A156, 609 (1970).
C. S. Ellegaard P. D. Barnes E. R. Flynn G. J. Igo	Inelastic Scattering of Tritons and Protons from ^{210}Pb	Nucl. Phys. A162, 1 (1971).
E. R. Flynn J. G. Beery A. G. Blair	^{122,124}Sn(t,p)^{124,126}Sn Reaction at 20 MeV	Nucl. Phys. A154, 225 (1970).
E. R. Flynn G. J. Igo P. D. Barnes R. F. Casten J. Erskine	^{182}W(t,d)^{183}W Reaction at 20 MeV Triton Energy	Nucl. Phys. A159, 598 (1970).
J. R. Sites W. A. Steyert	Angular Distribution of Gamma Rays Resulting from Polarized ^{124}Sb, ^{192}Ir, and ^{194}Ir	Nucl. Phys. A156, 19 (1970).

J. D. Garrett R. Middleton D. J. Pullen S. A. Andersen O. Nathan O. Hansen	Spectroscopy of ^{22}Na with the $^{20}Ne(^{3}He,p)$ and $^{20}Ne(^{6}Li,\alpha)$ Reactions	Nucl. Phys. A164, 449 (1971).
R. E. Alcouffe T. J. Hirons R. D. O'Dell	Effect of Collapsing Cross Section Data on Fast Breeder Physics Parameters	Nucl. Sci. Eng. 43, 173 (1971)
J. R. Lemley G. A. Keyworth B. C. Diven	High Resolution Fission Cross Section of ^{235}U from 20 eV to 100 keV	Nucl. Sci. Eng. 43, 281 (1971).
C. J. Orth	Average Number of Neutrons Emitted in the Spontaneous Fission of Some Even-Even Heavy Nuclides	Nucl. Sci. Eng. 43, 54 (1971).
J. C. Vigil	3DDT, A Three-Dimensional Multigroup Diffusion Burnup Program	Nucl. Sci. Eng. 42, 114 (1970).
D. M. Drake S. L. Whetstone I. Halpern	Spectra of High Energy Photons Emitted from the Compound System ^{64}Zn in Various Nuclear Reactions	Phys. Letters B32, 349 (1970).
D. F. Beckstrand E. B. Shera	$^{40}K(n,\gamma)^{41}K$ Reaction and the Level Structure of ^{41}K	Phys. Rev. C3, 208, (1971).
H. C. Britt J. D. Cramer	Fission of Odd-A Uranium and Plutonium Isotopes Excited by (d,p), (t,d), and (t,p) Reactions	Phys. Rev. C2, 1758 (1970).
J. D. Cramer H. C. Britt	Fission Studies of Thorium, Uranium, and Plutonium Isotopes with (t,pf) Reactions	Phys. Rev. C2, 2350 (1970).
P. Fessenden W. R. Gibbs R. B. Leachman	Nuclear State Widths of Medium Weight Nuclei in the Continuum	Phys. Rev. C3, 807 (1971).
D. G. Foster,Jr. D. W. Glasgow	Neutron Total Cross Sections, 2.5-15 MeV. I. Experimental	Phys. Rev. C3, 576 (1971).
D. W. Glasgow D. G. Foster,Jr.	Neutron Total Cross Sections, 2.5-15 MeV. II. Effects of Nuclear Deformation	Phys. Rev. C3, 604 (1971).
W. R. Gibbs	Multiple Scattering of Pions by Deuterons	Phys. Rev. C3, 1127 (1971).
G. J. Igo E. R. Flynn B. J. Dropesky P. D. Barnes	$^{210}Pb(p,d)^{209}Pb$ Reaction at 20.6 MeV	Phys. Rev. C3, 349 (1971).

N. Jarmie J. H. Jett J. L. Detch, Jr. R. L. Hutson	Proton-Proton Elastic Scattering from 9.6 to 13.6 MeV	Phys. Rev. C3, 10 (1971).
E. T. Jurney R. K. Sheline E. B. Shera H. R. Koch B. P. K. Maier U. Gruber H. Baader D. Breitig O. W. B. Schult J. Kern G. L. Struble	Study of the Levels in ^{140}La Using the ^{139}La(n,γ)^{140}La Reaction	Phys. Rev. C2, 2323 (1970).
M. Minor R. K. Sheline E. T. Jurney	Nuclear Levels in ^{177}Lu and ^{175}Lu	Phys. Rev. C3, 766 (1971).
M. S. Moore G. A. Keyworth	Analysis of the Fission and Capture Cross Sections of the Curium Isotopes	Phys. Rev. C3, 1656 (1971).
G. S. Mutchler W. B. Broste J. E. Simmons	Neutron Polarization in the d+T → n+^{4}He Reaction at 30° from 3 to 15 MeV	Phys. Rev. C3, 1031 (1971).
R. H. Stokes P. G. Young	Search for Excited States of ^{6}He	Phys. Rev. C3, 984 (1971).
B. E. Watt W. T. Leland	Deuteron Scattering from a Polarized ^{3}He Gas Target	Phys. Rev. C2, 1677 (1970).
B. E. Watt W. T. Leland	^{3}He(d,p)^{4}He Reaction Proton Asymmetry Using a Polarized ^{3}He Gas Target	Phys. Rev. C2, 1680 (1970).
K. Wolfsberg G. P. Ford	Thermal-Neutron Fission of ^{242m}Am: Mass and Charge Distribution	Phys. Rev. C3, 1333 (1971).
J. P. Balagna, Jr. G. P. Ford D. C. Hoffman J. D. Knight	Mass Symmetry in the Spontaneous Fission of ^{257}Fm	Phys. Rev. Letters 26, 145 (1971).
W. B. Broste G. P. Lawrence J. L. McKibben G. G. Ohlsen J. E. Simmons	Polarization Transfer in the Reaction T(d,n)^{4}He at 0 Degrees from 3.9 to 15 MeV	Phys. Rev. Letters 25, 1040 (1970).

L. Rosen	Particle Accelerators: Instruments of Basic Research	Phys. Teacher 8, 432 (1970).
H. T. Motz E. T. Jurney E. B. Shera R. K. Sheline	Low-Lying Configurations in ^{210}Bi	Phys. Rev. Letters 26, 854 (1971).
D. D. Armstrong H. E. Wegner	Supercollimation of Negative Icn Beams with Apertures	Rev. Sci. Instr. 42, 40 (1971).
L. Forman C. U. Benton D. A. Garrett A. D. Schelberg	Technique for Obtaining Neutron Radiographs in the Resonance Region	Rev. Sci. Instr. 41, 1900 (1970).

Papers recently submitted for presentation at meetings included the following:

Third Conference on Neutron Cross Sections and Technology, Knoxville, Tennessee, March 15-17, 1971

M. V. Harlow K. D. Ferrell R. Plaisted A. N. Phillips	RAYMATH-A Problem Oriented Language Designed for Processing Neutron Cross-Section Data
G. F. Auchampaugh	A Study of the Uniqueness of the R-Matrix Parameters Using the Fortran Code, MULTI
M. S. Moore	Status and Comparison of Techniques for Resonance Measurements
M. G. Silbert R. W. Lougheed J. E. Evans R. W. Hoff	Fission Cross Section of ^{249}Cf
G. F. Auchampaugh J. A. Farrell D. W. Bergen	Subthreshold Fission in ^{242}Pu and ^{244}Pu
L. Forman A. D. Schelberg J. H. Warren M. V. Harlow H. A. Grench N. W. Glass	Thorium-232 Neutron Capture in the Region 20 eV-30 keV
R. E. Hunter T. J. Hirons	Calculation of CH_2 and CD_2 Reactivities in Jezebel

R. E. Hunter C. C. Cremer D. R. Worlton	Integral Comparisons for Fast Critical Assemblies
D. W. Muir L. R. Veeser	Neutron Induced Fission Cross Sections of ^{230}Th and ^{231}Pa
D. J. Dudziak	Photon Production Data Review and Retrieval in the ENDF/B
F. McGirt M. Asprey M. Hoyt	Cross Section Processing in a Modular Environment
M. M. Hoffman G. J. Berzins W. M. Sanders L. J. Brown D. D. Phillips	Neutron Scattering Cross Section of ^{197}Au
D. R. Harris	Statistical Distribution of Kapur-Peierls Parameters for Fissile Nuclides

American Physical Society Meeting, New York, New York, 1-4 February, 1971; Bull. Am. Phys. Soc. Ser. 2, V. 16, No. 1:

J. R. Sites H. A. Smith W. A. Steyert	Comparison of ^{54}Mn and ^{60}Co γ Ray Angular Distribution Thermometers
R. H. Stokes P. G. Young	Search for ^{6}He Excited States

American Physical Society Meeting, Washington, D. C., 26-29 April 1971; Bull. Am. Phys. Soc. Ser. 2, V. 16, No. 4:

J. Amato R. Burman R. Macek W. Shlaer J. Oostens E. Arthur S. Sobottka W. Lam P. Barns P. Fessenden W. Swenson D. Axen M. Solomon	New Measurement of $(\pi^+, 2p)$ Reaction on Light Nuclei

R. Macek J. Amato R. Burman W. Shlaer J. Oostens E. Arthur S. Sobottka W. C. Lam	Search for (π^+,p) Reaction on ^{16}O, ^{12}C, and ^{9}Be
D. D. Armstrong P. W. Keaton,Jr. G. P. Lawrence L. L. Catlin	A Study of the Elastic Scattering of Polarized Deuterons from Nuclei
D. K. McDaniels M. Drosg J. C. Hopkins J. T. Martin J. D. Seagrave	The $T(d,n)^4He$ Neutron Source Reaction
J. H. Jett J. L. Detch,Jr. N. Jarmie	Accurate d-^4He Scattering Cross Sections at 12.0 MeV
G. P. Lawrence G. G. Ohlsen J. L. McKibben P. W. Keaton,Jr. D. D. Armstrong	Precise Proton and Deuteron Polarization Standards Determined with the LASL Lamb Shift Ion Source
J. E. Brolley	Supersonic Jet Target in Vacuo
P. W. Keaton,Jr. G. G. Ohlsen J. L. Gammel	Quadratic Relations for Simple Spin Systems
R. F. Casten P. W. Keaton,Jr. G. P. Lawrence	Levels in ^{185}W and ^{187}W Excited in the (d,p) Reaction with Polarized Deuterons
D. C. Slater E. R. Cosman O. Hansen E. R. Flynn	The $^{87}Sr(t,p)^{89}Sr$ Reaction and the Two-Particle, One-Hole States of ^{89}Sr
J. E. Brolley	Primary Solar Reaction Dependence on Deuteron Structure
R. F. Casten O. Hansen E. R. Flynn T. J. Mulligan	Shapes of Neutron Rich Nuclei Near A = 110 Studied with the (t,p) Reaction

The following LASL reports may also be of interest:

B. S. Jackson, Comp.	Bibliography - Neutron Interactions with Nuclei (A>2), in an Energy Range of 100 MeV or Higher. ISD-Bib-4
B. S. Jackson, Comp.	Bibliography - Total Cross Sections of the Elements Using Neutrons or Protons as the Incident Beam with an Energy Range of 100 MeV or Higher. ISD-Bib-5
G. G. Ohlsen	Los Alamos Lamb-Shift Polarized Ion Source: A User's Guide. LA-4451
J. L. Gammel P. W. Keaton, Jr. G. G. Ohlsen	Formalism for the $T(d,n)^4He$ and $^3He(d,p)^4He$ Reactions. LA-4492-MS
D. R. Harbur J. W. Anderson W. J. Maraman	Studies on the U-Pu-Zr Alloy System for Fast Breeder Reactor Applications. LA-4512
P. A. M. Gram	Proposal for P^3, a Versatile High-Energy Pion Beam Facility. LA-4535-MS
D. D. Armstrong P. W. Keaton, Jr.	Polarization of Elastically Scattered Tritons and ^3He. LA-4538
D. R. Harris	ANDYMG3, The Basic Program of a Series of Monte Carlo Programs for Time-Dependent Transport of Particles and Photons. LA-4539
J. J. Devaney M. L. Stein	Energy Loss by Nuclear Elastic Scattering. LA-4543
G. C. Hopkins	CONVERT: An IBM--To-CDC Program Conversion Code. LA-4555
R. M. Steffen	Angular Distributions and Correlations of Radiation Emitted from Oriented Nuclei. LA-4565-MS
K. D. Lathrop F. W. Brinkley	TWOTRAN SPHERE: A Fortran Program to Solve the Multigroup Transport Equation in Two-Dimensional Spherical Geometry. LA-4567
E. D. Dunn, Comp.	Quarterly Status Report on the Medium-Energy Physics Program for the Period Ending October 31, 1970. LA-4571-MS
L. Stewart R. J. LaBauve P. G. Young	Evaluated Nuclear Data for Hydrogen in the ENDF/B-II Format. LA-4574
F. W. Brinkley	TRANZIT: A Program for Multigroup Time-Dependent Transport in (ρ,z) Cylindrical Geometry. LA-4575
J. L. Detch, Jr.	Accurate Cross-Section Measurements of the Reactions $T(p,p)T$, $T(p,d)D$, $T(p,^3He)N$, and $T(p,\hat{p})T$ at 13.600 MeV. LA-4576

L. E. Agnew K. Harper B. F. Miller, Comps.	Proceedings of the Fourth LAMPF Users Meeting Held at the Los Alamos Scientific Laboratory of the University of California, Los Alamos, New Mexico, October 30-31, 1970. LA-4578-MS
	Quarterly Status Report on the Advanced Plutonium Fuels Program, October 1-December 31, 1970. LA-4595-MS
W. B. Broste	Polarization Effects in Neutron-Helium Scattering and the $T(d,n)^4He$ Reaction. LA-4596
G. R. Keepin	Nuclear Safeguards Research and Development. Program Status Report September-December 1970. LA-4605-MS
P. A. M. Gram	Method for Measuring the Energy and Intensity of a Proton Beam by Detecting Forward Scattered Electrons. LA-4612
	Proceedings of LAMPF Theoretical Study Group, January 25-29, 1971. LA-4637-MS
	Quarterly Status Report on the Medium-Energy Physics Program for the Period Ending January 31, 1971. LA-4639-MS
	Advanced Plutonium Fuels Program. Quarterly Status Report, July 1 - September 30, 1970. LA-4646-MS
NCSAC, Comp.	Compilation of Requests for Nuclear Cross Section Measurements. LA-4652-MS (NCSAC-35)

OAK RIDGE NATIONAL LABORATORY

Publications

Following is a list of papers of general interest published since the last meeting of the NCSAC December 1970:

Allowed Values of Coupled Angular Momentum and i-Spin for Nucleons in a Single Shell in j-j Coupling, L. B. Hubbard, Computer Phys. Comm., Vol. 1, 453-57 (1970).

Exchange Effects with a Realistic Interaction for Inelastic Scattering, W. G. Love and G. R. Satchler, Nucl. Phys. A159, 1-44 (1970).

Total Neutron Cross Section of Oriented ^{165}Ho from 2 to 135 MeV, H. Marshak, A. Langsford, T. Tamura, and C. Y. Wong, Phys. Rev. C2, 1862-81 (1970).

Reaction List for Charged-Particle-Induced Nuclear Reactions. Z = 1 to 98 (H to Cf), F. K. McGowan and W. T. Milner, Nucl. Data Tables, Vol. 8, 199-322 (1970).

Beta-Decay Rates and the Role of the $d_{3/2}$-Orbit in Light s-d Shell Nuclei, J. B. McGrory, Phys. Letters 33B, 327-30 (1970).

Ion-Ion Potentials in a Two Center Model, U. Mosel, T. D. Thomas, and P. Riesenfeltd, Phys. Letters 33B, 565-67 (1970).

Exchange Effects in the Nucleon-Nucleus Optical Potential, L. W. Owen and G. R. Satchler, Phys. Rev. Letters 25, 1720-24 (1970).

Observation of the Phase of the Effective Interaction for Inelastic Scattering of Complex Particles, G. R. Satchler, Phys. Letters 33B, 385-87 (1970).

Static Quadrupole Moment of the First 2+ States of the Even Tin Nuclei, P. H. Stelson, F. K. McGowan, R. L. Robinson, and W. T. Milner, Phys. Rev. C2, 2015-2022 (1970).

Following is a list of papers of general interest presented at meetings since the last meeting of the NCSAC December 1970:

Factorization and Folded Diagrams in the Goldstone Linked-Cluster Series, R. L. Becker and R. W. Jones, American Physical Society Meeting, Washington, D.C., April 26-29, 1971.

Dynamical Distortion of Nuclei in Heavy-Ion Reactions, A. S. Jensen and C. Y. Wong, American Physical Society Meeting, Washington, D.C., April 26-29, 1971.

Products of the $^{58,60}Ni(^{16}O,x)$ Reactions, R. L. Robinson, H. J. Kim, J. L. C. Ford, Jr., E. Collins, and J. H. Hamilton, American Physical Society Meeting, Washington, D.C., April 26-29, 1971

Coulomb Excitation of ^{197}Au, ^{204}Hg and ^{238}U, J. L. C. Ford, Jr., P. H. Stelson, R. L. Robinson, F. K. McGowan, W. T. Milner, and C. E. Bemis, American Physical Society Meeting, Washington, D.C., April 26-29, 1971.

Coulomb Excitation of ^{93}Nb, P. H. Stelson, R. L. Robinson, W. T. Milner, F. K. McGowan, and M. A. Ludington, American Physical Society Meeting, Washington, D.C., April 26-29, 1971.

Comparisons of ENDF/B Evaluated Neutron Scattering Cross Sections for Eight Elements with Recent Experimental Data from 1 to 8.5 MeV, W. E. Kinney and F. G. Perey, Third Conference on Neutron Cross Sections and Technology, University of Tennessee, Knoxville, Tennessee, March 15-17, 1971.

Experimental Nuclear Cross-Section Data for Spacecraft Shield Analysis, R. W. Peelle, F. R. Bertrand, W. R. Burrus, W. A. Gibson, N. W. Hill, T. A. Love, F. C. Maienschein, R. T. Santoro, R. J. Scroggs, J. H. Todd, V. V. Verbinski, J. W. Wachter, and W. Zobel, National Symposium on Natural and Manmade Radiation in Space, Las Vegas, Nevada, March 2-5, 1971.

Experimental Nuclear Cross Sections for Spacecraft Shield Analysis, R. W. Peelle, National Symposium on Natural and Manmade Radiation in Space, Las Vegas, Nevada, March 2-5, 1971.

The POPOP4 Library and Codes for Preparing Secondary Gamma-Ray Production Cross Section, W. E. Ford III, National Symposium on Natural and Manmade Radiation in Space, Las Vegas, Nevada, March 2-5, 1971.

TUNL Publications November 1970-April 1971

6-70Sc01 "Polarization Measurements and Phase Shifts for p-^{4}He Scattering between 3 and 18 MeV"
P. Schwandt, T. B. Clegg and W. Haeberli, Nuclear Physics A163, 432 (1970)

6-70Me01 "A DWBA Analysis of the Cross Section and Polarization Data for the ^{14}N(d,n)^{15}O Reaction at 3.5 MeV"
M. M. Meier, R. L. Walter and T. R. Donoghue, Nuclear Physics A159 (1970) 273

6-71Ev01 "Energies of Some ^{25}Al Levels from the ^{24}Mg(p,γ)^{25}Al Reaction and the Coulomb-Energy Differences of Analog Rotational Bands"
F. Everling, G. L. Morgan, D. W. Miller, L. W. Seagondollar, and P. W. Tillman, Jr., Canadian Journal of Physics 49, 402 (1971)

6-70La01 "An Angular Correlation Study of the Low Lying Levels of ^{29}P"
G. P. Lamaze, C. R. Gould, C. E. Moss, N. R. Roberson and D. R. Tilley, Nuclear Physics A158, 43 (1970)

6-71Ra01 "Lifetimes in ^{37}Ar Using Doppler Shift Techniques"
C. E. Ragan, C. R. Gould, N. R. Roberson, G. E. Mitchell and D. R. Tilley, Phys. Rev. C 3, 1152 (1971)

6-70Go01 "Midstream Evaluation, A = 88"
C. D. Goodman, T. A. Hughes, M. W. Johns, and K. Way, Nuclear Data Tables A 8, 345 (1970)

6-70Jo01 "Midstream Evaluation, A = 89"
M. W. Johns, J. Y. Park, S. M. Shafroth, D. M. Van Patter, and K. Way, Nuclear Data Tables A 8, 373 (1970)

6-70Ba01 "Midstream Evaluation, A = 90"
J. B. Ball, M. W. Johns, and K. Way, Nuclear Data Tables A 8, 407 (1970)

TUNL Abstracts November 1970-April 1971

6-71Ou02a "The Mass of ^{80}Rb from the ^{80}Kr(p,n)^{80}Rb Reaction Threshold and the ^{80}Rb Half-life"
D. A. Outlaw, F. Everling, D. W. Miller, T. G. Dzubay, G. A. Bissinger, A. A. Jaffe, and S. M. Shafroth, Bull. Am. Phys. Soc. 16, 13 (1971)

6-71Wa01a "Excitation of Gold L X Rays by ^{197}Hg Electron Capture and Proton, Alpha and ^{16}O Bombardment"
A. W. Waltner, G. A. Bissinger, and S. M. Shafroth, Bull. Am. Phys. Soc. 16, 13 (1971)

6-71Sy01a "Mössbauer Effect following Coulomb Excitation in the 43.8-keV State of Dy^{161}"
S. C. Sylvester and D. Schroeer, Bull. Am. Phys. Soc. 16, 25 (1971)

6-71La01a "Coulomb-excitation Mössbauer Effect in Eu^{151}"
R. L. Lambe and D. Schroeer, Bull. Am. Phys. Soc. 16, 25 (1971)

6-71Bi01a "Excitation of Cu and Ag K X Rays by ^{109}Cd Electron Capture and Proton and ^{16}O Bombardment"
G. A. Bissinger, S. M. Shafroth, and A. W. Waltner, Bull. Am. Phys. Soc. 16, 125 (1971)

6-71Ha01a "Lifetime Measurements of Low Lying States in ^{27}Si"
E. C. Hagen, C. R. Gould, N. R. Roberson and D. R. Tilley, Bull. Am. Phys. Soc. 16, 491 (1971)

6-71Pi01a "High Resolution Neutron Total Cross Section Measurements of ^{88}Sr"
W. F. E. Pineo, E. G. Bilpuch, H. W. Newson, and J. G. Malan, Bull. Am. Phys. Soc. 16, 495 (1971)

6-71Di01a "Doorway Interpretation of Sr^{88} Neutron Resonances"
M. Divadeenam, E. G. Bilpuch, and H. W. Newson, Bull. Am. Phys. Soc. 16, 495 (1971)

6-71Ba01a "Proton Induced Fission Cross Sections of the Uranium Isotopes"
J. R. Boyce, T. D. Hayward, F. O. Purser, and H. W. Newson,

and H. W. Schmitt, Bull. Am. Phys. Soc. 16, 517 (1971)

6-71Ha01a "Measurements of the Fission Fragment Angular Distributions for Proton Induced Fission of ^{236}U, ^{235}U and ^{234}U for Proton Energies from 9.00 MeV to 30.00 MeV"
T. D. Hayward, J. R. Boyce, F. O. Purser, H. W. Newson, and H. W. Schmitt, Bull. Am. Phys. Soc. 16, 517 (1971)

6-71Ha01a "Polarization of Neutrons from the $D(d,n)^3He$ Reaction from 12 to 22 MeV"
R. A. Hardekopf, T. C. Rhea, R. L. Walter, and J. M. Joyce, Bull. Am. Phys. Soc. 16, 542 (1971)

6-71Bi02a "Characteristic X-Rays from Ag and Au Produced by ^{16}O Beams from 12 to 42 MeV"
G. A. Bissinger, P. H. Nettles, S. M. Shafroth, and A. W. Waltner, Bull. Am. Phys. Soc. 16, 545 (1971)

6-71Mi01a "Decay of ^{36}K"
D. W. Miller, D. A. Outlaw, F. Everling, T. G. Dzubay, G. A. Bissinger, and S. M. Shafroth, Bull. Am. Phys. Soc. 16, 554 (1971)

6-71Go01a "Lifetimes of Low Lying Levels in ^{42}Sc"
C. R. Gould, J. D. Hutton, N. R. Roberson, G. E. Mitchell, and D. R. Tilley, Bull. Am. Phys. Soc. 16, 555 (1971)

6-71La02a "Study of ^{51}Ti from the $^{50}Ti(d,p\gamma)^{51}Ti$ and $^{48}Ca(\alpha,n\gamma)^{51}Ti$ Reactions"
G. P. Lamaze, C. R. Gould, N. R. Roberson, and D. R. Tilley, Bull. Am. Phys. Soc. 16, 556 (1971)

6-71Pr01a "Fine Structure of Analog States in ^{49}V"
N. H. Prochnow, H. W. Newson, E. G. Bilpuch, and G. E. Mitchell, Bull. Am. Phys. Soc. 16, 557 (1971)

6-71Pe01a "Gamma Decay of The Fine Structure of The Isobaric Analog of the Ground State of ^{55}Cr"
W. C. Peters, E. G. Bilpuch, G. E. Mitchell, and G. L. Morgan, Bull. Am. Phys. Soc. 16, 557 (1971)

6-71Dz01a "Improved Beam Energy Resolution for a Tandem Accelerator"
T. G. Dzubay, E. G. Bilpuch, F. O. Purser, J. D. Moses, H. W.

Newson, and G. E. Mitchell, Bull. Am. Phys. Soc. 16, 582 (1971)

6-71Lu01a "The Cross-Section and Polarization Angular Distribution for ^{3}He Particles Scattered from ^{27}Al at 21 MeV"
E. J. Ludwig, W. S. McEver, T. B. Clegg, J. M. Joyce, and R. L. Walter, Bull. Am. Phys. Soc. 16, 600 (1971)

6-71Wa01a "Investigation of Charge Symmetry and Spin-Dependent Effects in (d,t) and (d,h) Reactions Using Polarized-Deuteron Beams"
A. C. Watkins, E. J. Ludwig, T. B. Clegg, and T. G. Dzubay, Bull. Am. Phys. Soc. 16, 621 (1971)

6-71Ne01a "Measurement of Spectroscopic Factors in the $^{24}Mg(d,t)^{23}Mg$ and $^{24}Mg(d,^{3}He)^{23}Na$ Reactions"
R. O. Nelson, N. R. Roberson, and R. A. Hilko, Bull. Am. Phys. Soc. 16, 621 (1971)

6-71Ea01a "An Elastic Scattering Optical Model Code for Small Computers"
R. J. Eastgate and R. A. Hardekopf, Bull. Am. Phys. Soc. 16, 647 (1971)

6-71Th01a "Alpha-Cluster Effects in Elastic Alpha Scattering"
W. J. Thompson, Bull. Am. Phys. Soc. 16, 647 (1971)

Articles Published, November 1970-April 1971, in Journals edited at TUNL by K. Way

Nuclear Data Tables

Vol. 8, No. 4	"Quasi-Ground, Quasi-Beta, and Quasi-Gamma Bands", Mitsuo Sakai
	"Midstream Evaluation, A= 88", C. D. Goodman, T. A. Hughes, M. W. Johns, and K. Way
	"Midstream Evaluation, A = 89", M. W. Johns, J. Y. Park, S. M. Shafroth, D. M. Van Patter, and K. Way
	"Midstream Evaluation, A = 90", J. B. Ball, M.W Johns, and K. Way
Nos. 5-6	"Catalogue of γ-Rays Emitted by Radionuclides", M. A. Wakat
Vol. 9, No. 1	"A Tabulation of Gamma-Gamma Directional-Correlation Coefficients", H. W. Taylor, B. Singh, F. S. Prato, and R. McPherson
Vol. 9, No. 2	"One-Particle, j-j Coefficients of Fractional Parentage in the Isospin Representation for $n \leq 5$ in the $j = 7/2$ Shell", L. B. Hubbard
	"Contribution of Outer Atomic Shells to Total Internal Conversion Coefficients", O. Dragoun, Z. Plajner, and F. Schmutzler
	"The $^1H(n,n)^1H$ Scattering Observables Required for High-Precision Fast-Neutron Measurements", J. C. Hopkins and G. Breit
	"Tables of Single-Particle Reduced Matrix Elements of Spherical Tensors", W. K. Bell and G. R. Satchler

Atomic Data

Vol. 2, No. 1	"Matrix Elements of Atomic Interaction Operators for d^n Configurations", J. A. Barnes, B. L. Carroll, L. M. Flores, and R. M. Hedges

Atomic Data Vol. 2, No. 1 (Continued)	"Magnetic Interactions in Transition Metal Ions. Part I. Electronic Configurations d^2, d^3, and d^{4}", Wai-Kee Li
	"Magnetic Interactions in Transition Metal Ions. Part II. Bivalent Cations of the First Transition Series", Wai-Kee Li
	"Calculated Ionization Potentials for Multiply Charged Ions", Thomas A. Carlson, C. W. Nestor, Jr., Neil Wasserman, and J. D. McDowell
Vol. 2, No. 2	"Configuration Interaction Matrix Elements for d^n Configurations", J. A. Barnes, B. L. Carroll, and L. M. Flores
	"Potential-Energy Curves for Molecular Hydrogen and Its Ions", T. E. Sharp

YALE UNIVERSITY

PUBLICATIONS

"Low Energy Photonuclear Reactions", F.W.K. Firk, Ann. Rev. of Nucl. Science 20 39 (1970).

"Analysis of the High-Energy Photonucleon Emission from O^{16} and C^{12} in a Direct Reaction Model", M.G. Mustafa and F.B. Malik, Phys. Rev. C1 753 (1970).

"Evidence of E_2 and M_1 Transitions in High-Energy Photonuclear Reactions in O^{16}", M.G. Mustafa and F.B. Malik, Phys. Rev. C2 2068 (1970).

*"Structure of the Nucleon-Nucleus Scattering Matrix in the Random-Phase Approximation", J.N. Ginocchio, T.H. Schucan, and H.A. Weidenmuller, Phys. Rev. C1 55 (1970).

"The Scattering of 60 MeV Electrons from ^{90}Zr", J. Bellicard, P. Leconte, T.H.Curtis, R.A. Eisenstein, D. Madsen, and C.K. Bockelman, Nucl. Phys. A143 213 (1970).

"Inelastic Scattering of 60 MeV Electrons from K^{39}", R.J. Peterson, H. Theissen, and W.J. Alston, Nucl. Phys. A143 337 (1970).

"Total Neutron Cross Section Measurements", F.W.K. Firk and E. Melkonian, Experimental Neutron Resonance Spectroscopy (ed. by J. Harvey) Academic Press, New York 1970.

"Inelastic Electron Scattering from ^{56}Fe", R. J. Peterson, H. Theissen and W.J. Alston, Nucl. Phys. A153 610 (1970).

*"Extraction of Spectroscopic Factors from Isobaric Analogue Resonances with Strong Inelastic Background", J.N. Ginocchio and T.H. Schucan, Nucl. Phys. A156 629 (1970).

* Partially supported by Electron Accelerator Project Funds.

PUBLICATIONS SUBMITTED AND IN PROGRESS

"Electron Scattering Tests of Nuclear Models", R.J. Peterson, accepted for publication in Annals of New York Academy of Science.

"Anomalous Electron Scattering from $^{142,146,150}Nd$", D.W. Madsen, L.S. Cardman, J.R. Legg, and C.K. Bockelman, accepted for publication in Nuclear Physics.

ABSTRACTS SUBMITTED FOR THE 1971 WASHINGTON MEETING OF THE AMERICAN PHYSICAL SOCIETY

"Differential Polarization of Photoneutrons from Deuterium", R. Nath, F.W.K. Firk, H.L. Schultz, and F.D. Brooks.

"Electron Scattering Studies on Some Even Isotopes of Samarium", L.S. Cardman, C.K. Bockelman, J. Legg, D. Kalinsky, and R. Yen.

"$N^{14}(\gamma,p_x)$ Angular Distributions to the Excited Residual State", E.J. Bentz, J.E.E. Baglin.

"$N^{14}(\gamma,p_o)$ Angular Distributions," R.W. Carr, E.J. Bentz, Jr., J.E.E. Baglin.

"Absolute Differential Cross Sections for the $D^2(\gamma,p)$ Reaction at Low Energies", J.E.E. Baglin, E.J. Bentz,Jr., R.W.Carr.

INTERNAL REPORTS

"Computer Analysis of Elastic Electron Scattering", D. Kalinsky, EAL Report #116.